FINDING THE ACHILLES HEEL: INVESTIGATING HOW TO CONTROL MAJOR BACTERIAL PATHOGENS

Maria Solsona Gaya

100317176

62,445 words

A thesis submitted in fulfilment of the requirements of the University of East Anglia for the degree of Doctor of Philosophy

Quadram Institute Bioscience

Norwich Medical School, University of East Anglia

June 2024

ABSTRACT

Biocides are critical in the control and prevention of healthcare-associated infections. The emergence of bacterial tolerance/resistance to biocides and cross-resistance to antibiotics is a potential concern. Understanding how nosocomial pathogens respond to biocidal agents is key to improving infection prevention and control products and practices.

An evolution model was used to study how *Staphylococcus aureus* and *Enterococcus faecalis* responded to challenge with commonly used biocides and a novel biocidal formulation. Biofilm and planktonic lineages were exposed to repeated sub-lethal concentrations of chlorhexidine digluconate (CHX) and octenidine dihydrochloride (OCT) when grown both planktonically and as a biofilm. Both pathogens could adapt to both biocides with planktonic lineages able to survive higher concentrations of CHX and OCT before growth was inhibited. Evolved isolates had no major fitness deficit and low-level changes to susceptibility to various other antimicrobials were observed after biocide exposure. RNA sequencing identified multiple pathways involved in envelope homeostasis changed expression after biocide exposure.

Sequencing of *S. aureus* mutants from independent lineages identified repeated loss of function changes within fatty acid kinase (*fakA*) after exposure to CHX and OCT in all conditions. Analogous changes were observed within the homologous gene (*dak2*) in parallel experiments with *E. faecalis*. Significantly lower ethidium bromide accumulation and differences in the cell envelope were observed in isolates with *fakA* mutation when compared to the WT, suggesting differences in membrane permeability and fluidity. A final evolution experiment with a novel biocidal formulation however identified no changes in genes known to confer biocide tolerance after exposure.

This work shows *in vitro* evolution methods can be highly informative in understanding mechanisms of action and bacterial responses to biocides, and has identified a novel important role of FakA in biocide susceptibility. Different biocides impart different selective impacts and future work is needed to understand bacterial responses to diverse biocides.

Keywords: healthcare-associated infections, biocides, novel formulation, infection prevention control, *fakA.*

DEDICATION

To my parents, Montse and Miquel, for their constant sacrifices.

Dad, I wish you were here to share this with us. T'estimo papi.

ACKNOWLEDGEMENTS

First and foremost, I would like to thank both my supervisors Prof. Mark Webber and Prof. Cynthia Whitchurch for their constant support. I have greatly enjoyed our scientific discussions and all the constructive feedback you gave me during these years. Thank you to the Medical Research Council, the DART iCASE programme, and GAMA Healthcare Ltd. for funding this research. Special thanks to Dr Benjamin Evans, Michelle Eastman, and Natasha Montgomery for all their help in running the DART programme and organising all our cohort trainings.

My PI has been my mentor since the beginning, so I cannot possibly continue the acknowledgment section without thanking him again. Mark, thank you for giving me the opportunity to start my PhD in the UK, and become a little more British every day. I cannot possibly thank you enough for the amount of support (and banter) I have received during these years, which is unmeasurable. There was not a single day when your office door was not open, what a privilege to learn from you. I hope one day I can be as amazing a mentor (and person) as you are. Thank you and gracias for everything.

To Dr. Heather Felgate, who not only has been my postdoc but also my friend. Heather, thank you for making the nonsense make sense every day, for sharing walnuts (but not bananas), and for being there for me every time I needed it. I loved being part of our little Staph Club.

I would like to thank past and present members of the Webber group: Emma, Gregory, Ryan, Iliana, Justin, Eleftheria, Noemi, Yasir, Keith, Ho Yu, Leanne, Caroline, Josh, Tristan, Haider, Sarah, Sam, Yan, Maria Diaz, the medics (all of them) and the various students I had the joy and privilege of helping supervise. Especial thanks to Dr Muhammad Yasir for all his help during the cloning nightmare. It has been an honour to be part of the Webblings for 4 years. Especial thanks to Iliana and Agata (who may as well be a Webbling by now) for sharing this roller coaster journey together since our first dinner, and forever now.

To the QIB office gang, and especially Noemi, Claire (and the penguins), Alice, Steven, Gab and Oleksii, for making thesis writing much more fun (and noisy). To the Young Entrepreneurs Scheme (YES) *In-Ball Diagnostics®* team: Gloria, Federico, and Ari – what an amazing experience we had. To my Catalan microbiologists, Ari and Lluis, what a gift it has been to meet you here in Norwich and share jamón together. To the QIB sequencing team, especially Dave Baker and Rhiannon Evans; the bioimaging department, especially Kathryn Gotts and Dr James Lazenby for helping with the TEM and 3D-SIM work. Thank you to everyone at the

QIB Media kitchen for always helping us produce high-quality research with the best quality media.

To everyone I met during my placement at GAMA Healthcare Ltd. and during my AMS/MRC science policy internship at the Academy of Medical Sciences, thank you for welcoming me since the beginning. From GAMA – thank you to my industry supervisors James Clarke, Dr Maria Rubiano and Harsha Siani. A special thanks to Harsha for always believing in me, you are truly inspiring. Thank you to Giles Crowley for the chemistry lessons, and to Thomas Langford and Natalie Maguire for teaching me all about industry standards. Thank you to Katie, Jake, Louis, and my favourite undergrads (Eleanor, Harriet, Alex and Eren) because sharing the experience together made it so much better. From the Academy of Medical Sciences – thank you to the policy team, and special thanks to my supervisor Monica Dahiya for showing me what science policy really means. I really enjoyed both of these experiences!

To all the amazing scientists who I have been fortunate enough to meet along the way, from my undergraduate to my masters, thank you for helping me become a better scientist. Especially to Dr Juan-Carlos Jiménez-Castellanos for encouraging me to start a PhD.

To all the friends and flatmates that Norwich gave me, especially Georgie, Rik, and Rosie for the long night conversations in the sofa (and bad TV shows) during lockdown. To my Leamington Spa friends, it has been a joy to be closer to you again after all these years of living in different countries, and of course Leam would have never happened without you, Carlos – we miss you every day. To my friends from Catalunya, who are my family, and have always been a phone call away.

To my parents, because a simple dedication will never be enough, and to my grandpa for always being proud of my successes. I wish you could celebrate this one with me.

To Jesús, for being the best team from the beginning, and even more so at 10 hours' flight apart.

And last but not least, to me. In-between the good and the bad, the rainy days and the sunny ones, this has been a truly rewarding experience where not only have I grown as a researcher but also as a person.

Thank you everyone. Sometimes home can be another person (or people), thanks for being mine. Here is to 4 years full of adventures, challenges, and lifetime friendships. Norwich really is a fine city. On to the next chapter – "See you never!"

LIST OF PUBLICATIONS

List of publications arising from the project:

Darby, E. M., Trampari, E., Siasat, P., Gaya, M. S., Alav, I., Webber, M. A., Blair, J.M.A. 2023. Molecular mechanisms of antibiotic resistance revisited. *Nature Reviews Microbiology*, 21(5), 280–295.

Felgate, H. and Gaya, M.S., Sims, L., Bastkowski, S., Webber, M.A. (In Preparation). RNA Sequencing in staphylococci: commonalities and differences under biocide stress.

Gaya, M.S., Felgate, H., Siani, H., Whitchurch, C.B., Webber, M.A. 2024. FakA impacts antiseptic susceptibility in *Staphylococcus aureus* and *Enterococcus faecalis*. *bioRxiv.* https://doi.org/10.1101/2024.02.13.580087. (Submitted for publication).

Gaya, M.S., Felgate, H., Crowley, G., Rubiano, M., Clarke, M., Siani, H., Whitchurch, C.B., Webber, M.A. (In Preparation). Assessing bacterial adaptation to GAMA Healthcare's novel Clinell® proprietary formulation.

Gaya, M.S., Webber, M.A., GAMA Healthcare Ltd. (In Preparation). Technical performance evaluation of GAMA Healthcare's novel Clinell® proprietary formulation.

Invited talks and poster presentations:

ESCMID Global 2024, Barcelona (Spain) – Poster presentation

Microbiology Society Annual Conference 2024, Edinburgh (UK) – Oral presentation

BAMPS 2024, San Francisco (USA) – Poster presentation

Infection Prevention 2023, Liverpool (UK) – Poster presentation and Oral presentation

Microbiology Society Annual Conference 2023, Birmingham (UK) – Poster presentation

Medical Research Foundation National PhD Training Programme in AMR Annual conference 2023, Bristol (UK) – Poster presentation

Biennial Microbes in Norwich Symposium 2023, Norwich (UK) – Poster presentation (prize)

Understanding and Predicting Microbial Evolutionary Dynamics 2023, Manchester (UK) – Poster presentation

Microbiology Society Annual Conference 2022, Belfast (Ireland) – Poster presentation

BSAC Antimicrobial Resistance Workshop 2022, Birmingham (UK) – Poster presentation

TABLE OF CONTENTS

ABSTRACT ..... **ii**
DEDICATION ..... **iii**
ACKNOWLEDGEMENTS ..... **iv**
LIST OF PUBLICATIONS ..... **vi**
LIST OF FIGURES ..... **xiii**
LIST OF TABLES ..... **xvii**
LIST OF ABBREVIATIONS ..... **xviii**
CHAPTER 1: INTRODUCTION **1**
1.1. Healthcare-associated infections 2
1.1.1. Staphylococci and enterococci infections 3
1.2. Antimicrobial resistance 4
1.2.1. Introduction of antibiotics 4
1.2.2. AMR crisis: Post-antibiotic era 6
1.2.3. Antimicrobial stewardship and surveillance 8
1.2.4. Mechanisms of bacterial resistance to antibiotics 9
1.3. Infection Prevention and Control 11
1.4. Biofilms 14
1.4.1. Biofilm formation 14
1.4.2. Biofilms in healthcare settings 16
1.4.3. Biofilm control 17
1.5. Biocides 17
1.5.1. Classification of biocidal products 18
1.5.2. Biocides used in this project 18
1.6. Methods for testing biocide susceptibility 20
1.7. Mechanisms of bacterial tolerance/resistance to biocides 22
1.7.1. Mechanisms determining biocide susceptibility 25
1.8. The link between biocide and antibiotic resistance 26
1.9. Disinfectants and biosecurity in healthcare settings 28
1.10. COVID-19 impact on AMR and biocides 29
1.11. Gaps and limitations 29
1.12. Project aims and objectives 31
1.13. Hypothesis 31
CHAPTER 2: MATERIALS AND METHODS **32**
2.1. Bacterial strains 33

2.2. Media and growth conditions 34
2.3. Antimicrobial agents and other materials 34
2.3.1. Antibiotics 34
2.3.2. Biocides and formulations 34
2.3.3. Neutralizers 35
2.3.4. Stainless steel beads 35
2.4. Antimicrobial susceptibility testing 35
2.4.1. Minimum inhibitory concentration 35
2.4.2. Minimum bactericidal concentration 36
2.4.3. Minimum biofilm eradication concentration 37
2.5. Experimental microbial evolution 37
2.5.1. *In vitro* bead-based evolution model at the Quadram Institute Bioscience 37
2.5.2. Evolution experiments at GAMA Healthcare Ltd. 39
2.6. Phenotyping 40
2.6.1. Population sampling 40
2.6.2. Biofilm biomass production 41
2.6.3. Congo Red assay 41
2.6.4. Growth determination 42
2.7. Concentration dependent killing assays 42
2.8. Biocide efficacy testing at GAMA Healthcare Ltd. 43
2.9. *Galleria mellonella* infection model 44
2.10. Genotyping 45
2.11. Whole genome sequencing 45
2.11.1. DNA extractions 45
2.11.2. DNA quantification 47
2.11.3. Illumina NextSeq Short Read Sequencing 47
2.11.4. Nanopore MinION Long Read Sequencing 47
2.12. Bioinformatic Analysis 47
2.13. RNA sequencing 48
2.14. Characterisation of selected evolved isolates with FakA mutations 50
2.15. Attempts to create a defined *fakA* mutant 51
2.15.1. Plasmids 52
2.15.2. Restriction enzymes 52
2.15.3. Primers 52
2.15.4. Plasmid DNA purification 52
2.15.5. Polymerase chain reaction 53

2.15.6. Agarose gel electrophoresis 53
2.15.7. DNA extraction and purification 53
2.15.8. Restriction digests 54
2.15.9. Ligation and transformation 54
2.16. Data visualisation and statistical analysis 55
CHAPTER 3: IDENTIFICATION OF GENES IMPLICATED IN BIOCIDAL STRESS 57
3.1. Introduction 58
3.2. Aims 58
3.3. Results 59
3.3.1. The transcriptomic responses of *E. faecalis* and *S. aureus* when exposed to CHX, OCT and FM104 59
3.3.1.1. Gene expression changes in response to biocide exposure 61
3.3.1.2 Comparison of differentially expressed genes between *E. faecalis* and *S. aureus* 69
3.3.1.3. Relationship between stress responses in two clinical isolates 71
3.3.1.4. Functional pathway analysis 75
3.3.2. Similarities and differences in staphylococci exposed to CHX and OCT 80
3.4. Discussion 84
3.5. Conclusion 87
CHAPTER 4: *IN VITRO* BEAD-BASED BIOFILM EVOLUTION: OPTIMISATION AND NEWLY ESTABLISHED MODEL FOR STAPHYLOCOCCI AND ENTEROCOCCI 88
4.1. Introduction 89
4.2. Aims 90
4.3. Results 90
4.3.1. Test a panel of different staphylococci and enterococci isolates for baseline susceptibility and biofilm formation 90
4.3.2. Model optimisation 92
4.3.2.1. Bead preparation and contamination tests 92
4.3.2.2. Bead population capacity testing 92
4.3.2.3. Optimising use of the bead model to generate an effective population size 95
4.3.3. Further characterisation of the two selected isolates for susceptibility and virulence 105
4.3.4. *In vitro* bead-based evolution model for staphylococci and enterococci 108
4.3.4.1. Productivity of the evolved populations in the presence of biocides 108
4.4. Discussion 111
4.5. Conclusion 112

CHAPTER 5: PHENOTYPIC AND GENOTYPIC CHARACTERISATION OF THE BIOCIDE-EVOLVED ISOLATES 113

5.1. Introduction 114

5.2. Aims 114

5.3. Results 116

5.3.1. Phenotypic characterisation of the 308 evolved populations 116

5.3.1.1. Biofilm biomass production 116

5.3.1.2. Colony morphology of the evolved isolates 118

5.3.1.3. Fitness measurements of the WT and evolved populations 120

5.3.1.4. Studying the link between biocide tolerance and antibiotic cross-resistance 123

5.3.2. Genotyping 127

5.3.2.1. Characterization of the two parental clinical strains 127

5.3.2.2. Genotyping the selected evolved isolates 129

5.3. Discussion 134

5.4. Conclusion 135

CHAPTER 6: CHARACTERISATION OF FAKA AND ITS LINK WITH BIOCIDE TOLERANCE 137

6.1. Introduction 138

6.2. Aims 139

6.3. Results 140

6.3.1. Conserved regions and changes in FakA 140

6.3.2. Selection of *fakA* mutant isolates for further characterization 143

6.3.2.1. Susceptibility testing to assess cross-resistance to other antimicrobials in selected evolved isolates with *fakA* mutations 144

6.3.2.2. Other phenotyping tests in selected evolved isolates with *fakA* mutations 145

6.3.3. Construction of a *fakA* deletion mutant 150

6.4. Discussion 157

6.5. Conclusions 159

CHAPTER 7: STUDYING GAMA HEALTHCARE'S NOVEL CLINELL® PROPRIETARY FORMULATION 160

7.1. Introduction 161

7.2. Aims 163

7.3. Results 164

7.3.1. BS EN Standard testing with two Gram-positive isolates and a reference strain 164

7.3.2. Concentration dependent killing assays 165

7.3.3. MIC and MBC testing for biocides 166
7.3.4. Evolution experiment 171
7.3.5. Genotyping 174
7.3.6. Phenotyping 176
7.3.6.1. Biocide-antibiotic cross-resistance 176
7.3.6.2. Colony morphology of the evolved isolates 178
7.3.6.3. Growth curves 178
7.4. Discussion 180
7.5. Conclusions 182
CHAPTER 8: GENERAL DISCUSSION 183
8.1. General discussion 184
8.2. Concluding remarks 188
8.3. Future work 188
REFERENCES 190
APPENDICES 218
APPENDIX I: List of bacterial isolates used in the optimisation experiments 219
APPENDIX II: Standard Operating Procedure: *In vitro* bead-based biofilm evolution experiment for *Staphylococcus aureus* and *Enterococcus faecalis* 220
APPENDIX III: Calibration curves for *S. aureus* ST188 and *E. faecalis* ST40 232
APPENDIX IV: Primer list 233
APPENDIX V: Detailed PCR programmes used to construct Δ*fakA* mutants 234
APPENDIX VI: Calculation of the theoretical bead surface occupied by bacterial cells 235
APPENDIX VII: Survival of *E. faecalis* ST40 and *S. aureus* ST188 in the control condition 236
APPENDIX VIII: Wilcoxon-Mann-Whitney test to assess differences within conditions for each sample in *E. faecalis* isolates exposed to CHX 237
APPENDIX IX: Wilcoxon-Mann-Whitney test to assess differences within conditions for each sample in *E. faecalis* isolates exposed to OCT 238
APPENDIX X: Wilcoxon-Mann-Whitney test to assess differences within conditions for each sample in *S. aureus* isolates exposed to CHX 239
APPENDIX XI: Wilcoxon-Mann-Whitney test to assess differences within conditions for each sample in *S. aureus* isolates exposed to OCT 240
APPENDIX XII: Distribution of the MICs in *E. faecalis* ST40 evolved isolates 241
APPENDIX XIII: Distribution of the MICs in *S. aureus* ST188 evolved isolates 242
APPENDIX XIV: Summarised sequencing details for *S. aureus* ST188, *E. faecalis* ST40 and *S. aureus* NCTC 12973 243
APPENDIX XV: Ethidium bromide accumulation in isolates with *fakA* mutations previously exposed to biocides 244

APPENDIX XVI: Productivity of the control lineages 245

APPENDIX XVII: Summary of the SNPs in annotated and hypothetical genes from the evolution experiment at GAMA Healthcare Ltd. 246

LIST OF FIGURES

Figure 1.1. Molecular mechanisms of antibiotic resistance summarised. 10

Figure 1.2. Eight Infection prevention core components. 12

Figure 1.3. Biofilm development cycle. 15

Figure 2.1. Overview of the experimental design of the *in vitro* bead-based biofilm evolution model. 38

Figure 3.1. Multidimensional scaling plots (MDS) of (A) *E. faecalis* ST40 and (B) *S. aureus* ST188 RNA-Seq datasets coloured by stress. 60

Figure 3.2. Volcano plots showing feature counts of *E. faecalis* when exposed to ½ MIC of (A) CHX; (B) OCT; (C) FM104. 63

Figure 3.3. Volcano plots showing feature counts of *S. aureus* when exposed to ½ MIC of (A) CHX; (B) OCT; (C) FM104. 67

Figure 3.4. Stacked barplots showing the overall number of differentially expressed genes. 69

Figure 3.5. Heatmaps displaying all the significantly expressed (FDR < 0.05; LFC ≥ 2) genes for *E. faecalis* and *S. aureus* for the four tested conditions.). 70

Figure 3.6. Venn diagram showing the shared and unique number of DEGs for each condition and the overlap between stresses after 30-minute exposure. 71

Figure 3.7. Treemap indicating the names and sizes of GO biological processes for the upregulated genes shared between CHX-OCT in *E. faecalis* ST40. 72

Figure 3.8. Venn diagram showing the number of DEGs for each condition and the overlap between stresses after 30-minute exposure. 73

Figure 3.9. Treemap indicating the names and sizes of GO biological processes for the upregulated genes shared between all stresses (CHX-OCT-FM104) in *S. aureus* ST188. 74

Figure 3.10. Major biological processes upregulated in *E. faecalis* ST40 with significant enrichment of gene expression after exposure to (A) CHX, (B) OCT, (C) FM104. 76

Figure 3.11. Major biological processes upregulated in *S. aureus* ST188 with significant enrichment of gene expression after exposure to CHX. 77

Figure 3.12. Major biological processes (A) upregulated and (B) downregulated in *S. aureus* ST188 with significant enrichment of gene expression after exposure to OCT. 78

Figure 3.13. Major biological processes upregulated in *S. aureus* ST188 with significant enrichment of gene expression after exposure to FM104. 79

Figure 3.14. Stacked barplots showing the overall number of differentially expressed genes. 80

Figure 3.15. Venn diagrams showing the number of DEGs for each condition and the overlap between stresses after 30-minute exposure. 81
Figure 3.16. Genes significantly downregulated and upregulated on exposure to subinhibitory concentrations CHX and OCT across two or more *Staphylococcus* species..... 83
Figure 4.1. Comparison of planktonic growth of *S. aureus* NCTC 12973 with/without beads. 93
Figure 4.2. Test to measure bead size effect on bacterial colonisation. 94
Figure 4.3. Number of theoretical and observed *S. aureus* NCTC 13383 cells/bead. 95
Figure 4.4. Flow diagram showing the different optimisation experiments performed to increase the number of CFU of the biofilm and control condition in the evolution experiments. 96
Figure 4.5. Addition of different sera to the media for conditioned biofilms and planktonic conditions in *S. aureus* isolates 60 and 353. 99
Figure 4.6. Pre-conditioning bead surface model..... 100
Figure 4.7. Addition of sera 24 hours before inoculation in *S. aureus* isolate 60 (in blue) for the biofilm and planktonic state. 102
Figure 4.8. Test a panel of isolates with different biofilm forming activity..... 104
Figure 4.9. Colour change in *G. mellonella* model. 106
Figure 4.10. Kaplan-Meier survival plots from *G. mellonella* larvae infected with *S. aureus* ST188 and *E. faecalis* ST40. 107
Figure 4.11. Survival of *E. faecalis* (top panels) and *S. aureus* (bottom panels) after growth in increasing concentrations of CHX and OCT. 110
Figure 5.1. Schematic representation of the phenotypic and genotypic characterisation of biocide-tolerant mutants from the evolution experiment. 115
Figure 5.2. Biocide exposure had species-specific impacts on biomass production. 117
Figure 5.3. Colony morphology and ranking scores of *E. faecalis* and *S. aureus* on Congo red agar plates..... 118
Figure 5.4. Total distribution of Congo red intensity of the *E. faeca*lis evolved isolates. 119
Figure 5.5. Total distribution of Congo red intensity of the *S. aureus* evolved isolates..... 120
Figure 5.6. Growth curves of the WT isolates grown in TSB. 120
Figure 5.7. Relative growth of mutants isolated after antiseptic exposure. 122
Figure 5.8. Resistance profile of *E. faecalis* and *S. aureus* evolved isolates. 126
Figure 5.9. *De novo* hybrid assembly graphs from the WT genomes. 128

Figure 5.10. Phylogenetic trees from alignment of (A) *S. aureus* ST188 and (B) *E. faecalis* ST40 evolved isolates with the reference wild-type genomes. 130
Figure 5.11. Non-synonymous SNPs present in selected evolved *S. aureus* isolates. 131
Figure 5.12. Schematic representation of the gene environment for *fakA* and the homologous gene *dak2* in the two WT isolates. 132
Figure 5.13. Graphical overview of SNPs present in FakA/Dak2 domains recovered from both species for CHX and OCT stress. 133
Figure 6.1. Pathways for fatty acid biosynthesis in *S. aureus*. 138
Figure 6.2. Occurrence profiles of *fakA* (identified using the sequence from *S. aureus*) across genomes in the three kingdoms. 140
Figure 6.3. Sequence logo of FakA residues in (A) staphylococci excluding *S. aureus*; (B) related non-staphylococcal species using multiple sequence alignment data. 142
Figure 6.4. Heat maps of fold changes in (A) MIC and (B) MBC values (compared to the WT) against the two tested biocides (CHX/OCT) and daptomycin in MH. 144
Figure 6.5. Growth curves of the selected *E. faecalis* and *S. aureus* evolved isolates with *fakA* mutations (represented by dark lines), and the WT (indicated by dotted lines) grown in TSB. 145
Figure 6.6. Biofilm formation of the WTs and each selected evolved isolate with *fakA* mutation 146
Figure 6.7. Ethidium bromide accumulation assay with *E. faecalis* ST40. 147
Figure 6.8. Ethidium bromide accumulation is reduced in isolates with *fakA* mutations. 148
Figure 6.9. Biocide adapted FakA mutants exhibit increased mesosome formation. 149
Figure 6.10. Flow diagram summarising the construction of a *fakA* deletion mutant. 150
Figure 6.11. Schematic representation of both cloning strategies from Approach 1. 152
Figure 6.12. Agarose gel electrophoresis of pKOR1-mcs double digested with KpnI/ApaI (Vector 1) and SacI/XmaI (Vector 2). 152
Figure 6.13. Agarose gel electrophoresis of colony PCR products from both strategies. 153
Figure 6.14. Agarose gel electrophoresis of pKOR1-mcs vector digested with XmaI/ApaI, containing bot inserts. 155
Figure 6.15. Schematic representation of Approach 2. 156
Figure 6.16. Results from fusion PCR. 156
Figure 7.1. Efficacy testing for FM104 against *S. aureus* ST 188, *E. faecalis* ST40 and *E. hirae* NCTC 13383. 164

Figure 7.2. Productivity of planktonically evolved isolates for each stress. 173
Figure 7.3. Phylogenetic trees from alignments of the evolved isolates with the reference wild-type genomes. 175
Figure 7.4. Susceptibility profiles of the evolved isolates. 177
Figure 7.5. Congo red intensity of the WTs and the evolved samples. 178
Figure 7.6. Growth curves for the evolved isolates. 179
Figure 8.1. Proposed protocol to predict development of biocide tolerance/resistance and cross-resistance to antibiotics. 185
Figure A.III. Calibration curves for (A) *S. aureus* ST188 and (B) *E. faecalis* ST40. 231
Figure A.VI. Calculation of the theoretical bead surface occupied by bacterial cells. 234
Figure A.VII. Survival of (A) *E. faecalis* and (B) *S. aureus* in the control condition (no stress with beads). 235
Figure A.VIII. Biofilm biomass production in *E. faecalis* isolates exposed to CHX for (A) biofilm; (B) planktonic; (C) control (no stress). 236
Figure A.IX. Biofilm biomass production in *E. faecalis* isolates exposed to OCT for (A) biofilm; (B) planktonic; (C) control (no stress). 237
Figure A.X. Biofilm biomass production in *S. aureus* isolates exposed to CHX for (A) biofilm; (B) planktonic; (C) control (no stress). 238
Figure A.XI. Biofilm biomass production in *S. aureus* isolates exposed to OCT for (A) biofilm; (B) planktonic; (C) control (no stress). 239
Figure A.XII. Distribution of the MICs of 6 different antibiotics and 2 biocides against *E. faecalis* evolved isolates. 240
Figure A.XIII. Distribution of the MICs of 6 different antibiotics and 2 biocides against *S. aureus* evolved isolates. 241
Figure AXV. Ethidium bromide accumulation in isolates with *fakA* mutations previously exposed to biocides. 243
Figure A.XVI. Productivity of the control lineages. 244

LIST OF TABLES

Table 1.1. Selected cationic biocides and their application. 19

Table 1.2. Examples of definitions available in the literature for biocide resistance/tolerance. 24

Table 2.1. List of bacterial strains used. 33

Table 3.1. Selected hits from the volcano plots for *E. faecalis* ST40 under biocide stress. ... 64

Table 3.2. Selected hits from the volcano plots for *S. aureus* ST188 under biocide stress. .. 68

Table 4.1. Selected panel of 10 isolates. MIC of CHX and OCT, and biofilm forming ability (mean biofilm) included. 91

Table 4.2. Determination of the MIC, MBC and MBEC for CHX and OCT against the selected strains and control isolate in TSB/TSA media 105

Table 4.3. Number of generations of evolution completed for each stress in *S. aureus* ST188 and *E. faecalis* ST40. 108

Table 5.1. MICs for 6 different antibiotics and 2 biocides against *E. faecalis* ST40 determined in two different media: MH (in purple) and TSB (in green). 123

Table 5.2. MICs for 6 different antibiotics and 2 biocides against *S. aureus* ST188 determined in two different media: MH (in purple) and TSB (in green). 124

Table 5.3. Summary of the SNPs in annotated and hypothetical genes with known biological function from *E. faecalis* ST40 evolved isolates stressed with CHX and OCT. 132

Table 6.1. Selected *S. aureus* (SA) and *E. faecalis* (EF) evolved isolates with SNPs in *fakA*. 143

Table 7.1. Log_{10} CFU/mL reductions for *S. aureus* S188 and *E. faecalis* ST40 at different concentrations of CHX/OCT. 165

Table 7.2. MIC and MBC values of the tested agents against *S. aureus* ST 188, *E. faecalis* ST40 and *E. hirae* NCTC 13383. 168

Table A.I. List of bacterial isolates used in the optimisation experiments. 218

Table A.IV. Primers used to create Δ*fakA* mutants. 232

Table A.V. PCR programmes used in the cloning strategy (Step 1) to create Δ*fakA* mutants. 233

Table A.XIV. Summarised sequencing details for *S. aureus* ST188, *E. faecalis* ST40 and *S. aureus* NCTC 12973. 242

Table A.XVII. Summary of the SNPs in annotated and hypothetical genes in isolates evolved under different stresses (BZK+DDAC, FM104, Chassis). 245

LIST OF ABBREVIATIONS

ADAC	Alkyl dimethyl ammonium chloride
AMR	Antimicrobial resistance
AMU	Antimicrobial use
BPR	Biocidal product regulation
BZK	Benzalkonium chloride
CFU	Colony forming units
CHX	Chlorhexidine digluconate
CoNS	Coagulase-negative staphylococci
DEG	Differentially expressed genes
DDAC	Didecyldimethyl ammonium chloride
ECOFF	Epidemiological cut-off
ESPAUR	English surveillance programme for antimicrobial use and resistance
EUCAST	European committee on antimicrobial susceptibility testing
FM104	Novel formulation number 104
HAI	Hospital-associated infection
HCAI	Healthcare-associated infection
IPC	Infection prevention and control
LMIC	Low- and middle-income countries
MBC	Minimum bactericidal concentration
MBEC	Minimum biofilm eradication concentration
MDROs	Multidrug-resistant organisms
MIC	Minimum inhibitory concentration
NICU	Neonatal intensive care unit
OCT	Octenidine dihydrochloride
POE	Phenoxyethanol
QAC	Quaternary ammonium compound
SNP	Single nucleotide polymorphism
TEM	Transmission electron microscopy
WHO	World Health Organisation
WGS	Whole-genome sequencing

CHAPTER 1: INTRODUCTION

"Nothing in life is to be feared, it is only to be understood. Now is the time to understand more, so that we may fear less." – Marie Curie

1.1. Healthcare-associated infections

Healthcare-associated infections (HCAIs) affect people of all ages and can occur due to contact with a pathogen in a healthcare setting – care facilities, a patient's own house and hospitals – or medical interventions, where the infection is often directly linked to devices used in medical procedures (NICE, 2017, 2014).

HCAIs are a major concern in public health due to the clinical outcomes – patient discomfort, safety decrease, morbidity, and mortality increase – and associated healthcare costs (NICE, 2014; PHE, 2012). A wide range of factors can increase the risk of acquiring HCAIs such as: age, long hospital stays, immunocompromising conditions, invasive surgical procedures, and home wound management, among others (WHO, 2011). The impact is normally worst in hospitals due to the high-risk that these environments pose for the spread of infections (WHO, 2011).

Hospital-acquired infections (HAIs), occurring within 48 hours of a patient's admission to the hospital are alarming. According to the Centers for Disease Control and Prevention (CDC), the most common types of HAIs include central line-associated bloodstream infection, ventilator-associated pneumonia, catheter-associated urinary tract infections and surgical site infection. The increase in hospital stays associated to HAIs has an effect on environmental contamination; nosocomial pathogens can be found in the inanimate environment for a long period of time, which is directly linked to transmission of infection (Hu et al., 2015; Kramer et al., 2006). Due to the increase in antibiotic-resistant bacteria, HAIs are still one of the biggest causes of death worldwide.

Globally, the incidence of HCAIs is higher in low- and middle-income countries (LMICs), where healthcare settings have several limitations; 7 % of the patients in healthcare facilities have a risk of acquiring at least one HCAIs in high-income countries (HICs), compared to 10 % of the patients in LMICs (Allegranzi et al., 2011; WHO, 2011). The number of publications describing HCAIs worldwide has increased, however data is still missing from certain regions (Raoofi et al., 2023).

The last point prevalence survey (PPS-3) by the European Centre for Disease Prevention and Control (ECDC) analysed HCAIs and antimicrobial use in hospitals in 2022 - 2023. It was estimated that each year 4.3 million patients in the European Economic Area (EU/EEA) acquire a HCAIs, with *Escherichia coli*, *Klebsiella* spp., *Enterococcus* spp. being the microorganisms most frequently isolated (ECDC, 2024). Additionally, an increase in antimicrobial use compared to the PPS-2 in 2016-2017 (ECDC, 2023a) was seen.

In England, 834,000 HCAIs were estimated to occur between 2016 - 2017 within the National Health Service (NHS) which represented an economical cost for the NHS of £ 2.7 billion (Guest et al., 2020). The UKHSA (formerly known as Public Health England) is now leading an updated point-prevalence survey on HCAIs, antimicrobial use (AMU) and antimicrobial stewardship (AMS) to collect updated information since the last survey (2016-2017).

Despite infection prevention and control (IPC) strategies, multidrug resistant organisms (MDROs) are still present in healthcare settings and the burden of disease has remained difficult to reduce. The growth of Gram-positive and Gram-negative bacteria within biofilms in the environment, represents a major challenge in the treatment of HCAIs due to the difficulty in removing bacteria within a biofilm and their common tolerance to antimicrobials including biocidal agents (Percival et al., 2015).

1.1.1. Staphylococci and enterococci infections

In 2017, the World Health Organization (WHO) published a list of global bacterial priority pathogens (BPPL) (WHO, 2017), which has recently been updated (WHO, 2024). The catalogue initially included 12 families of bacteria (now expanded to 15 families) categorised by critical, high, and medium antibiotic resistance levels, for which new and effective antibiotics are required. All the pathogens in the critical category are Gram-negative bacteria. These are more difficult to kill due to the synergy between the outer membrane and the efflux machinery, a permeability barrier that impedes antibiotic entry and reduce intracellular concentration of antibiotics (Blair et al., 2015; Lewis, 2020; Mehla et al., 2021).

The focus of this project is on Gram-positive pathogens, which have been understudied in the recent years but as shown in the latest GRAM report (Murray et al., 2022), many resistant infections caused by Gram-positive organisms lead to high mortality rates. Particularly, we focus here on two common opportunistic pathogens: *Staphylococcus aureus* and *Enterococcus faecalis*, which are frequently reported in HCAIs in the EU/EEA (ECDC, 2023a): *S. aureus* were implicated in 11.6 % of HCAIs, *Enterococcu*s spp. in 9.8 %, and coagulase-negative staphylococci (CoNS) in 7.1 %. Among the CoNS group, *S. epidermidis* and *S. haemolyticus* are the most significant nosocomial pathogens (Becker et al., 2014).

S. aureus is a common coloniser of the human nasopharynx and skin, but also plays a role in disease. In fact, *S. aureus* was one of the six leading pathogens responsible for more than 250,000 deaths associated with AMR (after *E. coli,* the main causative agent). In HICs, *S.*

aureus was the main pathogen linked to half of the fatal AMR burden (more than *E. coli*), with methicillin-resistant *S. aureus* (MRSA) strains, currently listed as high-priority pathogen in the WHO BPPL, being responsible for more than 100,000 deaths attributable to resistance.

Biofilm formation on medical devices (Hegstad et al., 2010; Lee et al., 2019; Lister and Horswill, 2014; Percival et al., 2015) represents an important clinical problem. *S. aureus* and CoNS can adhere and form biofilms in medical devices causing catheter-associated urinary tract infections and prosthetic joint infections (Abraham and Jefferson, 2010). The risk of *S. aureus* infection is higher for patients that are in intensive care units, and in children in the neonatal intensive care units (NICU), where *S. aureus* and CoNS, are frequently associated with neonatal late onset sepsis (Felgate et al., 2023).

Enterococci are also commensal organisms which can also act as major opportunistic pathogens and one of the most frequent causes of HCAI, specially in intensive care units (García-Solache and Rice, 2019; Murray, 1990). Amongst enterococci, *Enterococcus faecalis* (80 - 90 % clinical isolates) and *E. faecium* (5 - 10 % clinical isolates) are the main causative agents of human infection, mainly causing urinary tract infections (Bonten et al., 2001; Moellering, 1992). *E. faecalis*, is also one of the six pathogens responsible for 100,000 - 250,000 deaths associated with AMR (Murray et al., 2022), and vancomycin-resistant *Enterococcus* (VRE) is listed as a high-priority pathogen in the WHO BPPL.

Given the impact of HCAIs and specifically the costs caused by AMR strains, there is a clear unmet need to control the global burden of AMR (NAO, 2000). Any new control measures will need to be effective against a range of pathogens including *S. aureus* and enterococci.

1.2. Antimicrobial resistance

1.2.1. Introduction of antibiotics

The introduction of antibiotics in clinical settings revolutionized medicine as it represented a solution for the treatment of many bacterial infections, leading to a decrease in mortality and morbidity (Walsh and Wright, 2005). Nonetheless, the golden era of antibiotics was short lived with most classes of current antibiotics discovered over 40 years ago (Lewis, 2020) followed by an increase in antibiotic resistance, due to the misuse of these compounds (Hutchings et al., 2019).

The problem of antibiotic resistance is escalating, with fewer antibiotics being discovered, although with some recent improvements in global clinical development (Laxminarayan et

al., 2020; Lewis, 2020; Theuretzbacher et al., 2020). Positively, since December 2022 there has been an increase in antibacterial drugs in the clinical pipeline, with 62 antibacterial candidates being investigated and a total of 26 phase-I candidates (Butler et al., 2023).

Recently possible new classes of antibiotics have been discovered. For example, using the power of artificial intelligence (AI) an antibiotic which exhibits activity against MRSA and VRE was discovered (Wong et al., 2023). In 2024, the promising discovery of zosurabalpin (Zampaloni et al., 2024), which is a novel class of macrocyclic antibiotics (Pahil et al., 2024), has recently entered human clinical trials showing activity against *Acinetobacter*, including Carbapenem-resistant *Acinetobacter baumannii*.

Additionally, traditional culturing methods, which do not allow the growth of uncultured bacteria, pose a scientific limitation to the process (Lewis, 2013). The invention of new discovery platforms can lead to the cultivation of uncultured organisms – a promising source for antibiotic discovery – and the screening of novel compounds. For example, the development of the *iChip* technology led to the discovery of a novel compound (teixobactin) from uncultured bacteria (Ling et al., 2015) that was active against tested Gram-positive bacteria. Other compounds like malacidins (Hover et al., 2018), amycobactin (Quigley et al., 2020) or the recent discovery of clovibactin (Shukla et al., 2023) are other examples of antibiotics with novel modes of action discovered from uncultured bacteria.

The discovery of more compounds is essential, especially against Gram-negative bacteria for which available treatments are already scarce (Jackson et al., 2018; Lewis, 2020). The challenging regulatory requirements and economic limitations in the research and development (R&D) area have both played a role in the antibiotic development pipeline decline (Payne et al., 2007). After the discovery of a new antibiotic, obtaining regulatory approval can delay the entry of the drug to the market; hence making the process non profitable for pharmaceutical industries. New funding strategies such as the subscription-type payment model (also known as “Netflix-style” model), which pays the manufacturers a fixed annual fee, was designed to incentivise pharma companies in investing in R&D (Leonard et al., 2023). In England, after the success of the NICE-NHS England pilot study (NICE, 2021) the model will now be expanded to the other UK devolved administrations. Additionally, targeted funding initiatives for R&D (e.g., CARB-X, INICATE, REPAIR Impact Fund, AMR Action Fund) can also attract investment and collaboration between different stakeholders.

Increasingly, much research is also focused on developing alternatives to antibiotics. Some examples of innovative treatments and/or technologies to combat antimicrobial resistance

include phage therapy, antimicrobial peptides (AMPs), or the new alternative antimicrobial polymers synthetically nanoengineered (SNAPS) (Laroque et al., 2023). Importantly, AI or other deep learning tools have accelerated the discovery or guide the design of AMPs (Boaro et al., 2023) by discovering novel peptides with antimicrobial activity in the human gut microbiome (Ma et al., 2022), or even by reintroducing AMPs from extinct organisms (Maasch et al., 2023). Interestingly, a search for 'ancientbiotics' in ancient remedies including Bald's eyesalve, which was effective against killing MRSA in a mouse chronic wound model (Harrison et al., 2015), and plant-based sources that also possess antimicrobial properties (e.g., garlic, medical-grade honey, vinegar) have also been studied (Harrison et al., 2023).

Other examples of alternative antimicrobial approaches include the use of genetic engineering (CRISPR), or faecal microbiota treatments that effectively decolonise the gut of AMR bacteria such as the FDA-approved and orally administered VOWST™ (by Seres Therapeutics and Nestle Health Science) to prevent *C. difficile* recurrent infections. It is important to highlight the burden of AMR is higher in LMICs (Nadimpalli et al., 2021), whilst the focus on novel approaches has mainly been explored in HICs, in LMICs there is still often insufficient access to antibiotics (Laxminarayan, 2022) or excessive/inappropriate use with over-the-counter sales of antibiotics being a problem.

Whilst development of new antibiotics or alternative anti-infective treatments is important, infection prevention and control approaches remain critical to control the burden of infection. This has become even more important due to the difficulty in treating infections caused by AMR bacteria.

1.2.2. AMR crisis: Post-antibiotic era

Humanity is now heading towards a post-antibiotic era in which there is a decrease in efficacy of antibiotics because of a rapid increase in the number of bacteria able to resist multiple antibiotics, including those needed to treat serious infections.

AMR represents one of the greatest global health threats and was declared in 2019 by the WHO as one of the top 10 biggest global public health threats. According to the O'Neill report (2016), the number of global deaths per year attributed to infections caused by drug-resistant bacteria could increase from 700,000 to 10 million by 2050. More recently, the Global Research on AntiMicrobial resistance (GRAM) report estimated higher numbers: around five million deaths were associated with AMR in 2019, with 1.27 million deaths of those were

directly attributable to resistance (Murray et al., 2022). The highest burden from AMR is estimated to be in Sub-Saharan Africa. Six MDROs were the causative agents of most deaths: *Escherichia coli*, *Staphylococcus aureus*, *Klebsiella pneumoniae*, *Streptococcus pneumoniae*, *Acinetobacter baumannnii* and *Pseudomonas aeruginosa.* Regarding distribution of pathogens in different countries, *S. aureus* and *E. coli* accounted for most of the deaths in HICs whereas *S. pneumoniae* and *K. pneumoniae* contributed to the highest numbers in Sub-Saharan Africa.

In England, the English Surveillance Programme for Antimicrobial Use and Resistance (ESPAUR) collected data on antimicrobial use and resistance patterns. Data for 2019-2020 (PHE, 2020) showed a small decrease in the number of antibiotic resistant infections between 2015 and 2019. AMR infections were mostly driven by the key resistant pathogens: *E. coli, K. pneumoniae, K. oxytoca*, *Acinetobacter spp*., *Pseudomonas spp*., *Enterococcus spp*., *S. aureus* and *S. pneumoniae*. However, the incidence of bloodstream infections (BSI) caused by key resistant pathogens increased from 2015 to 2019 with *E. coli* remaining the main cause (32.5 %) of sepsis in England, followed by *S. aureus*. Whilst overall levels of AMR in this study did not increase, there was variation by pathogen and drug with an increased incidence of Gram-negative bacteria resistant to quinolones and third-generation cephalosporins. Regarding Gram-positive infections, the incidence of infections caused by *S. aureus* increased by 14 %, from 20.5 per 100,000 population in 2015, to 23.5 per 100,000 population in 2019. This included a change in the nature of strains causing infections with a decline in methicillin-resistant isolates seen by 2019 where only 6 % of BSI isolates were MRSA.

To try and reduce selection for AMR, stricter policies on antibiotic usage have been implemented in many settings. Antibiotic consumption rates in England decreased between 2014 to 2019 from 19.4 to 17.9 defined daily doses (DDDs) per 1,000 inhabitants per day. However, despite this overall reduction the use of antibiotics in healthcare settings, especially in hospitals, increased by 3.5 % over the last 5 years (PHE, 2020).

Most recent data has illustrated the impact of the Coronavirus disease 2019 (COVID-19) pandemic where the percentage of isolates which were antibiotic resistant increased although total numbers of bacteria isolated decreased (UKHSA, 2022, 2021). There was a reduced incidence between 2019 - 2020 of bloodstream infections (BSIs), as less procedures in patients were performed due to the COVID-19 pandemic, however the use of broad-spectrum antibacterials for respiratory infections in primary and secondary care increased due to the risk of bacterial superinfection in these patients (Andrews et al., 2021). The latest

ESPAUR report (2022 - 2023) published in 2023 (UKHSA, 2023), shows antibiotic use and rates of priority pathogens returning to the pre-pandemic health situation.

As well as the costs to health, MDROs represent a threat to the global economy as it is predicted that AMR infections will cost £66 trillion in lost productivity by 2050 (O'Neill, 2016). The World Bank has estimated that by 2050 the global annual GDP loss could range from 1.1 % to 3.8 %, and the additional healthcare costs needed to combat MDROs would reach to $US 1 trillion (World Bank, 2017). In EU/EEA countries infections caused by MDROs now cost 1.1€ billion per year to healthcare and societal costs as estimated by the Organisation for Economic Co-operation and Development (OECD, 2022).

The burden from MDROs is considered a One Health challenge as it not only affects the health of people but also animals and crop health, where costs in lost production and treatment are also significant (Larsson et al., 2023; Robinson et al., 2016; Spagnolo et al., 2021). The spread of AMR is now restricted by national boundaries and has been accelerating due to different factors – globalization of human travel, changes to our food system, poor sanitation practices, and uncontrolled antimicrobial use – which facilitates the emergence of new resistance strains (Robinson et al., 2016).

1.2.3. Antimicrobial stewardship and surveillance

A coordinated response between different sectors – a One Health approach – is required to prevent and/or reduce the development and transmission of AMR (Van Belkum et al., 2019). Antimicrobial stewardship and surveillance approaches aim to monitor and promote responsible use of antimicrobials.

International and national institutions are already implementing various initiatives. For example, the United Nations Inter-Agency Coordination Group (IACG) on AMR – a tripartite collaboration between the WHO, the Food and Agriculture Organization and the World Organization for Animal Health – launched a global action plan on Antimicrobial Resistance (WHO, 2015) at a national, regional, and global levels. Additionally, the Global Leaders Group, a cross-sector group focused on antimicrobial resistance, has also established an action plan to address AMR.

Globally, the WHO introduced a new index for antibiotic stewardship in 2017 (and updated in 2019 and 2021) known as the Access, Watch, Reserve (AWaRe) classification. This tool categorizes antibiotics into 3 categories to monitor antimicrobial consumption (AMC) and

promote antibiotic stewardship and reduce AMR (WHO, 2019a). The target is to reduce the use of Watch and Reserve antibiotics, aiming to reach at least 60 % of antibiotic consumption to come from the Access group by 2023. Furthermore, the WHO also launched the Global Antimicrobial Resistance and Use Surveillance System (GLASS) in 2015 to collect AMR data, including antibiotic consumption, and standardise surveillance data. The latest report (WHO, 2022a), shows that only 65 % of the reporting countries have achieved the AWaRe-target so far.

European antimicrobial resistance surveillance networks, such as European Surveillance of Antimicrobial Consumption Network (ESAC-Net) and the European Antimicrobial Resistance Surveillance Network (EARS-Net), along with the Central Asian and European Surveillance on Antimicrobial Resistance (CESAR) network, provide data on AMC. According to the latest ESAC-Net report, the overall AMC had reduced between 2013-2022 in EUU/EEA (ECDC, 2023b). However, there were significant increases in AMC of broad-spectrum and last-line antibiotics during the COVID-19 pandemic.

In the UK, a series of five-year national action plans (NAP) have been implemented to achieve a 20-year Vision to effectively contain and control AMR by 2040 (DHSC, 2019a). The 2019-2024 NAP (DHSC, 2019b) achieved several milestones, including reductions in antibiotic use in food-producing animals, strengthening in surveillance systems, and establishment an NHS "Netflix-style" payment model for antibiotics. The updated 2024-2029 NAP (DHSC, 2024) expands on previous actions. Additionally, resources like the Treat Antibiotics Responsibly (TARGET) toolkit, which focuses on reducing AMU (DHSC, 2019b), are other national initiatives being implemented.

Better stewardship measures are needed to control the emergence and spread of MDROs, (Frieri et al., 2017; Velez and Sloand, 2016). Given the difficulty in therapeutic options, prevention becomes critically important. The implementation of IPC measures – like the use of biocides – is a viable option to prevent antibiotic-resistant strains in healthcare settings (Mc Carlie et al., 2020).

1.2.4. Mechanisms of bacterial resistance to antibiotics

Resistance to antimicrobial agents readily evolves in response to selective pressures exerted by antibiotics (Lewis, 2020). This leads to the survival of bacteria with an innate resistance phenotype or those that have acquired resistance genes via horizontal gene transfer or

gained beneficial mutations (Darby et al., 2023). There are different mechanisms of antibiotic resistance (**Figure 1.1.**), which can be grouped into three main categories: (1) prevention of antibiotic accumulation, (2) modification of drug targets and (3) drug modification or inactivation.

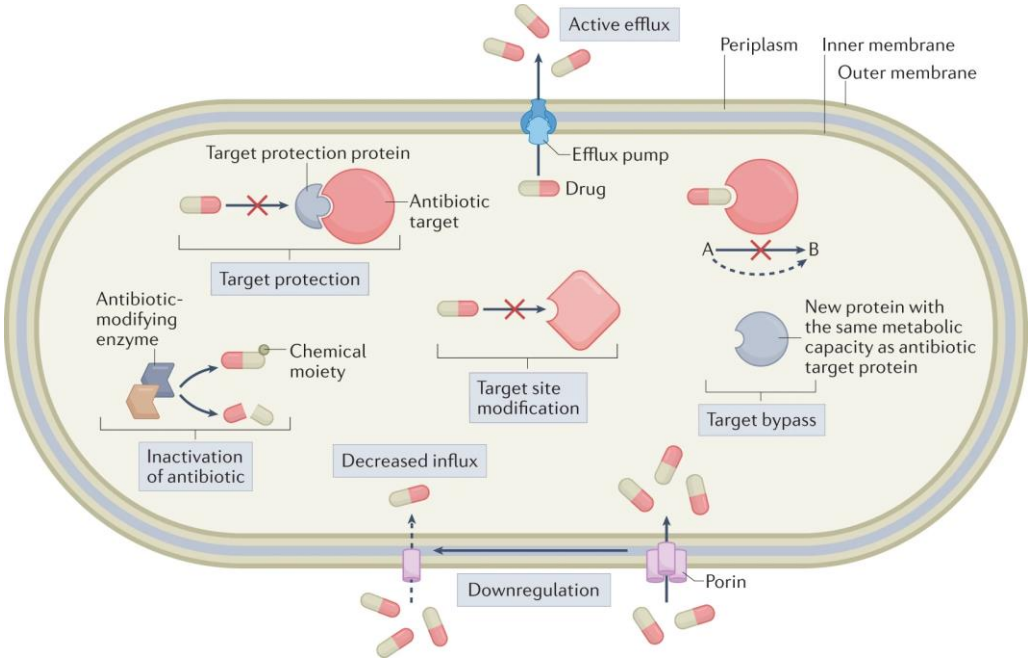

Figure 1.1. Molecular mechanisms of antibiotic resistance summarised. An overview of the various mechanisms by which bacteria resist antibiotics. From Darby et al. (2023).

(1) Prevention of antibiotic accumulation: Bacteria can prevent and decrease the concentration of drugs in the intracellular bacterial compartment by the downregulation of porins (decreased influx) and/or upregulation of efflux pumps (active efflux), which both (and often synergistically) reduce accumulation of antibiotics at their target sites.

As an example of active efflux of antibiotics, efflux pumps from the resistance-nodulation-division (RND) family are common examples that contribute to resistance in clinically relevant Gram-negative pathogens (Alav et al., 2021). In Gram-positives pathogens such as *S. aureus*, overexpression of the NorA efflux pump, from the major facilitator superfamily (MFS), confers resistance to many antibiotics (e.g., ciprofloxacin) (Neyfakh et al., 1993).

(2) Modification of drug targets: In order to avoid an antibiotic binding to its target, bacteria can change the target structure by mutation of the gene encoding the target, or by enzymatic action to decorate the target (target site modification). Target bypass, where an

alternative pathway is produced making the original drug target redundant, is another mechanism of resistance.

A well-known example of bypass is the development of MRSA (Stapleton and Taylor, 2002). β-Lactam antibiotics (e.g., methicillin), bind to penicillin-binding proteins (PBPs) and inhibit the transpeptidase domain, leading to disruption of the cell wall synthesis. *S. aureus* can acquire an exogenous PBP (PBP2a) that is homologous to the original target but with lower affinity for β-lactam antibiotics. When methicillin binds to this alternative target site, inhibition of cell wall synthesis is prevented as the transpeptidase activity of PBP2a is maintained, and *S. aureus* can bypass the action of methicillin ensuring cell survival.

(3) Drug modification or inactivation: Bacteria can also resist the action of antibiotics by directly modifying (or inactivating) these drugs through hydrolysis or addition of chemical groups (inactivation of antibiotic).

For example, the addition of phosphate-containing groups (by nucleotidyltransferases) can modify lincosamide antibiotics widely used to treat staphylococci infections. The gene *lnu(A)*, which encodes for a lincosamide nucleotidyltransferase, is a plasmid-located gene that confers resistance to these antibiotics by the transfer of a chemical group. This gene has been described in *S. aureus* and CoNS (Feßler et al., 2018), and a related gene, *lnu(G),* located in a transposon, has recently been identified in *E. faecalis* (Zhu et al., 2017).

1.3. Infection Prevention and Control

IPC strategies are practical solutions to stop, reduce or prevent the spread of infections in healthcare settings (PHE, 2012). IPC is linked to patient safety and quality universal health coverage; and plays an essential role in preventing and reducing the rates of infections and addressing the challenge of AMR (NICE, 2014; PHE, 2012).

The WHO developed a list of recommendations (WHO, 2016) which include eight core components for effective IPC standards (**Figure 1.2.**).

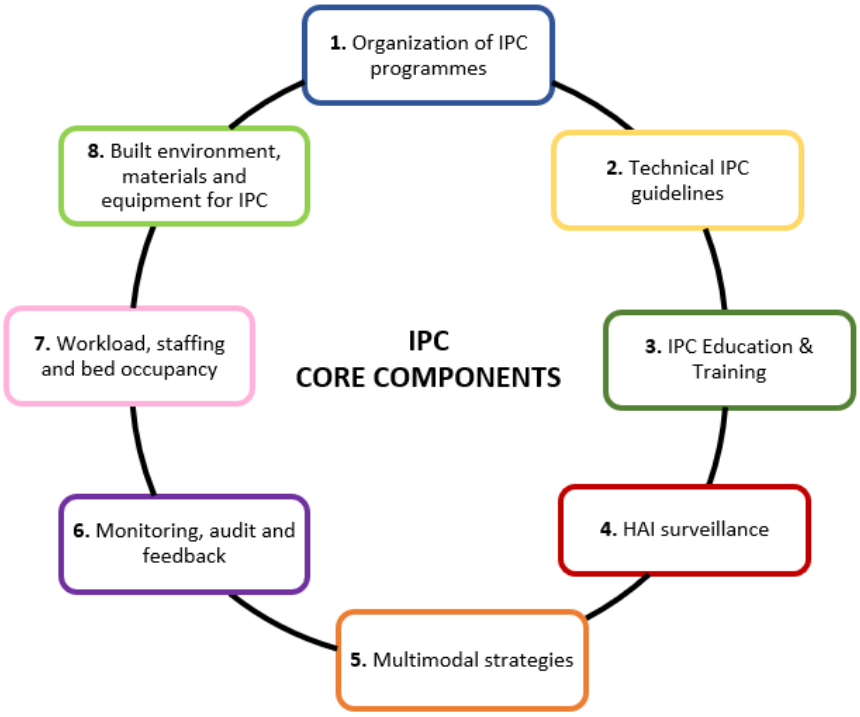

Figure 1.2. Eight Infection prevention core components. The circular flow diagram represents the 8 IPC components developed by the WHO for effective IPC programmes globally.

The first core component focuses on the organization of IPC programmes, which should also support the Global Action Plan on Antimicrobial Resistance (WHO, 2015). The second and third core component recommend the implementation of IPC guidelines as well as training to essential healthcare workers. For example, evidence on how training has reduced environmental contamination has been shown in several examples (Siani and Maillard, 2015). The fourth core component implements HAI surveillance programs, including AMR, to detect potential outbreaks. Some examples of surveillance networks include the HAI-Network (in the EU) and the Nosocomial Infection National Surveillance Scheme (in the UK), which are essential components of IPC programmes. Multimodal interventions, which include a variety of cross-organizational changes, constitute the fifth core component. The sixth component aims to periodically audit, monitor, and give feedback in order to modify quality care and practices. The last two core components are good practice statements recommended for acute health care facilities only.

Despite this proposed set of activities, implementation of the IPC core components is not the same in different countries, due to differences in their capacities. For this reason, the WHO

stated “the IPC minimum requirements” (WHO, 2019b) from these core components, implemented in a five-step cycle approach which should guarantee a better progress towards implementing all the core components. In May 2022, the WHO issued the first global report on IPC which provided a situation analysis of IPC programmes and activities worldwide (WHO, 2022b) and highlighted the importance of implementing IPC programmes to not only control the burden of HAI and AMR but work towards global health security and Sustainable Development Goals (SDGs) (Ferdinand et al., 2023).

Implementing these IPC core components in healthcare facilities and at a national level will help control priority infections and lead to a reduction of HCAIs and AMR. In the UK, the five-year AMR National Action Plan will also implement different IPC strategies to control infections (DHSC, 2019b), and there are already national evidence-based guidelines (Loveday et al., 2014) to prevent HCAIs and to have effective IPC protocols in place. More specifically, AMS, hand hygiene and environmental cleanliness were identified as key areas to combat HCAIs.

Environmental hygiene is essential to reduce the number of microorganisms that usually reside on surfaces (Boyce, 2007). Pathogens can persist on surfaces for a long time (Kramer et al., 2006) and contribute to the spread of infections. Surface contamination has been linked to HCAI especially from microorganisms that are able to persist on hospital surfaces where transmission can then be mediated by healthcare workers (Siani and Maillard, 2015). Surface disinfection of noncritical surfaces and patient items also needs to be considered in IPC practices (Rutala and Weber, 2004).

Effective cleaning and disinfection protocols can reduce contamination in the environment and consequently minimize the incidence of HAIs (Carling and Bartley, 2010). Cleaning removes visible inorganic or organic substances from surfaces or devices either manually or mechanically; it is essential to perform before disinfection (BICSs, 2020). A disinfection process eliminates most of the pathogenic microorganisms on inanimate objects, with varying levels of sporicidal activity (Spaulding et al., 1968). Choosing the best practice is essential in reducing HCAI (Siani and Maillard, 2015).

Biocides are widely used as disinfectants to control microorganisms and prevent transmission (Further information in **Chapter 1**, **Section 1.5.**). In the UK hospitals and other healthcare facilities, different cleaning programs and disinfectant agents (e.g., quaternary ammonium compounds, hydrogen peroxide, alcohol-based solutions and chlorine products) are available

to clean and disinfect equipment, patient-care supplies or surfaces (BICSs, 2020). The choice of agent depends on the location, materials as well as cost and ease of applications.

Despite the IPC strategies and surveillance programmes available, MDROs are still present in healthcare settings (Hu et al., 2015). Bacterial growth within biofilms represents an additional difficulty in the treatment of HCAIs due to the increased resistance of biofilms to antimicrobials (Percival et al., 2015). Prevention and control of biofilms is also an important aspect of IPC.

1.4. Biofilms

Bacteria can experience planktonic – single cells in suspension – or biofilm lifestyles. Biofilm is the usual mode of growth for many bacteria (Flemming et al., 2016). Biofilms are very important in IPS as they allow organisms to persist in the hospital environment and are also often tolerant to disinfection.

A biofilm is a consortium of microorganisms that grow in an aggregated community within an extracellular matrix (Costerton et al., 1995; Mack et al., 1975; Vickery et al., 2012). The extracellular polymeric substance (EPS) matrix is mainly formed by polysaccharides, but it can also comprise proteins, lipids, and extracellular DNA (eDNA) which is essential for biofilm formation (Whitchurch et al., 2002). This EPS confers several advantages to the cells within the biofilms, such as increased persistence in the environment and its compositions varies with species and conditions (Galié et al., 2018).

1.4.1. Biofilm formation

Different factors – opportunity, starvation, temperature, pH, desiccation, stresses including exposure to antimicrobials – act as triggers leading to the formation of biofilms from planktonic cells (Cândido et al., 2019; Percival et al., 2015). Five main stages (**Figure 1.3.**) are involved in the development of a biofilm: (1) single-cell attachment to the surface, (2) formation of a monolayer and EPS matrix production, (3) microcolony multi-layer formation and (4) formation of mature biofilms. At the end of the cycle, (5) dispersion of the cells can reverse to a planktonic state (Costerton et al., 1987). In the transition from planktonic cells to mature biofilms, cells will also undergo morphological and physiological alterations, as well as gene/protein expression changes (Costerton et al., 1987). Cell expression and

communication within the biofilm is regulated by quorum sensing, a phenomenon that has been a common target for antibiofilm therapies (Roy et al., 2018).

Biofilm formation is not always dependant on surfaces (Sønderholm et al., 2017). For instance, in the biofilm lifestyle, two types of cells are commonly found: surface-attached aggregates – cells that are attached to a surface – and suspended aggregates – bacteria that are attached to other cells (Alhede et al., 2011; Flemming et al., 2016). Surface attached biofilms have an increase tolerance to antibiotics than the same bacteria in a planktonic form (Alhede et al., 2011). Persister cells – found in a dormant state and common within biofilms – have increase antibiotic tolerance (Conlon et al., 2015; Dewachter et al., 2019).

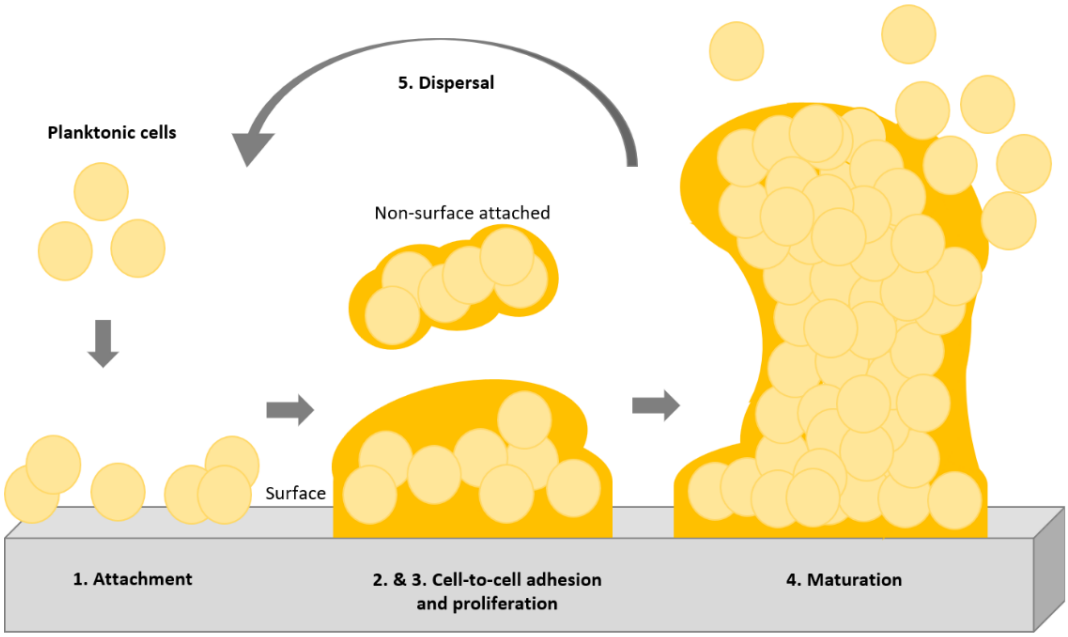

Figure 1.3. Biofilm development cycle. The five main stages involved in biofilm development include: (1) attachment (on the surface or non-surface attached), (2) cell-to-cell adhesion, (3) proliferation, (4) maturation and (5) dispersal. Cycle representative of cocci-shaped bacteria.

Depending on the presence of bacterial species, biofilms can be classified as: monospecies where only one species makes up the biofilm, or polymicrobial where the biofilm is formed by multiple species that interact with each other. Multispecies biofilms are commonly found in the environment. The interactions between species in a biofilm can have several advantages when compared to mono-species biofilms (Bridier et al., 2012; Galié et al., 2018) such as increased resistance to biocides since biofilms can act as protective cacoons against these agents (Charron et al., 2023). This poses a negative impact on disinfection processes

(Hu et al., 2015). Nonetheless, many *in vitro* studies are based on mono-species biofilms, which are less variable and hence easier to analyse (Alfa, 2019).

1.4.2. Biofilms in healthcare settings

Biofilms are a problem in healthcare settings. According to the National Institutes of Health (NIH), 80% of all bacterial infections in humans possess a biofilm component (NIH, 2002). *In vivo*, suspended cell aggregates are often responsible for chronic infections of wounds or indwelling devices (Alhede et al., 2011; Percival et al., 2015; Vickery et al., 2012).

Bacteria can grow as a biofilm on biomedical devices such as tracheal tubes, orthopaedic implants, catheters, or endoscopes (Donlan and Costerton, 2002; Percival et al., 2015). In this case, microorganisms grown in an aqueous/moisture environment on a biofilm are known as "wet biofilms" (Almatroudi et al., 2015; Ledwoch et al., 2018). The percentage of HCAIs associated with "wet biofilms" is around 65 % (Percival et al., 2014). In 2021, biofilms were also observed to be present within the hospital environment on dried surfaces (Almatroudi et al., 2015; Vickery et al., 2012) in what are known as "dry surface biofilms" (DSB) (Almatroudi et al., 2015), although no official definition is yet available (Maillard and Centeleghe, 2023). Regardless of the discovery of the presence of dry surface biofilms on a variety of surfaces in hospitals (Alfa, 2019; Ledwoch et al., 2018; Vickery et al., 2012) most studies have focused on wet or hydrated biofilms.

One study showed that than 90 % of the ICU surfaces had bacteria in a biofilm form (Hu et al., 2015). Recently, a study with dual species dry surface biofilm (DSB) showed that environmental species were still present on surfaces even after the disinfection treatment (Centeleghe et al., 2022). More research is essential to determine the role of dry surfaces biofilms in HCAIs. Additionally, there have been different calls for consistency and biofilm standardisation (NBIC, 2023).

Due to the high prevalence of biofilms in healthcare settings surfaces and their formation on medical devices and other critical points (Percival et al., 2015), biofilm prevention and control strategies are of vital importance.

1.4.3. Biofilm control

Bacteria within a biofilm typically have a higher survival rate than bacteria that grow in a planktonic form when exposed to antimicrobials. For example, a study suggested that the quantity of disinfectants (such as QACs and CHX) needed to kill planktonic *Salmonella* is less than the amount required to kill biofilms (Wong et al., 2010). Similarly, this was observed with common hospital biocides against planktonic and biofilms forms of MRSA and *P. aeruginosa* (Smith and Hunter, 2008).

Different parameters need to be considered in IPC practices to account for biofilm control and when applying different cleaning and disinfectant practices (Maillard and Centeleghe, 2023). Stronger cleaning and disinfectant practices are often required to provide biofilm control. Besides selection of biocides, considering the physicochemical characteristics of the medical devices or the surfaces to be treated is also essential to balance the need for efficacy without degrading the surface (Percival et al., 2015).

1.5. Biocides

Biocides are active chemical or biological agents (McDonnell and Russell, 1999) used as antimicrobials to control pathogens – virus, bacteria and fungi – and prevent transmission of infections (Mc Carlie et al., 2020).

Biocides might also be combined with other excipients in a product (biocidal product) to increase the overall effectiveness. The components of these formulations play a role in the efficacy of the biocide (Maillard, 2018) but also pose potential disadvantages (Weber et al., 2019) such as the ecological risks, or safety/toxicity-related issues risks for highly exposed populations such as healthcare personnel. In fact, during COVID-19 the number of adverse health effects of exposures from cleaning and disinfectants in healthcare workers increased (Rosenman et al., 2021), as well the increase exposure to QACs indoors has also been reported (Zheng et al., 2020). Nonetheless, biocides are key in preventing HCAIs and the benefits are greater than the disadvantages (Rutala and Weber, 2004).

The appearance of biocide tolerance/resistance represents a potential concern. Several factors like concentration, temperature, pH, contact time, or the presence of other organic materials (known was Interfering materials) can affect biocide performance (Maillard and Pascoe, 2024), and need to be taken into consideration. Resistance to biocides is higher in

biofilms than in the planktonic form (Fux et al., 2005); hence the concentration of biocides required to remove biofilms is often higher (Vickery et al., 2012).

Residual concentrations of the biocides which could be deposited on healthcare surfaces also need to be considered (Edwards et al., 2020). Example of re-contamination after using the same wipe was shown to increase transmission of infections hospital environments (Edwards et al., 2020). Therefore, it is of vital importance that biocides and biocidal products are correctly regulated to meet health and quality standards (Mc Carlie et al., 2020) in order to increase effectiveness and avoid contributing to outbreaks associated with inappropriate use or contaminated disinfectants and antiseptics (Weber et al., 2007).

1.5.1. Classification of biocidal products

According to the European Chemicals Agency (ECHA), biocidal products are classified in the Biocidal Products Regulations (BPR, Regulation (EU) 528/2012) into 22 types and 4 main areas: disinfectants, preservatives, pest control and other biocidal products. Regarding the main group 1, these can be used as skin antiseptics for human hygiene (Product Type 1), or as disinfectants to destroy microorganisms on non-living objects (Product Type 2) in several areas (e.g., surfaces, patient instruments).

Disinfectants were classified for the first time by E.H. Spaulding in three categories: high-level, medium-level and low-level disinfectants, according to their level of effectiveness against microorganisms (Russell, 1999; Spaulding et al., 1968). Disinfectants from the high-level category inactivate all microorganisms except high numbers of bacterial spores (Weber et al., 2019).

1.5.2. Biocides used in this project

There are multiple classes of biocides, with specific modes of action and several applications (Maillard and Pascoe, 2024), these include: alkylating agents, oxidising agents, cationics, phenolics, alcohols, weak organic acids, metal ions, antimicrobial dyes.

In this project, cationic biocides were used. This class of biocides, which are positively charged, interact with the negatively charged membrane leading to reduction in membrane fluidity, lysis and eventually cell death (Fox et al., 2022; McDonnell and Russell, 1999;

Sommers et al., 2022). Among these biocides, quaternary ammonium compounds (QACs) and biguanides (**Table 1.1.**) were selected.

Table 1.1. Selected cationic biocides and their application.

Name	Abbreviation	Application
Quaternary ammonium compounds (QACs)		
Benzalkonium chloride or Alkyl Dimethylbenzyl ammonium chloride	BZK, BKC, BAK, BAC or ADBAC	Food industry, healthcare settings (surface, skin and wound care, hand disinfection), household cleaning
Didecyldimethyl ammonium chloride	DDAC	Agriculture, healthcare settings, industrial settings
Alkyl dimethyl ammonium chloride	ADAC	Food industry, healthcare settings, household cleaning
Biguanides		
Chlorhexidine digluconate	CHX, CHG	Skin antiseptic, hand hygiene, oral and wound care
Octenidine dihydrochloride	OCT	Skin antiseptic, surface disinfection, wound care

Quaternary ammonium compounds

QACs were firstly introduced in 1935, and have been widely used in the food industry, medical environments, among other applications (Arnold et al., 2023; Boyce, 2023). QACs have also been incorporated into textiles conferring these materials with antimicrobial properties (Morais et al., 2016).

BZK is a nitrogen-based QAC, widely used in hospitals for surface, and hand disinfection (Pereira and Tagkopoulos, 2019), with many controversies in safety studies. Especially used in food industry to disinfect surfaces, where bacteria that can survive disinfectant practises are a main problem for food spoilage. DDAC is a water-soluble QAC, used for many applications and with a strong initial absorption to cell wall (Ioannou et al., 2007). Nonetheless, it can cause eye and skin irritation after topical application (Anderson et al.,

2016). ADAC is similar to DDAC, but with differences in the alkyl chain length (chains ranging from C12 to C16, while DDAC has C10 alkyl chains).

Biguanides

CHX and OCT represent different compound classes – biguanide and bispyridine respectively – and both have a similar mode of action (membrane disruption) although with different effects on the membrane as recently elucidated (Kholina et al., 2020; Malanovic et al., 2022; Rzycki et al., 2021; Waller et al., 2023).

CHX is one of the most used antiseptics for wound dressings, hand hygiene and in oral care (Jones and Joshi, 2021; Lim and Kam, 2008). It is also listed in the WHO essential medicine list to be used during pregnancy and childbirth and marketed as a general disinfectant. CHX has residual antimicrobial activity when applied in inanimate surfaces or skin (Rutter et al., 2014). Some studies have shown that CHX shows cytotoxicity activity *in vitro* in different cell types (Waller et al., 2023), and side effects *in vivo* such as allergic reactions (Chiewchalermsri et al., 2020), or oral mucosal lesions (Plantinga et al., 2016). Less is known about the effect of chlorhexidine as a gel for nasal applications.

OCT also has broad spectrum activity against Gram-positive and Gram-negative bacteria and a long-term effect after disinfection (Köck et al., 2023). Similarly to CHX, OCT is commonly used as a skin antiseptic and wounds thanks to its activity on a broad pH range and lower cytotoxicity (Hübner et al., 2010; Seiser et al., 2021). The effectiveness of OCT as a body wash in reducing HCAIs has been shown (Messler et al., 2019).

Assessing resistance to cationic compounds in more realistic context is needed (Fox et al., 2022). The use of biocides or biocidal products in hospitals, pharmaceutical industry, farms, home and in other settings like food industry (Fraise, 1999; Vijayakumar and Sandle, 2019; Webber et al., 2015) is an important part of infection prevention and control measures. For this project, we are interested in the use of biocides as surface disinfectants.

1.6. Methods for testing biocide susceptibility

The Biocidal Products Regulation (BPR, Regulation (EU) 528/2012) requires information on the risk of resistance, cross-resistance or tolerance development in organisms targeted by the biocidal product. However, there is no currently agreed standard protocol available to

predict the likelihood of bacteria becoming resistant to a biocidal product. The BPR and the Food and Drug Administration (FDA) do not stipulate standard tests or protocols, but rather recommendations, to predict the mechanisms of biocide resistance and cross-resistance to antibiotics. Although different expert groups and agencies such as the French Agency for Food, Environmental and Occupational Health & Safety (ANSES) are leading the review and guidance on this topic.

Minimum inhibitory concentration (MIC) and minimum bactericidal concentration (MBC) assays are used to test for microbial susceptibility to biocides (McDonnell and Russell, 1999; Wu et al., 2015). Nonetheless, there are no defined breakpoints for biocides. Another more time-consuming *in vitro* method to measure bacterial resistance to biocides could be laboratory evolution. Additionally, growth kinetics can also be used to study reduced susceptibility (Whitehead et al., 2011), and even more powerful in combination with MIC/MBC assays. One of the limitations of MIC/MBC testing is that the growth of these microorganisms in a biofilm form is not included (Macià et al., 2014). Additionally, the presence of interfering substances, such as presence of organic soil, is often not considered in these *in vitro* assays.

Laboratory evolution is a powerful tool to study the effects of drug exposure on bacteria and to understand the genetic basis of evolution (Cooper, 2018; Elena and Lenski, 2003; Lenski et al., 1991; Poltak and Cooper, 2011), which has also been used with biocides (Guérin et al., 2021; Nordholt et al., 2021; Pereira et al., 2021). Low level exposure to some disinfectants has also been shown to be able to select for antibiotic resistance in various species (Hardy et al., 2018; Kampf, 2019a, 2018; Webber et al., 2015). This has recently been used to study how low levels of antibiotics impact biofilm evolution which revealed strong pressure for emergence of resistance from sub-lethal concentrations of a panel of antibiotics (Trampari et al., 2021).

Other methods like transposon mutagenesis have been used to characterise modes of action and mechanisms of biocide tolerance/resistance including in essential genes (with TraDIS-*Xpress)* for example to Triclosan (Yasir et al., 2020), as well as further study the effects of biocides and the link with AMR in pathogens such as *Acinetobacter baumannii* (Li et al., 2023). Proteomic (Zhou et al., 2023) and transcriptome analysis to understand changes in proteins and gene expression levels under biocide stress (Casey et al., 2014; Felgate and Solsona, In Preparation) have also been used.

More realistic models, such as the simulated clinical setting sink model (Aranega-Bou et al., 2019) showed that *P. aeruginosa* can adapt to octenidine with cross-resistance to other biocides and may also represent a reservoir for biocide-tolerant bacteria (Garratt et al., 2021; Shepherd et al., 2018). The role of sinks as reservoirs during HAIs and outbreaks in hospital settings has also been highlighted by others (Fucini et al., 2023), and how wet surface biofilms could be effectively controlled by having correct IPC protocols in practise.

Nonetheless, biocides are often used at concentrations higher than MIC values (Fox et al., 2022) and in different cases these exceed the MIC/MBC values. Additionally, quality control ranges for biocide susceptibility testing (BST) (Schug et al., 2022) should also be implemented for standardisation. Hence, the absence of realistic exposure concentrations and growth conditions as well as the clinical relevance of laboratory-adapted strains could also be downside of these *in vitro* methods. Testing biocides in BST also do not reflect the real product, hence full formulations should be tested.

1.7. Mechanisms of bacterial tolerance/resistance to biocides

The emergence of bacterial tolerance and resistance could become a major challenge. Additionally, the widespread use of disinfectants might also exacerbate the emergence of antimicrobial resistance although the total amount of biocides that are being used in the EU is still not known (SCENIHR, 2010). The increased use of disinfectants on surfaces can also contribute to high concentrations of biocides seen in wastewater systems. Accumulation in the environment can exert selective pressures leading to bacterial tolerance/resistance over time. More safety studies to improve the use of biocidal products in HCAIs and avoid residual accumulation in the environment (Maillard, 2018; Paul et al., 2019) are still needed.

The BPR acknowledges the issue of bacterial resistance and cross-resistance to antibiotics, and other biocides, after biocide exposure. In this area, the European Union Good Manufacturing Practice (EU GMP) and the FDA suggested to rotate in-use disinfectants – with different mode of action – in order to avoid resistance (Vijayakumar and Sandle, 2019). Understanding the mechanisms by which bacteria evolve resistance to biocides is essential in the first place to determine which agents are least likely to select for resistance in practice, and guide any potential implementation of rotation policies.

Biocides must be used at concentrations recommended by the manufacturer to be effective. The use of these products at sub-inhibitory concentrations could also be a problem since

tolerance or resistance might develop in real life scenarios. The knowledge regarding resistance to biocides is limited when compared to antibiotic resistance (Mc Carlie et al., 2020) although there are common mechanisms of bacterial resistance to biocides and antibiotics (Maillard and Pascoe, 2024). Although no harmonised definitions have been agreed, several working groups are trying to stablish universal definitions.

As seen (**Table 1.2.**), the variety of terms used and the criteria to interpret results in BST is extensive and confusing (Neuhaus et al., 2022). According to Russell (2001), defining "resistance" to biocides can be done in the microbiological context. Therefore, a microorganism is resistant to a biocide when there is no inactivation by the biocidal concentration used; or when the concentration of that biocide does not inactivate the targeted microorganisms. Additionally, many different terms – "resistance", "tolerance", "reduced susceptibility", "insusceptibility – are often used as interchangeable due to the absence of scientific consensus (Maillard, 2018). In general, biocide resistance implies bacterial survival to exposure of an in-use concentration of the biocide (Maillard et al., 2013).

Tolerance is characterised by a reduced susceptibility to a biocide although not an ability to survive high level exposure (McDonnell and Russell, 1999). The terms "reduced susceptibility" or "tolerance" in the area of disinfectants are based on an increase in minimum inhibitory concentrations (MICs) or minimum bactericidal concentrations (MBCs) of a biocide (Maillard, 2018; Weber et al., 2019). When tolerance occurs in a subpopulation of phenotypic variants, it is known as persistence (Dewachter et al., 2019).

Table 1.2. Examples of definitions available in the literature for biocide resistance/tolerance.

Definition	Reference
Biocide resistance	
Insusceptible to a concentration of disinfectant used in practice	(Russell, 1999)
For the disinfection field, the word “resistance” be preferred when the phenomenon under discussion is killing	(Cerf et al., 2010)
biocide resistance implies bacterial survival to exposure of an in-use concentration of the biocide	(Maillard et al., 2013)
A bacterium surviving in a biocidal product is resistant to that product, whatever the concentration of biocide is in the product.	(Maillard, 2018)
Where a biocide concentration that inactivates other organisms but not the organism of concern	(Vijayakumar and Sandle, 2019)
Reduction in susceptibility of a microorganism to an antibacterial biocide because of its ability to withstand the dose(s) of use	(ANSES, 2019)
we propose that in-use concentrations should serve as the basis for the identification of bacterial resistance to biocidal substances	(Neuhaus et al., 2022)
Biocide tolerance	
Tolerance is characterised by a reduced susceptibility to a biocide although not an ability to survive high level exposure	(McDonnell and Russell, 1999)
Decrease of biocide susceptibility in laboratory culture include the two terms used here ("insusceptibility”, “reduced susceptibility”), “tolerance”, and “tolerant”	(Russell, 2001)
“tolerance” when it is adaptation to inhibitory concentrations	(Cerf et al., 2010)
Thus, the term “resistant” is incorrect when applied to pathogens exhibiting an elevated MIC to a germicide. The more accurate terms are “reduced susceptibility” or “increased tolerance”	(Weber et al., 2019)
Because many of the reported instances of reduced effectiveness of biocides are at concentrations significantly below the specified in-use concentrations, we will use the term biocide tolerance	(Coombs et al., 2023)
Isolates that are insufficiently killed by below-use concentrations of a disinfectant solution in suspension tests can be regarded as tolerant	(Kampf, 2023)

1.7.1. Mechanisms determining biocide susceptibility

Bacteria may acquire resistance to disinfectants either by intrinsic or acquired resistance mechanisms (Debarati et al., 2019; Maillard and Pascoe, 2024; McDonnell and Russell, 1999; Russell, 1999). The mechanisms of biocide tolerance and resistance are however less well understood than for antibiotic resistance, and for some biocides no mechanisms have been described yet.

Intrinsic resistance mechanisms

Intrinsic resistance mechanisms are present in all members of a species and often include permeability barriers, presence of alternative targets or active efflux. Reduced uptake of disinfectants often occurs in bacteria that are intrinsically resistant to biocides (Russell, 1999). Penetration of the disinfectant in the matrix barrier is incomplete or reduced. Therefore, the concentration of the disinfectant that reach the target site is not high enough to kill the bacterial cell (Russell, 1999).

Bacterial endospores are also a clear example of biocide resistance due to intrinsic properties. Physiological alterations like the growth of bacteria within a biofilm, are also part of bacterial intrinsic resistance. The biofilm phenotype confers reduced susceptibility to biocides, mainly due to the EPS architecture (Hu et al., 2015; Percival et al., 2015) as previously described. Polymicrobial biofilms are also commonly more resistant than mono-species biofilms (Hu et al., 2015). In this context persister cells and viable but non-culturable (VBNC) states increase the rate of resistance (Dewachter et al., 2019).

Acquired resistance mechanisms

Acquired resistance can arise due to a mutation or acquisition of mobile genetic elements. Mobile genetic elements (e.g., plasmids, transposons) are acquired through horizontal gene transfer (HGT). Among HGT, conjugation is the most well-known mechanisms of transfer of disinfectant genes, nonetheless the mechanisms of disinfectant resistance transferability still remain unknown (Mc Carlie et al., 2020). In this context, the *qac* genes encoding biocide exporter proteins, present in many staphylococcal species (but not exclusive to them) is an example of plasmid-mediated resistance (Mc Carlie et al., 2020; Vijayakumar and Sandle, 2019). During HGT, the movement of biocide resistant genes (BRG) and antibiotic resistant genes (ARG) can also be coupled (Mc Carlie et al., 2020).

Unlike antibiotics, biocides typically have multiple cellular target sites so there is a decreased likelihood of resistance due to target alteration (Bailey et al., 2009; Maillard, 2018). However, there are some cases (e.g., triclosan) in which bacteria have showed decreased susceptibility to biocides (Webber et al., 2008b; Whitehead et al., 2011). Additionally, certain mutations might lead to an overexpression of efflux pumps in bacteria, the selection of these efflux mutants by biocides represents a major issue (Webber and Piddock, 2003).

Efflux is a major mechanism of both acquired and intrinsic disinfectant resistance (Mc Carlie et al., 2020). Five classes of bacterial efflux pumps have been largely characterized: the multidrug and toxic-compound extrusion (MATE) family, the major facilitator superfamily (MFS), the small multidrug resistance (SMR) family, the resistance-nodulation-division (RND) and the ATP-binding cassette (ABC) superfamily (Du et al., 2018). Lately, two new transporter families have been identified: the paminobenzoyl-glutamate transporter (AbgT) family and the proteobacterial antimicrobial compound efflux (PACE) family (Hassan et al., 2018). The PACE family – highly conserved in Gram-negative bacteria – is responsible for biocide resistance to a wide variety of disinfectants and antiseptics (Debarati et al., 2019; Hassan et al., 2018). Further research on the role the PACE family plays on biocide resistance is important. Efflux-mediated tolerance to cationic biocides has been widely described. For example, the QacA pump (from the MFS family) which has been linked to disinfectant tolerance to QACs, although more literature is available describing CHX and BZK tolerance than for OCT (Wand and Sutton, 2022).

A combination of multiple mechanisms of tolerance to biocides have also been reported in *Salmonella* against chlorhexidine (Condell et al., 2014) and triclosan (Webber et al., 2008a). In fact, triclosan is a unique example of high-level tolerance by target alteration in FabI (Heath et al., 1999) or FabV in *P. aeruginosa* (Zhu et al., 2010); and upregulation of multiple efflux pump genes (Zeng et al., 2020) have also been shown to mediate triclosan tolerance.

1.8. The link between biocide and antibiotic resistance

The link between biocide and antibiotic resistance is of major importance. Despite several updates on the mechanisms of biocide tolerance/resistance (the latest by Maillard and Pascoe, 2024), there are no major changes from when these mechanisms were firstly described (McDonnell and Russell, 1999). Nonetheless, the knowledge on how biocides impact AMR has hugely increased.

Low level exposure to disinfectants, which contain biocidal active ingredients, can produce stress to the bacterial cell and promote antibiotic resistance due to co-selection (Debarati et al., 2019; Mc Carlie et al., 2020; Whitehead et al., 2011). This co-selection can be caused by cross-resistance and co-resistance (Hegstad et al., 2010).

Cross-resistance

Bacterial cross-resistance occurs when a resistance mechanism of action against a specific anti-infective agent triggers resistance to different antimicrobial agents (Cândido et al., 2019). In various Gram-negative and Gram-positive species (Kampf, 2019a, 2018), after low level exposure to biocides bacteria become resistant to antibiotics and other disinfectants (Debarati et al., 2019). Different mechanisms – alterations of the target site, drug inactivation and efflux systems – can be associated with bacterial cross-resistance to anti-infectives (Cândido et al., 2019). The formation of biofilms is also linked with cross-resistance events. For example, exposure to triclosan – a biocide that has been used in healthcare settings – lead to the development of cross-resistance to clinically relevant antibiotics in many microorganisms such as *E. coli, P. aeruginosa* and *S. aureus*, among others (Schweizer, 2001). Another study using biocidal products (with QAC as active ingredients) from household settings found a correlation between high QAC MICs and reduced susceptibility to antibiotics in staphylococci (Carson et al., 2008).

Co-resistance

Co-resistance events happen when different resistance mechanisms present in the same bacterial strain can lead to resistance to more than one category of anti-infectives (Debarati et al., 2019). Usually, mobile genetic elements, which contain more than one resistance gene, are transferred from the host and transferred to another microorganism. Consequently, resistance to both antibiotics and biocides occurs. For example, co-resistance between QACs and a range of antibiotics (and other disinfectants) can occur (Hegstad et al., 2010).

The evolution of biocide-antibiotic cross and co-resistance represents a major problem as it poses an increased challenge for IPC strategies (Wand et al., 2017). The presence of low levels of antimicrobials in the environment (Wellington et al., 2013) represent reservoirs and can exert selective pressure, which promotes microbial adaptation. The European Commission and the Scientific Committee on Consumer Safety (SCCS) reported this problem; but more

strict legislative measures should be implemented in order to study biocide-antibiotic cross-resistance and ultimately control antimicrobial resistance.

1.9. Disinfectants and biosecurity in healthcare settings

The emergence of bacterial resistance to biocides and cross-resistance to antibiotics would present a major challenge to IPC (Poole, 2002). MDROs which are also resistant to disinfectants pose a serious threat in HCAIs as both prevention and treatment of infection become compromised (McDonnell and Russell, 1999; Russell, 1999).

Although many can argue that biocide tolerance only develops in laboratory settings, there are also reported cases in real world scenarios. Several examples from intensive-care units showed biocide tolerance or decreased susceptibility to biocides (Batra et al., 2010; Edgeworth et al., 2007; Hardy et al., 2018).

For instance, in 2007, there was a clonal outbreak of MRSA at an intensive-care unit in London, where an endemic clone showed a 3-fold reduction in susceptibility to chlorhexidine. The widespread use of CHX was proposed to have contributed to the increased transmission of this strain in the unit (Edgeworth et al., 2007). In 2010, another clonal outbreak of MRSA sequence type 239 (TW) was linked to a chlorhexidine-based decolonization strategy (Batra et al., 2010), these TW MRSA strains carried the *qacA/B* genes were chlorhexidine and rapidly spread in the hospital. An example of high-level disinfectant resistance was observed in glutaraldehyde-resistant *Mycobacterium chelonae,* found from endoscope washer disinfectors (Griffiths et al., 1997). Other correlations between the increased use of chlorhexidine and octenidine when used as skin antiseptics and multidrug resistance have also been observed (Hardy et al., 2018).

Implementing strict biosecurity measures to use disinfectants in an effective way is of paramount importance to control HCAIs and prevent disinfectant resistance (Gibbens et al., 2001; Mc Carlie et al., 2020).

1.10. COVID-19 impact on AMR and biocides

The COVID-19 pandemic has influenced AMU, with an increased use of antimicrobials to treat co-infections causing changes in AMC (Knight et al., 2021; Rodríguez-Baño et al., 2021) which both accelerated and prevented the threat of AMR depending on the pandemic wave. A mathematical model developed by Smith et al. (2023) assessed the impact of COVID-19 outbreaks in HCAIs had on the spread of MDROs. The model revealed a 10 % increase in AMR rates and colonisation by 14 %. However, it also showed how COVID-19 control measures, along with more stringent IPC protocols, helped limit the spread of MDROs (with a 28 % reduction in patients acquiring MDROs).

The widespread use of disinfectants might also contribute to the rapid expansion of antibiotic resistant strains (SCENIHR, 2010). During the COVID-19 pandemic there was also an increase in biocide use, especially hand sanitizers and surface disinfectants in both hospitals and home settings (Ansari et al., 2021). Interestingly, besides surface disinfection and antiseptic use some biocides such as CHX were repurposed for oral use against SARS-CoV-2 (Stathis et al., 2021). The increased use of disinfectants on surfaces can also contribute to high concentrations of biocides in wastewater systems, which exerts selective pressures (McBain et al., 2002).

The importance of having good IPC practices on place was highlighted, with hospital-onset COVID-19 infections (HOCIs) reported although not yet fully understood (Myall et al., 2022), which posed a major challenge in effective IPC strategies. The focus on COVID-19 diverted attention from the ongoing issue of AMR, although it also highlighted valuable lessons learnt during the pandemics (Wilson et al., 2020) that can inform future preparedness in the fight against AMR.

1.11. Gaps and limitations

Many studies into biocides are available in the literature, but there are still many limitations such as the lack of universal definitions, standard protocols and the scarce number of safety studies of biocidal products.

Unlike for antibiotic resistance, there is still no universal definition for biocide resistance/tolerance. Additionally, the lack of standard guidelines or protocols for testing biocide susceptibility is an issue. For antibiotics, the European Committee on Antimicrobial Susceptibility Testing (EUCAST) ensures harmonization by stablishing antibiotic breakpoints.

The Biocidal Product Regulation and the FDA do not stipulate standard tests or protocols, but rather recommendations, to predict the mechanisms of biocide resistance and cross-resistance to antibiotics (Maillard, 2018; Vijayakumar and Sandle, 2019). Nonetheless, manufacturers need to prove that the biocidal product will not cause resistance or cross-resistance to antibiotics. The absence of standard methods and well-established breakpoints for MIC and MBC of biocides needs to be addressed, as it will improve the selection of suitable disinfectants.

More safety studies to improve the use of biocidal products in HCAIs (Maillard, 2018) and avoidance of residual accumulation in the environment are still needed. Understanding how the selected pathogens respond to different biocidal agents to inform risk assessment of the potential for resistance development between different biocide formulations is essential. The development of better IPC strategies and improved products is likely to be critical in the short-term fight against AMR pathogens with control of hospital acquired infections.

1.12. Project aims and objectives

Aim

To understand how nosocomial pathogens adapt to different biocides in a biofilm context, and to use this information to help develop improved biocidal formulations with my iCASE partner GAMA Healthcare Ltd.

Objectives

I. **To use laboratory evolution to identify genes determining susceptibility to test biocides:** Identification of genes that were involved in reduced susceptibility to commonly used biocides (quaternary ammonium compounds, chlorhexidine and octenidine) and GAMA Healthcare's novel Clinell® proprietary formulation (FM104).

II. **To identify genes responsive to biocidal stress and understand mechanisms determining biocide sensitivity:** RNA sequencing was used to identify genes involved in anti-infective susceptibility and candidate genes were validated.

III. **To develop and assess new product formulations and test efficacy:** Disinfectant products were tested for efficacy using the industry standard tests; a protocol for assessing bacterial adaptation to biocides was also developed. This data supported global regulatory submissions and marketing claims made by GAMA Healthcare Ltd.

1.13. Hypothesis

I. Bacterial biofilms can evolve resistance or tolerance to biocides leading to low-level changes to susceptibility to various other antimicrobials.

II. Biocidal products have different potentials for selection of resistance or tolerance depending on formulation.

CHAPTER 2: MATERIALS AND METHODS

Science knows no country because knowledge belongs to humanity and is the torch which illuminates the world." – Louis Pasteur

2.1. Bacterial strains

Two commensal isolates of *Staphylococcus aureus* (from a nose swab) and *Enterococcus faecalis* (an ear swab) were selected as representatives of each species (**Table 2.1.**). The selected *S. aureus* strain corresponds to sequence-type (ST) 188 which is a major lineage causing infection in humans (Wang et al., 2018) and the selected *E. faecalis* is ST40; the most common sequence type of this species isolates from humans (Zischka et al., 2015).

Table 2.1. List of bacterial strains used.

Isolate number	MLST type	Species	Source	Country
312	ST 40	*E. faecalis*	Ear swab	UK
678	ST 188	*S. aureus*	Nose swab	UK
NCTC 13383	NA	*E. hirae*	GAMA Healthcare	-
NCTC 12973	ST 5	*S. aureus*	-	-

These two strains were selected to represent common sequence types present within a large collection (> 2000 strains) of commensal isolates recently collected from babies in the NICU of the Norfolk and Norwich University Hospital (NNUH) where antiseptics are in regular use (Sethi et al., 2021). Both had been genome sequenced and initial biofilm formation characterised. A series of other CoNS isolates were used in optimisation experiments for methods to test for biofilm formation (**APPENDIX I**).

S. aureus NCTC 12973 (purchased from Public Health England, UK) was used as a control in susceptibility testing. *Enterococcus hirae* NCTC 13383 – commonly used in industry standard testing – was included in the experiments with GAMA Healthcare's novel Clinell® proprietary formulation (**Table 2.1.**).

For molecular cloning, NEB® 5-alpha competent *Escherichia coli* (derivative of *E. coli* DH5α by Hannahan, 1983) was purchased from New England Biolabs (UK) for high efficacy transformation. *Staphylococcus aureus* RN4220 (Kreiswirth et al., 1983) was used as a cloning intermediate strain (obtained from DSMZ, Germany).

2.2. Media and growth conditions

All strains were cultured in tryptic soy broth (TSB) media or tryptic soy agar (TSA) (Oxoid, Thermo Fisher Scientific, UK) plates at 37 ℃, unless otherwise stated. Cation-adjusted Mueller-Hinton (CaMH) broth and agar (Oxoid, Thermo Fisher Scientific, UK) were used for susceptibility testing and Lysogeny broth (LB) for molecular cloning. Mannitol-Salt agar (MSA) (Oxoid, Thermo Fisher Scientific, UK) was used for the identification of *S. aureus*, and Brain Heart Infusion (BHI) (Merck, UK) was the selected media for DNA extractions.

Foetal bovine serum (FBS) (Merck, UK) and bovine serum albumin (BSA) (Sigma-Aldrich, UK) were added to the media for initial *in vitro* bead-based model optimizations. For the evolution experiments, an orbital shaker at 40 revolutions per minute (rpm) inside a refrigerated incubator (22 ℃) was used to create controlled room temperature conditions that reproduce the environmental hospital surface. Crystal violet and Congo red assays were performed at 30 ℃ (skin temperature).

2.3. Antimicrobial agents and other materials

2.3.1. Antibiotics

Seven antibiotics (ciprofloxacin, cefotaxime, daptomycin, erythromycin, gentamicin, penicillin, vancomycin) from different classes (fluoroquinolone, 3rd generation *β-lactam*, cyclic lipopeptide, macrolide, aminoglycoside, β-lactam, glycopeptide) were used for antimicrobial susceptibility testing. For daptomycin, calcium (Sigma-Aldrich, UK) was added to media to a final concentration of 50 mg/L. Antibiotics were purchased from Sigma-Aldrich, UK.

2.3.2. Biocides and formulations

Chlorhexidine digluconate (CHX) and octenidine dihydrochloride (OCT), commonly used as skin antiseptics (Product Type 1) and disinfectants (Product Type 2) in hospital settings (Kampf, 2018), were the main biocides used in the project. Stock solutions of 20 % (v/v) CHX (Sigma-Aldrich, UK) and 0.5 % (w/v) OCT (Alfa Aesar, US) were prepared in double-distilled water (ddH_2O) and dimethyl sulfoxide (DMSO) respectively.

In the iCASE placement at GAMA Healthcare Ltd., a novel biocidal product (representing a formulation) and corresponding unformulated actives from the QAC family were used (**Chapter 7**). The biocidal ingredients from the GAMA Healthcare's novel Clinell® proprietary

formulation (also referred to as FM104) include: DDAC and ADBAC; due to a pending patent no further details of the respective concentrations can currently be disclosed.

2.3.3. Neutralizers

Polysorbate 80/Tween® 80 (Sigma-Aldrich, UK) was used as a neutralizer to quench the activity of biocides. Neutralizer efficacy and toxicity was assessed following the BS EN 13727:2012+A2:2015 (BSI, 2012a).

2.3.4. Stainless steel beads

For the *in vitro* bead-based evolution model, medical grade AISI 316 stainless steel beads (Grade 100) – a material widely used in hospital surfaces – were added to the selected media to allow biofilm formation (Konrat et al., 2016; Trampari et al., 2021). To distinguish different passage points in longitudinal evolution experiments stainless steel beads (Simply Bearings Ltd, UK) of different diameters (6 mm and 3 mm) were used.

2.4. Antimicrobial susceptibility testing

2.4.1. Minimum inhibitory concentration

Broth microdilution: this method was used to determine the minimum inhibitory concentration (MIC) of the tested antimicrobials against the controls and WT samples following the European Committee for Antimicrobial Susceptibility Testing (EUCAST) guidelines (EUCAST, 2024a). The MIC value equals the lowest concentration of a biocide needed to inhibit the growth of a microorganism.

The MICs of the selected antibiotics were determined for planktonically growing bacterial strains. Doubling serial dilutions of the antimicrobial agents (from 64 to 0.125 µg/mL) were prepared in TSB and inoculated with 10^5 colony-forming units per millilitre (CFUs/mL) of an overnight (O/N) culture. Plates were then incubated at 37 °C for 24 hours. The ability of the selected strains to grow at doubling concentrations of the antimicrobial agents was measured by the naked eye. The first clear well of the microplate where the microorganism stopped growing was detected by a change in turbidity in the media. In addition, the MIC was also determined by measuring absorbance (OD_{600nm}) with the FLUOstar® Omega spectrophotometer (BMG Labtech, UK) using the program "MicroPlate Manager 5.21;

Protocol: Endpoint". MICs for the different antibiotics and the two biocides were determined in triplicate for all the isolates; three biological replicates were included. The mean MIC of the tested antimicrobials was calculated for each isolate.

Agar dilution method: The agar dilution method following EUCAST guidelines (EUCAST, 2024a) was used to determine the MICs of a panel of antibiotics against the 306 evolved samples using the multipoint inoculator (Denley Instruments Ltd, UK) to identify any cross-resistance resulting from biocide exposure. Seven antibiotics of different classes (ciprofloxacin, cefotaxime, daptomycin, erythromycin, gentamicin, penicillin, vancomycin) were tested.

Overnight cultures from each master plate were grown in Mueller-Hinton broth (MH) (Sigma-Aldrich, UK) and diluted 1:100 in 96-deep-well plates to a total volume of 2 mL. For daptomycin, calcium (Sigma-Aldrich, UK) was added to media to a final concentration of 50 mg/L in accordance with EUCAST guidelines (EUCAST, 2024a). For each antibiotic, MH agar plates containing serially diluted concentrations of drug were used. Diluted cultures were spotted onto the agar (~10^4 cells) using a multipoint inoculator (Denley Instruments Ltd, UK) and incubated at 37 °C for 24 hours. Initial and end plates were added for each master plate as growth and sterility controls. To avoid colonies carriage on the pins and residual ethanol, washing time the pins were washed with 70 % ethanol for 4 minutes, and 8 minutes if there was a change in antibiotic, with a 4-minute waiting time.

Distribution of the MICs among the 306 evolved isolates was plotted for each antibiotic and biocides. The average $\log_2$ fold change in MICs (compared to the WT average) was calculated for each strain. avera

2.4.2. Minimum bactericidal concentration

The minimum bactericidal concentration (MBC), which is the lowest concentration of a drug that results in killing 99.9 % of the bacteria being tested, was determined using an agar plate assay. To assess the bacterial-killing activity of the selected biocides, 5 µL of the microtiter wells above the MIC (with no visible growth) were spotted on TSA plates and incubated at 37 °C for 24 hours. The MBC corresponded to the first clear area of the agar plate without bacterial growth.

2.4.3. Minimum biofilm eradication concentration

Minimum biofilm eradication concentration (MBEC) assays to determine the lowest concentration of an antimicrobial that can eradicate 99.9 % of biofilm-embedded bacteria was performed using a modified broth microdilution assay (Zaborowska et al., 2017). O/N cultures were prepared in 5 mL TSB glass tubes and incubated at 37 °C. After 24 hours, cultures were diluted (1:10000) into new microtiter plates. A semi-skirted 96-well polymerase chain reaction (PCR) plate (Starlab, UK) was then allowed to sit within the wells of the microtiter tray and incubated for 24 hours (150 rpm at 37 °C) allowing a biofilm to form on the outside of the wells of the PCR plate. The microtiter tray was discarded and the outside surface of the wells of PCR plate was washed for 10 seconds in 180 µL of PBS in a microtiter tray. The PCR plate was then allowed to rest within another microtiter tray in the same format for an MIC assay (previously described). Plates were incubated at 37 °C for 18 - 20 hours. On day 4, the MIC plate was then discarded, and the PCR plate was placed in a fresh microtiter tray containing 180 µL of TSB which was incubated for 18 - 20 hours at 37 °C, when the MBEC was determined.

2.5. Experimental microbial evolution

An *in vitro* bead-based evolution model was developed (Poltak and Cooper, 2011) to study the evolutionary process of biocide resistance. Two different evolution experiments were performed in the project to study the effects caused by the exposure to CHX and OCT (**Chapter 2**, **Section 2.5.1.**) and biocidal formulations, as well as other QAC agents and individual co-formulants (**Chapter 2**, **Section 2.5.2.**).

2.5.1. *In vitro* bead-based evolution model at the Quadram Institute Bioscience

This evolution experiment tested the effects of exposure to two common biocides against *S. aureus* and *E. faecalis* by exposing the isolates to escalating concentrations of CHX and OCT over a specific time (for an overview see **Figure 2.1.**). Biofilm and planktonic lineages were studied in parallel as in our recent work (Trampari et al., 2021), and the evolvability of each strain was measured after passaging.

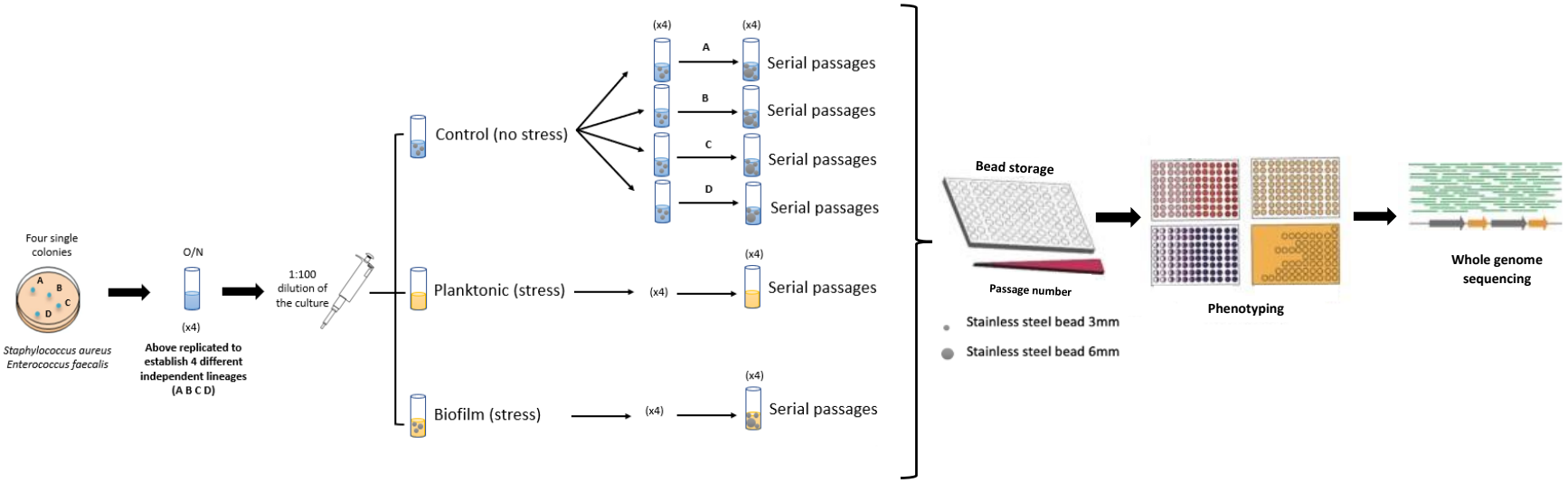

Figure 2.1. **Overview of the experimental design of the *in vitro* bead-based biofilm evolution model.** In the evolution model, isolates were repeatedly exposed for 72 hours (passage window). Phenotyping and genotyping assays performed with the resulting evolved isolates.

After previous optimisations (further details in **Chapter 4**), a Standard Operating Procedure (SOP) for the *in vitro* bead-based biofilm evolution model for the selected Gram-positive isolates was created (**APPENDIX II**). Briefly, the strains of interest were initially streaked out on TSA plates from O/N cultures. To establish independent lineages, four single colonies were randomly picked from each isolate to start the overnight cultures. A 1:100 dilution from the O/N cultures was performed and use to inoculate different conditions, giving a total of 4 independent lineages per condition (A, B, C, D). To mimic biofilm formation, stainless steel beads from different diameters (6 mm and 3 mm) were added to the selected media to allow biofilm formation. The bacterial population sizes supported by the beads of different sizes were not significantly different (further details in **Chapter 4**).

After each passage, the beads were washed with phosphate-buffered saline (PBS) in a 24-well microtiter plate and repeatedly exposed for 72-hour windows to each test condition before being passaged. New sterile beads were also added to the glass tubes to allow for bacterial regrowth. Planktonic cells were also passaged by 1:100 dilutions to fresh TSB glass tubes. Escalating concentrations of the biocides were added to the selected conditions after the parental generation and increased after every two passages (from 0.25 µg/mL to 64 µg/mL), following a ladder model. Control conditions had no biocides added. Beads, planktonic samples from the bead condition and planktonic samples were stored in 800 µL of TSB and 800 µL of 20 % glycerol in a 96-deep well plates. In parallel, samples were stored at -80 ℃ on preservation beads and at -40 ℃ glycerol after each passage.

Colony-forming unit per millilitre (CFU/mL) for planktonic, and colony-forming unit per square millimetre (CFU/mm^2) for biofilm, were calculated. The CFU/mm^2 value was obtained from dividing the CFU/bead value by the area of the spheric bead ($4\pi r^2$). The average number of generations expected in each condition for 18 passage cycles was calculated using a previously described method (Poltak and Cooper, 2011) by multiplying the number of passages by $\log_2$ of the relevant dilution factor.

2.5.2. Evolution experiments at GAMA Healthcare Ltd.

At GAMA Healthcare Ltd. an accelerated evolution experiment was also performed with some modifications from the previous SOP. For this experiment, modifications included removing the biofilm condition, reduction of the passage window (from 72 hours to 48 hours), and having a total of 3 planktonic lineages instead of 4. One set of controls was included per isolate.

The experimental set-up included the 3 selected isolates (*S. aureus* ST188, *E. faecalis* ST40 and *E. hirae* NCTC 13383), 3 different stresses: Stress 1 (50:50 combination of actives, BZK+DDAC), stress 2 (FM104) and stress 3 (chassis = FM104 minus actives). For stress 2, FM104 in the form of the bulk liquid was used (to standardise the concentration of actives), since each batch of a wipe package can have different percentages of actives. Stress 3 represents the chassis, which includes all the co-formulants without the active substances. This combination was created to determine if the preservative (and potentially other components of the formulation) exhibit any biocidal activity after removal de the biocidal actives. The experiment followed a ladder model, in which the concentration of stresses was increased (by double) over time. For stress 1 and stress 2 concentrations started at sub-MIC levels and increased 2-4 times before MIC. Values ranged from 0.0125 µg/mL - 12.8 µg/mL. For stress 3, the first three initial values were 0.0125 µg/mL, 93.75 µg/mL and 187.5 µg/mL, then doubling higher concentrations were selected (from 1000 µg/mL to 256,000 µg/mL). Samples from parental generation, early timepoint (2nd passage), middle timepoint (7th passage) and late timepoint (10 - 11th passage) were stored on 40 % glycerol at -80 °C at GAMA Healthcare Ltd.

2.6. Phenotyping

After the evolution experiments, different phenotypic assays were used to understand the evolutionary changes that occurred in each population.

2.6.1. Population sampling

Populations from the start ('early', passage 1), 'middle', and end ('late') of the evolution experiment were recovered from the stored glycerol stocks, grown overnight on TSB and plated on Tryptone Soy Agar (TSA) (Oxoid, Thermo Fisher Scientific, UK). The early timepoint corresponded to the first passage, middle timepoint corresponded to the passage 10 (except for some OCT samples where the middle of the experiment corresponded to the 8th passage) and the late timepoint was the 18th passage. For the control condition, two timepoints ('early' and ('late') were sampled to confirm no relevant changes had occurred. Three random colonies (C1, C2, C3) from a total of 77 populations were then selected to give 231 isolated strains. Overall, 308 isolates/populations were phenotypically characterised. From the evolution experiment at GAMA Healthcare Ltd., populations from the end were recovered from each isolate and stress, giving a total of 36 populations phenotypically characterised after sequencing.

2.6.2. Biofilm biomass production

Biofilm biomass production was quantified by crystal violet staining. O/N cultures of the desired bacterial strains were prepared in microtiter plates using 200 µL of TSB supplemented with 1 % (w/v) glucose (Sigma-Aldrich, UK) to facilitate biofilm formation (Croes et al., 2009; Lade et al., 2019; Lam et al., 2013). After 24 hours at 37 ℃ cells were diluted (1:10000) into new microtiter plates with fresh TSB supplemented with 1 % (w/v) glucose. The plates were sealed with gas permeable membrane (Thermo Fisher Scientific, UK) and incubated for 48 hours at 30 °C 200 rpm to mimic the skin temperature. After incubation, plates were washed with water and stained with 200 µL of 0.1 % (w/v) crystal violet (Sigma-Aldrich, UK) to each well and incubated at room temperature for 10 minutes. Plates were washed again with water and 200 µL of 70 % (v/v) ethanol was added to each well for 10 minutes. Absorbance measurements (OD_{600nm}) were determined for each well using the FLUOstar® Omega spectrophotometer (BMG Labtech, UK). 1 biological replicate with 3 technical replicates of each sample was included. Kruskal-Wallis test was performed to assess differences in biofilm biomass production between timepoints, both simultaneously across all conditions and for each individual condition. Subsequent Wilcoxon-Mann-Whitney tests were applied as a *post hoc* to study differences within conditions for each timepoint (early, middle, late) and samples (Population, C1, C2, C3).

2.6.3. Congo Red assay

To qualitatively assess biofilm formation and colony morphology, Congo red, which binds to amyloid fibres, assays were performed. On the first day, O/N cultures of the bacterial strains of interest were grown on in a microtiter with 200 µL of TSB and incubated at 37 °C. A manual pin replicator was used to copy each master plate and perform the assay. On the second day, O/N were diluted (1:100 and 1:100) and 20 µL were spotted on LB agar without salt (LB-NaCl) supplemented with 40 µg/mL of Congo red dye (Sigma-Aldrich, UK). Three technical replicates were included for each sample. Plates were incubated without shaking at 30 °C for 48 hours.

The intensity of the Congo red colour of the colonies is qualitatively associated with higher or lower biofilm production. Measurements are ranked on a 1-3 scale: light red (indicated as 1+) associated with low biofilm production, and dark red (3+), associated with higher biofilm production. Colonies with a mixture of light and dark red (2+), have a mixed biofilm production.

2.6.4. Growth determination

Growth rates were determined as a measure of general fitness over 12 hours at 37 °C using a BMG LABTECH microplate reader (FLUOstar Omega Microplate Reader). O/N cultures of the strains of interest were prepared in TSB and diluted 1:10000 before 200 µL were added to each well. Plates were sealed with a gas permeable membrane (Thermo Fisher Scientific, UK) and inserted into the plate reader to measure OD_{600nm}. Readings were taken every 30 minutes of absorbance of each well (scanned at 600 nm). Each growth curve included 300 cycles and a cycling time of 150, with shaking before each kinetic measurement cycle (5 flashes/well) and incubation at 37 °C. Measurements were then exported from the MARS software. Absorbance (OD_{600nm}) for each isolate and the area under the curve (AUC) relative to the WT were plotted.

2.7. Concentration dependent killing assays

Without interfering agents: concentration dependent killing assays were performed to evaluate the bactericidal effects of the disinfectants over time (Kawamura-Sato et al., 2008) following a modification of the British Standard BS EN 13727:2012+A2:2015 (BSI, 2012a). The log_{10} reduction was then calculated (Mazzola et al., 2003).

O/N cultures of the WT isolates were prepared and incubated at 37 ℃. A 1:100 dilution in ddH_2O was done to adjust the bacterial suspension to 10^7 CFU/mL. Then, 500 µL were transferred to 10 mL of disinfectant solutions. Different in-use concentrations of OCT and CHX, as well as lower concentrations (0.02 %, 0.002 % (v/v) for CHX and 0.05 %, 0.0005 % and 0.00025 % (w/v) for OCT) were tested for each isolate. After a contact time of 5 minutes (at room temperature), 1 mL of the mixture was transferred to 8 mL of TSB, containing 1 mL of 1 % (v/v) Polysorbate 80/Tween® 80 (used as a neutralizer for QAC inactivation). The suspension was then serially diluted with PBS and 100 µL were spread on TSA plates. Plates were incubated O/N at 37 °C. The number of viable bacteria colonies were counted the next day. As a negative control, neutralizer solution was added to TSB only; the positive control was TSB with the inoculum. Toxicity tests were included by adding 1 mL of neutraliser into 9 mL of media and 1 mL of bacterial cultures. This was compared to the growth control, where no neutraliser was included.

Addition of interfering agents: More-realistic concentration dependent killing assays were performed as described before by adding interfering substances and tryptone sodium chloride solution was used as a diluent (instead of ddH_20) following the BS EN 13727 Standard. Interfering substances (blood and protein mixture) to simulate a contaminated spill and to reproduce the presence of organic matter and dirt present when cleaning and disinfecting in real life. For clean conditions, 0.3 g/L bovine serum albumin (BSA) were prepared. For dirty conditions, 3 g/L BSA were mixed with 3 mL/L of sheep erythrocytes prepared from fresh defibrinated sheep blood (purchased from Darwin Biological, UK) as stated in the protocol. The biocide was then added to this simulated spill, mixed, and left for contact time (5 minutes), and eventually neutralized to stop its antimicrobial activity.

2.8. Biocide efficacy testing at GAMA Healthcare Ltd.

British and European Standards specify testing methods for a chemical disinfection and/or antiseptics. To test for antimicrobial efficacy, the bacterial suspension test BS EN 13727 (BSI, 2012a) and the surface test BS EN 16615 (BSI, 2012b) were performed with all the isolates and FM104 formulation to determine the bactericidal activity. To give accurate insights into clinical performance, liquid extracted from a wipe under dirty conditions was used to reproduce the presence of organic matter and dirt present when cleaning/disinfecting in real life. The product is then added to this simulated spill, mixed, and left for the contact time before it is neutralised.

Initially, optical density graphs for estimating CFU/mL for *S. aureus* ST188 and *E. faecalis* ST40 were generated by following the calibration curve protocol from GAMA Healthcare Ltd. (**APPENDIX III**). The average absorbance (OD_{600nm}) and CFU/mL of three biological repeats were calculated to have the precise value since standardisation is vital for accurate and reproductible testing. Protocols were rigorously followed as per BS EN Standard testing. The inoculum suspension was adjusted to $1.5x10^8$ CFU/mL - $5.0x10^8$ CFU/mL, aiming for as close to $3x10^8$ CFU/mL as possible. The contact time for all the tests was 10 seconds.

2.9. *Galleria mellonella* infection model

To study the virulence of the WTs and determine differences in virulence, the *Galleria mellonella* infection model was used. Some advantages of this model (Pereira et al., 2018) include: similarity to the innate immune response of mammals, no need for ethics approval, inexpensive and easy maintenance. *G. mellonella* larvae (purchased from Livefood UK Ltd.) were stored in the dark in a refrigerated incubator at 15 ℃ before use.

Inoculum test: Preliminary experiments with the WT isolates were performed to identify the infection dose of the strain. Following literature, different inoculum (10^6, 10^7, 10^8, 10^9 CFU) were tested for *S. aureus* ST188 (Desbois and Coote, 2011; Peleg et al., 2009; Sheehan et al., 2019) and *E. faecalis* ST40 (La Rosa et al., 2012; Thieme et al., 2020). Bacterial strains were grown O/N and serially diluted in a 96-well plate in sterile PBS. Then, 5µL from each dilution were spotted onto a square TSA plate. Colonies were counted the following day, and CFU/mL calculated. Three technical replicates were platted per each strain.

Haemolymph dissection: Further optimizations to perform a viable count of the bacteria injected into the larva were done. Haemolymph dissection was performed by dissecting the last proleg of the larvae and adding it into an Eppendorf tube until the haemolymph was drained. Serial dilutions with 10 µL of haemolymph in 90 µL of PBS were performed. 5 µL were spotted in Mannitol Salt Phenol Red Agar (MSA) plates to confirm growth.

Larvae injection: *G. mellonella* larvae were injected with 10 µL of the *S. aureus* ST188 and *E. faecalis* ST40 strains at 10^6, 10^7, 10^8, 10^9 CFU/inoculum with a Hamilton syringe (Sigma-Aldrich, UK, 20779). To ensure sterility between inoculations, Hamilton syringes were disinfected twice with 70 % ethanol and once with sterile PBS. The inoculum was delivered into the third right proleg to standardize experiments. Ten larvae were infected per strain/condition; controls included ten uninfected larvae and ten larvae injected with sterile PBS. Infected larvae were placed on Petri dishes covered with filter papers and incubated at 37 ℃. Survival checks were performed three times per day, for 72 hours. Full systemic melanisation and immobile larvae were considered as dead. One independent experiment was performed with 10 larvae/group.

2.10. Genotyping

Evolved isolates from *in vitro* bead-based evolution experiment at the Quadram Institute Bioscience*:* After phenotyping 308 samples, 131 samples from the end timepoints (populations and random colonies) from each isolate and condition were selected for whole-genome sequencing to determine the genetic basis behind adaptation. A naming convention to identify samples was created: samples were identified with species (SA/EF), biocide (OCT/CHX), condition (planktonic/biofilm), origin (population/random colony [C1, C2, C3]), and lineage (A, B, C, D).

Evolved isolates from evolution experiment at GAMA Healthcare Ltd.: Populations from the evolution experiment (stored at the -80 ℃) were sent from GAMA Healthcare Ltd. to the Quadram Institute Bioscience, where cultures were confirmed on TSA plates and back-up stocks in cryovial tubes were generated. A total of 36 evolved population samples from the late timepoints (12 samples for each isolate, 3 samples/stress) were selected for genotyping.

2.11. Whole genome sequencing

2.11.1. DNA extractions

Zymo Miniprep Kit: DNA extractions from the WT isolates were performed following a modification of the protocol "Cell suspensions and Proteinase K Digested Sample" from the *Quick*-DNA™ Miniprep Kit D3024 (Zymo Research, UK).

O/N cultures of the selected strains were prepared from the glycerol stocks in 5 mL glass tubes with Brain Heart Infusion (BHI) (Sigma-Aldrich, UK) and incubated at 37 ℃. To obtain a higher quantity of DNA, BHI was used instead of TSB. 1 mL of the culture was added into an Eppendorf tube and spun at maximum rpm for 15 minutes. The supernatant was removed, and the pellet was resuspended in 100 µL of 0.5 mg/mL lysostaphin (from *Staphylococcus staphylolyticus,* Merck, UK), and incubated at 37 ℃ for 1 hour. The next steps were followed as per the manufacturer's instructions. Purified DNA was obtained, and DNA concentration was measured.

Zymo Quick-DNA 96-Well Kit: DNA extractions from the selected evolved isolates from the Quadram Institute Bioscience evolution experiment (131 samples) from the end

timepoints (populations and random colonies) and GAMA Healthcare evolution experiment were performed following a modified protocol from the *Quick*-DNA™ Fungal/Bacterial 96 Kit (Zymo Research, UK). O/N cultures of the selected strains were prepared in 96-deep-well plates with 1 mL of BHI and incubated at 37 ℃. Plates were spun at 4000 rpm for 15 minutes. The supernatant was removed, and the pellet was resuspended in 100 µL of 0.5 mg/mL lysostaphin (for staphylococci) and/or 0.5 mg/mL lysozyme (for enterococci) and added into a 96-well plate bead beater. Then 400 µL of BashingBead™ Buffer were added to each tube. Plates were incubated (180 rpm at 37 ℃) for 40 minutes and then vortexed for 2 minutes. Plates were then spun at 4000 rpm for 8 minutes. The next steps were followed as per the manufacturer's instructions (starting from Step 4). The elution plate containing purified DNA was stored at -20 °C.

Zymo Quick-DNA High Molecular Weight (HMW) MagBead Kit: DNA extractions for hybrid genome assembly were performed using a modified protocol from Quick-DNA™ High Molecular Weight (HMW) MagBead Kit (Zymo Research, UK). O/N cultures of the selected strains were prepared in 5mL of BHI and incubated at 37 ℃. 500 µL of the cultures were added and centrifuged at 8000 rpm for 1 minute to start the "Microbial Lysis" steps. For an efficient degradation of the Gram-positive cell wall, 100 µL of 0.5 mg/mL lysostaphin (from *Staphylococcus staphylolyticus,* Merck, UK) were added and incubated at 37 °C for 1 hour. The saved supernatant (230 µL) was combined with 125 µL digested sample. The next steps of "Microbial Lysis" were followed as per the manufacturer's instructions. From the "DNA purification", protocol started from step three where 50 µL of MagBinding Beads instead of 33 µL were added to each sample. Additionally, the elution buffer volume increased from 50 µL to 75 µL. The eluted DNA was stored at -20 °C.

Fire Monkey: A Fire Monkey kit (RevoluGen Ltd, UK) to extract high quality High Molecular Weight DNA from *E. faecalis* ST40 was used following the "Updated Gram-positive Cells Protocol (August 2021)". Modifications of the protocol included a longer incubation period to lyse the cells (1 hour instead of 30 minutes). The eluted DNA was stored at -20 °C, and Fraction B, which contained fewer smaller fragments than Fraction A, was used for Nanopore long-read sequencing.

2.11.2. DNA quantification

A Qubit 3.0 Fluorometer (Invitrogen, UK) was used for DNA quantifications from samples in individual tubes. To measure double-stranded DNA (dsDNA) concentrations from single tubes, the Qubit dsDNA HS (High Sensitivity) assay Kit Q32851 (Invitrogen, UK) and Qubit DNA BR (Broad Range) assay kit Q32853 (Thermo Fisher Scientific, UK) were used following the manufacturer's instructions.

To quantify the DNA in 96-well plates, the Quant-iT dsDNA high sensitivity assay kit (Thermo Fisher Scientific, UK) was used; fluorescence was measures with OPTIMAstar (BMG Labtech) using an excitation/emission wavelength of 485/520 nm.

2.11.3. Illumina NextSeq Short Read Sequencing

Genomic DNA was normalized to a concentration of 5 ng/µL with 10 mM Tris-HCl. Whole-genome sequencing was performed using Illumina technology with the Flex library preparation protocol as in Trampari et al. (2021).

2.11.4. Nanopore MinION Long Read Sequencing

To obtain more accurate and robust hybrid assemblies of the parent strain genomes, both isolates were also sequenced by long-read MinION sequencing (Oxford Nanopore Technologies, ONT) following a protocol recently reported (Felgate et al., 2023).

2.12. Bioinformatic Analysis

Genome sequencing data was stored and analysed using the Integrated Rapid Infectious Disease Analysis (IRIDA, version 19.09.2) (Matthews et al., 2018) and Galaxy (v19.05) (Afgan et al., 2018) platforms at the Quadram Institute Bioscience. For taxonomic classification at the species level the tool Centrifuge (v0.15) (Kim et al., 2016) was used with FASTQ files.

From the Illumina sequencing, reads were assembled with SPAdes (v3.12.0) (Bankevich et al., 2012). QUAST (v5.0.2) (Gurevich et al., 2013) was used to check genome assembly quality and filter out bad quality samples. Assembled genomes were annotated with Prokka (v1.14.5) (Seemann, 2014). A standard assembly and annotation pipeline included Multi-locus sequence typing assignment (MLST v0.42) (Seemann, 2016) to check sequence types and antimicrobial resistance genes which were detected using ARIBA (v2.13.2) (Hunt et al., 2017)

with the Comprehensive Antibiotic Resistance database (CARD v3.0.1; https://card.mcmaster.ca) (McArthur et al., 2013). For biocide resistance genes (BRG) prediction, the antibacterial biocide and metal resistance genes database (BacMet, v2.0) (Pal et al., 2014) was used to look for predicted resistance genes. Long-read sequence data reads were assembled with Flye (v3.12.0) (Kolmogorov et al., 2019) and polished with Pilon (v1.20.1) (Walker et al., 2014). Kraken2 (v2.1.1) (Wood and Salzberg, 2014) and Bracken (v2.8) (Lu et al., 2017) were used for taxonomic classification and to estimate abundance, respectively. Assembled genomes were annotated as above. For the reference strain *E. hirae* NCTC 13383, PacBio assembled genome (Assembly accession: GCF_900448015.1) was used.

Assembled Nanopore reads were combined with Illumina reads to create hybrid genome assemblies. Long-reads were filtered by quality with Filtlong (v0.2.0) (Wick, 2017). Illumina short reads were then mapped with Minimap2 (v2.17) (Li, 2018) and assemblies polished with two iterations of Racon (v1.3.1.1) (Vaser et al., 2017), one round of Medaka (v0.11.5) (https://github.com/nanoporetech/medaka). Genome completeness was estimated with CheckM (v1.0.11) (Parks et al., 2015) and Socru (v2.2.4) (Page and Langridge, 2019) used to validate organisation of assemblies. Assembled hybrid genomes were annotated as above.

Snippy (v4.4.3) (Seemann, 2015) was used to identify single nucleotide polymorphisms (SNPs) between reference genomes and evolved samples. Snippy-core (v4.4.3) (Seemann, 2015) combined multiple snippy outputs into a core SNP alignment. The core alignment was then run in FASTTREE (v2.1.10) (Price et al., 2009) to generate approximately-maximum-likelihood phylogenetic trees from nucleotide alignments and iTOL (v6.8.2) (Letunic and Bork, 2006) used for visualisation. Artemis (v18.2.0) (Carver et al., 2012) was used for genome visualisation and manual confirmation of SNPs.

2.13. RNA sequencing

RNA sequencing (RNA-Seq) experiments with *S. aureus* ST188 and *E. faecalis* ST40 after being exposed for 30 minutes to ½ MIC of CHX, OCT and FM104 were performed to identify genes expressed under stress.

RNA extraction: RNA extractions following an optimised "Quick-RNA™ Fungal/Bacterial Miniprep" protocol (Zymo Research, UK) for *S*. aureus ST188 and *E. faecalis* ST40. Overnight cultures were diluted 1:200 in previously warmed MH broth. Triplicate cultures (20 mL volume) were grown at 37 °C 180 rpm until the OD_{600nm} reached 0.2 - 0.3

(exponential phase) where they were then exposed (30 minutes at room temperature) to ½ MIC of CHX, OCT, and FM104, or no biocide for the control. After exposure, the cultures were spun at 4000 rpm, 4 °C for 10 minutes. The pellets were resuspended in 400 µL DNA/RNA Shield (Zymo Research, UK) and transferred to a ZR Bashing Bead Lysis Tube (0.1 & 0.5 mm). The samples were lysed using a FastPrep-24™ set to 6.5 m/s [60 seconds on, 5 minutes off] for 5 times (for *E. faecalis*) and 2 times (for *S. aureus*), and frozen at -80 °C. The lysis was then continued following the steps from "Quick-RNA™ Fungal/Bacterial Miniprep" protocol (Zymo Research, UK) with the additional step of DNAse I treatment in-column (Zymo Research, UK). Finally, RNA was eluted in 50 µL of DNase/RNase-Free water and stored at -80 °C.

Quality checks: RNA concentration was checked using Qubit™ RNA High Sensitivity reagents and RNA integrity was checked using the Agilent High Sensitivity RNA Screen Tape and Agilent Technologies 2200 TapeStation. DNA contamination was also checked for using Qubit™ DNA High Sensitivity kit. Absence of contaminants was checked by measuring ratios A260/280 and A260/230 with the NanoDrop® ND-1000 Spectrophotometer (Labtech, UK). RNA with a RIN of ≥ 6, a concentration of ≥ 50 ng/µL, ratio A260/280 = 1.8 - 2.2 and ≤ 10 % DNA contamination was sent to Azenta Life Sciences/GENEWIZ (UK).

RNA depletion, library preparation and sequencing: depletion of ribosomal RNA from bacterial total RNA (using a NEBNext® rRNA Depletion Kit (Bacteria), Cat. No. E7850X) and library preparation were performed at Azenta Life Sciences/GENEWIZ (UK). Illumina NovaSeq 2x150 bp sequencing, generating a minimum of 10 M read pairs.

RNA sequencing analysis: Raw fastq files were preprocessed using Fastp (v0.23.2) (Chen et al., 2018) and checked using FastQC (v0.72) (Andrews, 2010). The hybrid assemblies were annotated with Prokka (v1.14.5) (Seemann, 2014), or, when specified, with Bakta (v1.7.0) (Schwengers et al., 2021); '*.fna'* and '*.gtf';* outputs were used in the RNA sequencing analysis. The RNA fastq files were aligned to the reference using HISAT2 (v2.1.0) (Kim et al., 2015) and checked by SAMtools-stats (v2.0.2) (Li et al., 2009). Gene expression was measured using the HISAT2 alignment file and GTF format in featureCounts (v1.6.3) (Liao et al., 2014). To then identify differentially expressed genes (DEGs), with a false discovery rate (FDR < 0.05) and a $\log_2$ fold change (LFC ≥ 2), the featureCounts were ran using DESeq2 (v2.11.40.4) (Love et al., 2014) with the count data from the CHX, OCT, FM104 exposed experiments compared

to the control. The '*.gtf*' file was used as the reference in Annotate DESeq2 (v1.1.0) (Love et al., 2014) to annotate the geneID used in featureCounts and to provide the '*locus tag*', '*gene*' and '*product names*'.

2.14. Characterisation of selected evolved isolates with FakA mutations

To further identify the role of FakA/Dak2 in biocide tolerance for both Gram-positive pathogens, we characterised six evolved isolates with SNPs in different regions of *fakA*. To observe how conserved the positions where changes in *S. aureus* FakA were in other related Gram-positive bacteria we retrieved homologous sequences from the NCBI database using BLAST (searching against taxID 1239, excluding staphylococci) (Altschul et al., 1990) before alignments of FakA sequences were performed. Sequences were uploaded into ClustalW (v1.2.4) (Sievers et al., 2011) for multiple sequence alignment and sequence logos were then generated with WebLogo (v3.7.12) (Schneider and Stephens, 1990; Crooks et al., 2004) for 100 sequences. Predicted structure from both proteins was visualised using AlphaFold DB (v.2022-11-01) (Jumper et al., 2021; Varadi et al., 2022), and STRING (v12.0; https://string-db.org/) (Szklarczyk et al., 2023) used to generate *fakA* occurrence profiles across genomes.

Ethidium bromide assay: To measure potential changes in membrane permeability between the wild-types and the six evolved isolates with *fakA* mutations, ethidium bromide accumulation was measured. Overnight cultures in MH were prepared in triplicate and incubated at 37°C. These were diluted 1:200 in MH and incubated at 37 °C at 200 rpm until cultures reached mid log phase (OD_{600nm} = 0.2). Cultures were then exposed at room temperature for 30 minutes at ½ MIC of CHX, OCT and FM104; cells with no stress were included as controls. Tubes were centrifuged at 4000 rpm at 4 °C for 10 minutes, and pellets were resuspended in a volume of sterile PBS to normalise cultures (OD_{600nm} = 0.1). In a 96-well plate, 20 µL of ethidium bromide (to give a final concentration of 10 µM/well) and 180 µL of the cell suspensions were added to each well in triplicate. Positive control (dead cells, which were 70 % ethanol-lysed cells) and negative controls (PBS + ethidium bromide) were also included. Fluorescence (Excitation: 301 nm, Emission: 603 nm) was measured using a BMG LABTECH microplate reader (CLARIOstar®) over 6 hours with reads taken every 5 minutes. Graphs represent accumulation after 2 h 30 minutes of incubation representing a steady state.

Transmission electron microscopy: To study cellular morphology, strains with *fakA* mutations and parent strains of both species were prepared for transmission electron microscopy (TEM).

Cells were grown overnight in 5 mL glass tubes in TSB and incubated at 37 °C. Cells were centrifuged at 3000 rpm for 15 minutes (at 4 °C). Media was removed from pelleted cells which were fixed immediately with 2.5 % glutaraldehyde (Agar Scientific, UK) in 0.1 M sodium cacodylate (Agar Scientific, UK) buffer (pH 7.2) and left for 2 hours at room temperature. The fixative was replaced with 0.1 M sodium cacodylate buffer (pH 7.2). After 2 further washes with cacodylate buffer, the cell pellet was mixed with a small amount of molten aqueous 2 % low gelling temperature agarose (TypeVII, A-4018, Sigma-Aldrich, UK), which was solidified by chilling and then cut into small pieces, approximately 1 mm^3, with a razor blade. These pieces were post-fixed in 1 % aqueous osmium tetroxide (Agar Scientific, UK) for 2 hours then dehydrated through an ethanol series (30 %, 50 %, 70 %, 80 %, 90 % and 3X 100 % dry ethanol for 15 minutes each). After the final 100 % dry ethanol treatment, samples were infiltrated with LR White medium grade resin (Agar Scientific, UK) for 1 hour each in 1:1, 2:1 and 3:1 mixes of LR White resin to 100 % ethanol and finally with 100 % resin, also for 1 hour. After a 100 % resin change, the sample pieces were further infiltrated overnight on a rotator. The resin was removed and a 3rd portion of 100 % LR White was added before samples were returned to the rotator for 3 - 4 hours. Then 4X pieces from each sample were each put into their own BEEM capsule with fresh resin and polymerised at 60 °C overnight (20 - 24 hours) in the oven in a fume hood. The polymerised resin was left for another 24 hours to fully cure. 90 nm thick sections were cut using a Leica UC6 ultramicrotome with a glass knife, collected on carbon coated copper grids (EM Resolutions, UK), and stained sequentially with 2 % aqueous uranyl acetate (BDH, UK) and 0.5 % aqueous lead citrate (Sigma-Aldrich, UK). Sections were examined and imaged in an FEI Talos F200C transmission electron microscope at 200 kV.

2.15. Attempts to create a defined *fakA* mutant

A molecular cloning strategy to construct a *fakA* deletion mutant (Bose et al., 2014, 2013) was attempted following two different approaches (as described in **Chapter 6**). In this chapter, the materials and molecular biology methods used for construction of deletion mutants in *E. coli* (Step 1) and intermediate strain *S. aureus* RN4220 (Step 2) are described.

The final step of introducing the constructs into the selected *S. aureus* isolate (*S. aureus* ST188) was not performed.

2.15.1. Plasmids

pKOR1-mcs plasmid (Addgene plasmid #181755; http://n2t.net/addgene:181755; RRID: Addgene_181755; gift from Suzan Rooijakkers) was used. This is a modified vector from pKOR1 (Bae and Schneewind, 2006) and acts as a shuttle vector allowing creation of constructs in *E. coli* then delivery into staphylococci (Stapels et al., 2014). To check transformation efficiency, pUC19 vector (Yanisch-Perron et al., 1984) (New England Biolabs, UK; supplied with C2987I) was used as a positive control.

Plasmids delivered in bacterial stabs were recovered by spreading them onto a LB agar plate with carbenicillin (100 µg/mL) and were incubated at 37 ℃ and purified. For validation, plasmids constructs and vectors were sequenced by PlasmidsNG (UK) using R10.4.1 ONT long-read plasmid sequencing.

2.15.2. Restriction enzymes

Restriction enzymes (ApaI, KpnI, SacI and XmaI) and buffers (rCutSmart™ Buffer) were purchased from New England Biolabs, UK.

2.15.3. Primers

Oligonucleotides were designed using SnapGene® software (from Dotmatics; available at: www.snapgene.com). Primers (10 pmol/µL) were used and prepared from the 100 pmol/µL stocks (synthetised by Eurofins, UK). Complete list of primers available in **APPENDIX IV**.

2.15.4. Plasmid DNA purification

Plasmid DNA was isolated using NucleoSpin® Plasmid kit (Macherey-Nagel, 740588.50). To increase plasmid DNA yield, purification from 100 mL of overnight cultures were performed using ZymoPURE™ II Plasmid Midiprep Kits (Zymo Research, UK, Cat. No: D4200-A and D4200-B) following manufacturer's instructions. The eluted DNA concentration was measured using Qubit DNA Broad Range assay kit (Thermo Fisher Scientific, UK, Q32853). For step 2, isolation of low-copy plasmid in RN4220 was performed following Macherey-Nagel

(07/2021, Rev.12) as per manufacturer instructions using NucleoSpin® Plasmid kit (Macherey-Nagel, 740588.50) with a modification by adding 100 µL of 0.5 mg/mL lysostaphin (from *Staphylococcus staphylolyticus,* Merck, UK), and incubated at 37 ℃ for 1 hour before the cell lysis step.

2.15.5. Polymerase chain reaction

PCR reactions were performed using Veriti™ thermal cycler (Thermo Fisher Scientific, UK), following different programmes (**APPENDIX V**). PCR products were stored at -20 °C.

Gene amplification: PCR reaction (total volume 50 µL) consisted of 1 µL bacterial template DNA, 2.5 µL of each primer, 25 µL NEBNext® Ultra™ II Q5® Master Mix (New England Biolabs, M0544S) and 19 µL of double distilled and deionised water (Sigma-Aldrich, UK, W4502).

Colony PCR: To verify that the desired genetic construct was present, transformed colonies (10 - 20) were picked with a toothpick from the plates. Colonies were added into 100 µL of ddH_20 and boiled in an Eppendorf tube at 100 °C for 5 minutes, then centrifuged at 11,000 g for 1 minute. PCR reaction (total volume 10 µL) consisted of 4 µL of the selected colony, 0.5 µL of each primer and 5 µL of GoTaq® G2 Green Master Mix (Promega, M7822).

2.15.6. Agarose gel electrophoresis

Agarose gels were prepared at 1 % with 1xTBE buffer (Sigma-Aldrich, UK). SYBR™ Green (Invitrogen by Thermo Fisher Scientific, UK) used as a nucleic acid staining reagent and 1 kb DNA ladder (New England Biolabs, UK) used to measure the band size. Gel loading dye (New England Biolabs, UK) was used as per manufacturer's instructions. Gels were usually run in Mini-Sub cell GT systems (BioRad, UK) at 120 V, 400 A for 30 minutes.

2.15.7. DNA extraction and purification

DNA extraction from PCR products/agarose gels: DNA was cleaned using NucleoSpin® Gel and PCR Clean-up kit (Macherey-Nagel, 740609.50), following the manufacturer's instructions. DNA extraction from PCR products was performed, except in some cases where extraction was performed directly from agarose gels.

Phenol-chloroform: As an alternative method, phenol-chloroform extraction was used for DNA purification in specific cases. DNA was mixed with equal volumes of phenol chloroform solution (Sigma Aldrich), vortexed and centrifuged at 13,000 rpm for 2 minutes. The upper layer containing DNA was transferred into a new Eppendorf tube and used for ethanol precipitation.

For the ethanol precipitation step, 100 µL of DNA were mixed with: 4 µL of magnesium chloride (1 M $MgCl_2$), 40 µL of sodium acetate (3 M NaOAc) and 888 µL of ice cold 100 % (v/v) ethanol. The mixture was centrifuged for 10 minutes (at 4 °C), and the supernatant removed. Then, the pellet was washed with 1 mL of ice cold 100 % (v/v) ethanol and centrifuged again for 10 minutes (at 4 °C). The new pellet was dried in the Savant SpeedVac™ SC110 vacuum for 45 minutes. Finally, pellet was resuspended in 80 µL of distilled water.

2.15.8. Restriction digests

To set up restriction digests, reactions usually performed in a total volume of 50 µL with 5 µL of rCutSmart® buffer, 1 µL of each restriction enzyme and different volumes of DNA depending on the concentration. In some cases, reactions had a total volume of 200 µL. For confirmation steps, small scale digestions of 10 µL were done. Most reactions were set at one-hour incubation at 37 °C, unless otherwise stated. Before ligation, dephosphorylation of 5' ends of DNA using Quick CIP (NEB, UK) was performed to the digested plasmids in a total volume of 100 µL for 4 - 6 hours at 37 °C. DNA was cleaned using NucleoSpin® Gel and PCR Clean-up kit before ligation.

2.15.9. Ligation and transformation

Ligation: Molar ratios of 1:3 and 1:5 vector to insert were used per ligation mix, using T4 ligase (New England Biolabs, UK). The entire ligation mix was left on ice for 20 minutes, then incubated at room temperature for 3 hours, and back in ice. Then, 10 µL aliquots were used for transformation and 10 µL stored at room temperature.

Chemical transformation: 1 mL of chemically competent NEB® 5-alpha Competent *E. coli* (High Efficiency) from New England Biolabs, UK; C2987I) were added to 10 µL and transformed by heat shock (at 42 °C) for 2 minutes left in ice. Afterwards, 1 mL of *E. coli* S.O.C medium (New England Biolabs, UK; supplied with C2987I) was added and samples were

incubated at the shaking incubator (37 °C, 200 rpm). Culture was centrifuged at 13,000 g for 1 minute and the supernatant was removed. Finally, 100 µL of each transformation were spread on the selecting antibiotic plates and incubated at the appropriate temperature. For this first step, LB plates with carbenicillin (100 µg/mL) were incubated at 37 °C.

Transformation by electroporation: For the second step, transformation of the construct (Step 1) by electroporation into staphylococci RN4220 was performed by modifying the protocol from Grosser and Richardson (2016).

Fresh electrocompetent cells were prepared each time to ensure success. Overnights were prepared in 5mL BHI and grown overnight. Cultures were diluted 1:200 in previously warmed MH broth. Triplicate cultures (20 mL volume) were grown at 37 °C 180 rpm until the OD_{600nm} reached 0.2 - 0.3, and left in ice for 4 minutes, and centrifuged at 4 °C for 10 minutes. 2 mL of NaCl were added, and culture was centrifuged at 4 °C for 10 minutes.

A series of wash steps were repeated by sequentially adding reduced volumes of 10 % glycerol with 500 mM of sucrose (4 mL, 1.6 mL, 200 µL) and culture centrifuged at 4 °C for 10 minutes. In the last wash, the pellet was then mixed and transferred into a centrifuge tube at 10,000 rpm for 1 minute and resuspended again in 200 µL of 10 % glycerol with 500 mM of sucrose. Then this was divided into 50 µL aliquots in 1.5 mL microcentrifuge tubes and plasmid DNA was added (1 µL and 3 µL of construct) and incubated at room temperature for 20 minutes.

Cells were transferred to a 2 mm pulse cuvette (EP-202* with long electrode, Cell Projects Ltd, UK). Electroporation with GenePulser Xcell™ (Bio-Rad, UK) was performed at specific settings (Voltage: 2.2 kV, Cuvette: 2 mm, Resistance: 400 Ohm, Capacitance: 25 µF). Immediately after, cells were resuspended with 1 mL B2 recovery media (Schenk and Laddaga, 1992) and transferred into a 1.5 mL microcentrifuge tube. Cells were shaken for 3 hours (at 300 rpm, 30℃); the supernatant was discarded, and the pellet was resuspended. 100 µL were spread on TSA plates with a gradient of carbenicillin (10, 20, 40, 60 µg/mL), and plates were incubated overnight at 37 ℃.

2.16. Data visualisation and statistical analysis

Statistical analyses were performed using R (v4.1.2) and RStudio (v2021.09.2+381) (R Core Team, 2021; RStudio Team, 2021). Most figures were produced using the package ggplot2

(v3.3.5) (Wickham, 2016). All the statistical details of the experiments can be found in the figure legends.

Degust (v3.1.0) (Powell, 2013) was used for visualising RNA-Seq differential gene expression and creating multidimensional scaling (MDS) plots, heatmaps and volcano plots. Venn diagrams were generated by the web-based tool InteractiVenn (Heberle et al., 2015) with the selected parameters (adjusted *p-value* ≤ 0.05; Upregulated = $\log_2$FC ≥ 2, Downregulated = $\log_2$FC ≥ -2). For RNA-Seq data pathway analysis, iDEP (v0.96) (Ge et al., 2018) and ShinyGO (v0.80) (Xijin Ge et al., 2020) using Gene Ontology (GO) Biological Process for enrichment analysis (30 top GO pathways were selected; False discovery rate (FDR) cutoff set at < 0.05).

CHAPTER 3: IDENTIFICATION OF GENES IMPLICATED IN BIOCIDAL STRESS

"You are only as good as your controls" – Mark Webber (maybe)

3.1. Introduction

RNA-sequencing (RNA-Seq) has been widely used to study differential gene expression (Stark et al., 2019). In the field of biocides, transcriptomic studies could be useful to better understand the mechanisms of biocide tolerance/resistance, and the different pathways involved under biocidal stress.

Some examples of RNA-Seq with biocides compared the responses of Gram-negative pathogens when exposed to QACs. A study (Pereira et al., 2020) assessed transcriptomic responses to short-term and long-term exposures to different biocides in *Escherichia coli* and observed an increased expression in chaperones and antibiotic response after QAC stress for short term exposures (30 minutes). Another study with QACs analysed the transcriptomic response under BZK stress, a widely used disinfectant to control *Listeria monocytogenes* (Casey et al., 2014) in the food processing environment. Furthermore, by studying the transcriptomic response of *Acinetobacter baumanii* to CHX, a novel chlorhexidine efflux protein (AceI) was identified (Hassan et al., 2015, 2013). This AceI protein is in fact the prototype for a newly characterised family of efflux pumps (PACE) (Hassan et al., 2018), which also transport CHX among other biocides.

In this chapter, RNA-Seq was used to study how gene expression was affected when exposing two Gram-positive isolates: *S. aureus* ST188 and *E. faecalis* ST40 to commonly used biocides (CHX/OCT), and a novel biocidal formulation (FM104). The effect of exposure to low concentrations of biocides (½ MIC) was tested for 30 minutes to mimic those concentrations found in the environment after regular use/misuse of these products. In parallel, responses of 4 major staphylococcal species (*S. aureus*, *S. capitis, S. haemolyticus* and *S. epidermidis*) were also compared to identify shared genes that are rexpressed under biocidal stress.

3.2. Aims

- To identify the genes that are involved in response to biocide exposure in two common Gram-positive pathogens.
- To identify the major cellular pathways involved after exposure to unformulated biocides (CHX and OCT) and a novel biocidal product.
- To study the commonalities and differences in gene expression in four different staphylococcal species.

3.3. Results

RNA was extracted from samples exposed for 30 minutes to ½ MIC of CHX, OCT, FM104 or no biocide (control). After several optimisations, including the addition of DNA/RNA Shield for improved nucleic acid stabilization, and varying lysing times for *E. faecalis* and *S. aureus* (shorter lysis), high-purity RNA (A260/280 ratio of 1.8 - 2.2) was obtained. RNA integrity (RIN ≥ 6) and ≤ 10 % DNA contamination was achieved. A total of 24 samples (3 biological replicates/stress) were then sequenced (with a minimum of 10 M read pairs generated) and analysed as explained in **Chapter 2**.

The transcriptomic responses of *E. faecalis* ST40 and *S. aureus* ST188 when exposed to CHX, OCT and FM104 were studied (**Chapter 3**, **Section 3.3.1.**). Additionally, commonalities and differences in the transcriptomic responses of four frequently isolated staphylococcal species when exposed to CHX and OCT were also examined **Chapter 3**, **Section 3.3.2.**).

3.3.1. The transcriptomic responses of *E. faecalis* and *S. aureus* when exposed to CHX, OCT and FM104

Multidimensional scaling (MDS) plots showed clear differences between each set of the samples (**Figure 3.1.**). Similarities between the technical replicates for each stress show reproducibility of the data for the RNA-Seq experiments with both *E. faecalis* (**Figure 3.1. - A**) and *S. aureus* **Figure 3.1. - B**). Each stress conditions clustered together and was distanced from the other groups.

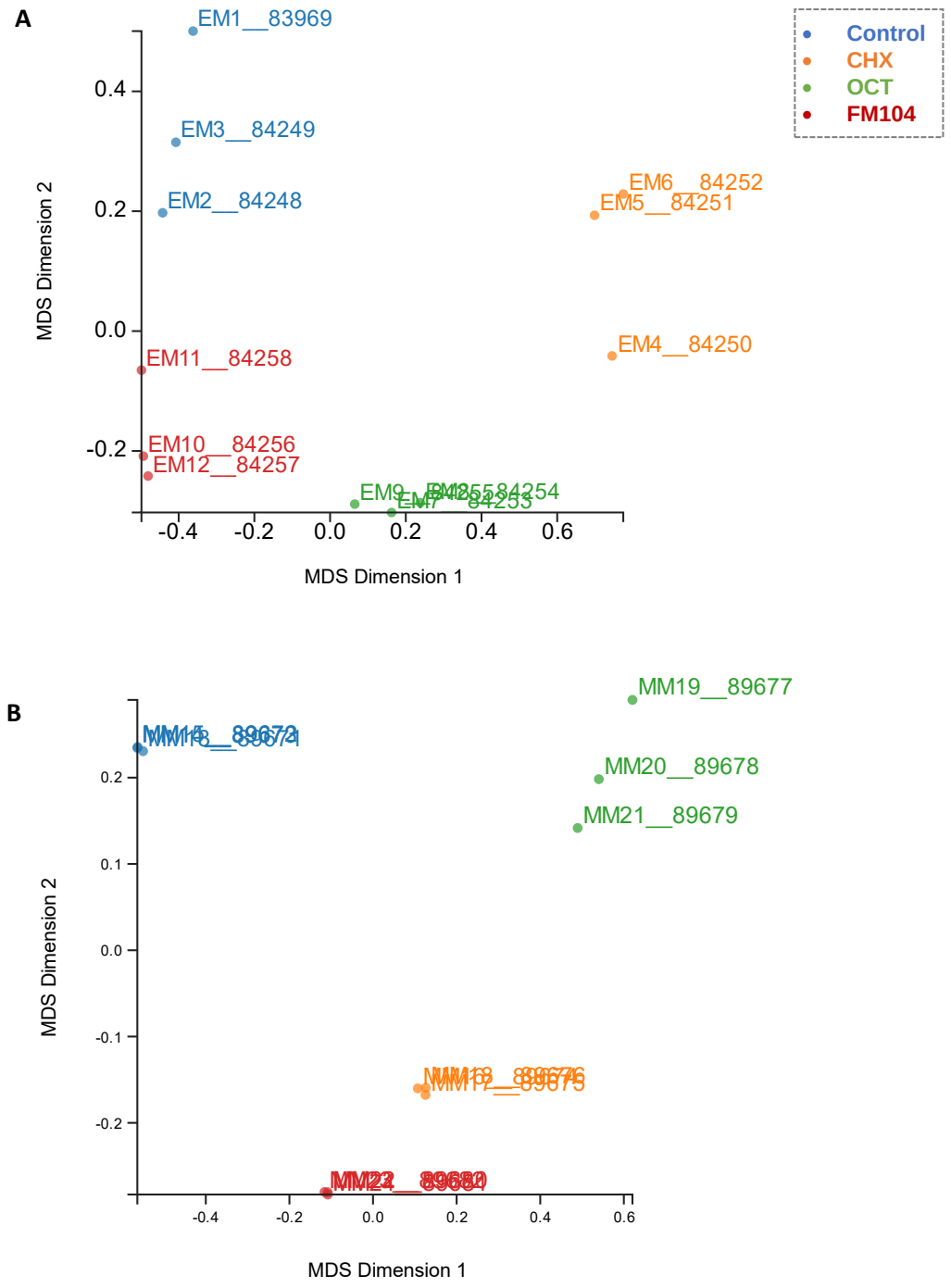

Figure 3.1. Multidimensional scaling plots of (A) *E. faecalis* ST40 and (B) *S. aureus* ST188 RNA-Seq datasets coloured by stress. Each dot represents one biological replicate. The four conditions are indicated by different colours: control (blue), CHX (orange), OCT (green) and FM104 (red). Three biological replicates are included for each condition. The X axis represents multidimensional scaling 1, and the Y axis represents the multidimensional scaling 2.

3.3.1.1. Gene expression changes in response to biocide exposure

Differences in gene expression in response to different stresses (CHX, OCT, FM104) were observed in *E. faecalis* ST40 and *S. aureus* ST188.

Gene expression changes in *E. faecalis* ST40: under CHX stress (**Figure 3.2. - A**), many genes were differentially expressed at statistically significant levels (FDR < 0.05; $\log_2$ fold change (LFC) ≥ 2). Focusing on the major hits significantly upregulated, there were four genes with a LFC more than 4: the serine protease Do-like *htrA* (6.27 LFC), polyisoprenyl-teichoic acid-peptidoglycan teichoic acid transferase *tagU* (7.25 LFC) and the HTH-type transcriptional regulators involved in the metabolism of cyanate *cynR_1* (7.17 LFC) and *cynR_2* (7.91 LFC).

There were three highly downregulated genes under CHX stress, with the highest $\log_2$ fold change (-8 LFC), belonging to a family of putative ABC transporter ATP-binding proteins. Significantly downregulated by more than 4-fold genes under CHX stress included the inner membrane ABC transporter permease *ydcV* (-4.49 LFC), sulfate/thiosulfate import ATP-binding *cysA* (-4.08 LFC) and the putrescine-binding periplasmic protein *spud* (-4.04 LFC). Additionally, glutaconyl-CoA decarboxylase subunit gamma *gcdC* (-3.82 LFC) and adenine deaminase *ade* (-3.66 LFC) were also significantly downregulated under CHX exposure.

For *E. faecalis* genes upregulated under OCT stress (**Figure 3.2. - B**), the top hits with the highest $\log_2$ fold change were the polyisoprenyl-teichoic acid–peptidoglycan teichoic acid transferase *tagU* (5.58 LFC), *lemA* (5.68 LFC) and *cynR_2* (5.42 LFC). Both *tagU* and *cynR_2* were also upregulated under CHX stress. Other genes that were also significantly upregulated under OCT stress were the niacin transporter *niaX* (4.13 LFC) and riboflavin transporter *fmnP* (3.71 LFC) at the bottom.

The downregulated hits under OCT stress included the PTS system fructose-specific EIIABC component *fruA* (-5.68 LFC) with the highest $\log_2$ fold change and tagatose-6-phosphate kinase *lacC* (-4.48 LFC). Other genes with a high $\log_2$ fold change were the guanine/hypoxanthine permease *pbuO* (-2.81 LFC), inner membrane ABC transporter permease *ydcV* (-3.68 LFC), glucitol operon repressor *srlR* (-3.64 LFC), adenine deaminase *ade* (-3.70 LFC) and melamine deaminase *triA* (-3.38 LFC). Interestingly, *ade, ydcV, cysA* and *spud*, identified in the CHX dataset, were also significantly downregulated under CHX stress.

While studying changes of gene expression in *E. faecalis* under ½ exposure to FM104 (**Figure 3.2. - C**), a cluster of genes. These upregulated genes highly expressed included many uncharacterised hits, and genes including hydroxycarboxylate dehydrogenase *hcxA* (4.13

LFC), aryl-phospho-beta-D-glucosidase *bglH* (3.15 LFC) and the PTS system lactose-specific EIIA component *lacF* (3.21 LFC) with the highest log_2 fold changes. Other highly significant upregulated genes included the PTS system 2-O-alpha-mannosyl-D-glycerate-specific EIIABC component *mngA* (3.58 LFC), trehalose transport system permease *sugB* (2.94 LFC), PTS system mannose-specific EIID component *manZ* (2.56 LFC) and the riboflavin transporter *fmnP* (2.75 LFC). The riboflavin transporter *fmnP* was also observed under OCT stress, but no other common hits were shared with the other stresses.

Fewer genes were significantly downregulated under ½ MIC exposure to FM104, in fact, there were only 7 differentially expressed genes. The major hit (-3.17 LFC) was uncharacterised followed by another major hit, the central glycolytic genes regulator *cggR* (-2.41 LFC) observed to be downregulated.

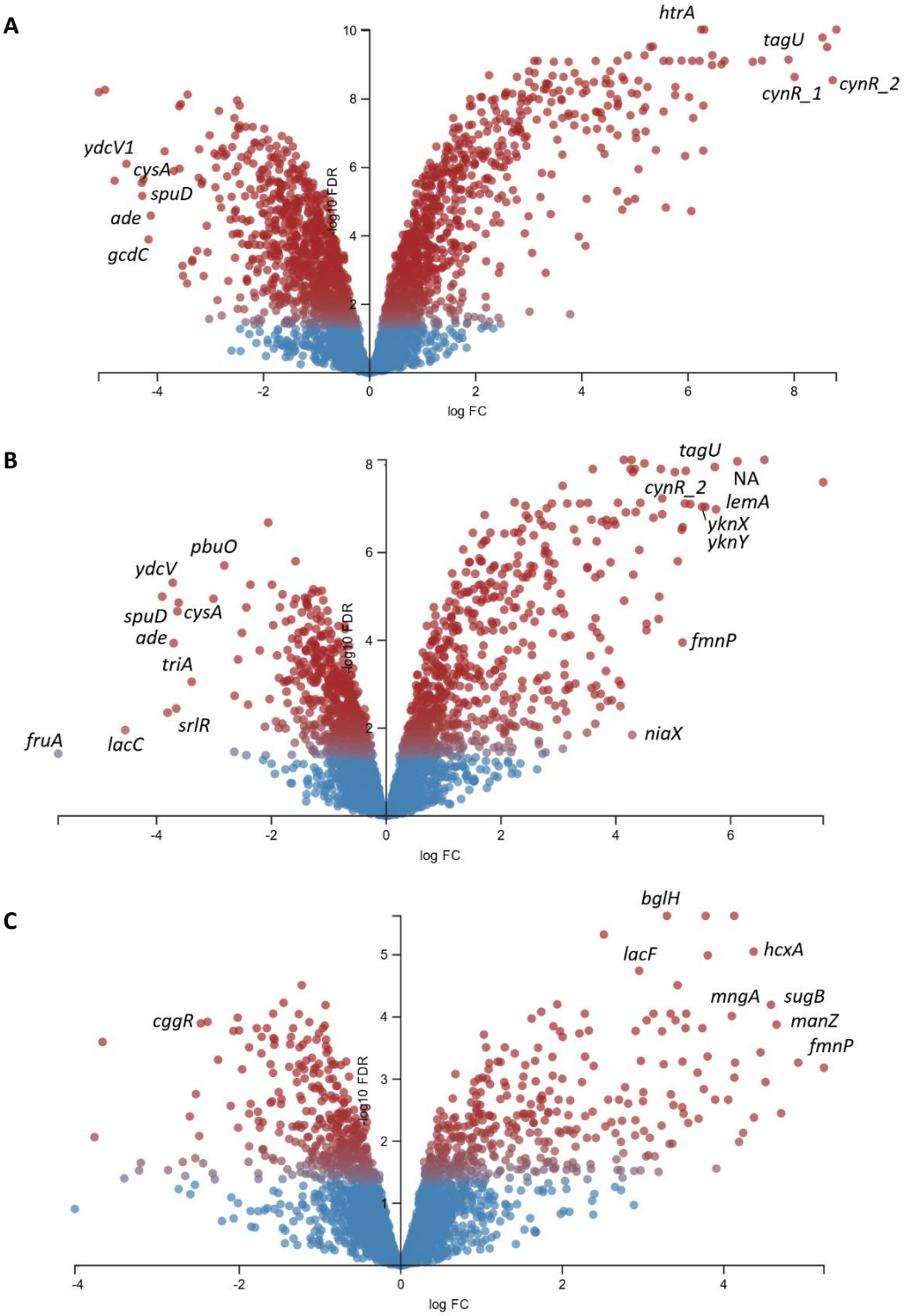

Figure 3.2. Volcano plots showing feature counts of *E. faecalis* when exposed to ½ MIC of (A) CHX; (B) OCT; (C) FM104. Y axis represents false discovery rate ($-\log_{10}$ FDR) and X axis fold change ($\log_2$ FC) and normalised to the control condition in Degust (v3.1.0). Each dot is a gene (n = 3051); Upregulated genes are on the right and downregulated on the left; red shows more significant FDR (FDR < 0.05) and blue less significant FDR. Function uncharacterised (FUN) genes not shown.

A summary of the parameters of selected statistically significant and differentially expressed hits are shown in **Table 3.1.**

Table 3.1. Selected hits from the volcano plots for *E. faecalis* ST40 under biocide stress.

Gene name	Log_2 fold change (LFC)	Adjusted *p-value*	Stress exposure
Downregulated			
ade	-3.66; -3.70	9.63E-12; 9.16E-53	CHX; OCT
cggR	-2.41	9.40E-26	FM104
cysA	-4.08; -3.60	6.29E-25; 1.36E-55	CHX; OCT
gcdC	-3.82	8.63E-12	CHX
fruA	-5.68	0	OCT
lacC	-4.48	3.26E-132	OCT
pbuO	-2.81	1.19E-66	OCT
spuD	-4.04, -3.64	1.28E-19; 1.76E-54	CHX; OCT
srlR	-3.64	1.23E-90	OCT
triA	-3.38	2.8-E-34	OCT
ydcV	-4.49; -3.68	9.86E-47; 5.54E-65	CHX; OCT
Upregulated			
bglH	3.15	1.48E-37	FM104
cynR_1	7.17	6.44e-126	CHX
cynR_2	7.91; 5.42	3.36E-130; 2.18E-133	CHX; OCT
fmnP	3.71	9.29e-07	OCT; FM104
hcxA	4.13	3.92E-46	FM104
htrA	6.27	2.48E-294	CHX
lacF	3.21	1.09E-28	FM104
lemA	5.68	2.42E-98	OCT
manZ	2.56	0.00014	FM104
mngA	3.58	4.23E-22	FM104
niaX	4.13	9.35E-67	OCT
sugB	2.94	2.30E-06	FM104
tagU	7.25; 5.58	4.08E-188; 4.16E-134	CHX; OCT
yknX	5.41	6.90E-97	OCT
yknY	5.07	2.84E-92	OCT

Gene expression changes in *S. aureus* ST188: under CHX stress, as observed in the volcano plot (**Figure 3.3. - A**), there were two highly upregulated genes: pyruvate formate-lyase-activating enzyme *pflA* (6.67 LFC) and formate acetyltransferase *pflB* (5.18 LFC). Other upregulated genes included the ATP-dependent Clp protease ATP-binding subunit *clpL* (3.96 LFC), and two genes from the *nar* cluster: a respiratory nitrate reductase 1 beta chain *narH* (4.93 LFC) and a putative nitrate transportase *narT* (4.29 LFC). Two genes from the *nas* cluster, an uroporphyrinogen-III C-methyltransferase *nasF* (4.55 LFC) and assimilatory nitrite reductase [NAD(P)H] small subunit *nasE* (4.79 LFC) were also significantlly upregulated under CHX stress.

Other significantly upregulated genes under CHX stress were part of the *ilv* cluster, especifically from L-valine biosynthesis: the acetolactate synthase large subunit *ilvB* (4.17 LFC), dihydroxy-acid dehydratase *ilvD* (4.16 LFC), ketol-acid reductoisomerase (NADP(+)) *ilvC* (4.78 LFC), and the acetolactate synthase small subunit *ilvH* (4.05 LFC). Additionally, two leucine biosynthetic genes were also found to be highly upregulated under CHX stress: 2-isopropylmalate synthase *leuA* (4.43 LFC) and 3-isopropylmalate dehydrogenase *leuB* (4.04 LFC).

Genes that were downregulated in *S. aureus* under CHX stress were the staphylococcal secretory antigen *ssA* (-4.38 LFC), N-acetylmuramoyl-L-alanine amidase *sle1* (-4.01 LFC) and the putative oxidoreductase *catD* (-3.36 LFC).

Under OCT stress (**Figure 3.3. - B**), the genes that were most significant and showed the highest differential expression were a putative HTH-type transcriptional regulator (7.95 LFC) and staphylococcal secretory antigen *ssaA* (-5.96 LFC), the latter also highly downregulated under CHX stress.

Significantly upregulated genes under OCT stress included the putative aldehyde dehydrogenase *aldA* (4.91 LFC), genes from the *ilv* operon: *ilvC* (6.91 LFC), *ilvH* (6.26 LFC), *ilvB* (5.08 LFC), *ilvD* (4.68 LFC), *ilvA* (5.44 LFC), and the *leu* operon: *leuA* (6.58 LFC), *leuB* (6.10 LFC), *leuC* (5.99 LFC) and the aspartokinase *lysC* (6.28 LFC). Additionally, genes from the lysine biosynthesis DAP pathway (*dapA, dapB, dapH*) were also upregulated by 5 LFC.

Among the significantly downregulated genes under OCT stress, those with a LFC higher than 2 included the putative transglycosylase *isaA* (-4.45 LFC), N-acetylmuramoyl-L-alanine amidase *sle1* (-4.01 LFC), the staphylopine synthase *cntM* (-4.69 LFC), the putative oxidoreductase *catD* (3.67 LFC) and the glycine betaine transporter *opuD* (-3.56 LFC).

Studying changes of gene expression in *S. aureus* under ½ exposure to FM104 (**Figure 3.3. - C**), was observed that most significantly upregulated hits were from the *pfl* cluster: *pflA* (7.13 LFC) and *pflB* (5.73 LFC), the *nas* operon: *nasE* (6.09 LFC), *nasF* (5.90 LFC), *nasD* (4.76 LFC), *narxX* (4 LFC) and *nar* operon: *narT* (5.35 LFC), *narH* (6.06 LFC) and *narG* (4.65 LFC). Furthermore, the L-lactate dehydrogenase 1 *ldh1* (4.03 LFC) and the ATP-dependent Clp protease ATP-binding subunit *clpL* (4.00 LFC) were also significantly upregulated.

A total of three genes were significantly downregulated: the aerobic glycerol-3-phosphate dehydrogenase *glpD* (-2.35 LFC), staphylopine synthase *cntM* (-2.14 LFC) and putative transglycosylase *sceD* (-2.07 LFC).

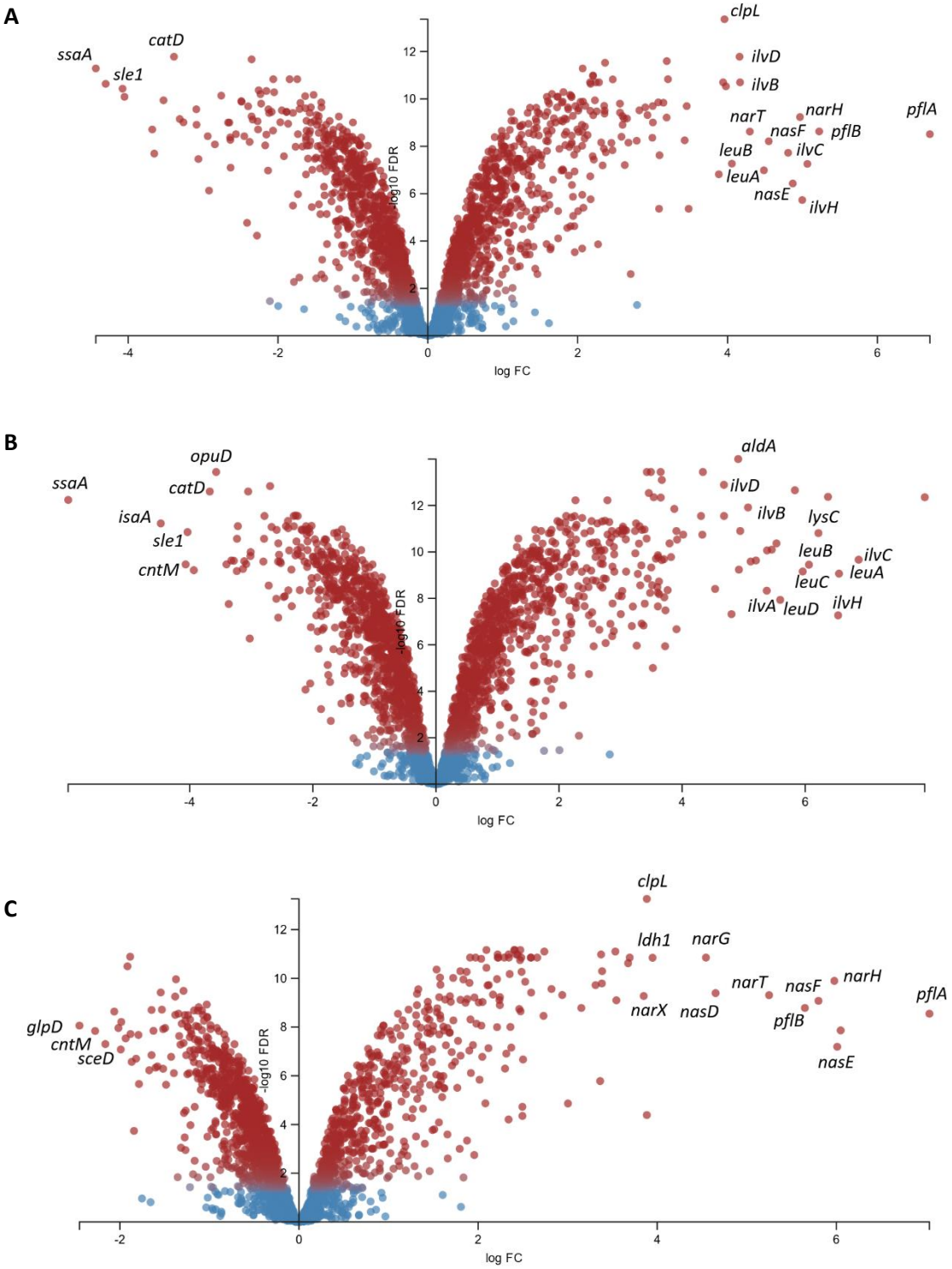

Figure 3.3. Volcano plots showing feature counts of *S. aureus* when exposed to ½ MIC of (A) CHX; (B) OCT; (C) FM104. Y axis represents false discovery rate ($-\log_{10}$ FDR) and X axis fold change ($\log_2$ FC) and normalised to the control condition in Degust (v3.1.0). Each dot is a gene (n = 2542); Upregulated genes are on the right and downregulated on the left; red shows more significant FDR (FDR < 0.05) and blue less significant FDR. Function uncharacterised (FUN) genes not shown.

A summary of the parameters of selected statistically significant and differentially expressed hits are shown in **Table 3.2.**

Table 3.2. Selected hits from the volcano plots for *S. aureus* ST188 under biocide stress.

Gene name	Log_2 fold change (LFC)	Adjusted *p-value*	Stress exposure
Downregulated			
catD	-3.36; 3.67	2.49E-299; 9.12E-261	CHX; OCT
cntM	-4.05; -2.14	4.69E-112; 6.11E-43	OCT, FM104
glpD	-2.35	3.73E-155	FM104
isaA	-4.45	3.24E-212	OCT
opuD	-3.56	0	OCT
sceD	-2.07	1.58E-69	FM104
sle1	-4.02; -4.01	1.25E-225; 2.03E-197	CHX; OCT
ssaA	-4.38; -5.96	0; 0	CHX; OCT
Upregulated			
aldA	4.91	0	OCT
clpL	3.96; 3.98	0; 0	CHX; FM104
ilvA	5.44	8.80E-141	OCT
ilvB	4.17; 5.08	0; 0	CHX; OCT
ilvC	4.78; 6.91	3.04E-220; 1.46E-251	CHX; OCT
ilvD	4.16; 4.68	0; 0	CHX; OCT
ilvH	4.05; 6.26	2.10E-14; 2.84E-23	CHX; OCT
ldh1	4.03	1.12E-88	FM104
leuA	4.43; 6.58	1.16E-193; 2.03E-163	CHX; OCT
leuB	4.04; 6.10	4.86E-160; 3.39E-204	CHX; OCT
leuC	5.99	2.49E-159	OCT
leuD	5.66	4.44E-125	OCT
lysC	6.28	1.95E-195	OCT
narG	4.65	0	FM104
narH	4.93; 6.06	0; 0	CHX; FM104
narT	4.29; 5.35	0; 0	CHX; FM104
narX	3.95	0	FM104
nasD	4.76	0	FM104
nasE	4.79; 6.09	3.04E-157; 7.68E-277	CHX; FM104
nasF	4.55	0	CHX
pflA	6.67; 7.13	0; 0	CHX; FM104
pflB	5.18; 5.13	0; 3.24E-181	CHX; FM104

3.3.1.2. Comparison of differentially expressed genes between *E. faecalis* and *S. aureus*

Overall, there were more upregulated than downregulated genes in both species in response to subinhibitory concentrations of biocide (**Figure 3.4.**).

Exposure to CHX resulted in a higher number of upregulated genes in *E. faecalis* ST40, while *S. aureus* ST188 had the highest number of upregulated genes following OCT exposure. Exposure to FM104 led to the lowest number of genes that were upregulated and downregulated in both species.

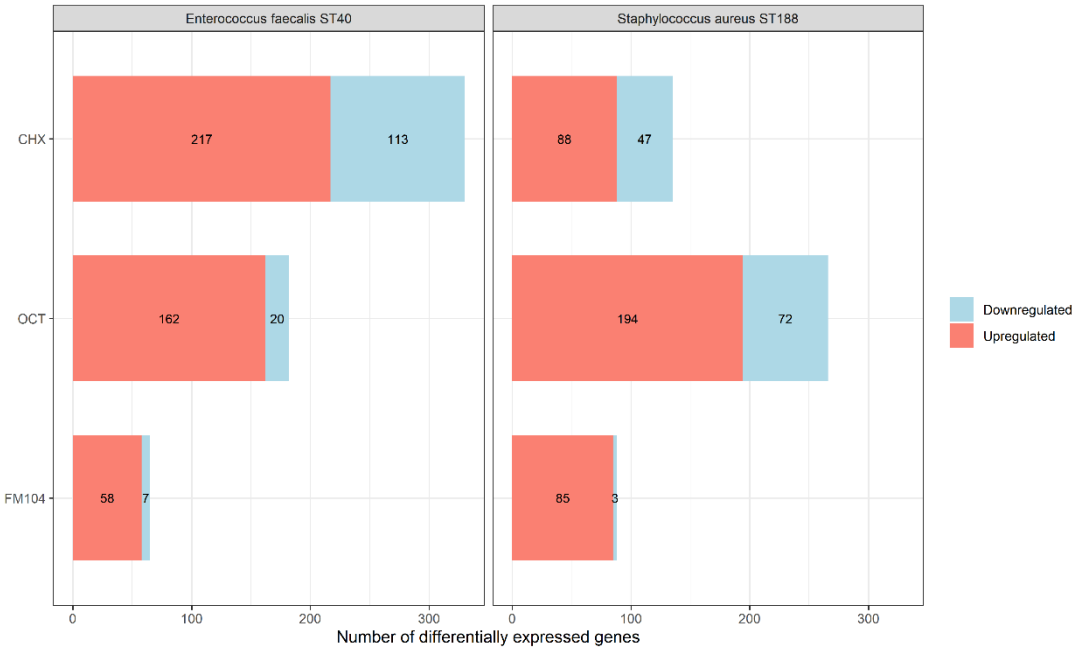

Figure 3.4. Stacked barplots showing the overall number of differentially expressed genes. DEGs for each stress (CHX, OCT, and FM104) and for each Gram-positive species are shown. Downregulated genes indicated in blue and upregulated in red.

As shown in the heatmaps (**Figure 3.5.**), responses to these agents are very distinct in both Gram-positive pathogens. There were however some common blocks of upregulated genes (red), which have higher expression in treatment, and downregulated genes (blue), which have lower expression in treatment, that were similar between 2 stresses. In *E. faecalis,* some similarities between the control and FM104 could be observed in terms of expression, whereas for CHX/OCT, even if these have a similar mode of action and are part of the same class of biocides (cationic biocides), the profile differed significantly between stresses and compared to the control. This was similarly observed in *S. aureus*.

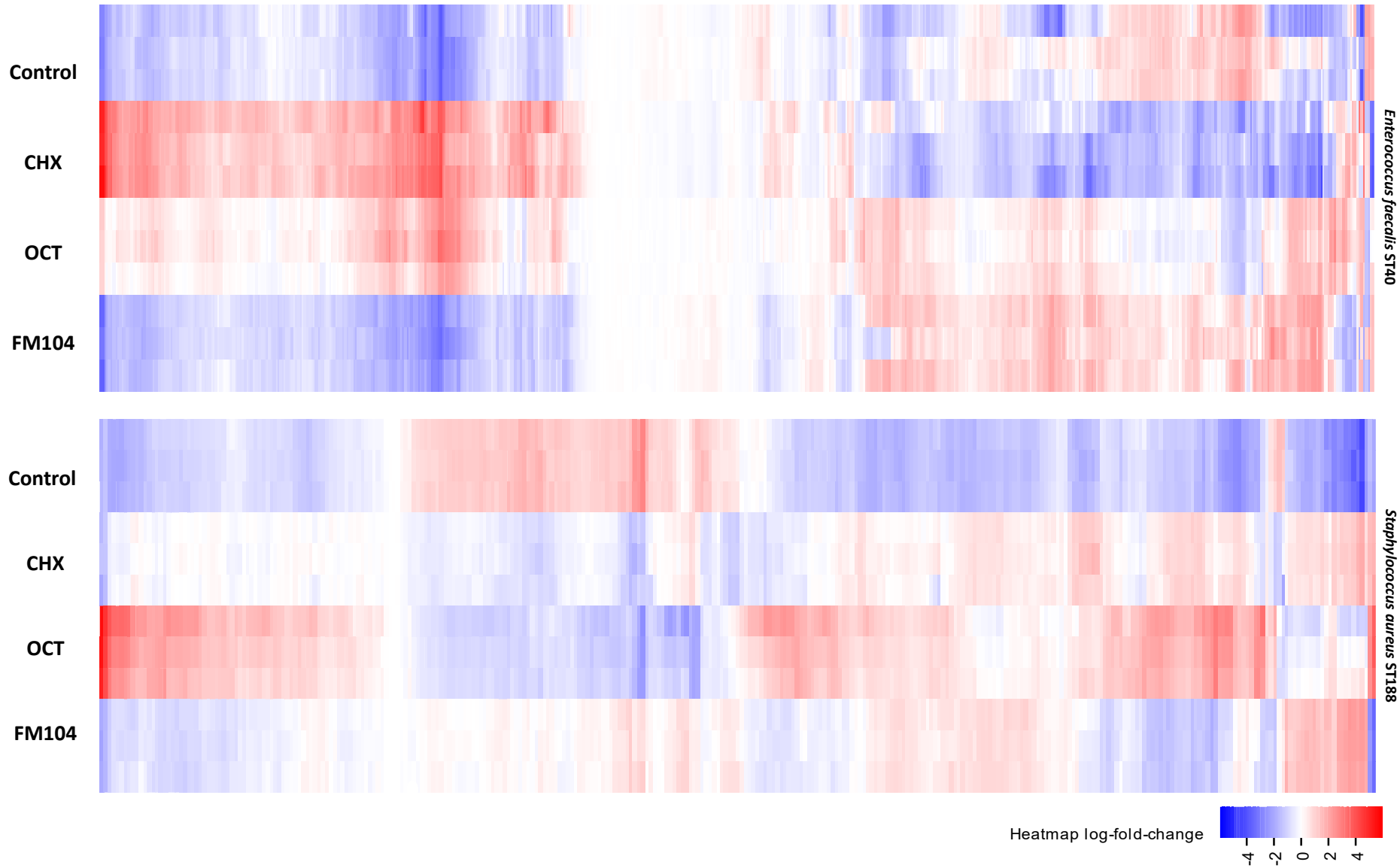

Figure 3.5. Heatmaps displaying all the significantly expressed (FDR < 0.05; LFC ≥ 2) genes for *E. faecalis* and *S. aureus* for the four tested conditions. Three biological replicates included per condition (Control, CHX, OCT, FM104); each block represents one gene. Upregulated (red) and downregulated genes (blue).

3.3.1.3. Relationship between stress responses in two clinical isolates

Links between stress responses in *E. faecalis* ST40: genes shared between all stress conditions were identified as illustrated in the Venn diagrams for *E. faecalis* ST40 (**Figure 3.6.**).

6 upregulated genes (*fmnP, niaX, thiW, thiM, thiE, thiD*) were shared between all stresses. From the upregulated genes shared between all stresses, four are part of the *thi* operon involved in thiamine biosynthesis (vitamin B1). The other two genes are both transporter genes for essential nutrients also belonging to the vitamin B group: *fmnP* for riboflavin (vitamin B2) and *niaX* for niacin (vitamin B3). There were no upregulated genes shared between CHX-FM104, and 35 upregulated genes were shared between OCT-FM104. CHX and OCT shared a total of 104 genes.

Regarding the genes with decreased expression (downregulated), only 1 gene of unknown function (*yusW*) was downregulated and shared between all stresses. OCT and FM104 shared one common gene, whereas no genes were shared between CHX and FM104. A total of 13 downregulated genes were shared between CHX and OCT (**Figure 3.6.**).

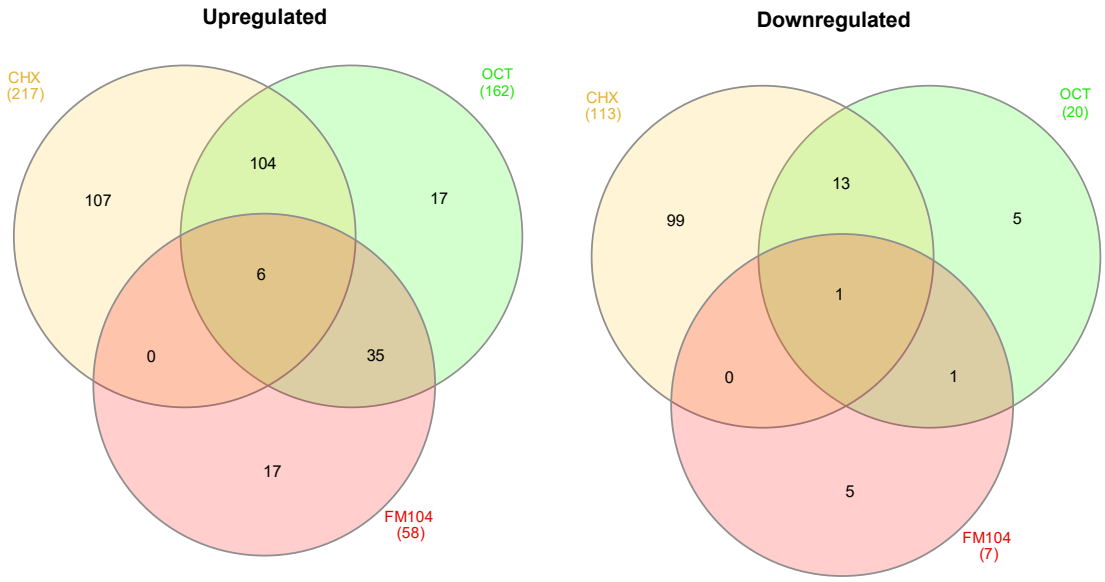

Figure 3.6. Venn diagram showing the shared and unique number of DEGs for each condition and the overlap between stresses after 30-minute exposure. Upregulated (left) and downregulated (right) in *E. faecalis* ST40. Colours represent different stresses (CHX: yellow, OCT: green, FM104: red).

To further analyse the common shared genes between two stresses, genes were classified into gene ontology (GO) biological processes.

Overall, there were 104 upregulated genes shared between CHX-OCT, 51 of those were uncharacterised. The characterised genes (**Figure 3.7.**) are involved in lipoteichoic biosynthesis and cation transport. From the 35 genes shared between OCT-FM104, most genes (n = 18) were of hypothetical function, and the other genes are mostly involved in carbohydrate and amino acid metabolism.

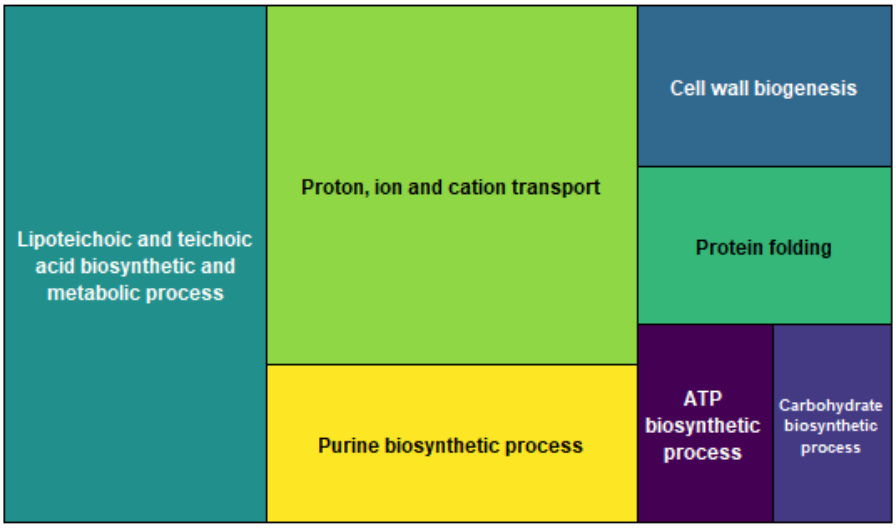

Figure 3.7. Treemap indicating the names and sizes of GO biological processes for the upregulated genes shared between CHX-OCT in *E. faecalis* ST40. Each biological process represented in a nested rectangle, and the sizes of the rectangles correspond to the number of genes in each process sorted by fold enrichment value.

From the 13 downregulated genes shared between CHX-OCT, 5 were of hypothetical function, and the rest are involved in nucleotide metabolism, transport processes (mainly sulfate/thiosulfate, polyamine and transmembrane transport), and protein degradation. The only shared gene between OCT and FM104 is a hypothetical protein.

Links between stress responses in *S. aureus* ST188: a total of 39 upregulated genes were shared between all stresses. In contrast, only 2 downregulated genes shared between the three stresses (**Figure 3.8.**).

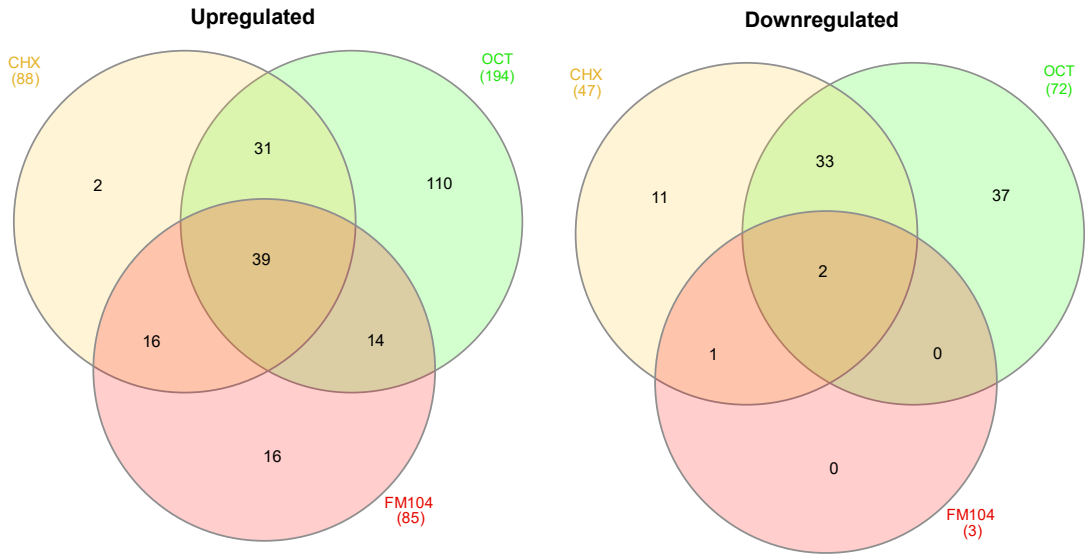

Figure 3.8. Venn diagram showing the number of DEGs for each condition and the overlap between stresses after 30-minute exposure. Upregulated (left) and downregulated (right) in *S. aureus* ST188. Colours represent different stresses (CHX: yellow, OCT: green, FM104: red).

The two downregulated genes shared between all stresses were the staphylopine synthase (*cntM*) and a putative transglycosylase (*sceD*), which are involved in metal acquisition and modification of bacterial cell wall peptidoglycan, respectively.

For the upregulated genes shared between all stresses, from the 39 upregulated genes in *S. aureus*, the majority were involved in amino acid biosynthesis from the *ilv* operon (*ilvB-H*) and *leu* operon (*leuA-D*), genes involved in nitrate metabolism (*nrtD*) and nitrite metabolism from the *nas operon (nasD-F), nar* operon (*narG, narH, narT*). Additionally, the other shared genes were involved in carbohydrate metabolism (*pflA, pflB, opuD, lctP, ldh1*) and other metabolic processes including those related to thiamine metabolism (*ydaP*), oxidative stress responses *(hmp*), aerobic respiration (*yghA, ythA*), cytolysis (*cidB*), sugar metabolism, and protein degradation (**Figure 3.9.**).

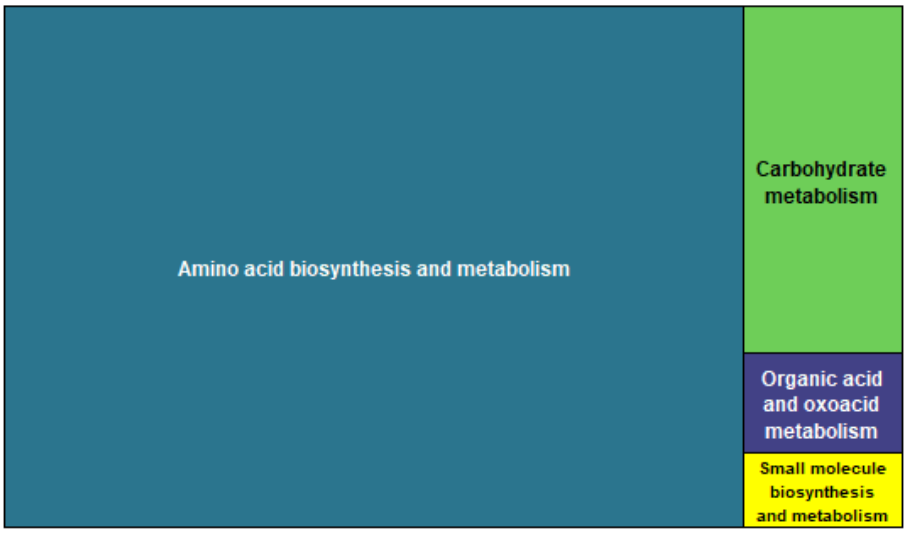

Figure 3.9. Treemap indicating the names and sizes of GO biological processes for the upregulated genes shared between all stresses (CHX-OCT-FM104) in *S. aureus* ST188. Each biological process represented in a nested rectangle, and the sizes of the rectangles correspond to the number of genes in each process sorted by fold enrichment value.

From the shared genes between 2 stresses in *S. aureus*, there were 31 upregulated and 33 downregulated (**Figure 3.8.**) genes shared between CHX-OCT. Upregulated genes shared between CHX and OCT were involved in several processes including protein folding, stress responses and amino acid biosynthesis/metabolism, which was the most common category in the set. Most downregulated genes shared between CHX-OCT were involved in metal ion transport, mainly cobalt transport.

There were 16 upregulated genes shared between CHX and FM104 (**Figure 3.8.**), and 14 upregulated genes shared between OCT and FM104 (**Figure 3.8.**). From the known functions, the 16 upregulated genes shared between CHX-FM104 are involved in nitrogen, carbohydrate and alcohol metabolism and protein signalling. The 14 upregulated genes shared between OCT-FM104 are involved in amino acid (arginine and glutamate), carbohydrate and fatty acid metabolism, and other stress responses**.**

Interestingly, OCT and FM104 did not share any downregulated genes (**Figure 3.8.**), and CHX and FM104 only shared one gene which was the aerobic glycerol-3-phosphate dehydrogenase (*glpD*).

3.3.1.4. Functional pathway analysis

To further understand which major cellular pathways were involved after biocide exposure and how many genes were present in each of those pathways, a pathway enrichment analysis was performed by searching against the GO database.

In *E. faecalis*, upregulated genes under CHX stress were categorised into different biological processes. Pathways that were significantly enriched under CHX stress (**Figure 3.10. - A**) were organic cyclic compound biosynthesis and other cellular biosynthetic processes. Under OCT stress (**Figure 3.10. - B**) thiamine biosynthesis had the highest number of genes significantly enriched. For FM104, upregulated genes were involved in thiamine and vitamin biosynthesis and metabolism, and phosphorus metabolism (**Figure 3.10. - C**).

While downregulated genes under CHX stress were mostly involved in purine transport, the main biological functions of downregulated genes under OCT stress included different metabolism processes (e.g., nucleotide, sugar, and amino-acid metabolism), ABC transporter proteins, and lipid-binding proteins. Regarding downregulated genes under FM104 stress, most of them were of hypothetical function but the 2 genes with non-hypothetical functions were involved in regulation of central glycolytic genes (*cggR*) and DNA repair and recombination (*ruvA*).

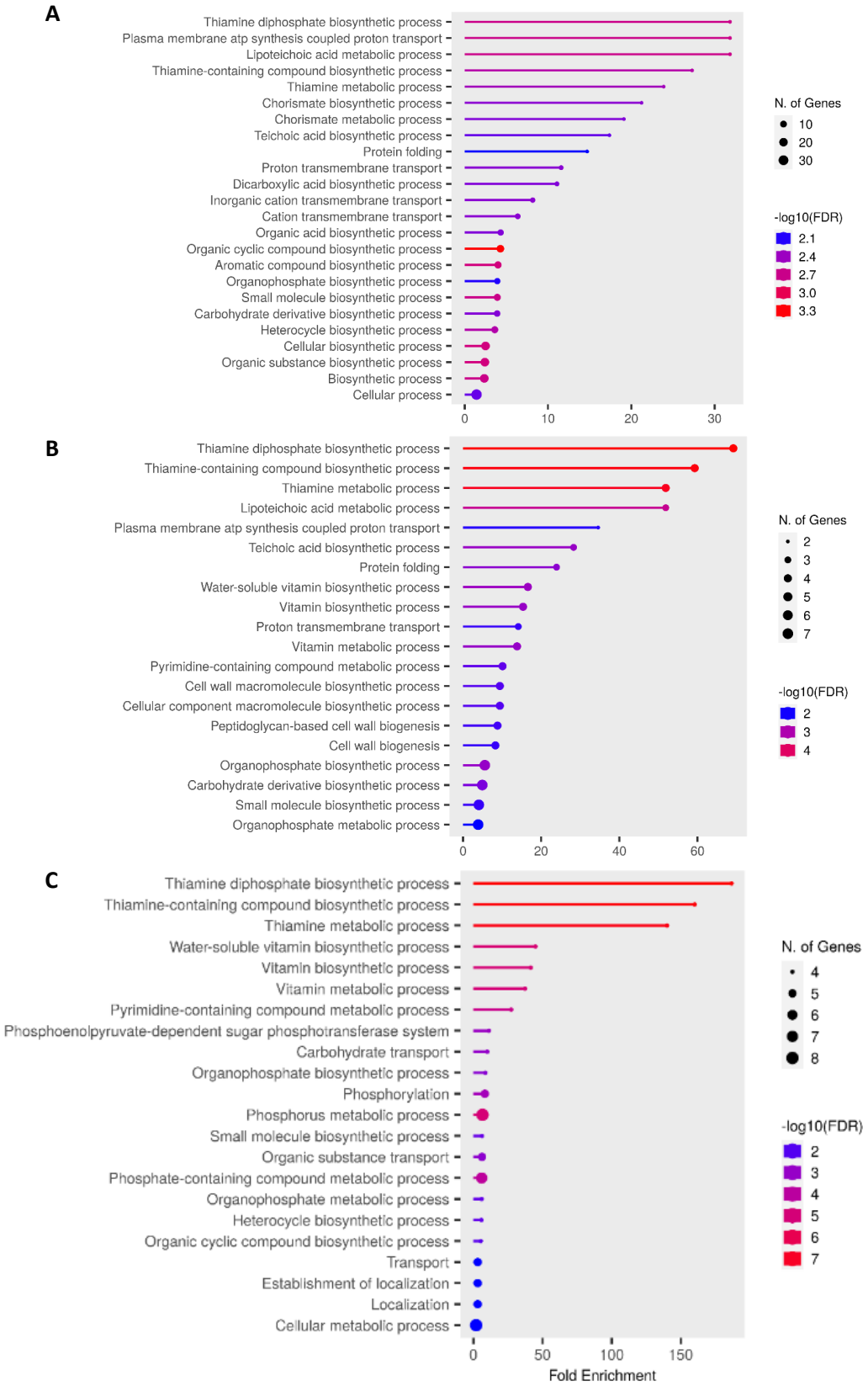

Figure 3.10. Major biological processes upregulated in *E. faecalis* ST40 with significant enrichment of gene expression after exposure to (A) CHX, (B) OCT, (C) FM104. GO Biological Processes generated using ShinyGO v0.80 (accessed March 2024). The bubble sizes indicate the number of genes, and the different colour shades represent the FDR.

In *S. aureus,* the pathway that had the highest number of upregulated and differentially expressed genes under CHX stress was branched-chain amino acid biosynthesis (**Figure 3.11.**). Downregulated genes under CHX were metal transport (e.g., cobalt, zinc, nickel, divalent metals, inorganic cations), genes involved in host-pathogen interactions and virulence (e.g., staphylococcal secretory antigen, Type VII secretion system).

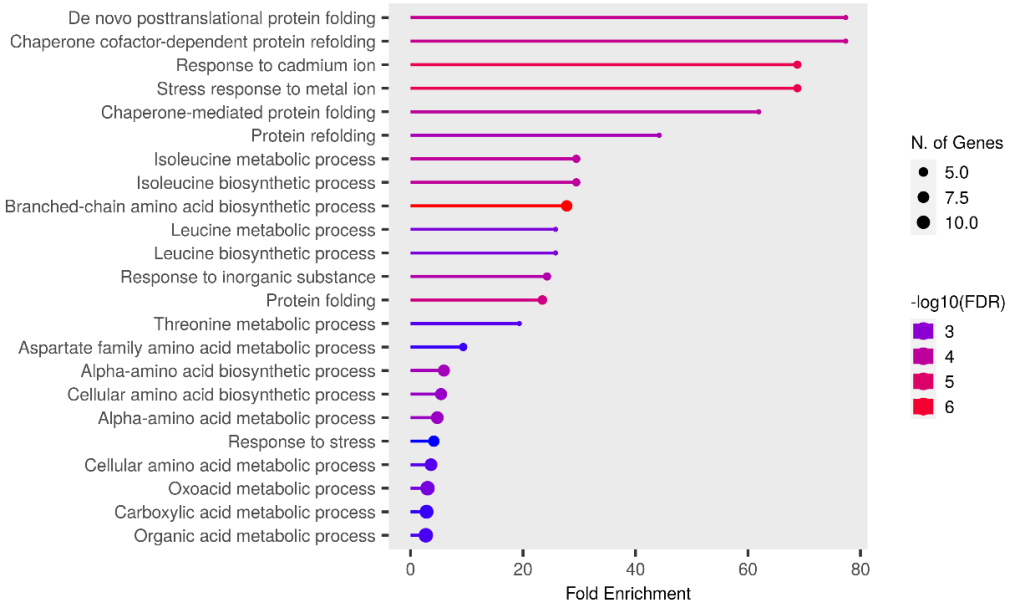

Figure 3.11. Major biological processes upregulated in *S. aureus* ST188 with significant enrichment of gene expression after exposure to CHX. GO Biological Processes generated using ShinyGO v0.80 (accessed March 2024). The bubble sizes indicate the number of genes, and the different colour shades represent the FDR.

Pathways that were significantly enriched under OCT stress in *S. aureus* were mostly involved in amino acid biosynthesis and histidine metabolic processes were upregulated (**Figure 3.12. - A**), while translation processes and metal transport were downregulated (**Figure 3.12. - B**).

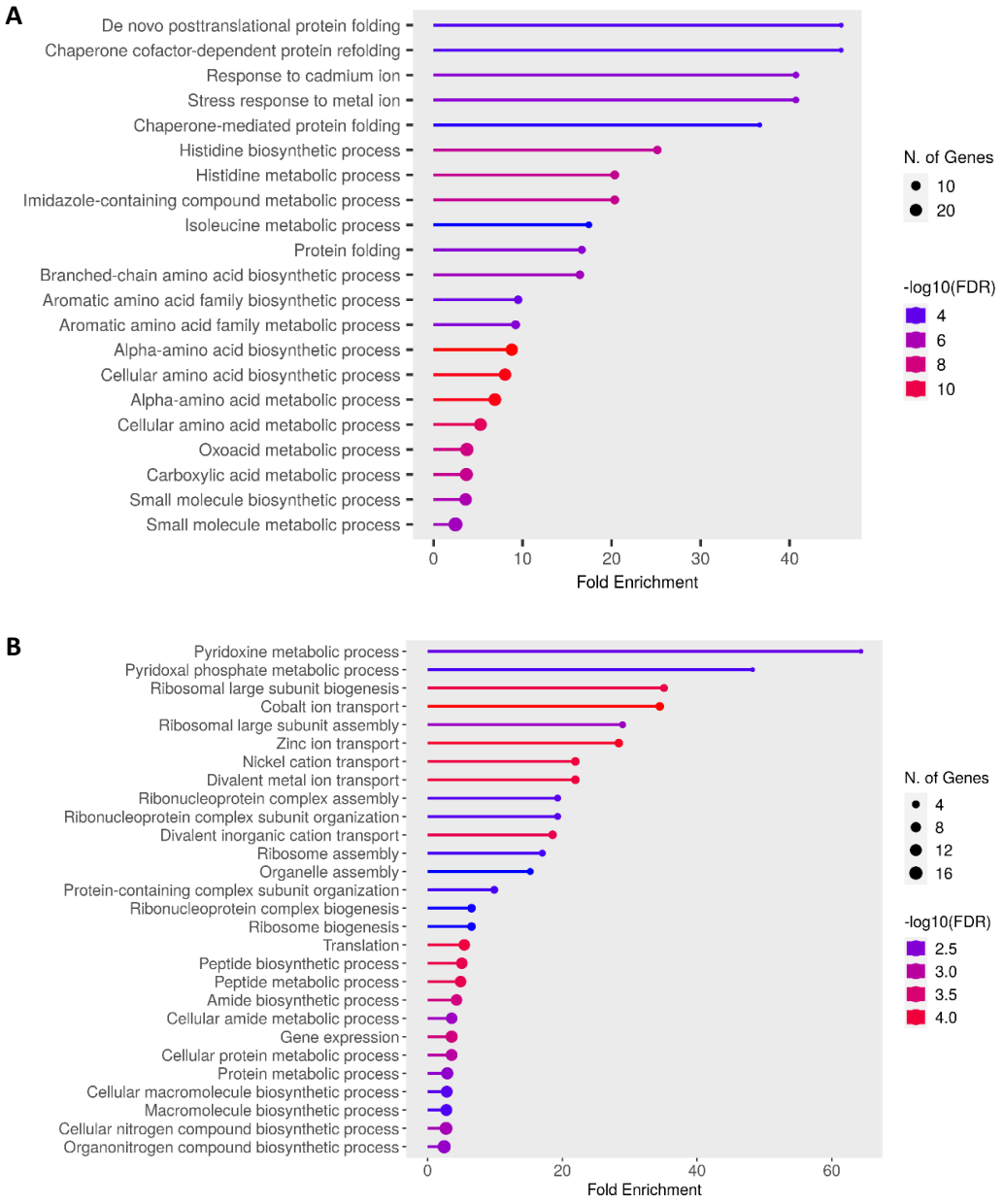

Figure 3.12. Major biological processes (A) upregulated and (B) downregulated in *S. aureus* ST188 with significant enrichment of gene expression after exposure to OCT. GO Biological Processes generated using ShinyGO v0.80 (accessed March 2024). The bubble sizes indicate the number of genes, and the different colour shades represent the FDR.

Finally, FM104 upregulated genes that were significantly enriched corresponded to carotenoid metabolic processes and branched-chain amino acid biosynthesis (**Figure 3.13.**). In contrast, from the three genes that were downregulated under FM104, two were involved in lipid metabolism/cell wall biosynthesis (*glpD* and *sceD*), and the third one was a staphylopine synthase gene (*cntM*) linked to metal ion homeostasis within the bacterial cell.

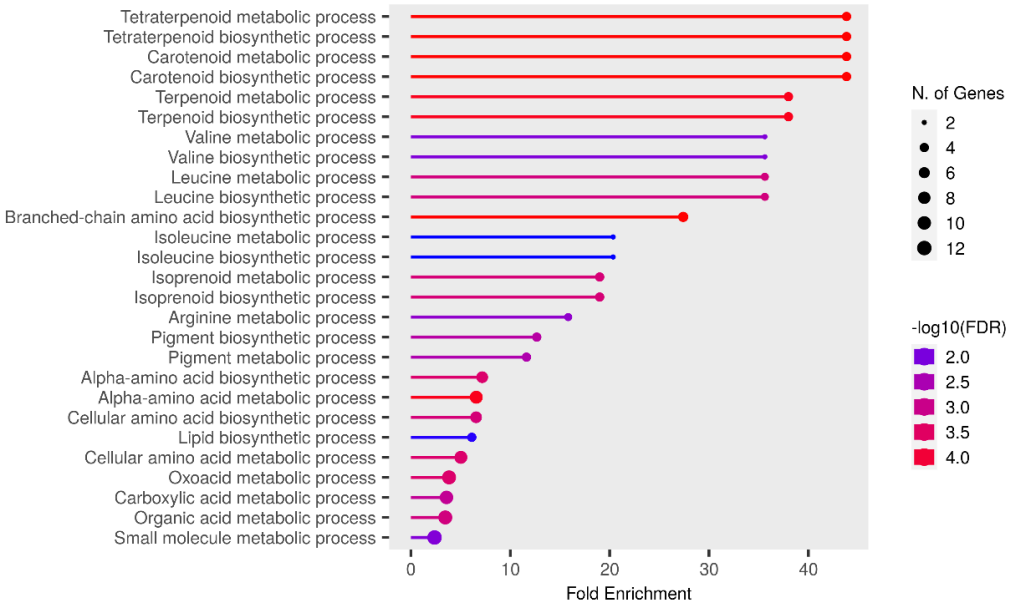

Figure 3.13. Major biological processes upregulated in *S. aureus* ST188 with significant enrichment of gene expression after exposure to FM104. GO Biological Processes generated using ShinyGO v0.80 (accessed March 2024). The bubble sizes indicate the number of genes, and the different colour shades represent the FDR.

3.3.2. Similarities and differences in staphylococci exposed to CHX and OCT

As part of a collaborative project (Felgate and Solsona, In Preparation), RNA-Seq was used to determine the commonalities and differences in gene expression between the 4 most frequently isolated clinical staphylococci: *S. aureus, S. epidermidis, S. haemolyticus* and *S. capitis* (NRCS-A isolates), when exposed to CHX and OCT.

Similarly to what was observed in the previous section, there were considerately more genes being upregulated on exposure to biocides than downregulated (**Figure 3.14.**), although the FDR cut-off was ≤ 0.01 for this study. *S. aureus* had the highest number of upregulated genes.

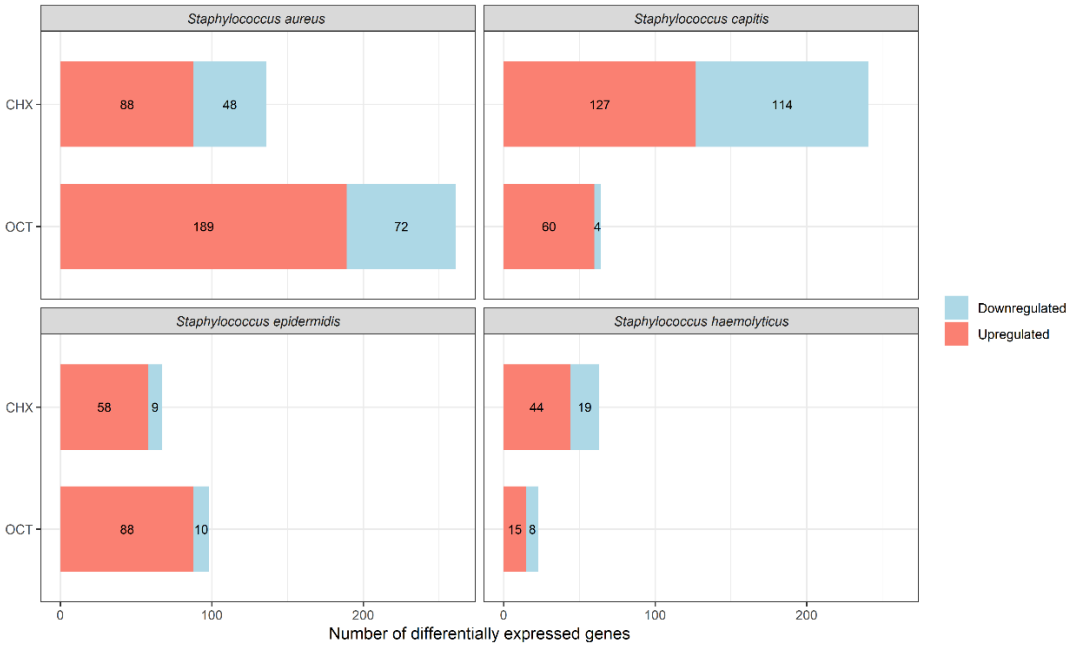

Figure 3.14. Stacked barplots showing the overall number of differentially expressed genes. DEGs for each stress (CHX, OCT) and for each *Staphylococcus* species shown. Downregulated genes indicated in blue and upregulated in red.

Results showed that gene expression in response to biocide stress was not consistent across staphylococci. In fact, only 6 upregulated core genes (*groES, groL, hrcA, grpE, dnaK* and *vraX*) were common between all species under CHX stress and a total of 9 genes (*vraX, dnaK, grpE, hrcA*, *ssA*, *liaF, vraS, qacA* and *clpB*) were common under OCT stress (**Figure 3.15. - A**). Surprisingly, there were no downregulated core genes as observed in the Venn diagrams (**Figure 3.15. - B**).

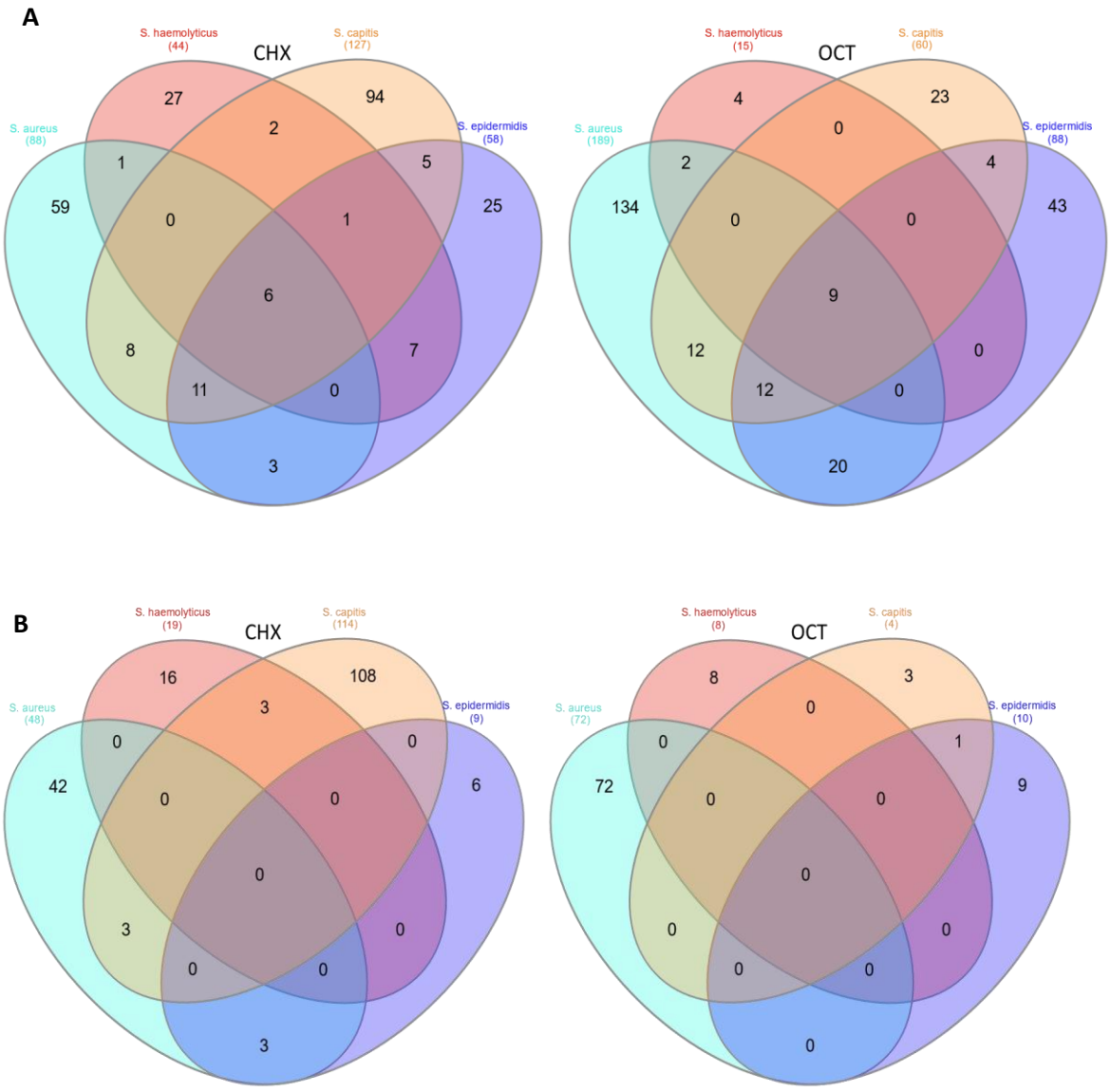

Figure 3.15. Venn diagrams showing the number of DEGs for each condition and the overlap between stresses after 30-minute exposure. (A) Upregulated and **(B)** downregulated results for CHX and OCT. Colours represent different species: *S. aureus* (cyan), *S. haemolyticus* (red), *S. capitis* (yellow), and *S. epidermidis* (blue).

To further understand the commonalities and differences in these genes, communal genes shared between 2 (or more) species were selected to further understand the biological processes involved. While studying the biological processes after biocide exposure, we have observed that many upregulated genes shared between CHX and OCT, mainly involved in stress responses, responses to antibiotics, amino acid biosynthesis, and cell wall metabolism (**Figure 3.16.**).

Downregulated shared genes were mainly involved in amino acid biosynthesis, translation, and heat shock response. There were no downregulated genes shared between the two stresses across all 4 species (**Figure 3.16.**) but some genes were present in more than one species. For example, the *emrA* gene, which is a multidrug resistance efflux pump involved in multiple biological processes, was downregulated in *S. capitis* and *S. haemolyticus* in response to CHX.

We have also observed (**Figure 3.16.**) that different genes from the same cluster were present. For example, genes from the same cluster of ribosomal proteins (*rpl/rps*) were downregulated in *S. capitis* (under CHX stress) and downregulated in *S. aureus* (under OCT stress). Another example was seen with the cold shock proteins from the *csp* operon, which were downregulated under OCT stress in *S. capitis (cspA), S. epidermidis (cspA)* and *S. haemolytiucs* (*cspC*).

Figure 3.16. Genes significantly downregulated and upregulated on exposure to subinhibitory concentrations CHX and OCT across two or more *Staphylococcus* species. Colours represent the biological processes associated with the genes, with the term 'multiple' indicating genes involved in more than one process (information provided by UniProt). In this study, Bakta (v1.7.0) was used for gene annotation; hypothetical and unannotated genes not shown. SA: *S. aureus*, SC: *S. capitis*, SH: *S. haemolyticus*, SE: *S. epidermidis*.

3.4. Discussion

Gene expression responses differed a lot between CHX, OCT and FM104 in *E. faecalis* ST40 and *S. aureus* ST188. One important difference between the agents is that FM104 is a fully formulated product rather than a single active agent. It also contains QACs as its active ingredients which differ from CHX and OCT.

Furthermore, the transcriptional response to subinhibitory concentrations of CHX and OCT varied significantly between four different species of *Staphylococcus*. Overall, there were considerably more genes being upregulated on exposure to biocides than downregulated.

E. faecalis ST40 and *S. aureus* ST188 under CHX, OCT and FM104 stress

In *E. faecalis* ST40, the upregulated genes shared between all stresses were transporter genes for essential nutrients belonging to the vitamin B group. From the thiamine operon, the genes are involved in thiamine biosynthesis (the active form of vitamin B1), which also plays an important role in growth and bacterial survival, as this operon is involved in many processes from central metabolism of carbohydrates and amino acids. In fact, this biosynthetic pathway, which is not present in humans, has been found in all ESKAPE pathogens (which include *S. aureus*), and in other major nosocomial pathogens like *E. faecalis* and has been explored as a potential target for developing new probes for bacterial inhibition (Barra et al., 2020), although biocides that specifically target this biosynthesis pathways have not yet been explored.

The downregulated gene shared between all conditions in *E. faecalis* was a gene with unknown function (*yusW*), which is an uncharacterised protein also present in some *Bacillus* strains (e.g., *B. subtilis, B. licheniformis, B. gobiensis*) and other Gram-negative bacteria. In our study, downregulated genes under CHX stress were mostly involved in purine transport. A study with another *enterococcus* (*E. faecium*) showed how nucleotide biosynthesis (purine and pyrimidine) and carbohydrate metabolism were critical pathways essential for fitness in the human serum (Zhang et al., 2017). Hence, the downregulation of genes involved in purine and pyrimidine transport under stress might be suggesting that this is a strategic response to metabolically conserve energy to cope with the stress posed by CHX.

Many upregulated genes shared between both stresses (CHX and OCT) were involved in lipoteichoic biosynthesis and cationic transport. For example, genes such as *tagU* (cell wall teichoic acid biosynthesis) or *cynR* (involved in cyanate metabolism) were significantly

upregulated under CHX and OCT stress. Increased expression of these cell wall genes and cations transporters might reflect changes to membrane structure caused by the mode of action of these biocides that attack and disrupt the membrane.

Downregulated genes under CHX and OCT stress included many ABC transporter ATP-binding proteins, although not known drug efflux pumps. For the novel formulation (FM104), downregulated genes controlled major carbohydrate metabolic pathways and transport genes involved in permeability were upregulated. Results also showed upregulated heat shock proteins under sub-inhibitory concentrations of CHX and OCT stress. For example, the serine protease *htrA* which was *t*he major hit in *E. faecalis* under CHX stress (6.27 LFC) and also upregulated under OCT stress (2.30 LFC). This highly conserved protein, which combines both chaperone and protease activity, has been showed to enhance bacterial survival under stress conditions (Wessler et al., 2017).

In *S. aureus*, upregulated genes shared between all stresses were involved in stress responses (e.g., heat shock proteins), similarly to what was observed with *E. faecalis,* which might indicate that these genes contribute to bacterial protection against biocidal stress. Additionally, many upregulated genes shared between all stresses were also involved in amino acid biosynthesis, especially branched-chain amino acids (BCAAS) from the *ilv-leu* operon: isoleucine, valine and leucine. One previous study showed that changes in different stresses (temperature, pH and NaCl) can induce changes in metabolic processes and amino acid biosynthesis (Alreshidi et al. 2022).

Chaperones from the Clp family, which are critical in bacterial stress survival (Alam et al., 2021; Singh et al., 2012), were also upregulated under both CHX and FM104 in *S. aureus*. These chaperones have been shown to have a direct impact on antibiotic resistance and virulence, among other functions (Frees et al., 2014). Two genes associated with anaerobic metabolism (*pflA* and *pflB)* had an increase in expression under CHX and FM104 in *S. aureus*. Changes in nitrate/nitrate metabolism or translation processes were also seen to be upregulated in *S. aureus* under CHX stress and FM104. The nitrate reductase operon recently has been found to contribute to virulence in an *agr*-dependent way or surface antigen proteins in *S. aureus* (Li et al. 2023). Additionally, the *agr* (accessory gene regulator) is a quorum-sensing regulator with a role in biofilm formation (Kleerebezem et al., 1997). How this system may impact biocide survival is however unclear.

In contrast, downregulated genes shared between all stresses in *S. aureus* were involved in metal transport (from the *cnt* operon) and the peptidoglycan hydrolase (*sceD*), which has a

role in cell wall hydrolysis and peptidoglycan turnover/remodelling (Wang et al., 2022). A study found that *S. aureus* lacking SceD had impairment in cell separation and clumping processes (Stapleton et al., 2007). Additionally, there have been studies about the role of peptidoglycan-related genes in cell growth, and virulence (Wang et al., 2022). Genes involved in virulence and intra-species competition like the staphylococcal secretory antigen (*ssa*) and genes from the *ess* locus, which encodes the type VII secretion system (T7SS) in *S. aureus* (Bowman and Palmer, 2021) were significantly downregulated for both CHX and OCT. Other downregulated genes shared between OCT and CHX stress were involved in metal transport and translation processes, such as *rpl* and *rps* ribosomal proteins. The downregulation of these processes (metal transport, peptidoglycan metabolism, virulence factors and translation) could suggested a global response is in place to reduce the impact of biocidal stress and enhance survival.

Comparing responses of 4 different staphylococci under CHX and OCT stress

When comparing the responses of 4 different staphylococci, we observed that biocide stress does not cause a conserved response in all staphylococci.

Overall, a large number of staphylococcal genes were involved. These played various roles in stress responses to antibiotics/antimicrobials, amino acid biosynthesis, heat shock, ribosomal hibernation, cell wall metabolism and virulence. Interestingly, changes in ribosomal proteins (*rpl* and *rps*) were also observed throughout the CoNS species. The *hbf* gene was found to be significantly upregulated in *S. capitis, S. aureus* and *S. epidermidis* in response to biocide exposure. This gene is also associated with ribosomal preservation, and involved in other processes such as enhanced antibiotic and stress tolerance, biofilm formation and general stress response (Basu et al. 2018).

Metal genes, for example genes involves in zinc and manganese transport, had an increased response to CHX in the three CoNS. However, in *S. aureus* there was a decrease in the expression of many metal chelating genes (e.g., from the *cnt* operon), which was also observed for *E. faecalis*. Changes in metal homeostasis could enhance cell protection, in this case, a reduction in metal scavenging might be beneficial for conserving energy or for biocide binding.

3.5. Conclusion

RNA sequencing revealed differences in gene expression after biocide exposure in two Gram-positive pathogens. Gene expression responses differed a lot between CHX, OCT and FM104. Furthermore, responses were also independent and species-specific between four common staphylococcal species.

Although CHX/OCT have a similar mode of action, these biocides differed in the number of genes and pathways that were upregulated and downregulated. There were considerately more genes being upregulated on exposure to CHX than OCT. When comparing it to the results from FM104, changes in gene expression also differed from the active biocides. Overall, general stress response and heat shock proteins, as well as genes involved amino acid biosynthesis were upregulated in both Gram-positive isolates, indicating these pathways are key for survival under biocide stress. Especially changes in branched-chain amino acids, observed for all three stresses, that are linked to membrane stability in *S. aureus* (Frank, Whaley and Rock 2021). This is consistent with the mode of action of these biocides, which act on the membrane (Rzycki et al. 2021) and might induce changes in the fatty acid composition of the cell membrane.

These transcriptomic analyses elucidated distinct gene expressions patterns in response to short-term exposure (30 minutes) to ½ the MIC of commonly used biocides and a novel formulation, with some commonalities observed between *E. faecalis* and *S. aureus*. Although a much wider set of genes seem to have a role in biocide susceptibility, there was no universal response or core set of genes observed across all biocides or species. To further evaluate the effects of biocides on bacterial adaptation, an evolution experiment was conducted with escalating concentrations of the selected biocides over a prolonged period of time in *S. aureus* ST188 and *E. faecalis* ST40 (**Chapter 4**).

CHAPTER 4: *IN VITRO* BEAD-BASED BIOFILM EVOLUTION: OPTIMISATION AND NEWLY ESTABLISHED MODEL FOR STAPHYLOCOCCI AND ENTEROCOCCI

"If you know you are on the right track, if you have this inner knowledge, then nobody can turn you off... no matter what they say." – Barbara McClintock

4.1. Introduction

S. aureus and *E. faecalis* are common opportunistic pathogens that can survive on dry surfaces for months which can help them persist in the hospital environment (Kramer et al., 2006; Porter et al., 2024). Biocides are widely used to control and prevent healthcare-associated infections, with surface disinfection a key goal. However, inappropriate biocidal use or ineffective disinfection processes can result in survival of these microorganisms on inanimate surfaces. Similarly, the residual effects of biocides applied as antiseptics remaining on the skin after several hours have also been shown to be ineffective in killing adhered bacteria (Wade and Casewell, 1991).

Laboratory evolution is a powerful *in vitro* tool to study the effects of drug exposure on bacteria and to understand the genetic basis of evolution (Cooper, 2018; Poltak and Cooper, 2011). In the context of biocides, several studies have shown how repeated bacterial exposures to low concentrations of biocides can lead to selection for mutants demonstrating reduced susceptibility to these biocides or cross-resistance to other antimicrobials. However, the conditions and mechanisms by which this may happen are not well understood and how biofilms may adapt to biocides is not currently clear. Understanding the bacterial responses to biocides and the link with antibiotic resistance will improve IPC. Additionally, understanding the clinical significance of biocide tolerance (Horner et al., 2012) is also essential.

Results after exposure to different classes of biocides have been reported for various species. For example, evolution experiments with QAC biocides showed that *Escherichia coli* formed persisters against BZK (Nordholt et al., 2021). In *S. aureus*, *in vitro* mutants with changes within the *norA* gene showed increased MIC to BZK and CHX (Furi et al., 2013). Similarly, reduced susceptibility to CHX and BZK was also observed in enterococci (Sobhanipoor et al., 2021). Another study also found that increased use of antiseptics (OCT and CHX) within one hospital trust was associated with reduced susceptibility of *S. aureus* clinical strains (Hardy et al., 2018).

Previously adapted protocols in our laboratory included a biofilm evolution model to study the sub-inhibitory effects of antibiotics against *Salmonella Typhimurium* (Trampari et al., 2021) and *Pseudomonas aeruginosa*. However, this model was not immediately translatable to Gram-positive pathogens nor use with biocides. Therefore, one of my initial goals was to optimise this model to obtain a robust *in vitro* bead-based evolution model and establish a

standardised protocol to be used with my clinical isolates and biocides. The preliminary tests and several optimisation steps are detailed in this chapter.

After establishing a newly robust model, a laboratory evolution experiment was used to investigate the impact of prolonged repeated exposure of *S. aureus* ST188 and *E. faecalis* ST40 to sub-lethal concentrations of CHX and OCT when grown planktonically and as biofilms over a period of almost 3 months (with a passage window of 72 hours).

4.2. Aims

- To optimise an *in vitro* bead-based evolution model for *S. aureus* and *E. faecalis*.
- To understand the responses after prolonged exposure to sub-inhibitory concentrations of biocide in both Gram-positive pathogens.
- To characterise the virulence of *S. aureus* and *E. faecalis* strains.

4.3. Results

4.3.1. Test a panel of different staphylococci and enterococci isolates for baseline susceptibility and biofilm formation

A panel of 10 isolates were chosen from > 1000 clinical isolates (Sethi et al., 2021) on the basis of being highly diverse and having high to low biofilm biomass production. Selected isolates included *S. aureus*, *E. faecalis* and CoNS species (*S. epidermidis*, *S. capitis* and *S. hominis*).

Baseline susceptibility testing

The MICs of CHX and OCT were determined against the panel of isolates. The MIC values of both biocides against the panel of strains corresponded to the first clear well of the microtiter plate which indicated no visible growth of microorganisms, as recommended by EUCAST for antibiotics. Results were consistent in the three biological replicates and between the three technical replicates (**Table 4.1.**).

MIC values of OCT were lower than MICs of CHX. Overall, values for OCT ranged from 1 µg/mL to 2 µg/mL, and most isolates had a mean value of 2 µg/mL (for OCT). For CHX, values ranged from 8 - 16 µg/mL, and many isolates had a mean value of 16 µg/mL (for CHX).

Biofilm forming ability

The biofilm forming ability of the isolates, indicated by the mean biofilm absorbance value, was quantified by crystal violet. Based on diversity and the ability to form biofilms, it was observed that there was a high diversity of species in the panel of 10 isolates to have high and low biomass production.

Out of the panel, a total of two *S. aureus* isolates (isolate 353 and 60) were selected to be used in optimising the *in vitro* bead-based evolution model.

Table 4.1. Selected panel of 10 isolates. MIC of CHX and OCT, and biofilm forming ability (mean biofilm) included.

Isolate number	Species	Mean MIC (µg/mL)		Mean biofilm*
		OCT	CHX	
312	*Enterococcus faecalis*	1	8	0.94
678	*Staphylococcus aureus*	1	4-8	1.52
60	*Staphylococcus aureus*	2	16	0.24
353	*Staphylococcus aureus*	1	16	0.56
379	*Staphylococcus capitis*	16	32	0.07
677	*Staphylococcus capitis*	2	16	3.32
567	*Staphylococcus epidermidis*	8	16	0.06
W01 - 42 - a	*Staphylococcus epidermidis*	2	8	3.49
349	*Staphylococcus haemolyticus*	2	16	3.44
W02 - 16 - t	*Staphylococcus hominis*	2	16	2.61

* Biofilm measured by crystal violet absorbance (OD_{600nm}).

4.3.2. Model optimisation

4.3.2.1. Bead preparation and contamination tests

Previous evolution models used in the laboratory by Trampari et al. (2021), adapted from Poltak and Cooper (2011), included coloured stainless-steel beads. However, after preliminary bead tests with Gram-positives, the paint used to colour the beads was removed over time in *S. aureus* cultures. Therefore, stainless steel beads of different sizes (diameters = 6 mm and 3 mm) were chosen to distinguish between passages.

Stainless steel beads were stored in 70 % ethanol in Duran bottles and tested for contamination. After O/N incubations, the turbidity of each tube containing beads was measured and compared to the controls. Results showed no cells grew in the presence of beads, confirming beads could be stored in 70 % ethanol throughout the evolution experiments.

4.3.2.2. Bead population capacity testing

Tests to compare bacterial growth with and without the beads, as well as differences between the numbers of cells recovered from beads with the two different diameters (6 mm VS 3 mm) were performed.

Qualitative test: To check for morphology changes, *S. aureus* NCTC 12973 was cultured in TSB media with and without the beads and plated on TSA. *S. aureus* forms gold-coloured colonies on TSA at 37 °C. As observed, the tested control isolate had the same colony morphology without beads and with beads. Additionally, the growth was the same when recovered from 6 mm and 3 mm beads. Hence, it was confirmed that with the addition of beads to the media no morphology changes in *S. aureus* NCTC 12973 were observed. Different bead sizes did not have an impact on growth, as pure cultures, which looked morphologically similar, were recovered on agar plates.

Quantitative test: As two different sizes of beads were used to distinguish between passages, it was important to verify there was not a bias in cell numbers introduced before the evolution experiments. Therefore, theoretical calculations to determine the total bead surface that could be occupied by bacterial cells were performed (**APPENDIX VI**) and compared with the number of cells recovered. The surface area of the sphere was calculated for the two types of bead sizes. The surface area of the 6 mm bead equated to 113.1 mm^2, and for the 3 mm bead to 28.7 mm^2. The surface area of the two bacterial types, the Gram-

positive cocci (*S. aureus* and *E. faecalis*) were also required to be calculated as to ascertain how many cells could be theoretically on each bead. The relative size of a coccus is between 0.5 - 1 µm of diameter; the theoretical number of cells/beads was then calculated by dividing the surface area of the beads by bacterial surface area for each stainless-steel bead. This approach assumes uniform binding of bacteria to the bead. The theoretical number of cells/beads are 1.44 x 10^8 cells (for 6 mm) and 3.60 x 10^7 cells (for 3 mm).

Preliminary growth tests to compare growth with and without the beads were performed. The productivity of the cells expressed in log CFU/mL (planktonic) and log CFU/mm^2 (biofilms) was quantified to also compare differences between bead sizes. A non-parametric Kruskal-Wallis test was performed to assess differences in planktonic growth with and without beads (**Figure 4.1.**). Differences between planktonic liquid (containing 3 mm and 6 mm beads) were not statistically significant (*p-value* = 0.77). Additionally, *S. aureus* NCTC 12973 growth was the same when grown planktonically without beads compared to the planktonic liquid with 3 mm (*p-value* = 0.77) and 6 mm beads (*p-value* = 1). This confirms the presence of stainless steel does not restrict planktonic growth.

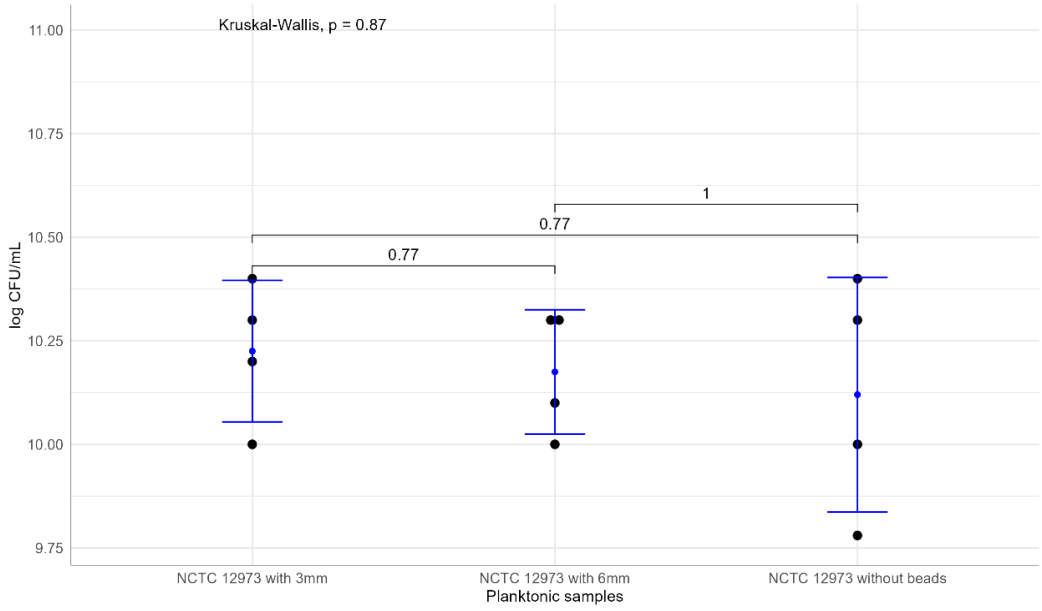

Figure 4.1. Comparison of planktonic growth of *S. aureus* NCTC 12973 with/without beads. CFU/mL (for planktonic) and CFU/mm^2 (for biofilm) were calculated; four technical replicates/sample were included. Kruskal-Wallis test showed non-statistically significant differences in the number of *S. aureus* NCTC 12973 cells when grown planktonically with and without beads.

A quantitative growth test was performed to obtain the actual recovered cells/bead. To observe if the bead size made a difference in bacterial growth, *S. aureus* NCTC 12973 was cultured in TSB media with 6 mm and 3 mm beads, and without beads. For the biofilm experiment, beads were washed with 1 mL of phosphate-buffered saline (PBS) and vortexed using a thermo mixer at 1200 rpm, 21 °C for 2 minutes to allow for the biofilm to detach from the surface. Planktonic and biofilm experiments were serial diluted in 96-well plates (total volume 200 µL), with 4 technical replicates/sample included for CFU counting. A control containing PBS only was also included. For the CFU counts 5 µL of each dilution were spotted in TSA plates and the log CFU/mL (planktonic) and log CFU/mm^2 (biofilms) were calculated for the recovered cells after 24 hours incubation at 37 °C.

A paired-samples T-test was used to test whether there was a significant difference in the number of *S. aureus* NCTC 12973 cells when using 3 mm and 6 mm beads. As seen (**Figure 4.2.**), the smaller beads (3 mm) had similar CFU/mm as the larger diameter beads (6 mm), no significant difference was observed between the CFU/mm^2 on either bead sizes (*p-value* = 0.06).

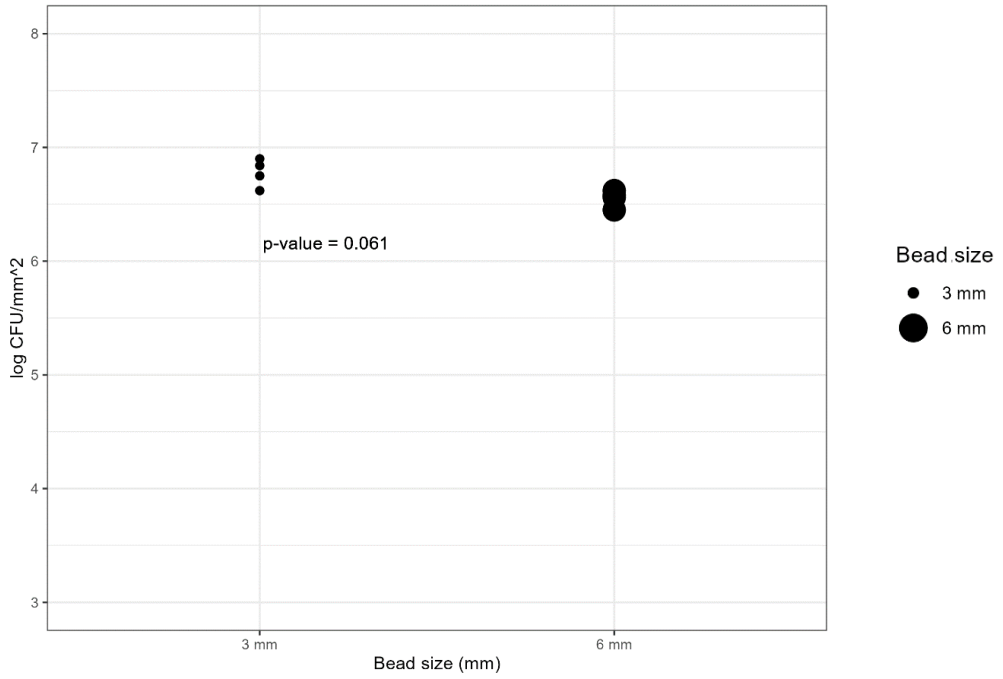

Figure 4.2. Test to measure bead size effect on bacterial colonisation. *S. aureus* NCTC 12973 cells recovered after growth on 3 mm and 6 mm beads were quantified (expressed as log CFU/mm^2). Points indicate independent replicates from two experiments. A paired-samples T-showed no significant difference (*p-value* > 0.061) in cell numbers between 3 mm and 6 mm beads, indicating bead size had no significant effect on cell counts.

Finally, the theoretical maximum carrying capacity and recovered data of the number of cells grown on beads (number of cells/bead) were plotted together (**Figure 4.3**.), potential differences between 3 mm and 6 mm were seen.

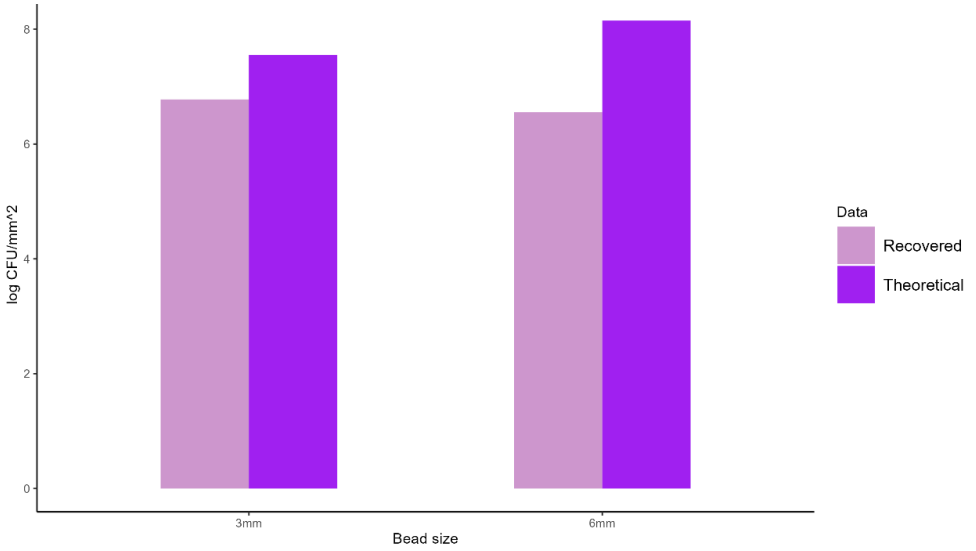

Figure 4.3. Number of theoretical and observed *S. aureus* NCTC 13383 cells/bead. Cells/bead (CFU/mm^2) calculated theoretically and with recovered data (one biological replicate) when grown in TSB with beads.

In summary, stainless-steel beads did not limit planktonic growth of *S. aureus* NCTC 13383 and similar numbers of cells were recovered from growth on beads of different diameters. Therefore, stainless-steel beads of different sizes were potentially suitable for evolution experiment.

4.3.2.3. Optimising use of the bead model to generate an effective population size

A preliminary evolution experiment was run with *S. aureus* (isolates 60 and 353) with the antiseptics CHX and OCT following a ladder model (increasing the concentration of the selective agent over time as passages progressed). However, after the first passage (without stress) no growth was observed in the biofilm and control plates (with beads), and planktonic samples showed a small number of colonies in the parental generation.

Therefore, several variables were changed (**Figure 4.4.**) to optimise growth in the system in order to obtain adequate numbers of colonies in the biofilm and control conditions. With the aim of increasing the number of CFU per bead, optimisations focused on the initial conditions

to obtain at least 10^5 cells per mm^2 of bead. This number was chosen to allow a population size suitable for evolution experiments, and to further proceed with the evolution experiments.

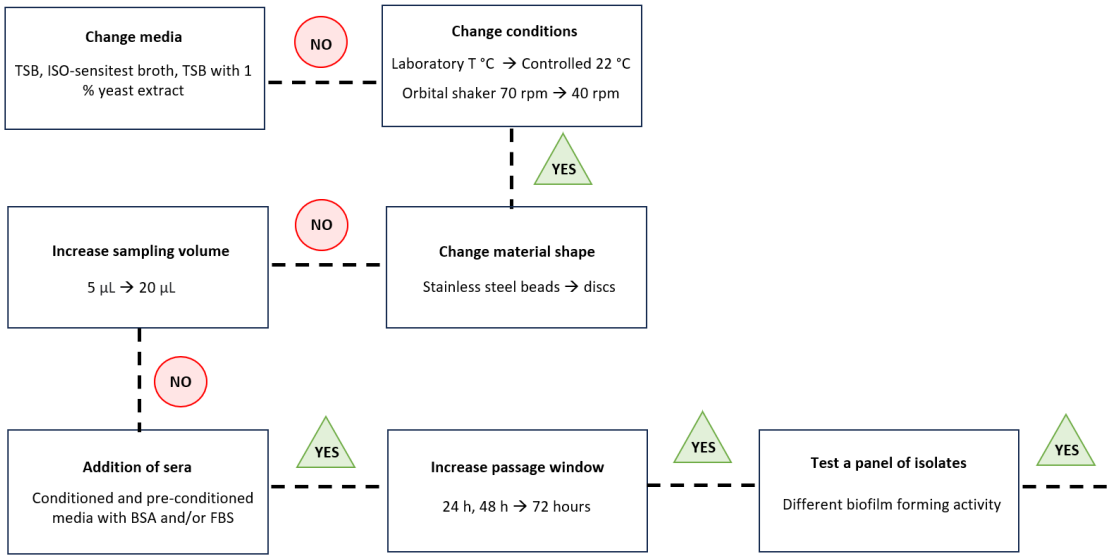

Figure 4.4. Flow diagram showing the different optimisation experiments performed to increase the number of CFU of the biofilm and control condition in the evolution experiments. In each square there is a different variable tested, circles indicate failure of the tested variable and triangles an observed improvement. Media and seria abbreviations: TSB (tryptic soy broth), BSA (bovine serum albumin) and FBS (fetal bovine serum).

(a) Test different media: the first optimization consisted of changing the TSB media for three different media: brain heart infusion (BHI) broth (Sigma-Aldrich, UK), ISO-sensitest broth (Thermo Fisher Scientific, UK) and TSB with 1 % yeast extract (Sigma-Aldrich, UK). No improvements in the number of CFUs were obtained with the different media. Therefore, TSB media, which is commonly used for staphylococci growth, was retained as a base for the next round of optimisation experiments.

(b) Temperature and agitation: a refrigerated incubator (set to 22 °C) was used to avoid temperature fluctuations from the laboratory and the speed of the orbital shaker was decreased from 70 rpm to 40 rpm. The results of those evolution experiments showed growth in the parental generation for the biofilm and control conditions (10^2 - 10^3 CFU/bead). The planktonic condition had higher number of cells (10^6 CFU/mL). In the first generation, 0.25 µg/mL of CHX and OCT were added. The number of colonies of the planktonic condition

started to decrease to 10^4 CFU/mL, but low CFU numbers were seen on the control/biofilm plate after 48 hours, which was the initial passaging window previously used in other experiments. The source of the problem was not related to the biocide, as in the control condition no stress was added. The only common point between the control/biofilm conditions were the beads.

(c) Change material shape and sampling volume: modification of different variables included changing the stainless-steel material shape (from beads to discs), and increasing the volume spotted on the plates but there were still no significant growth improvements in the biofilm, nor the control plates after the parental generation. The problem was potentially related to bacterial attachment to the beads, as recovery of biofilm forming cells from the beads was low or absent. To check if there were cells after the vortexing step, that allows for biofilms to detach to the bead surface, 20 µL of the culture (undiluted solution) were spotted in TSA. There were almost no colonies on the biofilm condition and a few on the control condition. Additionally, a vortexed bead (from a randomly selected sample) was added into a 5 mL TSB glass bottle and left O/N to check if there was bacterial growth. After 24 hours, there was turbidity in the tube, which indicated that after the vortexing step there were cells still attached to the beads, but numbers of cells were very low.

(d) Addition of sera in the media: different experiments were performed by adding sera to the media during the inoculation (conditioned conditions) or before the inoculation step (pre-conditioned conditions).

- **Addition of sera with the inoculation step (Conditioned)**

TSB was supplemented with 1 % (w/v) bovine serum albumin (BSA) [Condition A] and 1 % (v/v) foetal bovine serum (FBS) [Condition B] and compared to TSB [Condition C] to see if the sera had any effect in biofilm-formation (Abraham and Jefferson, 2010; Cendra et al., 2019; Hill et al., 2010; Monahan et al., 2014; Xie et al., 2020). Following a similar experimental design (**Chapter 2**, **Figure 2.1.**), four single colonies (unless otherwise stated) were randomly picked for each isolate to start the overnight cultures. A 1:100 dilution from the O/N cultures was performed and inoculated to planktonic and biofilm tubes for Condition A, B and C. Sera was filtered with a 0.22 micron filter and then added to TSB. Broth controls from the different conditions were also run in parallel to test for contamination. A conditioned planktonic control was run alongside to have a reference of the number of cells. Two independent

lineages per isolate were included in this experiment. No stress was added, and no serial passages were done here. A CFU/bead analysis was done 24, 48 and 72 hours after inoculation.

The conditioned biofilm results (**Figure 4.5.**) showed that no condition reached the desirable number of cells (10^5 CFU/mm^2). The number of cells was lower at 24 hours when compared to the two other timepoints, but no differences were observed between 48 and 72 hours. The highest CFU/mm^2 values were obtained with condition B at 48 hours (around 10^4 CFU/mm^2). Condition C also showed high values at 48 hours. The lowest cell numbers were obtained in condition A.

Conditioned planktonic results (**Figure 4.5.**) showed higher number of cells than biofilms (10^9 - 10^{10}CFU/mm^2), exceeding the set value of 10^5 CFU/mm^2. The number of planktonic cells was lower in Condition C. Overall, there was an improvement in the cell counting but further experiments were needed to reach a higher number of cells.

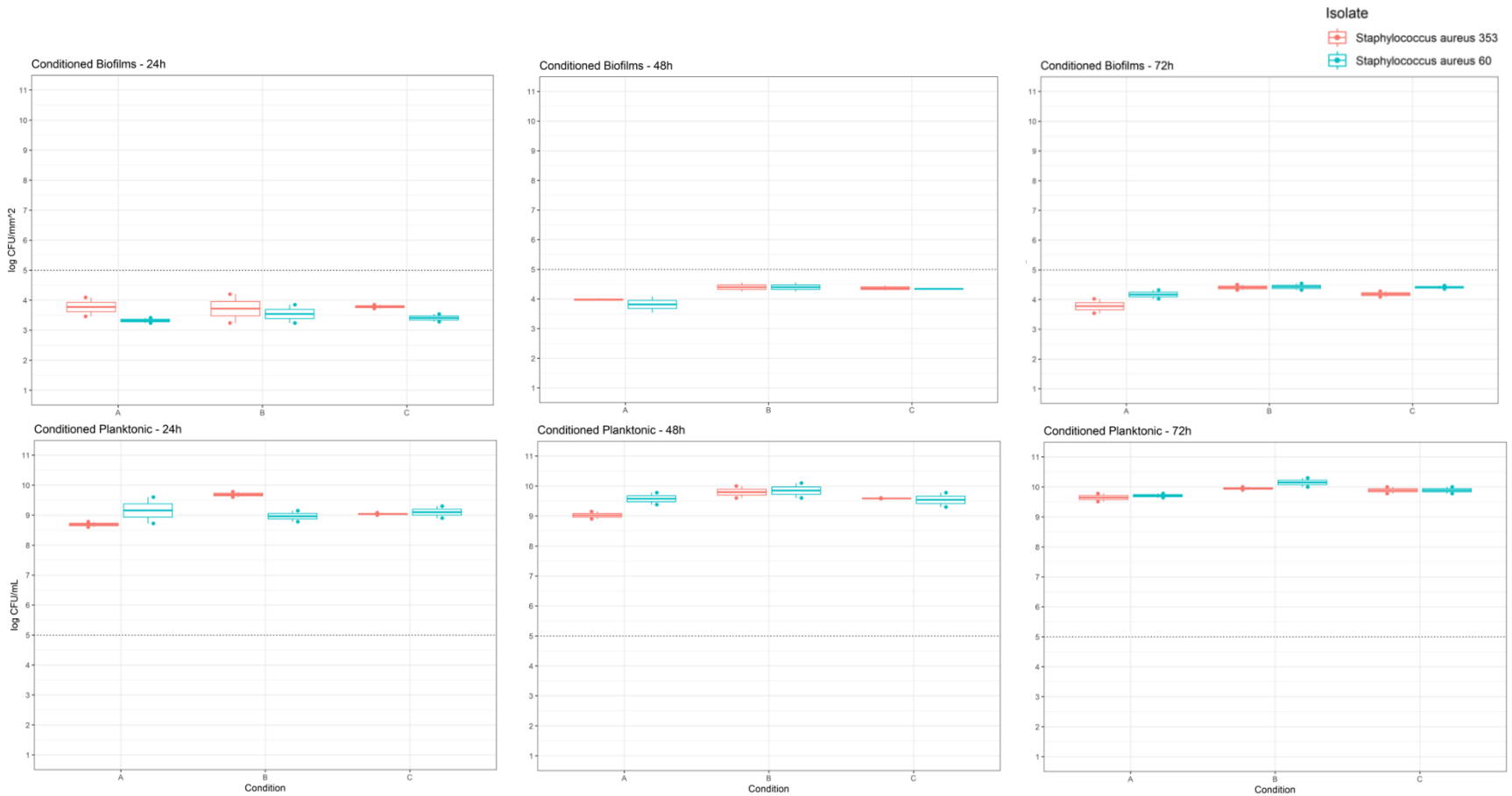

Figure 4.5. Addition of different sera to the media for conditioned biofilms and planktonic conditions in *S. aureus* isolates 60 and 353. Boxplots represent the number of cells for biofilm (log CFU/mm^2) and planktonic (log CFU/mL) in each condition: Condition A (TSB + 1 % BSA); Condition B (TSB + 1 % FBS) and Condition C (TSB only). Each graph represents data collected at different timepoints: 24, 48 and 72 hours after inoculation. Two independent lineages were included in this experiment; the dotted line corresponds to the desired number of cells (set value = 10^5 CFU/mm^2) on a logarithmic scale.

- **Addition of sera before the inoculation step (Pre-conditioned)**

A modification in the previous experimental design was then introduced: addition of the sera 24 hours before inoculation (**Figure 4.6.**) to determine if pre-conditioning the bead surface could increase the number of cells. By adding the sera 24 hours before inoculation, instead simultaneously (like previously performed), a layer of serum would pre-coat the bead surface and once the bead is conditioned enough, bacteria will be added to the culture. This approach mimics the *in vivo* conditions of *S. aureus* adhesion and biofilm formation in prosthetic joint infections.

Two potential outcomes could occur: (A) the bead is pre-coated with a good amount of serum, which can increase cell adhesion and CFU/mm^2, or (B) the bead is pre-coated with less amount of serum hence less CFU/mm^2 would be obtained.

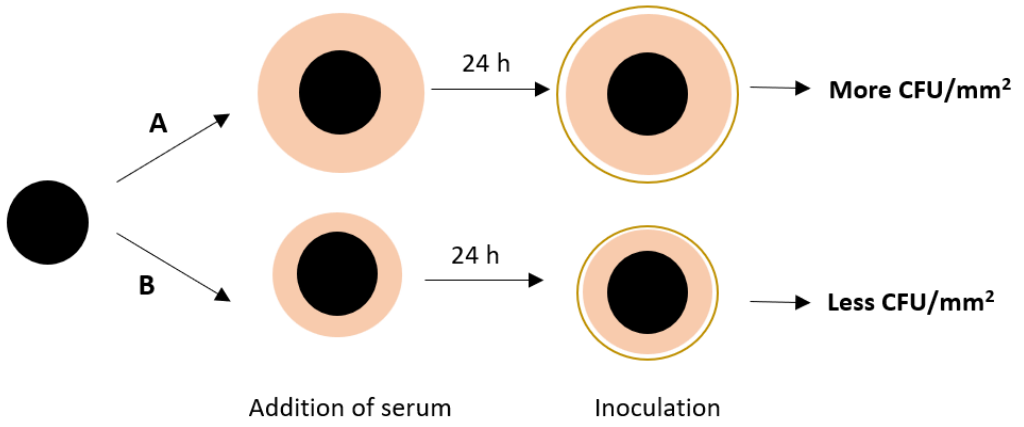

Figure 4.6. Pre-conditioning bead surface model. Addition of the sera 24 hours before inoculation can result in two potential outcomes with more or less CFU/mm^2 obtained.

For this optimisation, condition B (TSB + 1 % FBS) and condition C (TSB) were tested only, on *S. aureus* isolate 60, as it generally grew better than *S. aureus* isolate 353. Colony counting and CFU/mm^2 calculations were done after 24, 48 and 72 hours. Control tubes indicated no contamination in the media nor the beads.

The pre-conditioned biofilm results showed that at timepoint 72 hours, both conditions B and C reached the set value of 10^5 CFU/mm^2 (**Figure 4.7.**). Adding the sera 24 hours before did not make a statistically significant difference, as condition C also showed similar results at 72 hours. A paired-samples T-test was used to compare the mean difference in the number

of cells between the two tested conditions for the same isolate. Results showed a *p-value* higher than 0.05 (*p-value* = 0.73) with 95 % confidence intervals (CI: -0.398; 0.293), indicating insufficient evidence to reject the null hypothesis (H_0: No true difference, in terms of means, in the number of cells between the two conditions). To conclude, there was not enough evidence in the data for a genuine difference in the mean number of cells from *S. aureus* isolate 60 resulting from conditions B and C.

The number of cells was lower at 24 hours and 48 hours when compared to 72 hours (**Figure 4.7.**). Results from the pre-conditioning planktonic phase showed a higher number of cells (10^9 - 10^{10} CFU/mm^2) than in the biofilm state; with condition B a higher number of planktonic cells were obtained. Overall, pre-conditioning planktonic results were similar to the conditioning planktonic data.

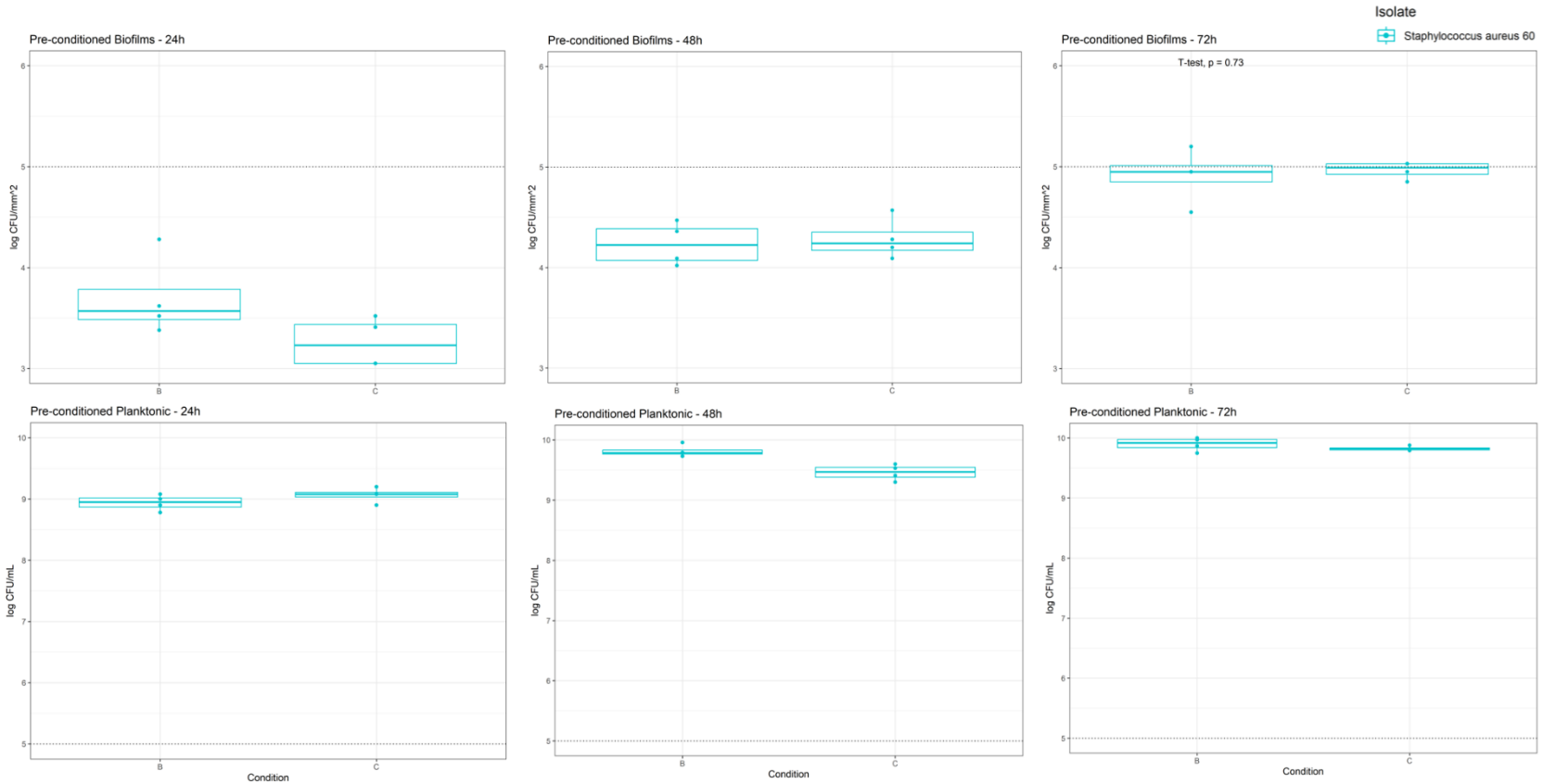

Figure 4.7. Addition of sera 24 hours before inoculation in *S. aureus* isolate 60 (in blue) for the biofilm and planktonic state. The boxplots represent the number of cells for biofilm (log CFU/mm^2) and planktonic (log CFU/mL) in each condition: Condition B (TSB + 1 % FBS) and Condition C (TSB only). Each graph represents data collected at different timepoints: 24, 48 and 72 hours after inoculation. Four independent lineages were included in this experiment; the dotted line corresponds to the desired number of cells (set value = 10^5 CFU/mm^2) on a logarithmic scale. At 72 hours, both conditions reached the set value, indicating that increasing the passage window could allow for more biofilm to attach in the beads.

After observing 10^5 CFU/mm^2 at timepoint 72 hours for both Condition B and C, and considering the significance probability (*p-value* = 0.73), to reduce the extra time of sera preparation, condition C (TSB only) was selected for the last optimisation experiment. The next step of optimisations was to identify if different strains of staphylococci/enterococci would vary significantly in biofilm formation in this model.

(e) Test a panel of isolates with different biofilm forming activity: to identify if the ability to form biofilms affected the productivity (measured by the number of cells), isolates from the initial panel (with different biofilm forming activity, and previously tested for MIC) were studied.

The experiment was performed with Condition C (TSB) and CFU/mm^2 were measured at 48 and 72 hours after inoculation in the biofilm state (with beads). Two independent lineages per isolate were included. Control tubes indicated no contamination in the media nor the beads.

Results showed differences in the number of cells depending on the isolate (**Figure 4.8.**). A one-way analysis of variance (ANOVA) was used to determine any statistically significant differences in the number of cells between the means of 10 different isolates. The ANOVA test showed the *p-value* was lower than 0.05 (*p-value* = 0.000273). Hence, the null hypothesis (H_0 = All population means are equal) was rejected in favour of the alternative hypothesis (H_1 = All population means are not all equal), indicating significant differences in the number of cells between the groups.

In this case, *E. faecalis* isolate 312 and *S. aureus* isolate 678 reached the desired value of 10^5 CFU/mm^2. As previously mentioned in **Chapter 2**, these isolates correspond to common sequence types: ST40 and ST188 respectively.

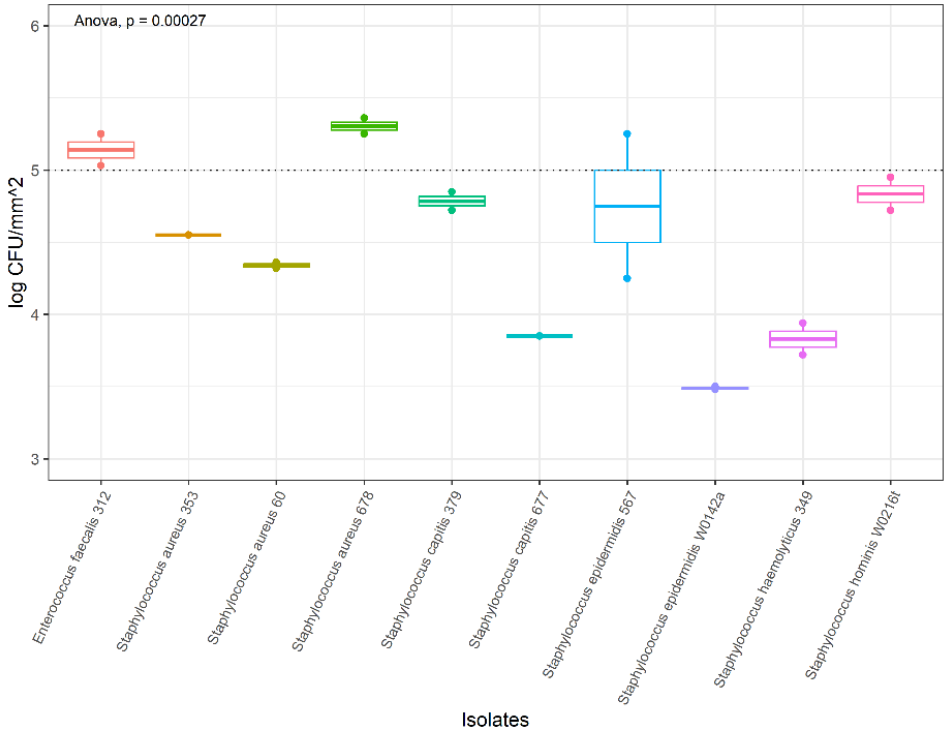

Figure 4.8. Test a panel of isolates with different biofilm forming activity. The boxplots represent the number of cells expressed on a logarithmic scale (log CFU/mm^2) obtained for Condition C (TSB only) after 48 hours. Two independent lineages/isolate were included; the dotted line corresponds to the desired number of cells (set value = 10^5 CFU/mm^2) on a logarithmic scale. Isolates 312 and 678 reached the set value. ANOVA test showed statistical significance (*p-value* = 0.000273).

Biofilm forming ability was therefore strain specific rather than species dependent and the number of cells recovered from beads did not necessarily correlate with crystal violet assays. As observed with the previously studied *S. aureus* isolate 60, low CFU/mm^2 were found, but with other isolates from the same species high CFU/mm^2 were obtained. Interestingly, the isolates with higher mean biomass production (**Table 4.1.**) were not the ones with higher mean log CFU/mm^2 numbers.

To conclude, after performing several optimisation experiments to increase the number of CFUs (to obtain at least 10^5 cells per mm^2 of bead), the selected parameters that showed optimal results included TSB media (with no sera, although similar results were also observed when adding FBS), slow rotation (40 rpm) at a controlled temperature (22 °C), increasing the passage window to 72 hours and selecting for specific isolates (independently of biofilm formation activity). The final experimental design, which includes the optimised selected parameters, is described in **Chapter 2**.

4.3.3. Further characterisation of the two selected isolates for susceptibility and virulence

The next step before starting the *in vitro* bead-based evolution experiments with *E. faecalis* ST40 and *S. aureus* ST188 was to further characterise the selected isolates for susceptibility (MBC/MBEC) and virulence.

Baseline susceptibility testing (MIC, MBC and MBEC): susceptibility of both isolates to CHX and OCT were determined. In addition to previously determined MIC, MBC and MBEC were also performed to assess the bactericidal concentrations for planktonic and biofilm conditions before the evolution experiment. Results (**Table 4.2.**) were consistent between the three biological replicates and between the three technical replicates.

The MICs for CHX ranged between 4 - 8 µg/mL and the OCT MIC was 1 µg/mL for both isolates. To complement the MIC measured on broth, agar MICs were also performed. Broth and agar MICs gave similar results, although generally agar MIC was one-fold above the broth MIC.

The bactericidal concentrations (MBC) for OCT were the same as the MIC, except for *E. faecalis* ST40 where the MBC increased to 2 µg/mL. For CHX, the MBC were one-fold above the MIC for all three isolates. In general, for biofilm eradication levels of antiseptic needed to be much higher. The MBEC for CHX was > 64 µg/mL for both species and 8 - 16 µg/mL for OCT.

Table 4.2. Determination of the MIC, MBC and MBEC for CHX and OCT against the selected strains and control isolate in TSB/TSA media.

Isolate number	MIC (µg/mL)		MBC (µg/mL)		MBEC (µg/mL)	
	CHX	OCT	CHX	OCT	CHX	OCT
S. aureus NCTC 12973	8	1	8 - 16	1	> 64	16
E. faecalis ST40	8	1	8 - 16	2	> 64	8
S. aureus ST188	4 - 8	1	8 - 16	1	> 64	8 - 16

Virulence assays: to determine the larval susceptibility to infection with *S. aureus* ST188 and *E. faecalis* ST40 strains, an *in vivo* infection model using *Galleria mellonella* was used. The colour change in *G. mellonella* was used as a measure of killing (**Figure 4.9.**).

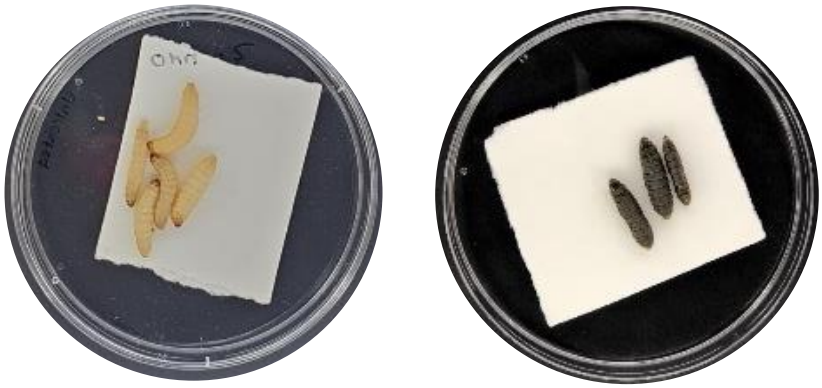

Figure 4.9. Colour change in *G. mellonella* model. Colour change indicates **(A)** PBS-injected control *G. mellonella* larvae at the start of the experiment; **(B)** *E. faecalis* ST40 infected and dead *G. mellonella* larvae.

From the different tested inoculums, it can be observed in the survival curves that 10^6 - 10^7 CFU/larva for *S. aureus* ST188 (**Figure 4.10. - A**) and 10^6 CFU/larva for *E. faecalis* ST40 (**Figure 4.10. - B**) correspond to an infectious dose resulting in approximately 60 % larval death within 48 hours. This represents an inoculum which can therefore be used to compare any mutants for changes in virulence compared to their parental strains.

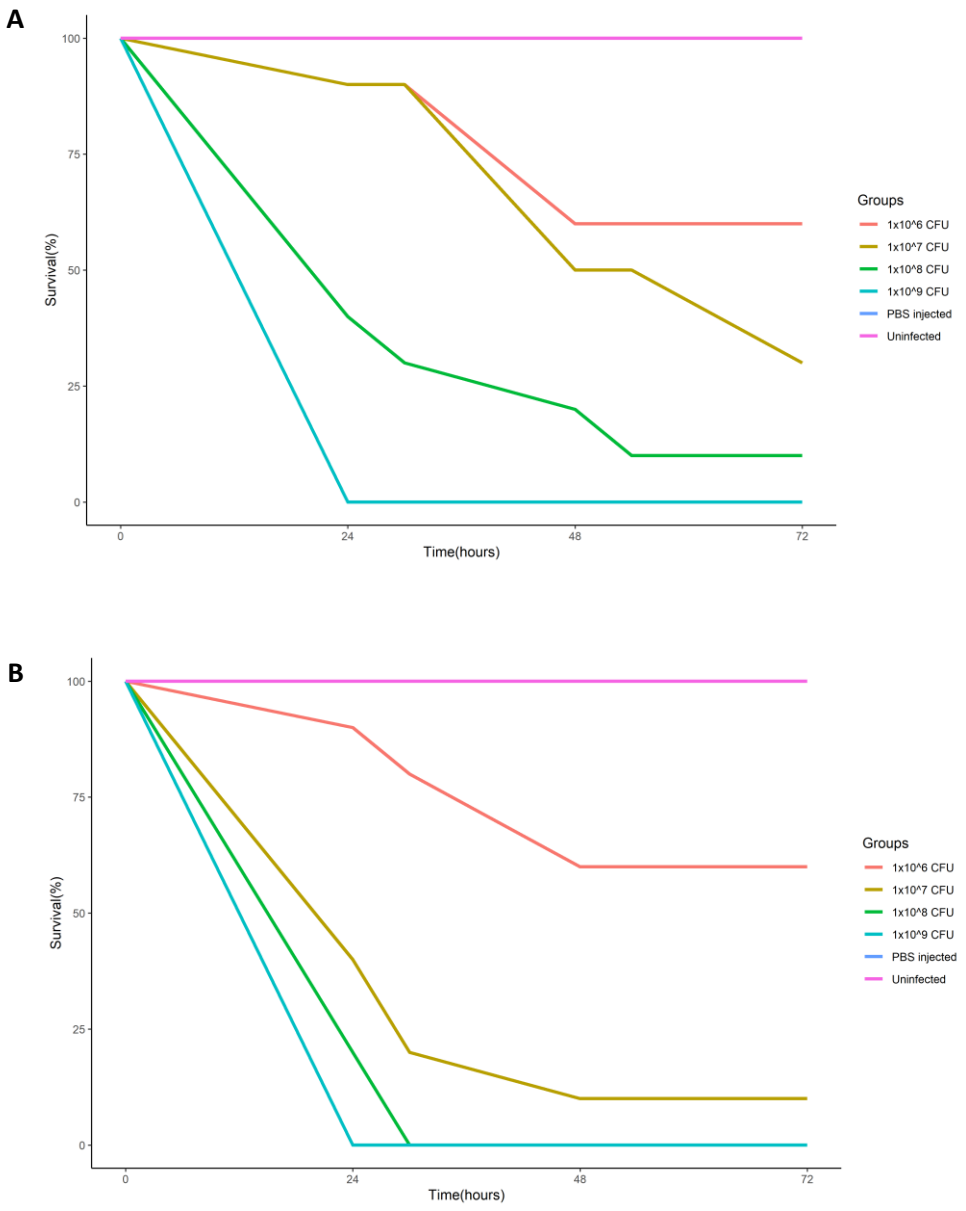

Figure 4.10. **Kaplan-Meier survival plots from *G. mellonella* larvae infected with *S. aureus* ST188 and *E. faecalis* ST40.** Survival of *G. mellonella* larvae after infection with different tested inoculums of **(A)** *S. aureus* ST188 and **(B)** *E. faecalis* ST40. PBS-injected larvae included as a negative control and non-infected larvae as positive controls. Plots show 1 independent experiment with 10 larvae per group (N = 60 larvae).

4.3.4. *In vitro* bead-based evolution model for staphylococci and enterococci

After previously optimized experimental conditions, an *in vitro* bead-based evolution model was used to study the evolutionary changes that occur in *S. aureus* ST188 and *E. faecalis* ST40 when exposed to two commonly used biocides (as previously described in **Chapter 2**). A total of 4 independent lineages of each strain in either biofilm or planktonic conditions were exposed to increasing concentrations of CHX or OCT (starting below the MIC before doubling every two passages) for 18 passages (passage window = 72 hours) giving ~250 generations in biofilms and ~120 in planktonic lineages.

The number of generations completed for each stress in the different conditions is shown in **Table 4.3.** As observed, different conditions resulted in more or less generations since the survival across the experiment differed between species, context and biocide.

Table 4.3. Number of generations of evolution completed for each stress in the different conditions in *S. aureus* ST188 and *E. faecalis* ST40.

Tested isolate	Control		Biofilms		Planktonic	
	For CHX	For OCT	CHX	OCT	CHX	OCT
E. faecalis ST40	250	259	252	220	119	119
S. aureus ST188	263	264	274	212	119	119

*Control condition (no stress + beads) for the CHX and OCT experiments.

4.3.4.1. Productivity of the evolved populations in the presence of biocides

Throughout the evolution experiment, the productivity, expressed as CFU/mL (for planktonic) and CFU/mm^2 (for biofilm recovered beads) was measured for each passage. Changes in the productivity in each generation can be found for *E. faecalis* and *S. aureus* for both stress conditions and non-stressed controls.

Both strains were able to adapt to grow in concentrations of biocides above the MIC to CHX (up to ~32 μg/mL) and to a lesser extent to OCT (2 - 4 μg/mL) until growth was compromised at the highest concentrations (**Figure 4.11.**). For control lineages (drug-free), growth in both planktonic and biofilm conditions remained stable across all experiments (**APPENDIX VII**).

E. faecalis biofilms were able to adapt to escalating CHX concentrations (up to ~32 μg/mL); with biofilm productivity maintained at a similar level to control conditions (10^5 CFU/mm^2) until populations were exposed to the highest concentrations of CHX (**Figure 4.11. - A**). Planktonic lineages were able to grow at higher concentrations of CHX than biofilms but growth in the highest concentrations was compromised, which is observed by a decrease in CFUs. *E. faecalis* planktonic lineages (**Figure 4.11. - A**) were able to grow up to 64 μg/mL and one lineage survived exposure to 128 μg/mL.

Similar patterns of growth were observed for *S. aureus* (**Figure 4.11. - C**) as for *E. faecalis* after CHX exposure. Biofilm productivity stayed relatively the same over time in controls. *S. aureus* biofilms were able to survive escalating CHX concentrations up to ~32 μg/mL, before eventually, biofilm productivity decreased. Planktonic lineages were also able to survive up to ~32 μg/mL of CHX. However, isolates from last exposures had very poor growth.

Both species were also able to adapt to escalating OCT concentrations, but to lower concentrations than for CHX. Biofilms were unable to survive beyond ~4 μg/mL of OCT for *E. faecalis* (**Figure 4.11. - B**) and ~2 μg/mL for *S. aureus* (**Figure 4.11. - D**). *E. faecalis* planktonic lineages were again able to survive higher OCT concentrations than biofilms (4 μg/mL) (**Figure 4.11. - B**) and for *S. aureus* one lineage was able to survive up to 8 μg/mL of OCT (**Figure 4.11. - D**). Biofilm productivity was maintained until growth was lost.

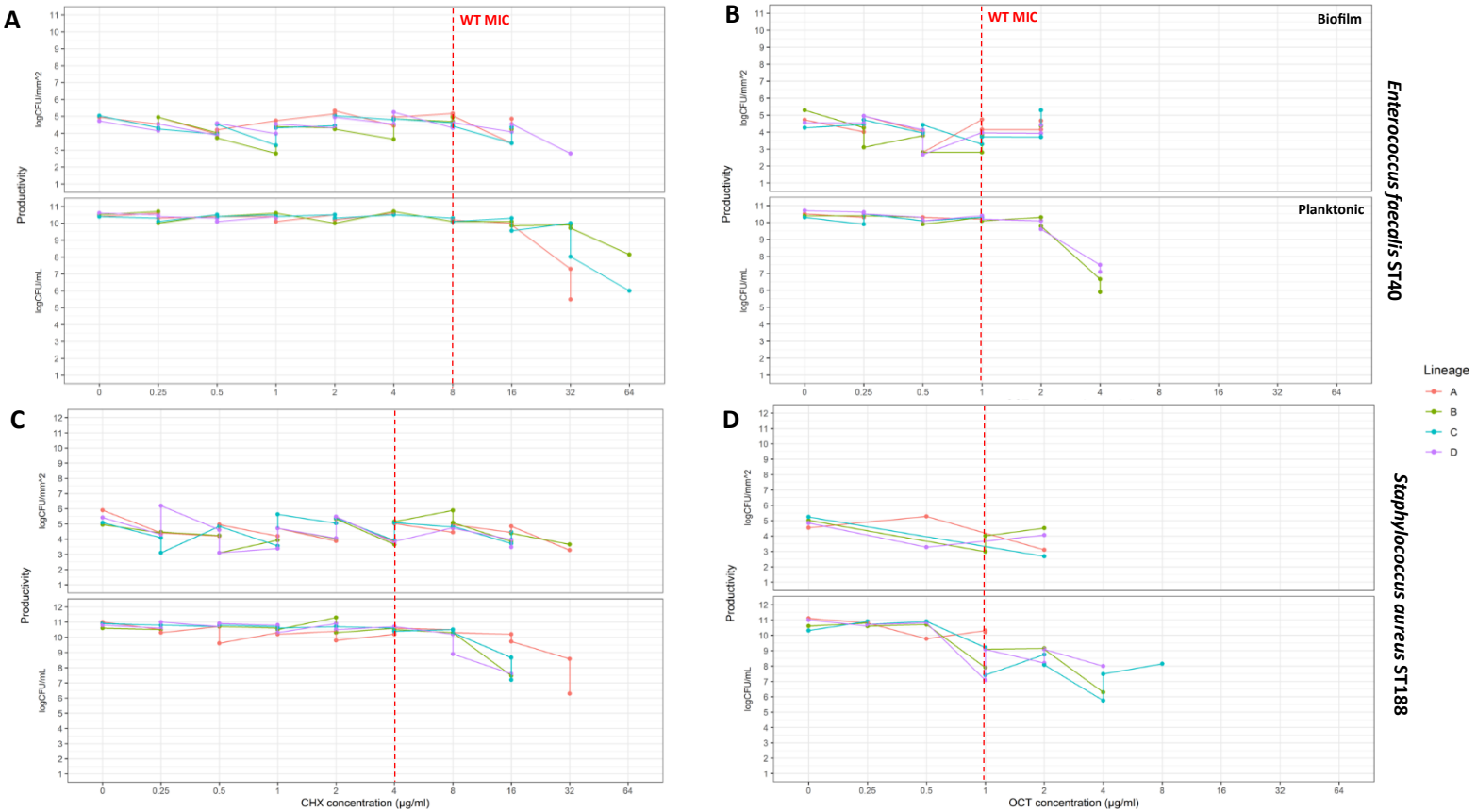

Figure 4.11. Survival of *E. faecalis* (top panels) and *S. aureus* (bottom panels) after growth in increasing concentrations of CHX and OCT. Productivity (expressed as CFU/mm^2 for the biofilm and CFU/mL for the planktonic) is plotted against the biocide concentrations for both conditions (biofilm and planktonic). The MIC of the WT is shown in a red dotted line in each panel. **(A)** *E. faecalis* isolates exposed to CHX; **(B)** *E. faecalis* isolates exposed to OCT; **(C)** *S. aureus* isolates exposed to CHX; **(D)** *S. aureus* isolates exposed to OCT.

4.4. Discussion

An *in vitro* bead-based evolution model was optimised from a previously established model to study *Burkholderia cenocepacia* (Cooper, 2018) for use with two Gram-positive species. The differences between Gram-negative and Gram-positive pathogens elucidated some difficulties in translating the model to Gram-positive pathogens. Additionally, biocides vary from antibiotics, with diverse modes of action and interacting uniquely with media. Therefore, various model optimisation steps were essential.

Results showed that bead size was not a limiting factor and had no significant effect on the number of cells able to attach to the surface allowing different sized beads to be used to distinguish between 'old and new' biofilms in the model. Other optimisation experiments were needed to increase the number of CFUs per bead which included changing different experimental conditions that could affect biofilm formation, such as the temperature, agitation, passage window and media. Choices of media included different compositions, for example, BHI medium (a nutrient-rich not defined media) and TSB (a less nutrient-rich medium). Both of these are frequently used for biofilm research, and media has been shown to affect matrix composition in staphylococcal biofilms (Sugimoto et al., 2018). Glucose and NaCl were shown to promote biofilm formation by various *S*. *aureus* strains via acidification of culture media (due to secretion of acidic metabolites). Since we wanted to develop a standard model with no external factors added, TSB was the media of choice for all the experiments. The addition of sera also showed no difference to cell growth or attachment when compared to TSB only, and so this was omitted from the experiment. During the optimisation process, it was also observed that the productivity (measured by the number of cells) does not necessarily depend on biofilm biomass, as isolates with high biofilm forming activity (based on crystal violet staining) did not show high number of cells produced by biofilms formed on beads. By altering the variables outlined above, it was possible to reliably grow biofilms on beads which produced populations large enough for evolution experiments to be run.

Results from these evolution experiments showed that both species were able to adapt to grow in increased concentrations of CHX and OCT, beyond the WT MIC; and it was easier to select tolerance to CHX than OCT. Studies have also shown adaptation to CHX (as detailed in Kampf, 2019b), but less is known about tolerance to OCT (Bock et al., 2021; Shepherd et al., 2018). Although biofilms are often intrinsically more tolerant of many antimicrobials, the planktonic lineages exhibited an ability to adapt to higher concentrations of both biocides

than the biofilm lineages. This may reflect the larger effective population size present in the planktonic lineages providing greater mutational supply. It is clear however that there was no inherently greater ability to adapt to these biocides when grown as single species biofilms for both tested Gram-positive isolates.

There is a clear gap in knowledge in regard to antimicrobial susceptibility testing of biocides/antiseptics due to the lack of standard guidelines for testing biocide susceptibility, and standard breakpoints. For antibiotics, EUCAST ensures harmonization for antibiotic susceptibility testing by stablishing clinical breakpoints and epidemiological cut-off (ECOFF). Previously though a suggested definition of a breakpoint for CHX tolerance has been proposed as 4 mg/L of CHX (Hardy et al., 2018; Horner et al., 2012). However, no MIC breakpoints for OCT have been proposed. This data here shows both strains adapt to CHX easily and above the proposed breakpoint. OCT exposure resulted in less adaptation however there was still a clear selection of phenotypically more tolerant mutants. Therefore, we can consider that the tested isolates have gained an increased tolerance to both CHX and OCT.

4.5. Conclusion

A robust and reproducible *in vitro* bead-based evolution model was optimised for two Gram-positive isolates.

This data shows important pathogens can evolve to survive at concentrations beyond the MIC of both biocides with planktonic lineages surviving at higher concentrations of both agents than biofilm lineages. The absence of standard methods and well-established breakpoints for susceptibility testing for biocides needs to be addressed, as it will improve the selection of suitable disinfectants (Htun et al., 2019; Vijayakumar and Sandle, 2019).

To determine the genetic basis behind this adaptation and correlate impacts on fitness and other phenotypes, a panel of randomly selected isolates drawn from the start, middle and end of each experiment were selected. In **Chapter 5**, results from phenotyping assays (biofilm-forming capacity, fitness, colony morphology and susceptibility to different antibiotics and biocides) and genotyping (WGS) are explained.

CHAPTER 5: PHENOTYPIC AND GENOTYPIC CHARACTERISATION OF THE BIOCIDE-EVOLVED ISOLATES

“Our genomes are like dense, coiled poems, and every poem has to be interpreted to be understood." - Siddhartha Mukherjee

5.1. Introduction

Phenotyping and genotyping of bacterial species can provide useful information on the consequences of microbial evolution and adaptation. Several studies have been investigating the link between laboratory-evolved biocide tolerant strains and the potential development of cross-resistance to antibiotics. For example, in the case of triclosan (a commonly used biocide) various studies have shown the use of this biocide is linked with antibiotic resistance. It was seen that mutations in *fabI* in *E. coli* selected by triclosan led to cross-resistance with other antimicrobials (Heath et al., 1999). QACs have also been widely studied and reported examples of cross-resistance are common, e.g., where exposure to these compounds has been shown to select resistance to ciprofloxacin in *L. monocytogenes* (Guérin et al., 2021), or cross-resistance between BZK-adapted *E. coli* and chloramphenicol (Langsrud et al., 2004).

In the context of cationic agents, studies showed that CHX and OCT exposure has also led to a decreased susceptibility to several antibiotics. For example, a study (Kõljalg et al., 2002) identified CHX-tolerant *S. aureus* strains that were less susceptible to β-lactams, quinolones, and aminoglycosides. Another study showed how sub-inhibitory CHX selected for Vancomycin-resistant *E. faecium* strains with increased tolerance to daptomycin (Bhardwaj et al., 2017). Prolonged exposure to CHX and OCT also lead to clinically decreased susceptibility to several antibiotics such as penicillin (Nicolae Dopcea et al., 2020).

In this chapter, characterisation of 308 biocide-tolerant mutants obtained from the evolution experiments (**Chapter 4**) was performed to assess different traits (fitness, biofilm-forming capacity, biofilm phenotypes, colony morphology, and cross-resistance) of the evolved populations and randomly selected isolates from these. Additionally, to better understand the genetic basis behind CHX-OCT adaptation, evolved isolates from the later timepoints were sequenced, and their genomes were compared to robust hybrid assembled WT references to identify any changes (as illustrated in **Figure 5.1.**).

5.2. Aims

- To phenotypically characterise the CHX and OCT evolved isolates.
- To generate robust hybrid genome assembles of the parental clinical isolates by combining long and short-reads sequencing.
- To identify the genes that are involved in reduced susceptibility to the tested biocides by using whole-genome sequencing.

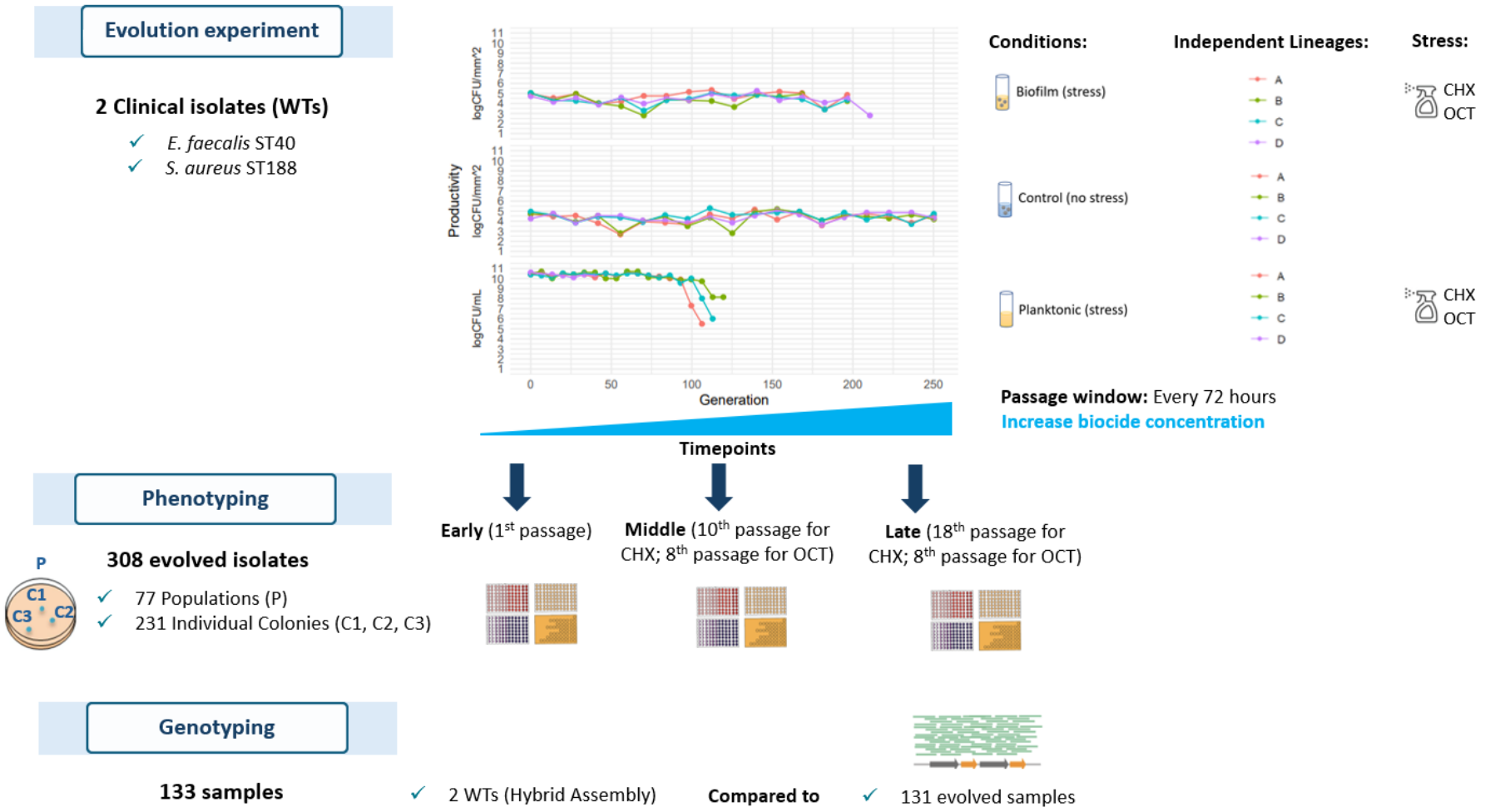

Figure 5.1. Schematic representation of the phenotypic and genotypic characterisation of biocide-tolerant mutants from the evolution experiment. Further characterisation of 308 evolved isolates obtained from different timepoints in the *in vitro* bead-based evolution model was performed. Samples from later timepoints were further selected for whole-genome sequencing.

5.3. Results

5.3.1. Phenotypic characterisation of the 308 evolved populations

Isolates were recovered from the start, middle and end of each experiment to assess changes over time (as explained in **Chapter 2**), giving a total of 308 isolates/populations to phenotypically characterise. Tests included assessing biofilm biomass production, colony morphology, fitness, and biocide-antibiotic cross-resistance.

5.3.1.1. Biofilm biomass production

The parental *S. aureus* strain had a higher biomass production (mean OD_{600nm} = 1.374, std error = ± 0.15) than the *E. faecalis* strain (mean OD_{600nm} = 0.858, std error = ± 0.16). Biofilm biomass production differed between evolved isolates recovered from different conditions.

E. faecalis evolved isolates showed lower biofilm formation after being exposed to CHX (**Figure 5.2. - A**) than in the control lineages but were able to maintain biofilm formation after exposure with OCT (**Figure 5.2. - B**) which increased when compared to the control. In contrast, *S. aureus* isolates exposed to either biocide (CHX and OCT) produced more biomass than control lineages (**Figure 5.2. - C and D**), although this reduced over time after CHX exposure (**Figure 5.2. - C**).

Wilcoxon-Mann-Whitney tests showed non-statistically significant changes (*p-value* > 0.05) within conditions for each sample (**APPENDICES VIII - XI**).

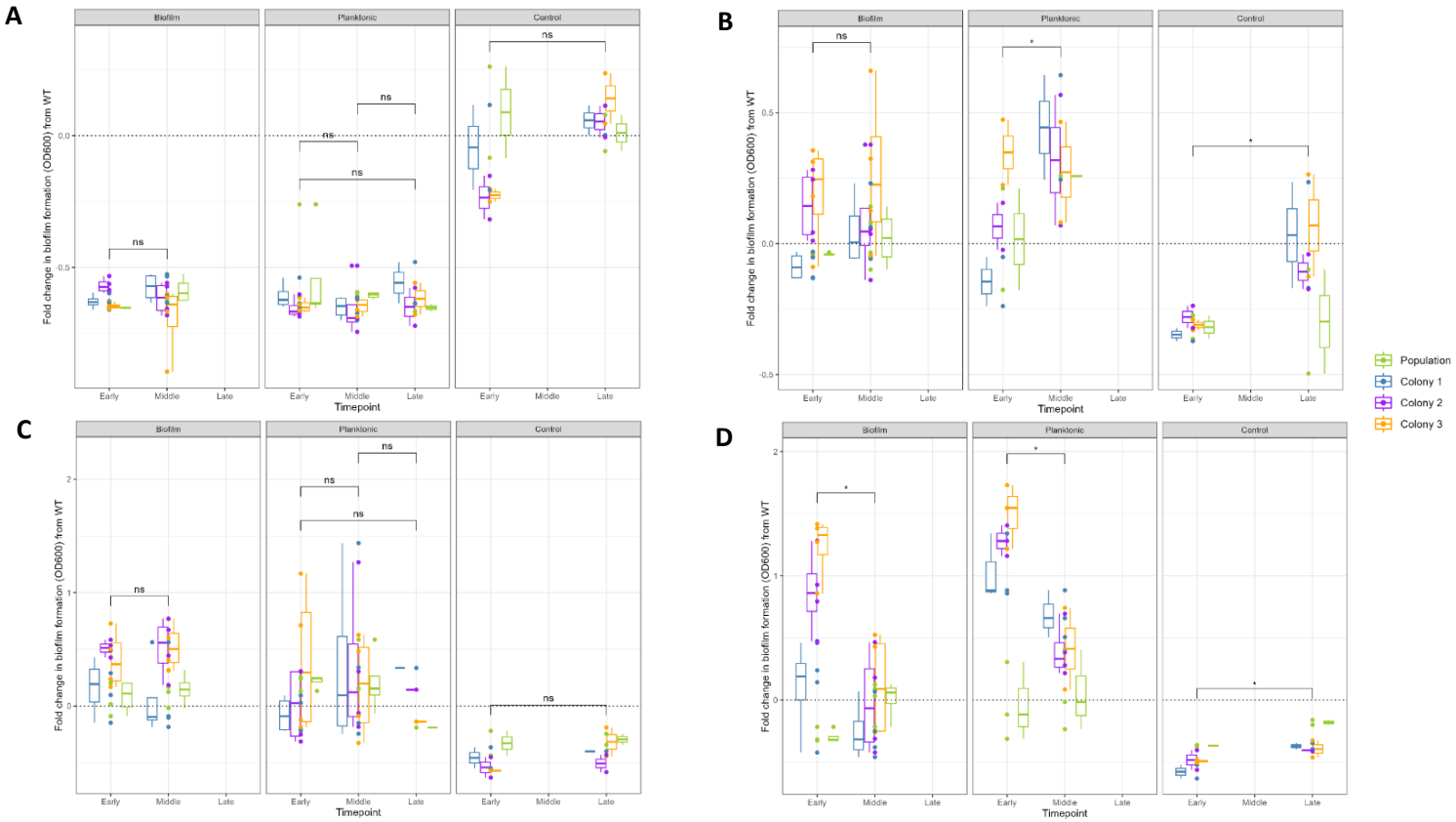

Figure 5.2. Biocide exposure had species-specific impacts on biomass production. Fold changes in biofilm formation ($OD600_{nm}$) from the WT baseline (black dotted line) are shown. Boxplots representing crystal violet staining with medians are shown; populations and individual isolates represented in different colours. **(A)** *E. faecalis* isolates exposed to CHX; **(B)** *E. faecalis* isolates exposed to OCT; **(C)** *S. aureus* isolates exposed to CHX; **(D)** *S. aureus* isolates exposed to OCT. Kruskal-Wallis test assessed differences between timepoints across conditions; Wilcoxon-Mann-Whitney test applied as a *post hoc* to study differences within conditions; *ns* indicates non-statistically significant changes (*p-value* > 0.05) with * indicating statistically significant differences (*p-value* ≤ 0.05) within conditions for each timepoint according to the Wilcoxon-Mann-Whitney test.

5.3.1.2. Colony morphology of the evolved isolates

Changes in the size and colony morphology of the colonies between timepoints (early, middle, late) were studied. In general, colony morphology was similar between the 308 evolved samples. For *E. faecalis*, in some earlier timepoints colonies seemed bigger and more undulate. This was also observed for *S. aureus* where smaller colonies were observed in some middle timepoints. Colonies from the control plates had similar colony morphology throughout.

Colonies of populations and isolates obtained over the evolution experiment were ranked on a 1 - 3 scale depending on the intensity of the Congo red (**Figure 5.3. - A**), which ranges from light red (1+), which was associated with lower biofilm production, to dark red (3+) which was associated with higher biofilm production. Colonies with a mixture of light red and dark red (indicated with 2+), had a mixed biofilm production. For the parental strains (**Figure 5.3. - B**), the colour of the *S. aureus* colony was dark red (3+) whereas for *E. faecalis* the colonies were paler (1+).

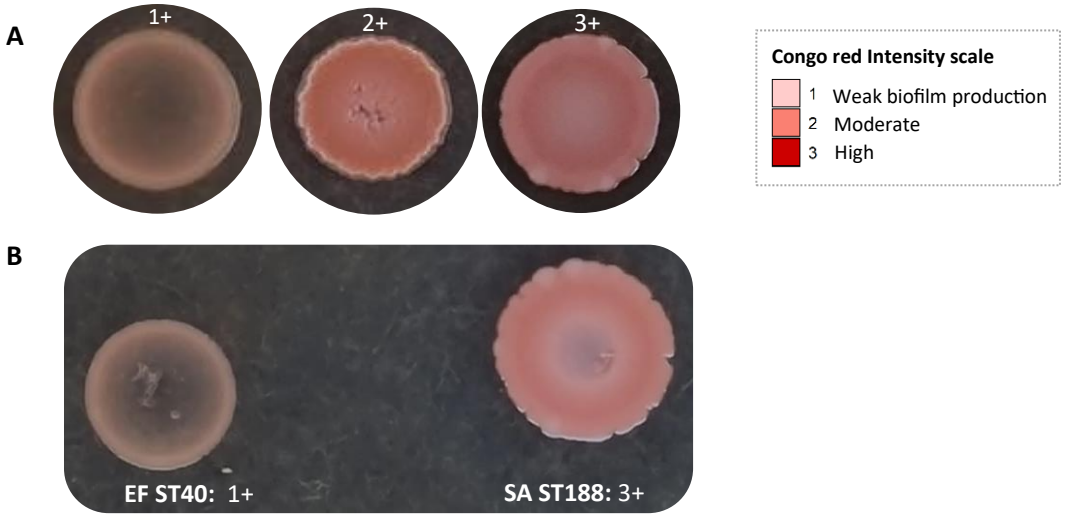

Figure 5.3. Colony morphology and ranking scores of *E. faecalis* and *S. aureus* on Congo red agar plates. (A) Colonies were scored on a 1 - 3 scale according to the Congo red intensity, each score was associated to a different level of biofilm production (three representative evolved samples shown). **(B)** Colony morphologies of *E. faecalis* (EF) and *S. aureus* (SA) WTs with their respective scores are shown.

E. faecalis evolved isolates had low biofilm production (1+) at both early and middle timepoints. Controls (no biocide) showed low biofilm production (1+) and no variation in biofilm production over time. Under CHX stress, colonies isolated from biofilms became paler over time after exposure to CHX. As seen at early timepoints colonies were darker (3+) than at middle timepoints (**Figure 5.4. - A**). In the evolution experiment, the biofilm condition did not reach the late timepoint hence only the planktonic condition is shown here. No differences were observed in colony morphologies over time for OCT for both conditions (**Figure 5.4. - B**).

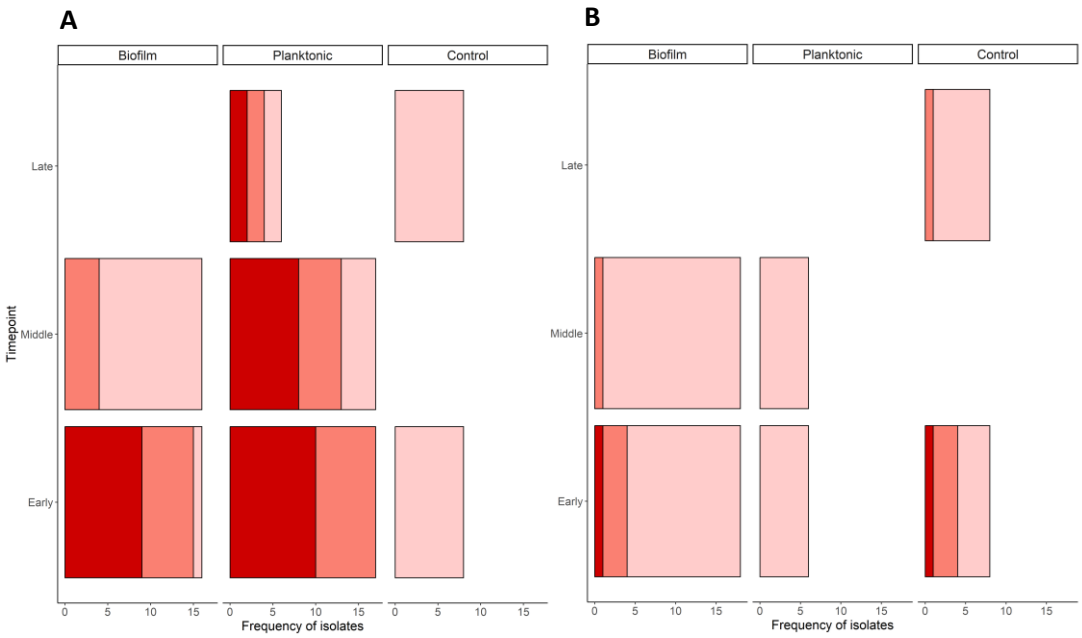

Figure 5.4. Total distribution of Congo red intensity of the *E. faeca*lis evolved isolates. Isolates that evolved in **(A)** CHX and **(B)** OCT stress are shown. Stacked barplots show changes in biofilm formation by timepoint (early, middle, late) in each condition.

A converse pattern was observed for *S. aureus* when compared to *E. faecalis*. For CHX, no differences in colony morphology were seen over time in both biofilm and planktonic conditions (**Figure 5.5. - A**). Most of the isolates showed mainly pale colony formation. Populations exposed to OCT showed higher biofilm production at early timepoints (3+) than at middle timepoints (1+) (**Figure 5.5. - B**). Controls for this experiment showed higher biofilm production at earlier timepoints than at late.

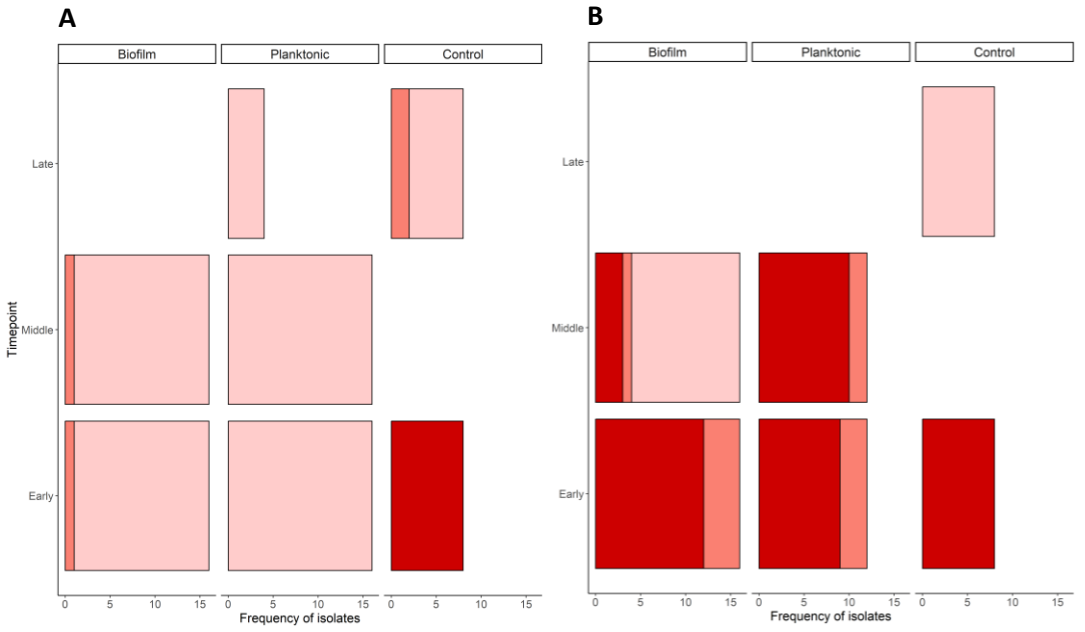

Figure 5.5. Total distribution of Congo red intensity of the *S. aureus* evolved isolates. Isolates that evolved in **(A)** CHX and **(B)** OCT stress are shown. Stacked barplots show changes in biofilm formation by timepoint in each condition.

5.3.1.3. Fitness measurements of the WT and evolved populations

The *S. aureus* ST188 growth in TSB broth with no biocide was higher than *E. faecalis* ST40 (**Figure 5.6.**). The area under the curve (AUC) for *S. aureus* was 10.32 A.U. and for *E. faecalis* 6.47 A.U.

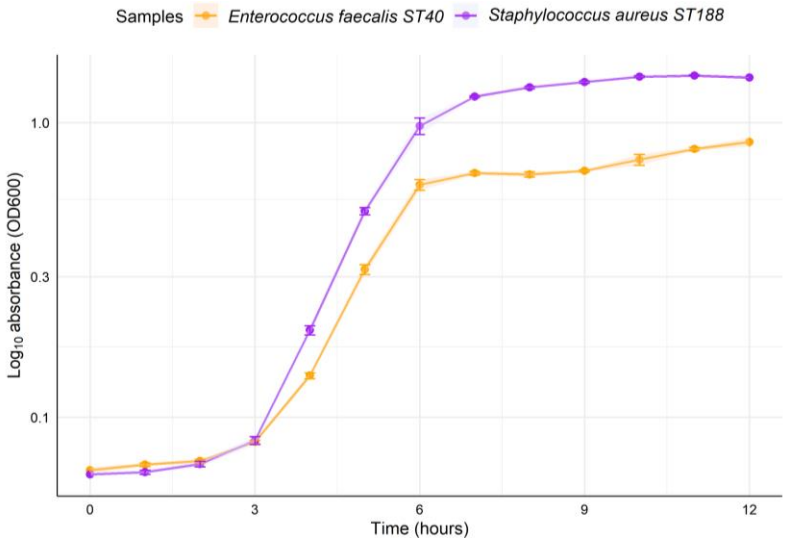

Figure 5.6. Growth curves of the WT isolates grown in TSB. Absorbance ($OD600_{nm}$) measured for 12 hours. Error bars (also represented as shaded areas) indicate the standard deviation of the mean.

Growth of the isolates in drug free media was determined to study fitness of evolved isolates compared with controls; area under the curve values calculated and plotted relative to the WT. For both species growth in the original experiment was largely maintained until a prohibitive biocide concentration was reached (**Figure 5.7.**).

E. faecalis isolates exposed to either agent recovered from the experiments were not inhibited in their ability to grow in planktonic culture compared to the parental strain and increased growth capacity slightly in line with control lineages. After CHX (**Figure 5.7. - A**) and OCT exposure (**Figure 5.7. - B**), biofilm growth was higher than in the planktonic condition and similar between timepoints. Control samples (early and late timepoints) had similar growth over time. Under OCT stress (**Figure 5.7. - B**), no late timepoint was plotted as isolates did not survive higher exposure to OCT in the evolution experiment.

S. aureus isolates recovered from across the time points demonstrated no significant change in growth capacity. When observing *S. aureus* after CHX exposure (**Figure 5.7. - C**), growth of *S. aureus* mutants was higher than the parent strain for the early timepoint. However, most isolates grew equally or less than the parental strain for the middle and late timepoint (**Figure 5.7. - C**). *S. aureus* grown under OCT stress (**Figure 5.7. - D**) showed no massive difference in growth between timepoints. The control condition (no biocide) from the late timepoint had lower growth than the WT.

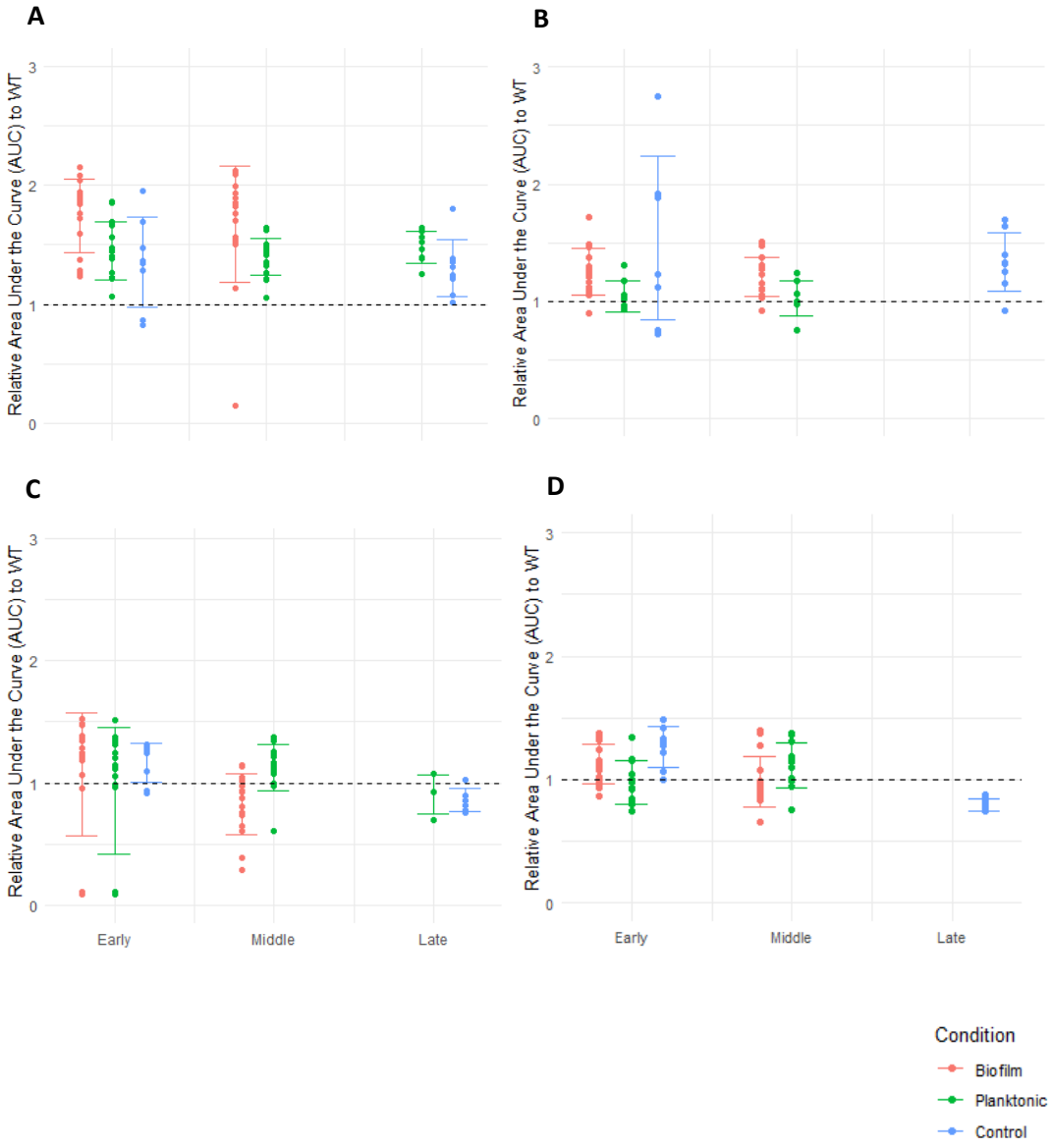

Figure 5.7. Relative growth of mutants isolated after antiseptic exposure. After growth kinetic experiments, the area under the curve (AUC) was determined for mutants recovered from each exposure experiment relative to the parental strain (black dotted line). Graphs show **(A)** *E. faecalis* isolates exposed to CHX; **(B)** *E. faecalis* isolates exposed to OCT; **(C)** *S. aureus* isolates exposed to CHX; **(D)** *S. aureus* isolates exposed to OCT. Error bars determined by the mean and standard deviation values of the samples, grouped by condition (biofilm, planktonic, control).

5.3.1.4. Studying the link between biocide tolerance and antibiotic cross-resistance

Determining the MIC of the two parental strains

Antibiotic susceptibility of the two parental clinical strains, *S. aureus* ST188 and *E. faecalis* ST40, was determined for 6 antibiotics and the 2 biocides. Additionally, MIC data was compared between two different growth mediums: TSB and MH. MH is the recommended media for determining antibiotic MIC according to the EUCAST guidelines (EUCAST, 2024a), and TSB is a media widely used media for *Staphylococcus* growth.

MICs determined in MH media were generally lower than those found in TSB for both *E. faecalis* ST40 (**Table 5.1.**) and *S. aureus* ST188 (**Table 5.2**.). In general, between 2-4-fold change increases in MICs were seen when comparing MH to TSB. For example, the MIC of gentamicin against *S. aureus* was 4 µg/mL in MH and between 8 - 16 µg/mL in TSB. The MIC of penicillin against *E. faecalis* was 1 µg/mL in MH but up to 16 µg/mL in TSB. In some cases, such as OCT and erythromycin, the MIC did not vary between media.

Table 5.1. MICs for 6 different antibiotics and 2 biocides against *E. faecalis* ST40 determined in two different media: MH (in purple) and TSB (in green).

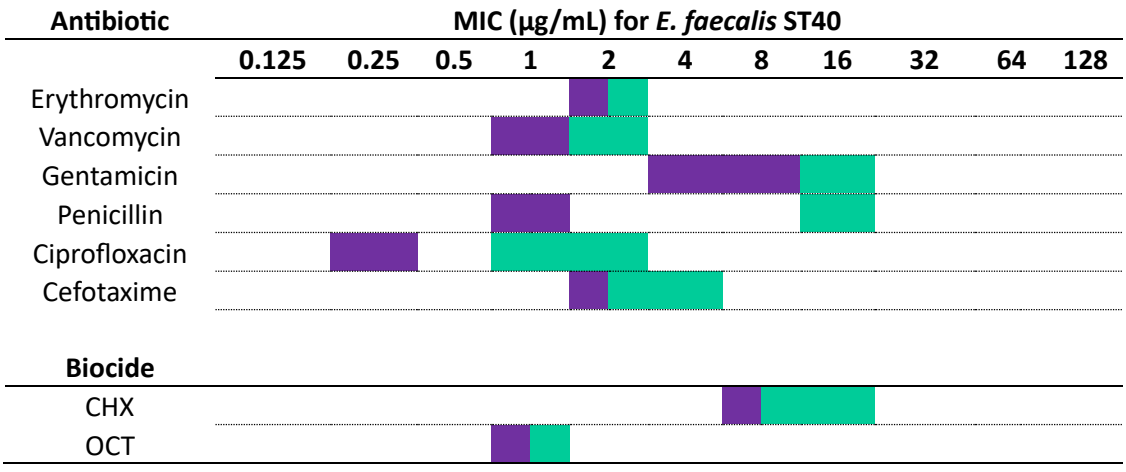

Table 5.2. MICs for 6 different antibiotics and 2 biocides against *S. aureus* ST188 determined in two different media: MH (in purple) and TSB (in green).

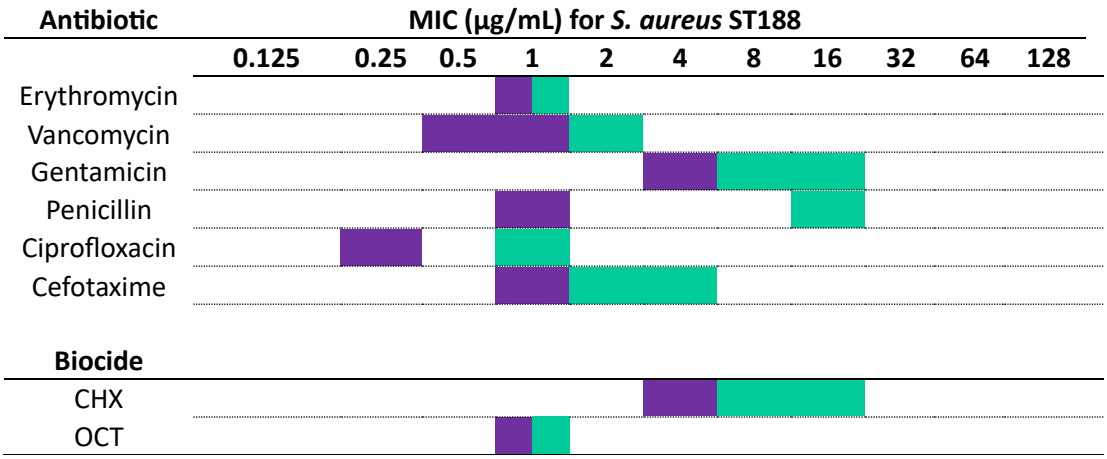

The MICs of both biocides and a panel of antibiotics were determined for the evolved isolates to identify changes in the susceptibility pattern from biocide exposure and any cross-resistance resulting from exposure to CHX or OCT. Results obtained with MH media were used as the parental strain reference to proceed with comparison of the evolved isolates.

Distribution of MIC values across the evolved samples

Distribution of MIC values of each antibiotic and biocide across the 306 evolved isolates was studied to better understand susceptibility patterns in the individual samples and within the population. Changes in the distribution of the MIC values across the samples were assessed, and differences between timepoints were observed.

In *E. faecalis* under CHX stress (**APPENDIX XII**), for some antibiotics (e.g., vancomycin), the MIC remained consistent amongst the isolates (n = 72), however, for some antibiotics (e.g., gentamicin) there was more of a distribution in MIC observed. Interestingly, for cefotaxime the MIC did not change, all the isolates showed an MIC higher than 64 µg/mL. The control samples (n = 16) distribution of MICs for the different antibiotics and biocides was similar to the stressed samples, with little change in the MIC. Under OCT stress (**APPENDIX XII**), distribution of MICs for the different antibiotics and biocides in the stressed samples (n = 48) was similar to the control samples (n = 16).

In *S. aureus* under CHX stress (**APPENDIX XIII**) for both tested biocides, the MIC was the same in all the evolved isolates (n = 68) whereas for the antibiotics changes in MIC were observed between timepoints. Control samples (n = 16) had a different distribution of the MICs for the

biocides and some antibiotics. Under OCT stress (**APPENDIX AXII**), variable MIC values were found in the evolved isolates (n = 56) for all antibiotics; the same MIC of CHX was found throughout the stressed isolates and controls (n = 16).

Change in susceptibility profiles in the evolved isolates compared to the WT

Changes in susceptibility profiles compared to the parental strains were determined for each stress. Early and late timepoints were selected for the control condition (hence the white space in the middle timepoint indicates no samples were represented). For the biofilm and planktonic conditions, three timepoints were selected. Overall, the MIC data obtained (**Figure 5.8.**) show very little impact on antibiotic susceptibility occurred as a result of biocide exposure in these conditions.

Decreased susceptibility to both antiseptics were seen in all exposed lineages although these were modest (mainly 2-$\log_2$ FC) (**Figure 5.8.**). Only low-level changes to various antibiotics were observed, increases in MICs of cefotaxime were consistently observed for both *E. faecalis* (**Figure 5.8. - A and B**), and *S. aureus* (**Figure 5.8. - C and D**) after exposure. Nevertheless, this was also seen in the control condition, which suggests this may be due to media adaptation rather that exposure to biocides.

In *E. faecalis* evolved isolates under CHX exposure (**Figure 5.8. - A**), had an increase in MICs which was not seen in the controls, indicating the low-level changes to CHX in the biofilm and planktonic condition are not due to media adaptation. No changes in the MIC of ciprofloxacin, penicillin, vancomycin, and erythromycin from the evolved isolates were seen when compared to the WT. For *E. faecalis* OCT stress, the average $\log_2$ fold change in MIC (compared to the WT average) showed low level changes to OCT were selected in both biofilm and planktonic condition but not observed in the control (**Figure 5.8. - B**). Low level changes to CHX stress were also seen in biofilm and not in the control condition. Interestingly, the MIC of gentamicin showed a reduction in the control condition. No changes in the MIC of ciprofloxacin, penicillin, vancomycin, or erythromycin were observed in any of the three conditions.

For *S. aureus* under CHX stress (**Figure 5.8. - C**), a 2-$\log_2$ fold increase to gentamicin were seen in biofilm (early and middle) and not in the control condition. Additionally, a 2-$\log_2$ fold change in the ciprofloxacin MIC was seen for early and late stages in the planktonic condition and not in the control. However, no changes were seen for the MIC of ciprofloxacin in any of the conditions under OCT stress (**Figure 5.8. - D**).

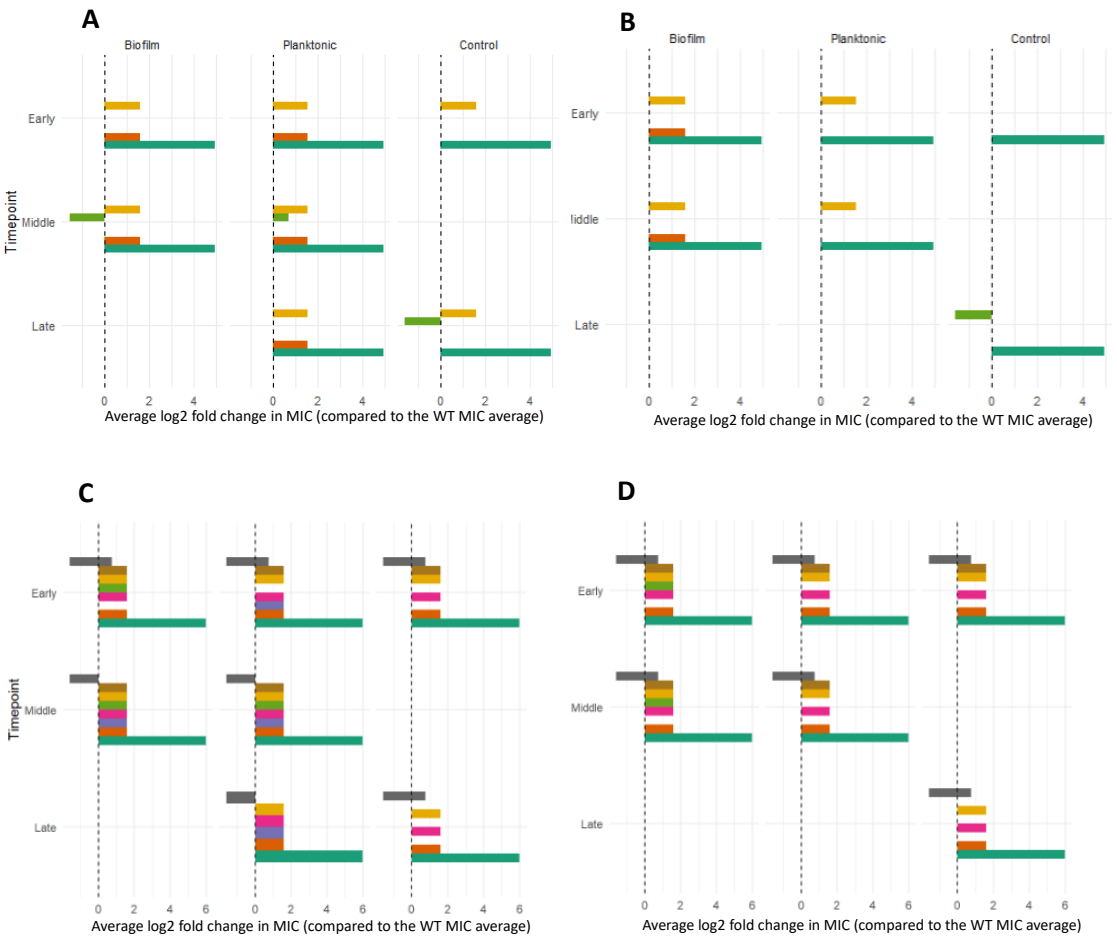

Figure 5.8. Susceptibility profile of *E. faecalis* and *S. aureus* evolved isolates. The average $\log_2$ fold change in MICs (compared to the WT MIC average) was calculated for 6 different antibiotics and 2 biocides. Results for each condition (biofilm, planktonic and control) are shown. **(A)** *E. faecalis* CHX-exposed; **(B)** *E. faecalis* OCT-exposed; **(C)** *S. aureus* CHX-exposed; **(D)** *S. aureus* OCT-exposed.

5.3.2. Genotyping

5.3.2.1. Characterization of the two parental clinical strains

To obtain robust reference genomes, *de novo* assemblies using short-reads (Illumina) and long-reads (Nanopore) were performed, and sequences were combined to make hybrid assemblies. Using the QI-Taxon pipeline from IRIDA (as explained in **Chapter 2**, **Section 2.12.**), taxonomic classification of reads was performed which confirmed the MLST of the sequenced isolates (**Figure 5.9.**).

E. faecalis parental genome (hybrid assembly) had a total of four contigs (**APPENDIX XIV**): a main circular chromosome (2.9 Mbp), and 3 smaller contigs of different lengths that correspond to plasmids and phage sequences. The *S. aureus* parental genome (hybrid assembly) showed a total of 3 contigs: the main circular genome (2.7 Mbp) and two plasmid contigs. *S. aureus* ST188 had the largest N50 (138 Kbp) compared to *E. faecalis* ST40 (114 Kbp); the guanine-cytosine content (GC %) of both assemblies were consistent with the expected species, with *E. faecalis* ST40 having a higher GC percentage (37 %) than *S. aureus* ST188 (32 %).

Antimicrobial resistance genes pipelines used included the Quadram Institute Bioscience AMR detection pipeline and ARIBA (Hunt et al., 2017). When using the AMR detection pipeline, which uses the RDI and StarAMR tools, common genes (e.g., *bla*Z) were found but more genes were obtained by ARIBA (searching the CARD database). Further investigation of the gene function of each AMR gene showed that most antimicrobial genes present in the WT genomes were mostly core efflux pumps. Additionally, with BacMet database, specific for BRG and metal resistance genes, showed some metal resistance genes with 100 % identical matches in the WTs.

Enterococcus faecalis ST40

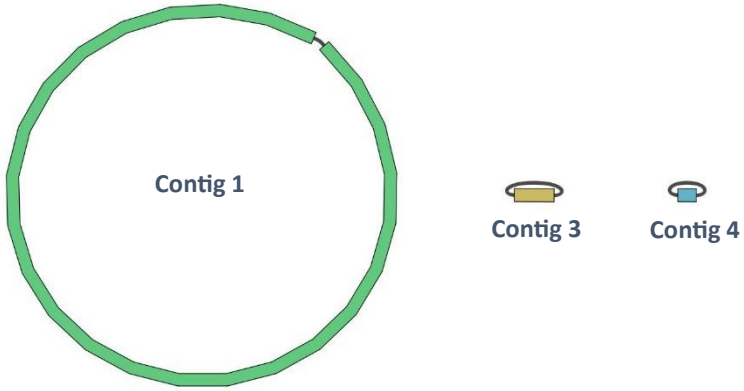

Sequence name	Length (bp)	Corresponds to	Circular
Contig 1	2,953,229	Genome	+
Contig 2	31,031	Phage	-
Contig 3	100,388	Plasmid	+
Contig 4	46,644	Plasmid	+

Staphylococcus aureus ST188

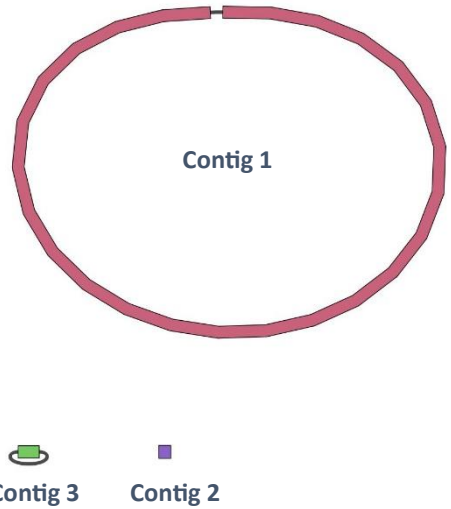

Sequence name	Length (bp)	Corresponds to	Circular
Contig 1	2,764,623	Genome	+
Contig 2	14,720	Plasmid	-
Contig 3	49,867	Plasmid	+

Figure 5.9. *De novo* hybrid assembly graphs from the WT genomes. Assemblies visualized with Bandage Image (v0.8.1), with additional information summarised in the tables.

5.3.2.2. Genotyping the selected evolved isolates

After phenotyping 308 samples from across the experiments (including 77 whole populations and 231 randomly selected individual colonies), 131 samples representing final timepoints from each strain and all exposure conditions were selected for whole-genome sequencing (WGS) to determine the genetic basis behind their adaptation to surviving in high biocide concentrations.

Sequencing of *S. aureus* evolved isolates identified various mutations present in the different groups (in intergenic and genetic regions) and phylogenetic trees indicate a divergence according to the stressor with groups seen relating to different exposure to OCT or CHX. When compared to the parental genome, *S. aureus* evolved isolates contained 60 core SNPs (out of 2,700,000 core-alignment) (**Figure 5.10. - A**) versus more than 600 SNPs (out of a 3,000,000 core-alignment) in *E. faecalis* evolved isolates (**Figure 5.10. - B**).

For both species, some isolates had multiple SNPs, and various SNPs were observed in the same or similar genes which independently arose in multiple lineages.

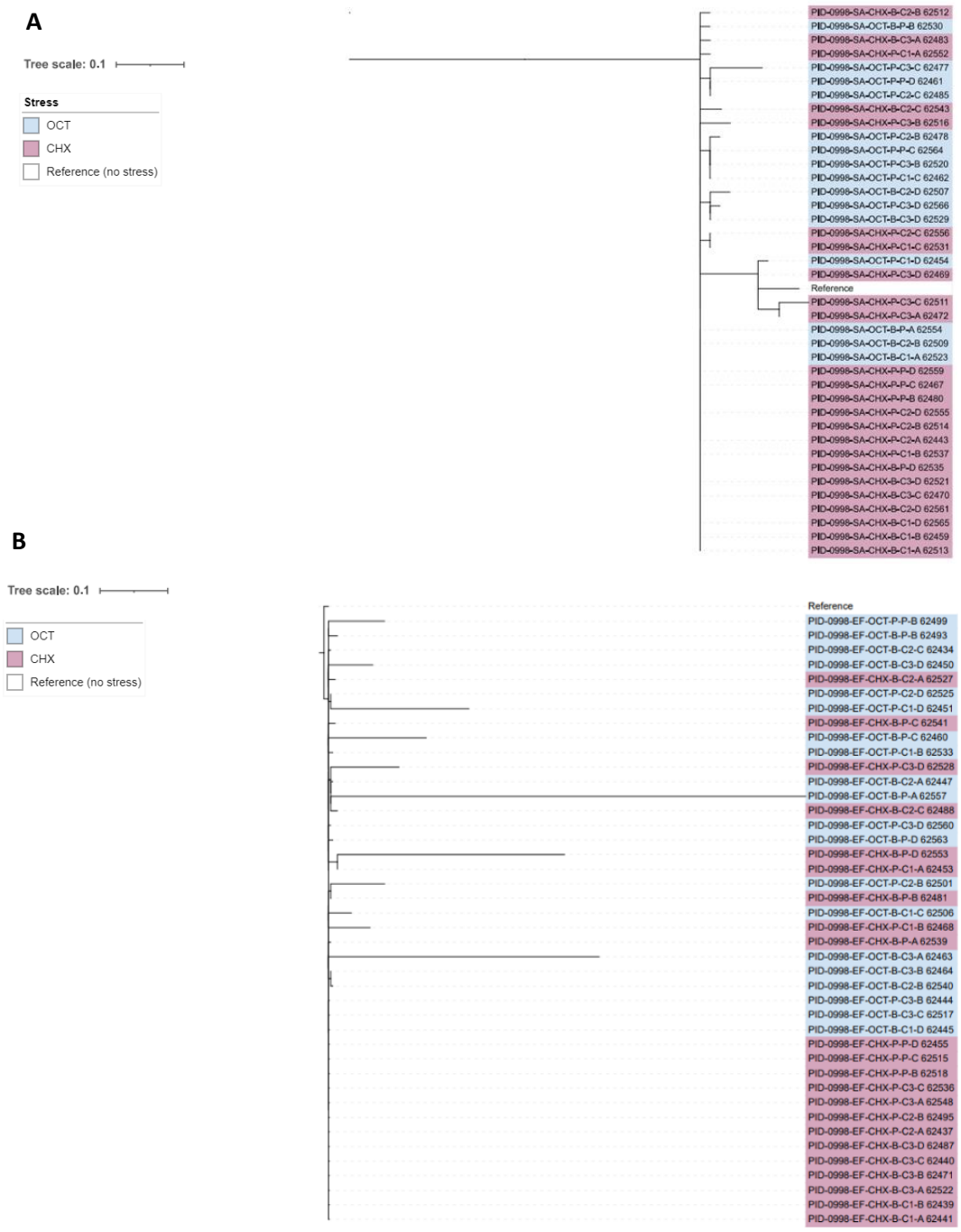

Figure 5.10. Phylogenetic trees from alignment of (A) *S. aureus* ST188 and (B) *E. faecalis* ST40 evolved isolates with the reference wild-type genomes. Approximately-maximum-likelihood phylogenetic trees from Snippy-core (v4.4.3) alignments generated with FASTTREE (v2.1.10) and visualised with iTOL (v6.8.2). The phylogenetic trees were rooted using the reference strain. Results show different groups selected by different stress conditions (CHX highlighted in pink, OCT in blue). Abbreviations: species (SA/EF), biocide (OCT/CHX), condition (planktonic/biofilm), origin (Population/Random colony [C1, C2, C3]), lineage (A, B, C, D).

In *S. aureus* isolates, a panel of SNPs were identified in genes involved in diverse cellular processes such as amino acid, siderophore and phospholipid biosynthesis, virulence, and transcriptional regulation (**Figure 5.11.**). Hypothetical genes with unknown biological functions are also included. Amongst these different isolates from independent lineages exposed to either OCT or CHX stress, all shared a common SNPs in the same gene fatty acid kinase (*fakA*), which is associated with phospholipid synthesis. Two independent isolates shared a mutation in the chorismite synthase (*aroC*) gene (**Figure 5.11.**).

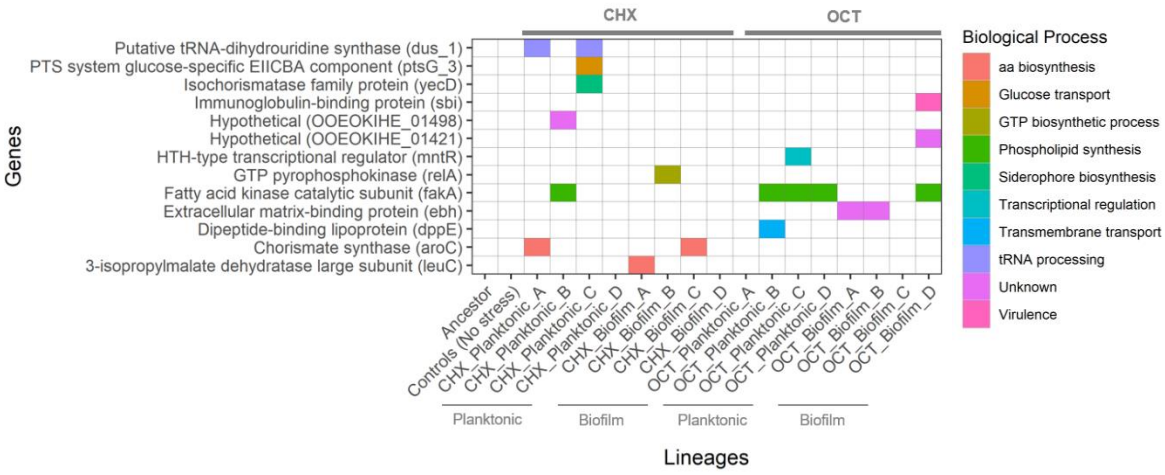

Figure 5.11. Non-synonymous SNPs present in selected evolved *S. aureus* isolates. Mutations in genes involved in many biological processes were found in in *S. aureus* ST188 evolved isolates stressed with CHX or OCT. Displayed are SNPs present in multiple lineages or in genes with a predicted association with antiseptic tolerance.

In the *E. faecalis* evolved isolates, a total of 12 SNPs were present in more than one evolved isolate. For this analysis, the search was narrowed into SNPs present in more than one evolved isolate (**Table 5.3.**). From these, 3 SNPs were found in intergenic regions and there was a mutation found in a hypothetical gene of unknown function. Of the 8 remaining SNPs, there were missense mutations in 2-hydroxyacyl-CoA dehydratase (which forms the 2-acyl-CoA product), *yitT* (required for protection against paraquat stress), *lysM*, encoding a peptidoglycan-binding domain-containing protein (with 4 SNPs in different positions of the same gene), *priA* (encoding a primosomal protein involved in DNA replication) and in a Dak2 domain-containing protein where two isolates exposed to OCT presented a non-synonymous mutation within this protein.

Table 5.3. Summary of the SNPs in annotated and hypothetical genes with known biological function from *E. faecalis* ST40 evolved isolates stressed with CHX and OCT.

Gene	Name or functions	Present in
Hypothetical (CIJKNMKJ_00813)	YitT family protein required for protection against paraquat stress	OCT and CHX
2-hydroxyacyl-CoA dehydratase	Forms the 2-acyl-CoA product	OCT and CHX
Hypothetical (CIJKNMKJ_00838)	LysM peptidoglycan-binding domain-containing protein	CHX
priA	Priomosomal protein involved in DNA replication	OCT
Hypothetical (CIJKNMKJ_01735)	Dak2 domain-containing protein	OCT

After individually studying all the genes, and from information obtained in the literature an observation was made. Interestingly, two isolates exposed to OCT presented a non-synonymous mutation in the gene encoding a Dak2 domain-containing protein. When studying the genetic environment (**Figure 5.12.**) in *E. faecalis* ST40 of the hypothetical gene (CIJKNMKJ_01735) and comparing it with the *fakA* gene from *S. aureus* ST188 they appear to be homologous genes, with the CIJKNMKJ_01735 corresponding to the gene *dak2*.

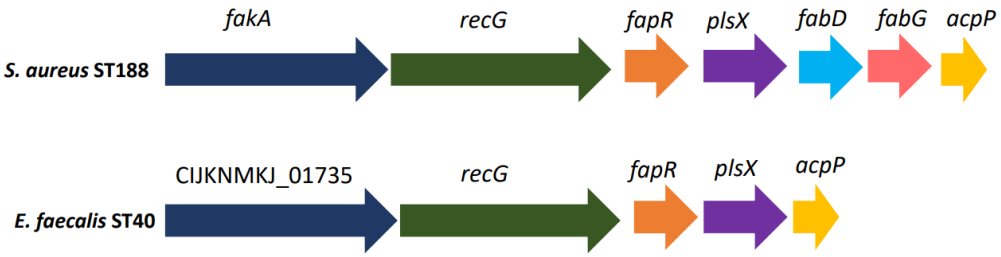

Figure 5.12. Schematic representation of the gene environment for *fakA* and the homologous gene *dak2* in the two WT isolates. Genes are plotted as arrows facing direction of transcription and ordered by their genomic positions. CIJKNMKJ_01735 corresponds to *dak2* (homologous to *fakA*).

A series of separate substitutions at five different positions from 14 isolates of both species were found in the 3 different structural domains (characterised by Subramanian et al., 2022) of the fatty acid kinase which were recovered from both species in biofilm and planktonic conditions. A graphical summary of the non-synonymous mutations in FakA/Dak2 identified in all conditions are shown (**Figure 5.13.**). As seen, changes in FakA were mainly predicted to result in loss of function as a result of either introduction of stop codons or missense mutations in completely conserved residues as later explained in **Chapter 6**.

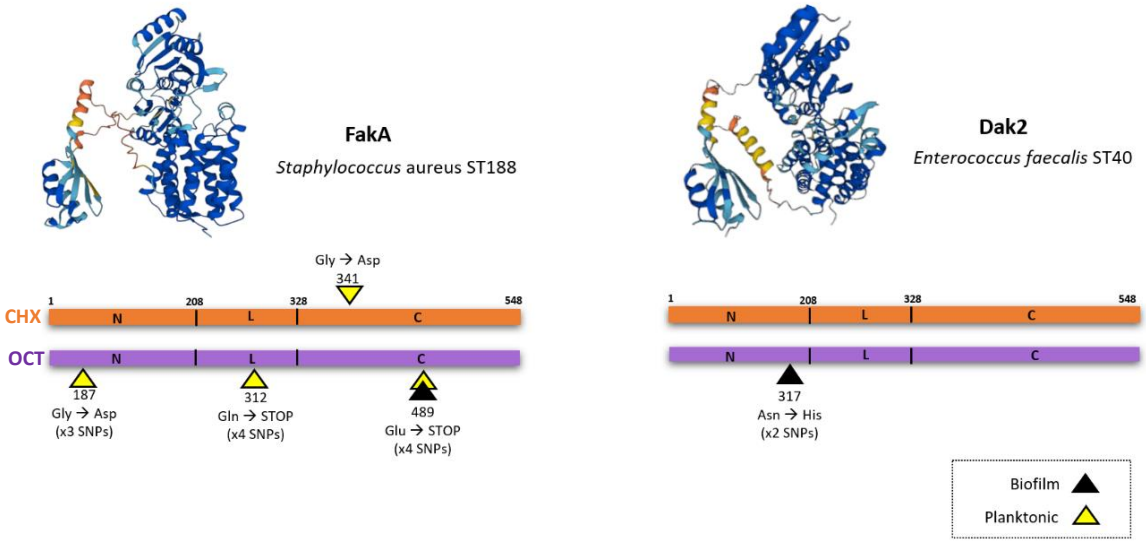

Figure 5.13. Graphical overview of SNPs present in FakA/Dak2 domains recovered from both species for CHX and OCT stress. Substitutions are indicated by triangles, with different colours representing biofilm or planktonic conditions. The number of SNPs per position in the 3 main structural domains (N = amino terminal domain; L = central domain; C = carboxy domain) are shown for each stress. FakA/Dak2 predicted structure from AlphaFold DB (v.2022-11-01).

5.3. Discussion

From the previous evolution experiments (**Chapter 4**) we observed that the two selected strains were able to adapt to increased concentrations of CHX and OCT (beyond the WT MIC) but growth was compromised in planktonic and biofilm conditions. Phenotypic characterisation was performed to understand the changes that occurred in the evolved populations and random isolates.

Exposure to CHX was linked with lower biofilm biomass production in *E. faecalis* although biofilm biomass increased for *S. aureus* isolates after exposure to both agents. Regarding colony morphology on Congo red plates, colonies taken from biofilms became paler over time after exposure to CHX for *E. faecalis*, suggesting adaptation to biocide has a negative effect in biofilm formation over time and further demonstrating constraint of biofilm formation by CHX exposure, although a converse pattern was observed for *S. aureus*. Interestingly, isolates from across the exposure series were not inhibited in their ability to grow in planktonic culture indicating no fitness deficit.

Antimicrobial susceptibility testing results showed that the MICs for the different antibiotics against the parent strains – representative of the staphylococci and enterococci group – were within the EUCAST ECOFF for normal populations (EUCAST, 2024b). Results against the evolved isolates showed very limited changes in antimicrobial susceptibility following exposure to either biocide and there were no significant changes between isolates recovered from planktonic or biofilm conditions. OCT showed less potential to select for tolerance than CHX.

Changes to cefotaxime susceptibility were observed in both species but also occurred in control conditions and are likely to represent media adaptation and not a specific response to either biocide. There is no cefotaxime MIC data available in EUCAST for *E. faecalis*, as this pathogen is considered intrinsically resistant to many cephalosporins. In *S. aureus*, the MIC of cefotaxime against isolates surpassed the ECOFF value (4 mg/L; EUCAST, 2024b) after exposure to both drugs, however the same pattern was also seen in control lineages indicating this is a result of adaptation to the experimental conditions rather than the antiseptics. This could explain high changes (4-$\log_2$ fold increase) in the MIC of cefotaxime in the three conditions when compared to the WT.

In *E. faecalis* evolved isolates there was no MIC that surpassed the EUCAST ECOFF for the tested antibiotics (EUCAST, 2024b). *S. aureus* isolates demonstrated a wider spectrum of other changes in susceptibility although this was usually only by 1-2 dilutions and similar

changes were seen in control lineages as well. For example, the MIC of gentamicin was increased for *S. aureus* isolates recovered after exposure to both biocides in in planktonic and biofilm conditions and these were above the ECOFF (2 mg/L; EUCAST, 2024b). Other studies have also shown an increase in the MIC of gentamicin after CHX exposure in several *S. aureus* isolates (Nicolae Dopcea et al., 2020; Wu et al., 2016) suggesting a mechanistic link is feasible. Additionally, for *S. aureus* evolved isolates, the MIC of erythromycin was one-fold above the erythromycin ECOFF (1 mg/L).

Sequencing of mutants identified various mutations including in genes associated with amino acid and phospholipid synthesis. Two *S. aureus* evolved isolates under CHX stress presented a mutation in *aroC*, which is essential in the aromatic amino acid biosynthesis. A study (Alreshidi et al., 2020) showed that the release of amino acid could potentially be involved in peptidoglycan biosynthesis and quorum-sensing – which is also linked in the biofilm life cycle in *S. aureus*.

The most interesting results were found in genes associated with phospholipid synthesis. SNPs in *S. aureus* fatty acid kinase (*fakA*) were repeatedly isolated from independent lineages in both planktonic and biofilm conditions, under both stresses, strongly suggesting a role of this novel gene in biocide tolerance. SNPs in *E. faecalis* identified the presence of a mutation in *dak2* which is an orthologue of *fakA* (Parsons et al., 2014a). From the literature, the protein FakA was previously known as Dak2 or VfrB (Bose et al., 2014). Additionally, a homologous (orthologous) relationship between the Dak2 domain-containing protein and FakA from *S. aureus* has been established (Bose et al., 2014; Parsons et al., 2014a) and further confirmed, as explained in **Chapter 6**. This repeated isolation of changes within FakA indicates this is a hotspot for antiseptic adaptation.

5.4. Conclusion

To conclude, these results show two common nosocomial pathogens can evolve limited tolerance to two common biocides. This had different collateral impacts between species and selective agents on biofilm formation, colony morphology and fitness costs.

There were some differences in the selective outcomes between the biocides and species, in general, lineages exposed to OCT retained higher biofilm-forming capacity than those stressed with CHX. Biofilm formation was also generally compromised more in *E. faecalis*

after biocide exposure than for *S. aureus*. Adaptation was relatively limited with small changes in susceptibility and little evidence of antibiotic cross-resistance.

Tolerant mutants selected by CHX and OCT were repeatedly found to have mutations within *fakA* in *S. aureus,* and the homologous gene *dak2* in *E. faecalis*. FakA appears to be a novel mediator of biocide sensitivity potentially acting by causing changes in membrane permeability. Further characterisation and understanding of the role of *fakA* in biocide tolerance is included in the next chapter (**Chapter 6**).

However, there were collateral impacts on fitness seen in populations able to grow in escalating concentrations of the biocides; no mutants were able to adapt to grow beyond relatively low concentrations of both agents. Whilst both biocides tested here showed limited selection for tolerance, in reality these are applied in formulation containing many other components that can impact product efficacy. Therefore, outcomes after exposure to different products containing CHX or OCT may vary. In **Chapter 7**, similar experiments were conducted during a 3-months iCASE placement at GAMA Healthcare Ltd. including a novel biocidal formulation (FM104) to observe if results from the CHX/OCT exposure series could be translated to real-world formulations.

CHAPTER 6: CHARACTERISATION OF FAKA AND ITS LINK WITH BIOCIDE TOLERANCE

“You can't connect the dots looking forward; you can only connect them looking backward. So you have to trust that the dots will somehow connect in your future” – Steve Jobs

6.1. Introduction

FakA has recently been shown to be necessary for the incorporation of exogenous fatty acids into the lipid membrane in a pathway known as type II fatty-acid biosynthesis (FASII) (Frank et al., 2020). Instead of using *de novo* synthesis, *S. aureus* and other Gram-positive pathogens can incorporate exogenous fatty acids and produce phosphorylated fatty acids using this bypass pathway. An analogous system is also present in Gram-negative bacteria (Parsons et al., 2014b) although with some differences.

More specifically, FakA is an ATP-dependent kinase that phosphorylates exogenous fatty acids, leading to their incorporation, whereas FakB1 and FakB2 activate saturated and monounsaturated host fatty acids, respectively (**Figure 6.1.**). A better understanding of the recognition between FakA and FakB, and activation of exogenous fatty acids in Gram-positive bacteria is vital.

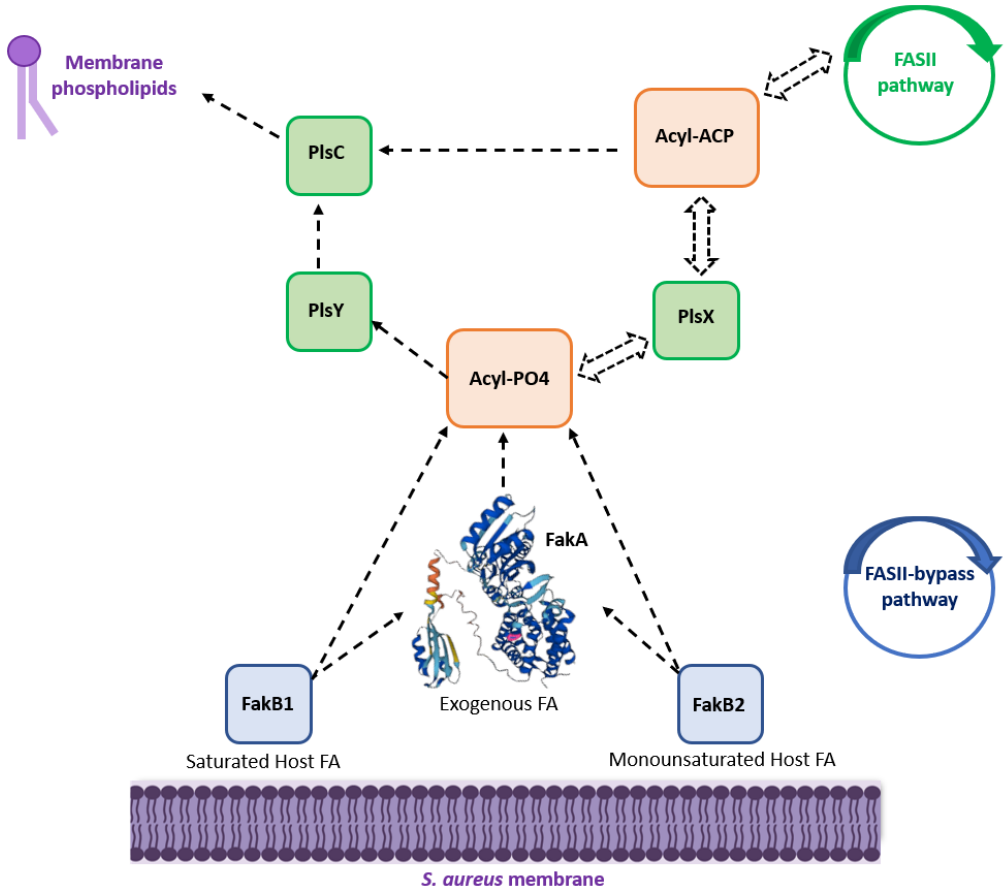

Figure 6.1. Pathways for fatty acid biosynthesis in *S. aureus*. PlsXYC and FASII pathways are the most widely distributed in Gram-positive bacteria. In the FASII-bypass pathway, FakA is essential for exogenous fatty acids (FA) incorporation into the membrane. Adapted from Frank et al. (2020).

Due to the essential role of FakA in incorporation of exogenous fatty acids (Parsons et al., 2014b), it has been shown that the absence of FakA results in more lipids containing longer acyl chains, leading to less membrane fluidity due to exogenous fatty acids not being incorporated into phospholipids (DeMars et al., 2020). The FASII pathway has been a target for development of new antimicrobial drugs. Therefore, this bypass system that uses exogenous fatty acids, which is not as energy intensive process as *de novo* synthesis, could represent a problem for the efficiency of anti-FASII inhibitors (Morvan et al., 2017). In this context, FakA could potentially be used as a therapeutic drug target (Lopez et al., 2017).

Studies showed that, besides being involved in fatty acid metabolism, FakA also has a role in virulence and modulation of pathogenesis during skin infection. Studies from Bose's group showed that the inactivation of FakA lead to hypervirulence during skin infection in a murine model (Bose et al., 2014; Ridder et al., 2020). Although other studies have shown *fakA* mutants had attenuated virulence (Kuiack et al., 2023; Lopez et al., 2017). In this chapter, virulence of the evolved isolates with a *fakA* mutation was not compared to the parental strains (**Chapter 4**, **Section 4.3.3.**), since it has previously been characterised by others. Additionally, FakA has also been suggested to have a negative impact on biofilm formation (Sabirova et al., 2015) although we saw no consistent impact across the mutants in this project (**Chapter 5**). In fact, data from our study showed that *S. aureus* mutants when stressed with OCT presented a loss of biofilm formation in later timepoints, although different strains and a different biofilm model were used in our study.

In this chapter, further characterisations of this gene included testing the drug accumulation activity of the evolved isolates with a mutation in *fakA* and assessing differences in the cell envelope by transmission electron microscopy. The creation of a deletion mutant (Δ*fakA*) has also been started.

6.2. Aims

- To assess the conservation of *fakA* across Gram-positive and Gram-negative isolates.
- To characterise selected isolates with *fakA* mutations and assess drug accumulation and differences in the cell envelope.
- To understand the role of *fakA* in biocide tolerance by creating a clear *fakA* deletion mutant.

6.3. Results

6.3.1. Conserved regions and changes in FakA

After confirming that FakA (*S. aureus*) and Dak2 (*E. faecalis*) are homologous proteins (**Chapter 5**), the first aim was to understand how conserved this gene/protein is across other bacterial species and kingdoms.

Homology of *fakA* across the three kingdoms: occurrence profiles to determine how conserved *fakA* (ABD30300.1) is across the three kingdoms showed that this is a conserved gene/protein across Bacteria and Eukaryota, but not present in the Archaea kingdom (**Figure 6.2.**). Results showed that it has the highest similarity detectable in Bacteria, and lower similarity in Eukaryota. In fact, in the Eukaryota kingdom it was only present in the Opistohonkonta group, more specifically in *Biomphalaria glabrata*, a species of freshwater snails. Although *fakA* is conserved across multiple groups and taxa, it is generally less conserved than *plsX*, which is part of the FASII pathway.

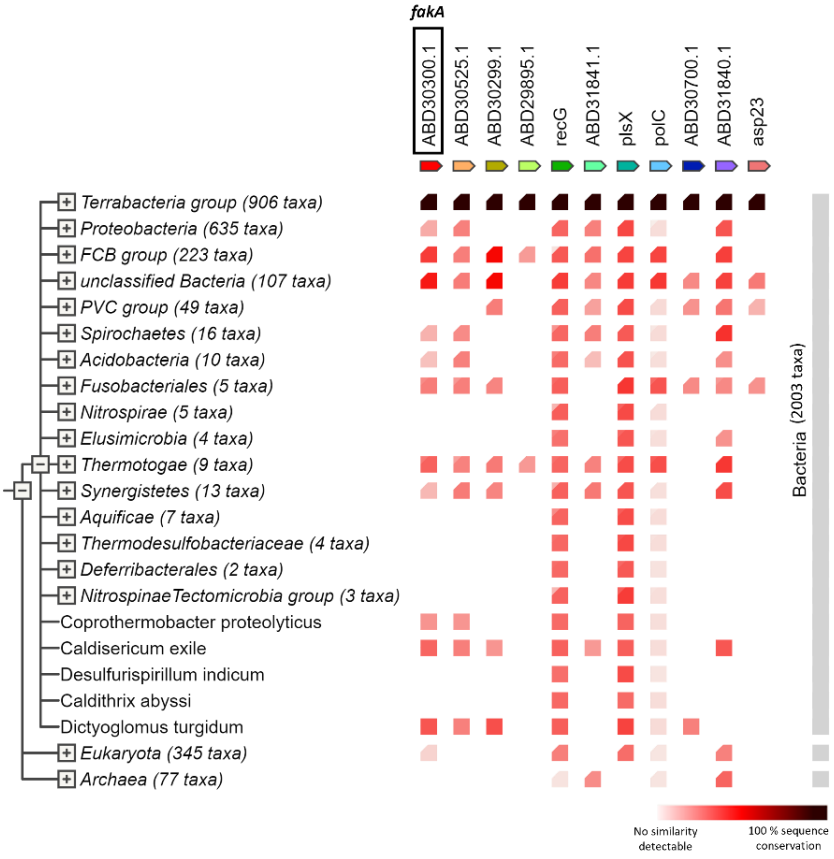

Figure 6.2. Occurrence profiles of *fakA* (identified using the sequence from *S. aureus*) across genomes in the three kingdoms. Colours indicate a similarity scale for *fakA* in the STRING genome database: lighter red shades (lower similarity) and black (highest similarity). Degree of conservation within each group is indicated by completeness of the squares.

Homology in Gram-positives and Gram-negatives: FakA homologs are present in both Gram-negative and Gram-positive bacteria (e.g., *Bacillus subtilis*, *Lactobacillus johnsoni*, *Streptococcus pneumoniae, Clostridium botulinum*, *Mycobacterium tuberculosis*), with some identical residues in all FakA proteins (Parsons et al., 2014a). As previously studied (Parsons et al., 2014a), the percentage of nucleic acid identity shared between *fakA* from *S. aureus* with *E. faecalis* is 53 %.

Comparison of available sequences of FakA found that residues 187, 312 and 341 (changed in mutants recovered in this study) are completely conserved across the genus *Staphylococcus* (**Figure 6.3. - A**). However, residue 489 is less conserved with various substitutions apparently tolerated. By expanding analysis to other Gram-positive species, excluding the *Staphylococcus* genus (**Figure 6.3. - B**), we found that residues 187 and 312 remained completely conserved suggesting that the changes seen at these sites in this study are likely to have functional impacts on FakA.

Figure 6.3. Sequence logo of FakA residues in (A) staphylococci excluding *S. aureus*; (B) related non-staphylococcal species using multiple sequence alignment data. The data for this logo consists of 100 sequences. Positions with SNPs in FakA (187, 312, 341, 489 aa) are highlighted in a red box.

Conservation in a panel of > 1000 clinical isolates: To determine the impact of these mutations in larger dataset of > 1000 clinical isolates (used in Felgate and Solsona, In Preparation), we studied if mutations in these residues were also present in different coagulase-negative staphylococci (CoNS) species (*S. epidermidis, S. capitis, and S. haemolyticus*). The aim was to further identify if the isolates with high CHX/OCT MICs from the CoNS collection had the same or similar SNPs in *fakA* as previously observed in *S. aureus*. Furthermore, to then determine if these mutations were absent in isolates with lower CHX/OCT MICs.

In *S. epidermidis* isolates, changes in position 187 were present in 6 different isolates isolated from different body sites (gut, skin, ear) which presented with high CHX MICs (64 µg/mL), and low OCT MICs (1 - 2 µg/mL). Changes in the other positions (312, 341, 489 aa) were not observed in these isolates. No changes in the selected residues were observed in *S. capitis* nor *S. haemolyticus* isolates.

6.3.2. Selection of *fakA* mutant isolates for further characterization

To assess the direct contribution of *fakA* mutation to different phenotypes, a series of six evolved isolates with SNPs present in *fakA* (in different residues) from both species were selected and analysed for further characterisation (**Table 6.1.**).

While most changes were nonsense mutations, the non-synonymous mutations were further studied to determine if there were differences in the type of in polarity and charge. For the observed missense mutations, no changes in polarity were observed, while most amino acids had a neutral charge, some can also have a different charge depending on the pH.

Table 6.1. Selected *S. aureus* (SA) and *E. faecalis* (EF) evolved isolates with SNPs in *fakA.*

Species	Position	Amino acid change	Sample ID	Biocide	Condition	Origin	Lineage
SA	187	Gly -> Asp	202	OCT	Planktonic	Population	D
SA	312	Gln -> STOP	200	OCT	Planktonic	Population	C
SA	341	Gly -> Asp	176	CHX	Biofilm	Colony 3	B
SA	489	Glu -> STOP	226	OCT	Biofilm	Colony 3	D
SA	489	Glu -> STOP	240	OCT	Planktonic	Colony 1	D
EF	317	Asn -> His	94	OCT	Biofilm	Colony 2	B

6.3.2.1. Susceptibility testing to assess cross-resistance to other antimicrobials in selected evolved isolates with *fakA* mutations

To assess whether changes in FakA result in changes in antimicrobial tolerance, MIC assays against a panel of antibiotics from differing classes regularly used to treat staphylococci and enterococci infections were determined in MH (**Chapter 5**). This analysis identified small decreases in susceptibility to various antibiotics and biocides tested for the evolved isolates.

In this chapter, daptomycin was added in this susceptibility testing since it is a widely used lipopeptide to treat severe infections with Gram-positive pathogens, such as MRSA and drug-resistant enterococci (Alder, 2005). Additionally, this antimicrobial disrupts cell membranes, which has a direct link with the role of *fakA.* This MIC experiment (**Figure 6.4. - A**) identified small decreases in susceptibility to daptomycin (4/6 isolates). MBCs were then determined for CHX, OCT and daptomycin against the selected evolved isolates to study susceptibility changes when compared with the parental strains (**Figure 6.4. - B**). In general, low-level changes to OCT, CHX and daptomycin were observed in isolates with SNPs in *fakA*. Interestingly, fold changes in MBC were significantly higher when compared to the WT in isolates ID226 (for all the tested antimicrobials) and ID240 (for CHX).

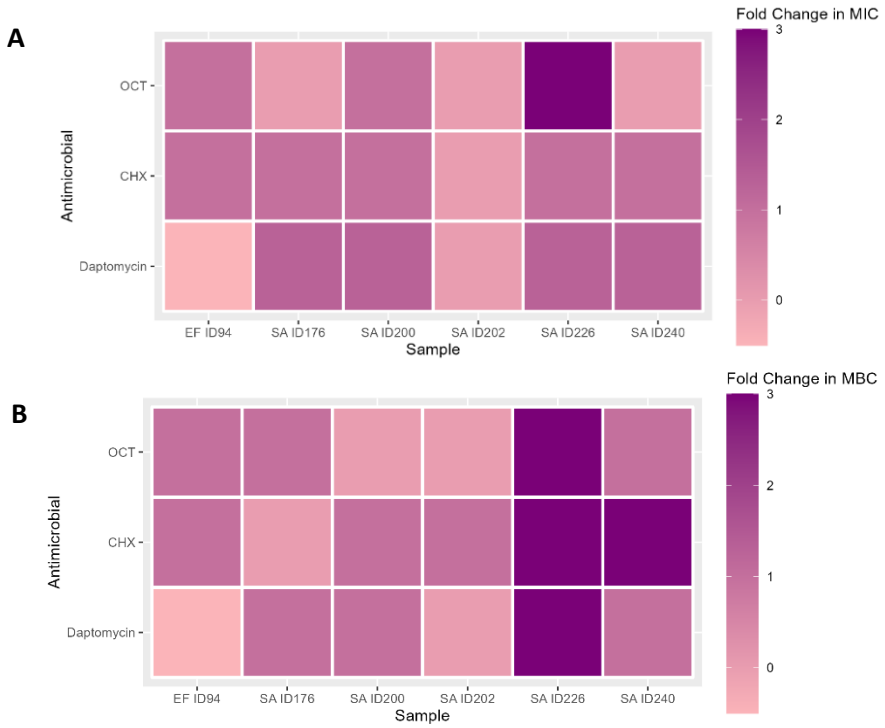

Figure 6.4. Heat maps of fold changes in (A) MIC and (B) MBC values (compared to the WT) against the two tested biocides (CHX/OCT) and daptomycin in MH. Evolved isolates (Sample ID shown) with different SNPs in the *fakA* gene are shown. Intensities represent fold changes in MIC/MBC for each sample (three biologicals with three technical replicates/sample).

6.3.2.2. Other phenotyping tests in selected evolved isolates with *fakA* mutations

To further understand if the selected isolates with *fakA* mutations had a fitness cost in growth and biofilm biomass production had, further phenotyping tests were performed.

Growth curves

As observed (**Figure 6.5.**), some *S. aureus* OCT-evolved isolates had an increase in fitness/growth, indicated by higher AUC relative to the parental strains: SA ID200 (relative AUC = 1.25), SA ID202 (relative AUC = 1.19), SA ID226 (relative AUC = 1.43). Other isolates from the same experiment had lower AUC than the parental strain: SA ID240 (relative AUC = 0.88) and SA ID176 (AUC = 1.03). However, none of these differences were statistically significant (Wilcoxon-Mann-Whitney test performed).

In *E. faecalis*, the selected evolved isolate EF ID94 had a higher AUC compared to the WT (relative AUC = 1.23), although the difference was not statistically significant.

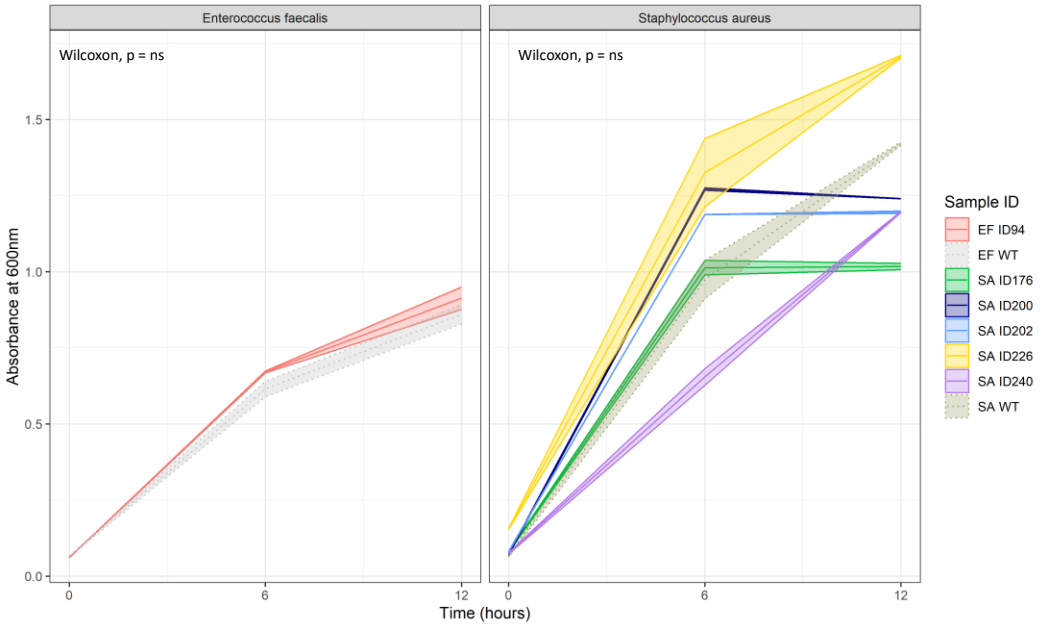

Figure 6.5. Growth curves of the selected *E. faecalis* and *S. aureus* evolved isolates with *fakA* mutations (represented by dark lines), and the WT (indicated by dotted lines) grown in TSB. Absorbance (OD_{600nm}) was measured for 12 hours for each isolate. Error bars (represented as shaded areas in the plots) show the variability observed across the three technical replicates per sample. Non-statistically significant changes (*p-value* > 0.05) were observed between the evolved isolates and the WTs according to the Wilcoxon-Mann-Whitney test.

Biofilm biomass production

The parent *S. aureus* strain had a higher biomass production (mean OD_{600nm} = 1.374) than the *E. faecalis* strain (mean OD_{600nm} = 0.858), when assessed by crystal violet.

Differences between isolates with *fakA* mutations were observed. Some OCT-evolved isolates with a mutation in *fakA* (EF ID94, SA ID226 and SA ID240) had an increased biofilm formation when compared to the parental strain, whereas other CHX-evolved isolates with a mutation in *fakA* (SA ID200, ID202, ID176) had a decrease in biofilm formation (**Figure 6.6.**). However, no statistically significant changes (*p-value* > 0.05) were observed between the evolved isolates and the WTs when applying a Wilcoxon-Mann-Whitney test.

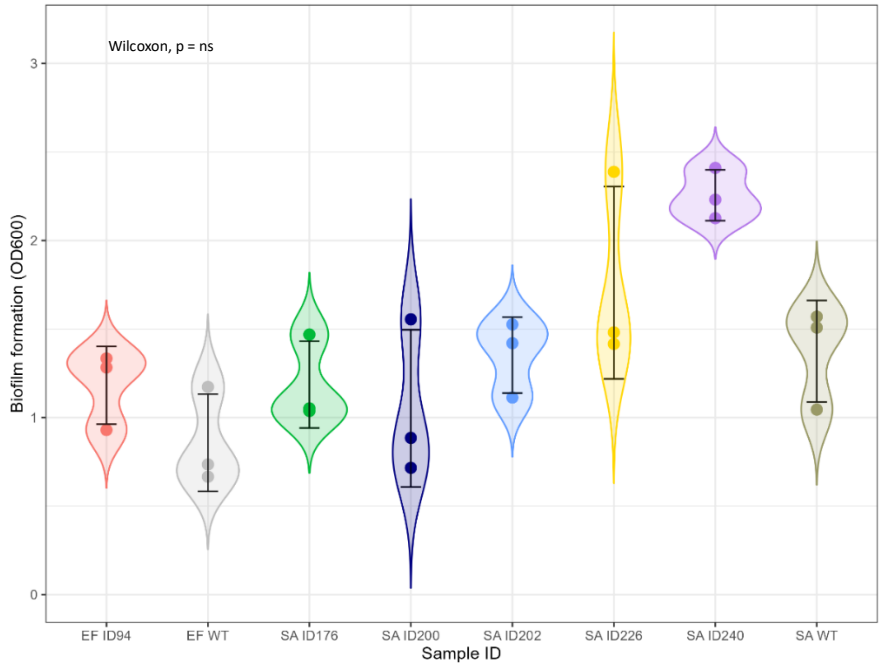

Figure 6.6. Biofilm formation of the WTs and each selected evolved isolate with *fakA* mutation. Violin plots representing crystal violet staining (OD_{600nm}); the dots represent the three technical replicates, and error bars indicate standard deviation of the mean. Group comparisons assessed by the Wilcoxon-Mann-Whitney test showed non-significant changes (*p-value* > 0.05) between the evolved isolates and the WTs.

Drug accumulation assays

Given the potential impact of changes to *fakA* on membrane fluidity, accumulation of ethidium bromide was also determined for the selected evolved *fakA* mutants. Changes in

the accumulation of ethidium bromide (measured by fluorescence) are indictive of changes in membrane permeability/fluidity changes.

Initially, a time period corresponding to the parental cells being in the steady state during the experiment (**Figure 6.7.**) was selected. As shown, in this case the steady state corresponded to 150 minutes for *E. faecalis* ST40 (green area). The same rationale was used for *S. aureus* ST188.

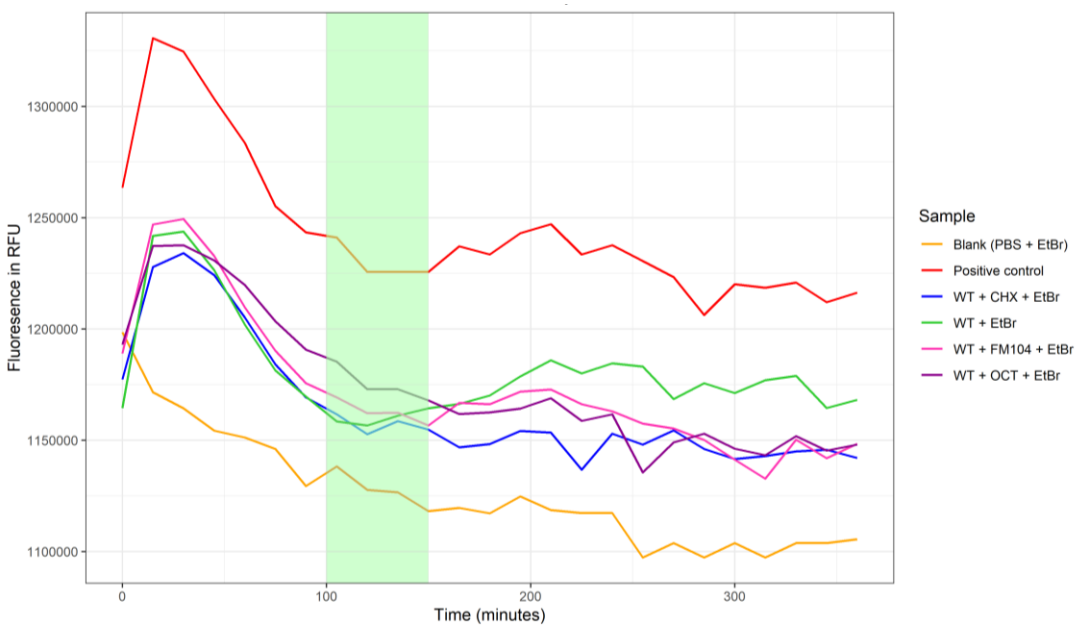

Figure 6.7. Ethidium bromide accumulation assay with *E. faecalis* ST40. Tested conditions include positive control (dead cells, which were 70 % ethanol-lysed cells), negative controls (PBS + ethidium bromide), cells with no stress and cells stressed at ½ MIC of CHX, OCT and FM104 for 30 min. The steady state (time: 150 minutes, cycle: 156) is shown in green. Curves indicate average of 3 technical replicates per sample Abbreviations: RFU (relative fluorescence units), EtBr (ethidium bromide).

Results showed that all the selected evolved *fakA* mutants (**Figure 6.8.**) accumulated significantly less ethidium bromide within the cell than the parental strains. Similar results were observed with exposure to ½ MIC of CHX, OCT and FM104 (**APPENDIX XV**).

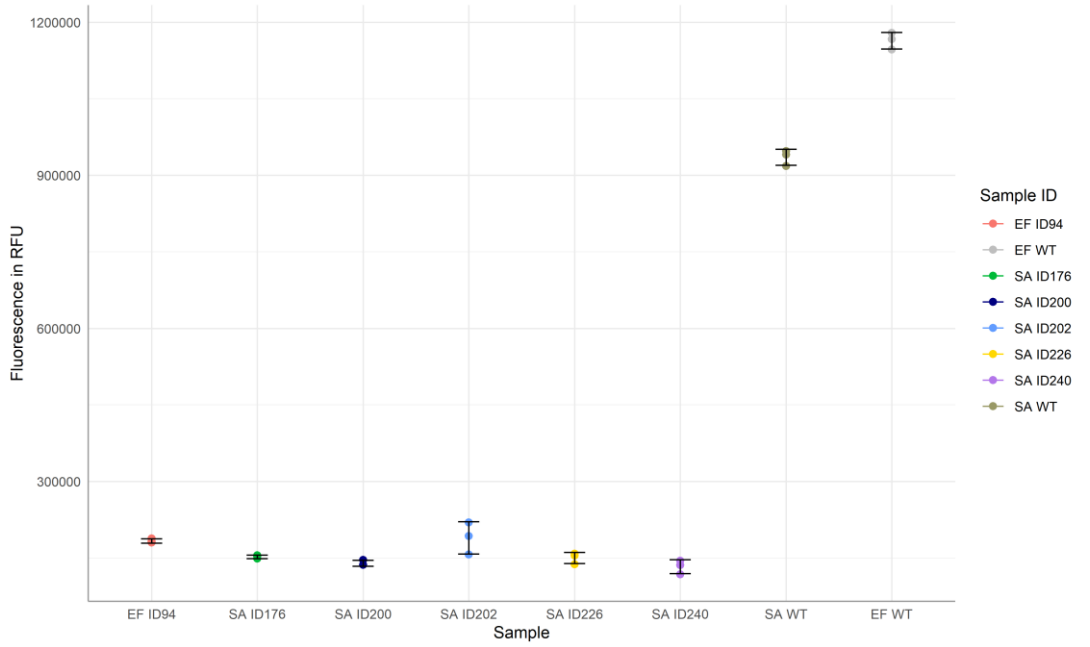

Figure 6.8. Ethidium bromide accumulation is reduced in isolates with *fakA* mutations. Ethidium bromide accumulation was measured based on fluorescence (excitation: 301 nm, emission: 603 nm) of cultures over 6 hours for *S. aureus* (SA) and *E. faecalis* (EF) evolved isolates and the parent strains. Accumulation was measured after 2 h 30 minutes of incubation representing a steady state; points show 3 independent replicates per sample with error bars indicating the mean and standard deviation values of the samples.

Differences in the cell envelope of FakA mutants using microscopy

Results from transmission electron microscopy (TEM) revealed differences in the cell envelope between the parental strains and evolved isolates carrying *fakA* mutations (**Figure 6.9.**). The membranes of evolved isolates consistently showed invaginations (mesosomes) at a higher frequency than the parental cells with more mesosomes per cell also being observed.

In *S. aureus*, 75 % of *fakA* mutants recovered after CHX treatment (and 53 % after OCT treatment) showed mesosomes compared to 40 % of WT cells. In an *E. faecalis* isolate recovered after OCT exposure with a *fakA* mutation (EF ID94), 75 % of cells had mesosomes, whereas no wild-type cells had any mesosomes visible.

Further analysis using three-dimensional structured illumination microscopy (3D-SIM), which uses fluorescence labelling instead of chemical fixation like TEM, confirmed the presence of the mesosomes in the *fakA* evolved isolates live (not shown).

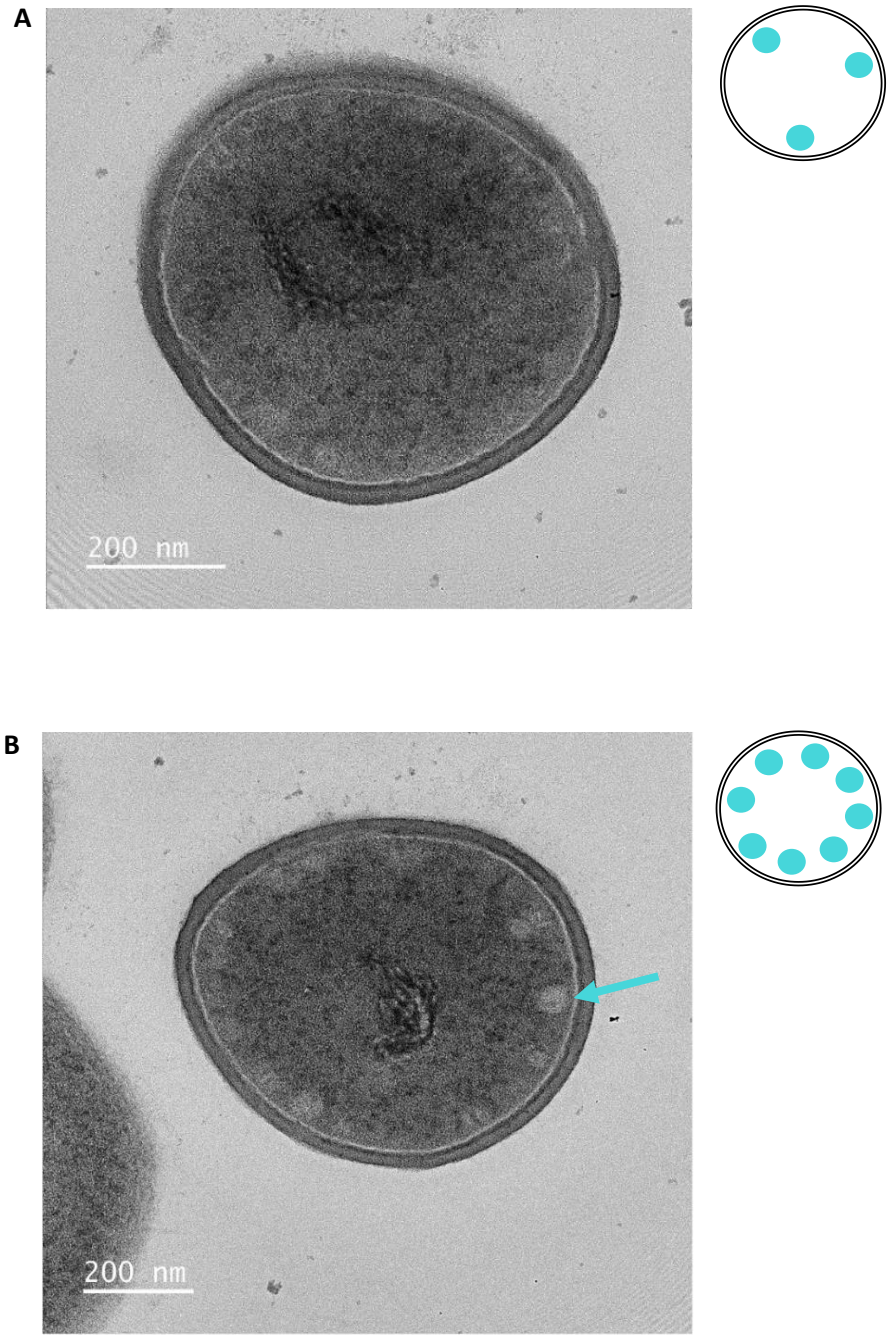

Figure 6.9. Biocide adapted FakA mutants exhibit increased mesosome formation. TEM shows representative images of **(A)** *S. aureus* WT and **(B)** a *fakA* evolved isolate (SA ID176). Mesosome indicated with the blue arrow, a schematic representation of the frequency of these structures is also shown.

6.3.3. Construction of a *fakA* deletion mutant

To better understand the role *fakA* plays in biocide tolerance, creation of a clear deletion mutant was started. A homologous recombination strategy to construct Δ*fakA* mutants (Bose et al., 2014, 2013) was designed following two different approaches based on a pKOR1-mediated allelic replacement in *S. aureus* (Bae and Schneewind, 2006) with some modifications (Stapels et al., 2014), with the overall process including three main steps (**Figure 6.10.**).

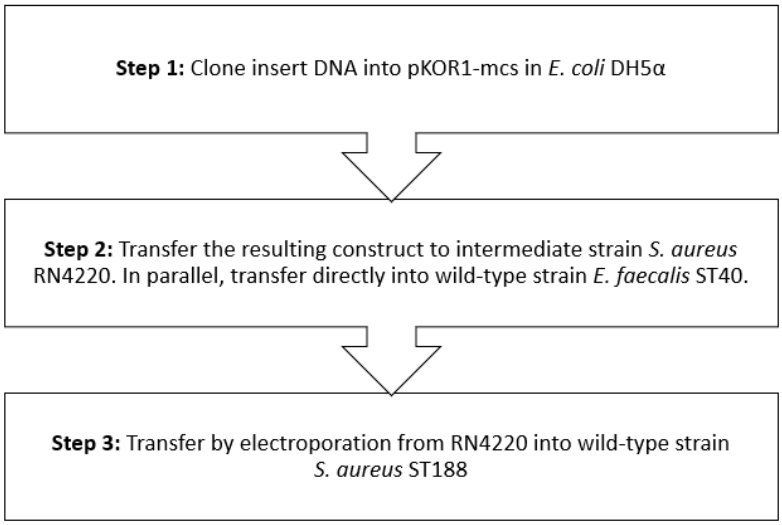

Figure 6.10. Flow diagram summarising the construction of a *fakA* deletion mutant. An overview of the three main steps used in the gene deletion process is shown.

Initially, flanking sequences that are 1 kb upstream and downstream of the region of interest (*fakA* gene) are amplified and cloned into pKOR1-mcs vector in *E. coli* DH5-α by a recombination reaction. Since the efficiency of the transformation into *S. aureus* is unknown, two different approaches were explored in this step. One approach includes using an antibiotic resistance marker (chloramphenicol) between the flanking sequences (Approach 1) and in the other approach (Approach 2), no antibiotic cassette is present between the two overlapping flanking sequences.

The second step involved using a shuttle strain (RN4220) before transformation into the strain of interest. Due to the dense wall of teichoic acids, transformation in *S. aureus* is tedious. Additionally, methylation and restriction-modification systems could also be responsible for the low transformation efficacy (Monk et al., 2012). For these reasons, the resulting constructs are first being transformed into RN4220, that does not have restriction endonucleases and specific methylation profiles. In theory, by using this intermediate strain

cleavage of the constructs grown in this strain would be avoided once these are transformed into the strain of interest.

In the last step, the construct of interest grown and isolated from RN4220 will be electroporated into the clinical isolate *S. aureus* ST188 (and directly into *E. faecalis* ST40), and grown at a non-permissive temperature for pKOR1-mcs vector replication (Bae and Schneewind, 2006; Stapels et al., 2014). Once the plasmid integrated into the bacterial chromosome, the target gene (*fakA*) will be substituted with the foreign DNA, as the flanking regions would be detected as homologous (homologous recombination). In theory the flanking regions will be incorporated and by this allelic exchange the target gene will then be deleted from the strain of interest.

<u>Step 1:</u> To clone insert DNA into pKOR1-mcs in *E. coli* DH5α

Approach 1

For this approach, constructs were created using two similar strategies, that initially differed in the pairs of restriction enzymes used (**Figure 6.11. - A**). Eventually, the same constructs (**Figure 6.11. - B**) are generated with both strategies, but having two almost-identical strategies was an option in case one was less efficient than the other.

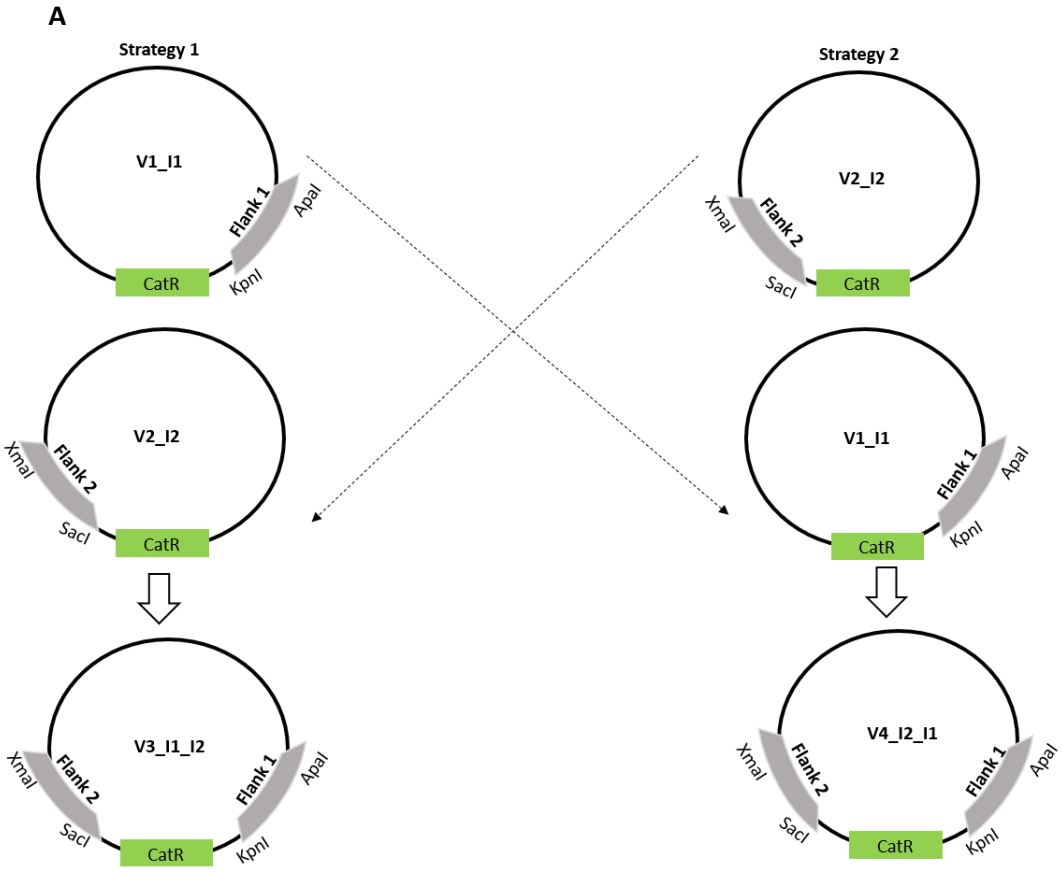

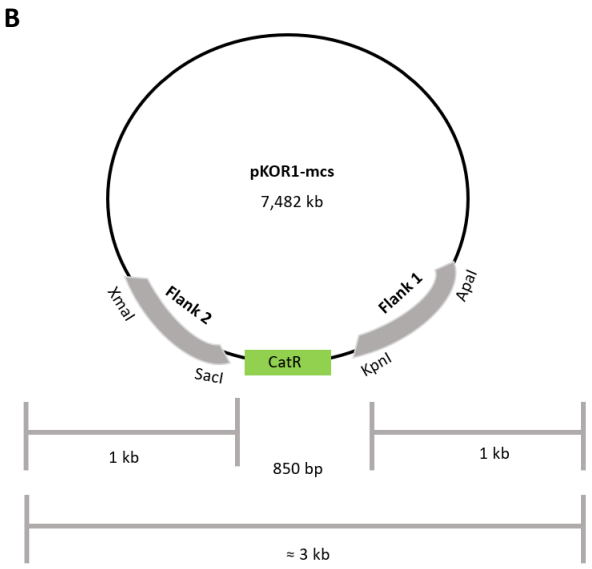

Figure 6.11. Schematic representation of both cloning strategies from Approach 1. (A) details of the two strategies are shown; **(B)** the final construct obtained from both strategies along with the respective sizes. Chloramphenicol (CatR) cassette is shown in green.

Creation of the vectors: Initially, pKOR1-mcs was double digested with ApaI and KpnI (Vector 1), and SacI and XmaI (Vector 2) for 2 hours. To obtain a bigger pool, three identical digestions were included (**Figure 6.12.**), and in this case, the fragments were then gel extracted.

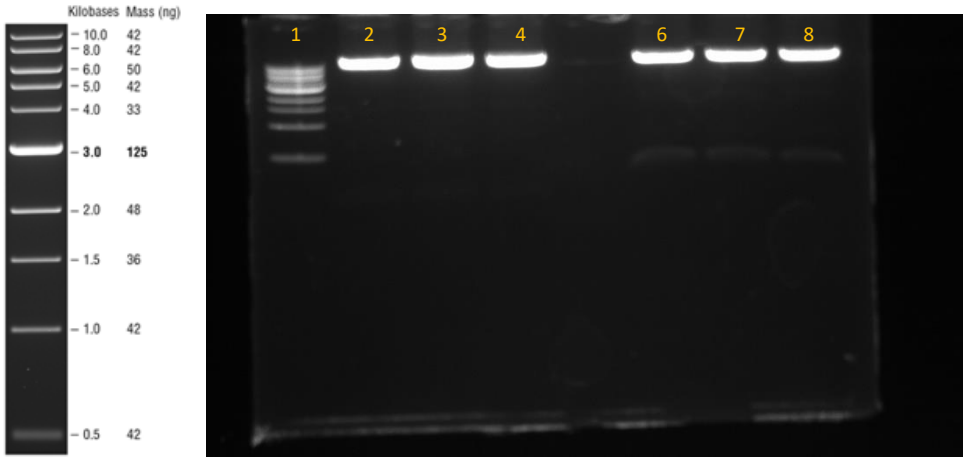

Figure 6.12. Agarose gel electrophoresis of pKOR1-mcs double digested with KpnI/ApaI (Vector 1) and SacI/XmaI (Vector 2). In this case, 200 µL from each reaction were loaded in each well. For reference, 1 kb DNA ladder (from NEB) is included. Lanes: 1st (1 kb ladder), 2nd - 4th (pKOR1-mcs digested with KpnI/ApaI), 6th - 8th (pKOR1-mcs digested with SacI/XmaI).

Creation of the inserts: inserts were created by PCR using *S. aureus* ST188 DNA as a template, with different primers for each flank 1 and flank 2 (**APPENDIX IV**). The resulting PCR products were then digested with KpnI/ApaI (for Flank 1), and SacI/XmaI (for Flank 2), respectively to ensure the insert ligated in the preferred directions. Finally, flank 1 was ligated into KpnI/ApaI-digested pKOR1-mcs, creating Vector 1_Insert1 (V1_I1). Additionally, Flank 2 was also ligated into SacI/XmaI-digested pKOR1-mcs, creating Vector V2_Insert2 (V2_I2).

After transformation into *E. coli* DH5α, 10 colonies were randomly picked from 1:5 LB plates with carbenicillin (as the antibiotic of selection) for both strategies, and further screened by colony PCR with the same primers used for each insert. In this strategy, carbenicillin, an ampicillin analogue, was selected since a β-lactamase (*bla)* gene that confers resistance to ampicillin is present in pKOR1-mcs; and to reduce the formation of satellite colonies (Medaney et al., 2016) on the transformation plates.

As observed (**Figure 6.13.**), more transformants were obtained in the second strategy (V2_I2) compared to the first strategy (V1_I1). In the first strategy, only two colonies (C9 and C10) showed a 1 kb band, whereas in the second strategy, six colonies displayed a 1 kb band. Colonies indicated with a yellow arrow represent the ones with higher DNA concentrations after plasmid preparation and were therefore selected for the next step.

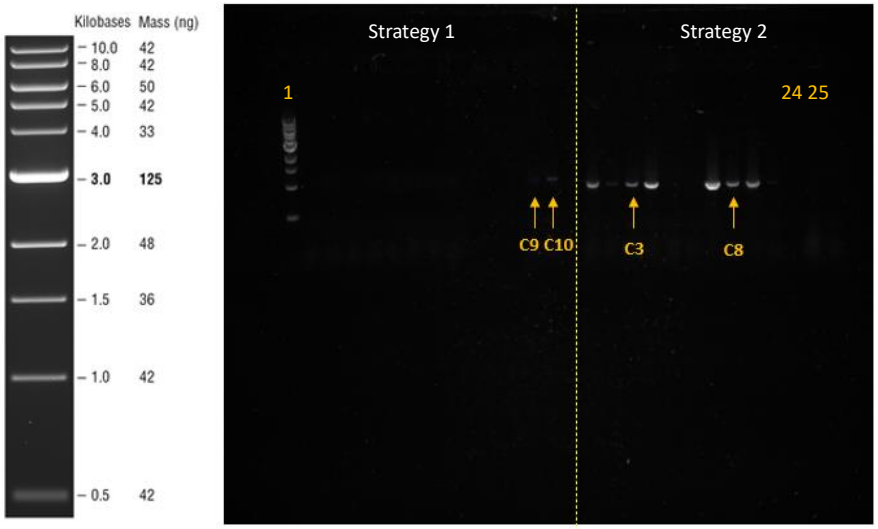

Figure 6.13. Agarose gel electrophoresis of colony PCR products from both strategies. 10 colonies from each strategy picked; 2 transformants (Strategy 1) and 6 transformants (Strategy 2) were obtained. Yellow arrow indicates the selected colonies with higher DNA concentrations for each strategy. C9 and C10 (selected colonies from strategy 1 with V1_I1); C3 and C8 (selected colonies from strategy 2 with V2_I2). 10 µL from each reaction were loaded in each well. Lanes: 1st (1 kb ladder); and 24th - 25th (negative controls).

Final construct: The next step was to create the final vector from construct 1 (V1_I1) and construct 2 (V2_I2), but now digested with the opposite restriction enzymes. Therefore construct 1 (V1_I1) was now digested with SacI/XmaI and construct 2 (V2_I2) now digested with KpnI/ApaI with the selected colony 9 (for strategy 1) and colony 3 (strategy 2).

Subsequently, now Flank 2 was ligated into KpnI/ApaI/SacI/XmaI-digested vector (Vector 3) having then both inserts in the construct 3 (V3_I1_I2). And in the same way for Flank 1, generating construct 4 (V4_I2_I1). Both construct 3 and construct 4 are, in theory, identical constructs containing both inserts and a chloramphenicol cassette in-between. In this case, better transformation results were obtained with construct 3 than with construct 4. Subsequent screening of 10 colonies from 1:3 ratio from construct 3 were performed.

Confirmation of the final constructs: to confirm for the presence of flank 2 (since flank 1 has already been previously confirmed) colony PCR was performed using the corresponding primers. From the 10 screened selected colonies, 7 colonies had a band around 1 kb, indicating the presence of the second insert (Flank 2). Therefore, these constructs now have 2 flanking regions with a chloramphenicol (CatR) cassette between them.

Further restriction digests to check these 7 constructs were also performed. All constructs were digested with KpnI/ApaI and XmaI/SacI separately to confirm for the presence of each insert bands (1 kb). A digestion with XmaI/ApaI was also used (**Figure 6.14.**) to confirm the nature of the total construct. As seen, vector bands should be around 7 kb and a band around 3 kb should also be present, which suggests the two inserts and the antibiotic cassette (850 bp) are present.

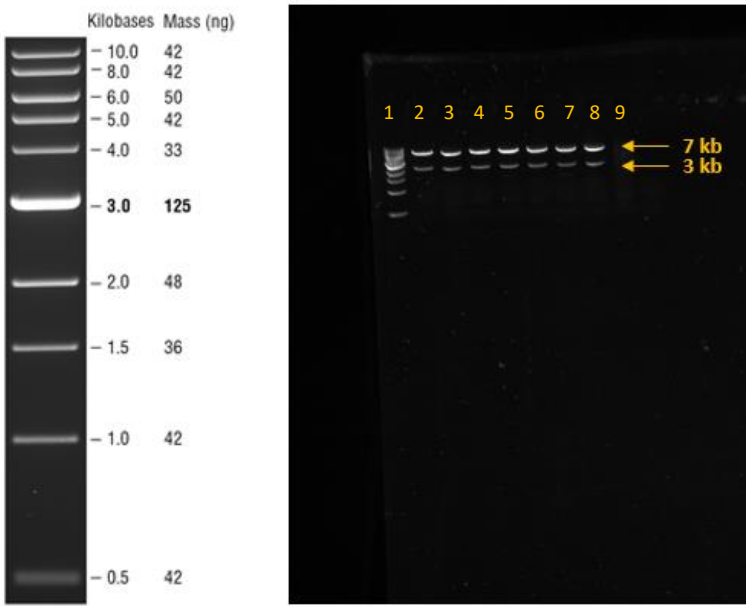

Figure 6.14. Agarose gel electrophoresis of pKOR1-mcs vector digested with XmaI/ApaI, containing both inserts. Seven selected colonies from strategy 1, construct 3 (V3_I1_I2) were selected for further confirmation. The yellow arrow indicates the desired band sizes obtained in all 7 constructs. 50 µL from each reaction were loaded in each well. Lanes: 1st (1 kb ladder), 2nd - 8th (selected colonies from strategy 1, construct 3), 9th (negative control).

To conclude, these 7 constructs from approach 1 were then sent to also be confirmed by sequencing. Overall, by having conducted two identical strategies in parallel from approach 1, we have increased the options of obtaining more constructs. Additional optimisations using phenol-chloroform for DNA purifications of were also performed as alternative plans.

Approach 2

Similarly to the first approach, regions flanking the gene of insert were selected. In this case, inserts (Up and Down) were created by PCR using *S. aureus* ST188 DNA as a template and different primers (**Figure 6.15.**). However, no chloramphenicol cassette was present between the flanking regions.

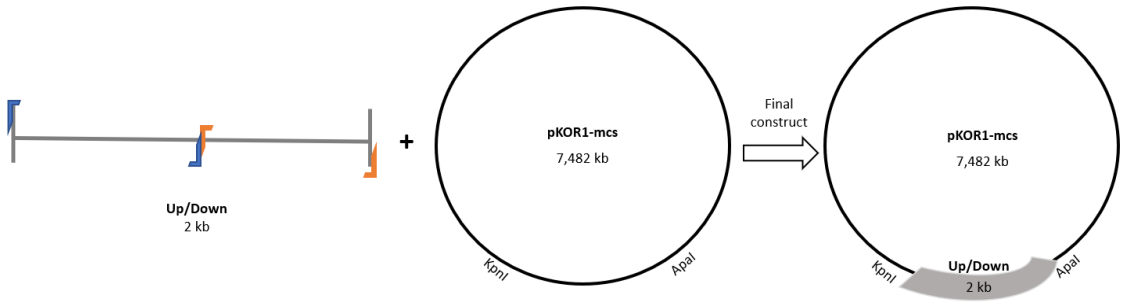

Figure 6.15. Schematic representation of Approach 2. The fusion insert (Up/Down) digested with KpnI/ApaI and ligated into KpnI/ApaI-digested pKOR1-mcs to create the final construct. Primers indicated in different colours.

Creation of the fusion insert: In this approach, a fusion PCR was successfully performed with the aim of merging these two fragments (of 1 kb each) into a bigger fragment (of 2 kb). As shown (**Figure 6.16. - A**), the bands had a total size of higher than 2 kb. To be precise, Insert Up had a total size of 1208 bp and Insert Down had a size of 1056 bp, giving a Fusion fragment (Up/Down) of 2208 bp (**Figure 6.16. - B**).

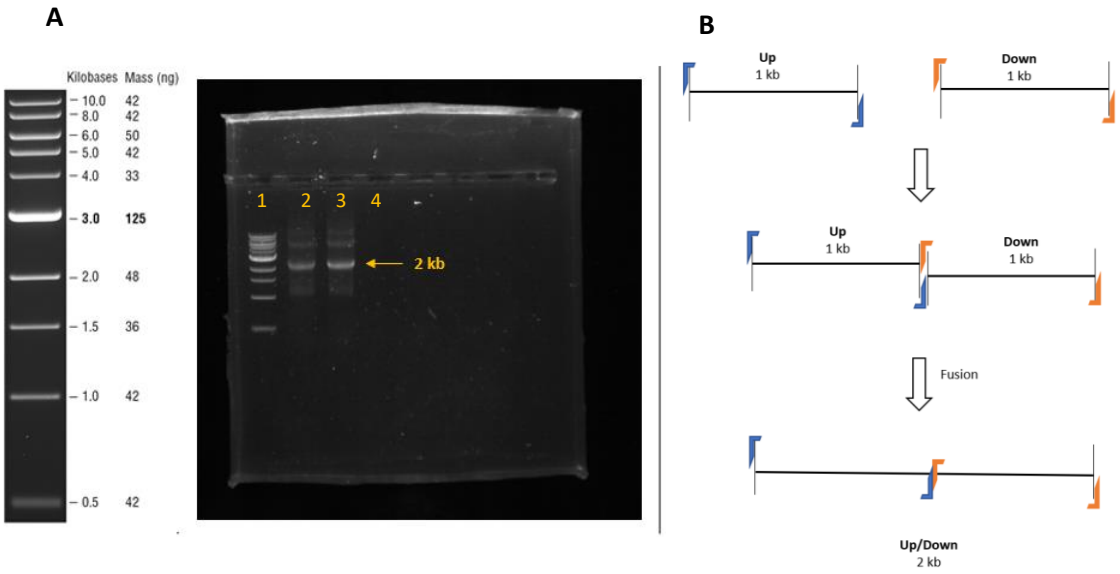

Figure 6.16. Results from fusion PCR. (A) Agarose gel electrophoresis of fusion PCR with both inserts. Reactions performed in duplicate to obtain a bigger pool. 5 µL from each reaction were loaded in the lanes (2nd and 3rd lanes). The yellow arrow indicates the desired band size. Lanes: 1st (1 kb ladder), 2nd - 3rd (fusion fragments), 4th (negative control). **(B)** Schematic representation of fusion PCR. To obtain the final insert of 2 kb (Up/Down) two consecutive PCRs were set to merge with each fragment. Primers indicated in different colours.

Creation of the construct: Fusion Insert (Up/Down) was digested with KpnI/ApaI and ligated into KpnI/ApaI-digested pKOR1-mcs (Vector 1), which had already been created in the first approach.

Confirmation of the construct: after transformation, 30 colonies from 1:5 ratio plates were screened by colony PCR with primers corresponding to Insert Up. Nonetheless, no positive results were observed. Subsequent screening of 20 additional colonies, but with different primers (for insert Down), showed only one colony with a band of approximately 2 kb, corresponding to the insert size. Additional confirmations included digesting the construct with KpnI/ApaI, and sequencing.

Step 2: To transfer the resulting construct to intermediate strain *S. aureus* RN4220

The resulting constructs from both approaches obtained in Step 1 were transformed by electroporation into *S. aureus* RN4220 intermediate strain. Due to difficulties in transformation of *S. aureus* (Monk et al., 2012; Prax et al., 2013), especially clinical isolates, work was paused at this point and further optimisations are needed.

6.4. Discussion

SNP changes in *fakA* were mainly loss of function and present in conserved residues across FakA homologs from different bacteria. We found some totally conserved residues in all homologues. These include residues 187 and 312 where we saw substitutions in evolved isolates whereas other residues where we observed changes were less conserved (341 and 489 aa).

When investigating conserved regions of *fakA* in a pool of > 1000 CoNS, we observed that there was a proportion of isolates with high OCT and CHX tolerance, but not all these isolates had a *fakA* signature in staphylococci. In fact, results showed that *fakA* mutations in the selected amino acids were only present in some *S. epidermidis* isolates with high CHX MIC, but this was not conserved in all species, indicating there was no strong correlation with the phenotypic data. However, differences between *S. aureus* and CoNS, might also be the reason why there is not a unique mechanism of biocide tolerance in all CoNS. In fact, this has been similarly found with FabK for triclosan resistance, where *fabK* conferred high (McMurry et al., 1998) and also low resistance (Khan et al., 2016) to triclosan in different species.

CHX and OCT are positively charged molecules and interact with negatively charged phospholipids, causing membrane disruption, lysis, and cell death, although recent studies have elucidated differences in their mode of action (Malanovic et al., 2022; Rzycki et al., 2021; Waller et al., 2023). The repeated isolation of *fakA* mutants after biocide exposure strongly suggests a role for *fakA* in disinfectant tolerance and we hypothesised that loss of FakA function would result in altered membrane composition and as a result increased tolerance to CHX and OCT. Ethidium bromide accumulation assays showed significantly lower accumulation of this intercalating dye in the evolved isolates than in the parental strains, supporting the idea that SNPs in *fakA* confers a reduction in membrane fluidity. Additionally, changes in MIC/MBC of daptomycin, another membrane targeting antibiotic (Alder, 2005), were observed and susceptibility was increased in some biocide adapted *fakA* mutants, which is consistent with membrane alterations. In a previous study (Song et al., 2013), isolates with a mutation in *fakA* (then hypothetical and referred to as *mw1109*) showed reduced susceptibility to daptomycin *in vitro*. A recent study (Gómez-Casanova et al., 2024) observed that isolates with reduced susceptibility to daptomycin had mutations in *fakA*, although causation could not be established in that study.

Further analysis into the selected *fakA* evolved isolates showed that two OCT-evolved isolates with a mutation in *fakA* (SA ID226 and SA ID240) had increased biofilm formation when compared to the parental strain. Interestingly, both isolates had a SNP in the same position (where it also contained the higher number of SNPs), with a loss of function as a change. This could suggest that the number or nature of SNPs impacts biofilm formation, but higher numbers would be needed to explore this. Nonetheless, differences in growth were seen among these isolates, since isolate SA ID240 had a higher growth than the WT, but SA ID226 showed lowest growth among all the evolved isolates, indicating a potential fitness cost might be associated regardless of the number of SNPs.

When investigating the morphological changes that resulted from the *fakA* SNPs, TEM showed differences in the cell envelope between the parental and evolved isolates. The membranes of the evolved isolates consistently showed invaginations on the inner membrane (mesosomes) at a higher frequency than the parental cells with more mesosomes per cell also being observed in both *S. aureus* and *E. faecalis* evolved isolates. Although mesosomes have been proposed to be artefacts of chemical fixation during the electron microscopy process (Silva et al., 1976), there are also observations that demonstrate mesosomes are a biological phenomenon in antibiotic-treated *S. aureus* (Raj et al., 2007). We propose that, with the presence of mesosomes, there will be an increase surface area hence

the biocide will be harder to penetrate on the bacterial membrane when compared to a cell with lesser membrane invaginations.

Results with 3D-SIM confirmed that mesosomes are real live events present in higher frequency in the *fakA* evolved isolates, and not artefacts from the chemical fixation of the TEM. Therefore, the data obtained are consistent with our prediction that *fakA* impacts membrane composition and as a result susceptibility to agents targeting the membrane, as elucidated in the *fakA* evolved isolates with reduced tolerance to the tested biocides.

6.5. Conclusions

Sequencing of biocide adapted mutants repeatedly identified mutations within a fatty acid kinase gene (*fakA*) in independent lineages of *S. aureus* after exposure to both biocides in all conditions (**Chapter 5**). Analogous changes were observed within the homologous gene in parallel experiments with *E. faecalis*. Interestingly, the changes were mainly loss of function and present in conserved residues across FakA homologs from different bacteria. This wider presence of this gene might indicate the impact this could have in predicting CHX/OCT tolerance not only for *S. aureus* and *E. faecalis* but across different bacterial species.

Further assays to study the mechanistic basis and relationship to phospholipid production showed that evolved isolates with *fakA* mutations accumulated less ethidium bromide than parent strains, exhibited altered cell envelope morphology and most of them showed decreased susceptibility to daptomycin, an antimicrobial that disrupts the cell membranes. FakA appears to be a novel mediator of biocide sensitivity potentially acting by causing changes in membrane permeability and fluidity leading to an increase tolerance to CHX and OCT, consistent with the mechanism of action of both biocides. Overall, this strongly suggests a potential role of FakA in biocide tolerance.

To conclude, understanding the mechanisms by which bacteria evolve resistance to biocides is essential in the first place to determine which agents are less likely to select for resistance in practice. Further optimisation in creating a clear *fakA* deletion mutant will better elucidate its role in the context of biocides. The FakA structural domains have been recently characterised (Subramanian et al., 2022) and the discovery of this fatty acid kinase involved in phospholipid biosynthesis is a recent finding, hence additional understanding of the interactions between biocides and this gene has yet to be further investigated.

CHAPTER 7: STUDYING GAMA HEALTHCARE'S NOVEL CLINELL® PROPRIETARY FORMULATION

"What you do makes a difference, and you have to decide what kind of difference you want to make." – Jane Goodall

7.1. Introduction

As discussed, the increasing number of HCAIs make infection prevention and control critical. There are however a relatively small number of biocidal agents in common use for surface disinfection in hospitals. Developing new products requires understanding of the impacts of all components of a formulation. Currently however, most tests are performed with biocides and/or the active ingredients of the formulation (unformulated products) without testing the formulation as a whole or the effects co-formulants and other excipients might have in biocide activity (Cowley et al., 2015; Maillard, 2018). Therefore, testing fully formulated products, single actives and co-formulants in a more realistic context is essential.

Biocides must be used at concentrations recommended by the manufacturer to be effective. Nonetheless, the use of these products at sub-inhibitory concentrations could also represent a problem since tolerance/resistance might develop in real life scenarios. The biocidal product regulation (BPR) now requires information on resistance, tolerance and cross-resistance development in organisms targeted by the biocidal product. Nonetheless, there is no current standard protocol developed to assess bacterial adaptation to biocides. GAMA Healthcare is an innovative company at the forefront of IPC products with multiple areas of expertise including the production of effective and efficient surface care products.

Biocide efficacy testing: BS EN Standard testing

According to the BPR, biocidal products need to comply with strict regulations for the product to be authorised. To make a disinfectant claim, the product needs to pass efficacy testing, where the tested organisms are in high concentrations (to reproduce worst case scenarios). Each disinfectant product needs to be validated to ensure its efficacy, and to support claims about how to kill different viruses or bacteria in different contact times.

British and European Standards specify efficacy testing methods for chemical disinfectants and/or antiseptics. Additionally, antimicrobial preservatives, which can be added to the product to prevent and/or limit microbial contamination, are also tested by preservative efficacy testing (PET). At GAMA Healthcare Ltd., a UK biocide producing company, the obligatory standards for disinfectants in the medical area are regularly performed; these include a bactericidal suspension test (BS EN 13727) to determine bactericidal activity of any novel formulation and the active ingredients and a surface test (BS EN 16615) to determine the bactericidal activity of disinfectant wipes.

Efficacy testing might also complement the data obtained with biocide susceptibility testing (Neuhaus et al., 2022), since the antibacterial activity of the biocide is tested against different reference organisms, concentrations and contact times.

FM104: A novel formulation

Due to regulatory changes, biocidal products containing polyhexamethylene biguanide (PHMB/CAS 27083-27-8) must not be sold in Great Britain since 2020. To meet these requirements, GAMA Healthcare has developed a novel formulation: GAMA Healthcare's novel Clinell® proprietary formulation (also referred to in this chapter as FM104, for formulation number 104), that can be used for everyday cleaning and disinfection. A patent was filed for this novel biocidal formulation hence some information is confidential.

This new formulation contains a combination of two quaternary ammonium compounds (QACs) as active ingredients: didecyldimethylammonium chloride (DDAC) and benzalkonium chloride (BZK). This QAC-based formulation also includes phenoxyethanol (POE) as an antimicrobial preservative, to protect the product and inhibit the growth of microorganisms that could be introduced during the manufacturing process. POE is highly effective against Gram-negative organisms, and at higher concentrations is also effective against Gram-positive organisms. Other co-formulants (e.g., ingredients which do not have biocidal activity but offer other performance benefits for application) are added in the formulation such as surfactants and chelating agents to improve stability and odour.

When designing biocidal formulations, different factors that might influence the antimicrobial activity of the biocide need to be considered (Maillard, 2005). Recent work (Jennings et al., 2024) has also studied material compatibility in the context of the biocidal product applied, to avoid phenomena like environmental stress cracking leading to a fracture of materials (plastic, stainless steel) on surfaces or polymeric medical devices (Block et al., 2018). When compared to other disinfectants, QACs are proven to be less reactive and to have good surface compatibility (Rutala and Weber, 2016). Additionally, the formulation's compatibility with other products that are used for the same purpose need to be considered. For example, when using CHX for skin, the bactericidal activity can be reduced or inactivated by the co-formulants of alcohol sanitizing gels, if applied (Kaiser et al., 2009).

In this chapter, to help prepare data to satisfy the BPR resistance claim, different methods were used to assess for tolerance/resistance of the novel FM104 formulation against selected isolates (*S. aureus* ST188 and *E. faecalis* ST40) and a reference strain (*E. hirae* NCTC 13383)

commonly used in biocide efficacy testing standards. Additionally, since exposure of bacteria to low level of biocides can select for antibiotic-resistant mutants (Webber et al., 2015), potential for selection of cross-resistance to a panel of antibiotics was also assessed.

7.2. Aims

As part of the MRC Doctoral Antimicrobial Research Training iCASE PhD programme, a three-month placement (September to December 2022) was undertaken at GAMA Healthcare Ltd., at the Fellows Research Centre (Halifax, UK). The aims of this iCASE partnership were:

- To generate data for the next generation of disinfectant formulations that GAMA Healthcare Ltd. have developed to be included in the BPR regulatory submission.
- To develop and implement a multi-step approach to assess bacterial adaptation to biocides (not only the active ingredients separately) but also including biocidal formulations.
- To test for disinfectant efficacy using the British and European Standards testing.
- To gain industrial perspective and understand the applicability of this PhD project by using real-world biocidal products.

7.3. Results

7.3.1. BS EN Standard testing with two Gram-positive isolates and a reference strain

To establish baseline efficacy of FM104, BS EN Standard testing in suspension (BS EN 13727) and in a wipe form (BS EN 16615) were performed with the two clinical isolates (*S. aureus* ST188 and *E. faecalis* ST40) and the reference strain *E. hirae* NCTC 133833, with a 10-second contact time. The log reduction, which is a measure of how effective the disinfectant was in eliminating microorganisms, was calculated. Achieving at least a 5-log reduction, which indicates that the product eliminates 99.999 % of pathogens, is desirable for a product to be considered effective.

Toxicity and efficacy of the neutraliser used was assessed. The selected neutraliser (Polysorbate 80/Tween® 80) had no antibacterial activity against *E. faecalis* ST40, *E. hirae* NCTCT 13383, and *S. aureus* ST188, and effectively neutralised the biocidal action when added.

Overall, when testing FM104 against the selected reference strain and the two clinical isolates, a 5-log reduction was achieved in 10 seconds (**Figure 7.1.**).

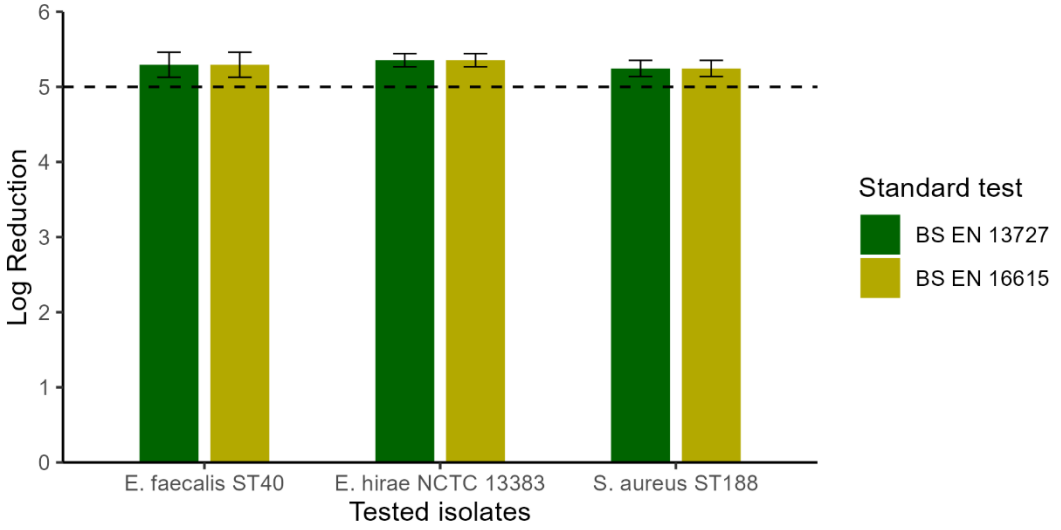

Figure 7.1. Efficacy testing for FM104 against *S. aureus* ST 188, *E. faecalis* ST40 and *E. hirae* NCTC 13383. Log_{10} CFU/mL reduction for the tested isolates; Bars represent 95 % CI. The black dotted line indicates the desired 5-log reduction needed to claim for bactericidal efficacy (contact time = 10 seconds).

7.3.2. Concentration dependent killing assays

In industrial settings, BS EN efficacy testing is performed to test for the efficacy of commercialised disinfectant, which better elucidates real-life scenarios. As a comparison, the bactericidal activity of CHX and OCT was also assessed using similar guidelines. Different concentrations of the biocides were studied against the two clinical isolates, with and without interfering substances. These concentration dependent killing assays were performed at 5-minute exposure time (instead of 10 seconds), with in-use concentrations of CHX/OCT and also lower concentrations of these biocides to determine which concentration gives at least a 5-log reduction. Log reductions in CFU/mL were then calculated for each tested isolate and the different disinfectant concentrations (**Table 7.1.**).

In-use concentrations of CHX (0.2 - 2 %) and OCT (0.05 - 0.5 %) eliminated both isolates, hence demonstrating the high efficacy of these products and neutralisers with a 5-minute contact time. With lower biocide concentrations than recommended by manufacturers, generally only a 3-log reduction was seen with the used neutraliser. Except for OCT (5 mg/L) in *E. faecalis* ST40 and CHX (200 mg/L) where a slightly higher reduction was observed with these lower doses. Similar results were observed for *S. aureus* ST188.

Table 7.1. Log_{10} CFU/mL reductions for *S. aureus* S188 and *E. faecalis* ST40 at different concentrations of CHX/OCT.

Tested isolate	Disinfectant concentration		Log Reduction
	%	µg/mL	
Octenidine dihydrochloride			
S. aureus ST188	0.5	5000	> 6
	0.05	500	> 6
	0.0005	5	4.94
	0.00025	2.5	3.93
E. faecalis ST40	0.5	5000	> 6
	0.05	500	> 6
	0.0005	5	> 6
	0.00025	2.5	4.7
Chlorhexidine digluconate			
S. aureus ST188	2	20,000	> 6
	0.2	2000	> 6
	0.02	200	5.4
	0.002	20	4.3
E. faecalis ST40	2	20,000	> 6
	0.2	2000	> 6
	0.02	200	2.59
	0.002	20	2.19

* Inoculum size = $5x10^8$ (for *S. aureus* ST188) and $1x10^8$ (for *E. faecalis* ST40); Exposure time = 5 minutes. Log > 6 indicated; Polysorbate 80/Tween® 80 used as neutraliser.

Concentration dependent killing assays were repeated with interfering substances to ensure more realistic conditions (not shown). With a 5-minute exposure time, the log reduction in clean conditions was higher than in dirty conditions, where blood was added to simulate dirty environment conditions present when cleaning/disinfecting. Although interfering substances reproduce real-life scenarios, and protein load would potentially have an effect in the efficacy of these agents, dirty conditions are not included in MIC/MBC assays (Koburger et al., 2010).

7.3.3. MIC and MBC testing for biocides

MIC and MBC assays were used to measure microbial susceptibility for the individual components of FM104, 50:50 combinations of the actives, preservatives and the full GAMA Healthcare's novel Clinell® proprietary formulation (bulk liquid and liquid extracted from the wipes) against the selected clinical isolates and the reference strain. Additionally, the formulation minus the active ingredients (chassis) and excluding the preservative were tested. A comparison between DDAC, and another regularly used QAC (ADAC), which has a different number and length of alkyl chains, and comparisons between two different suppliers for BZK were also performed.

Susceptibility testing was performed using 0.00625 - 12.8 µg/mL concentration ranges (two-fold dilution) by broth microdilution method (**Chapter 2**, **Section 2.4.1.**). For the preservatives and the whole formulation, higher concentrations were used: 125 - 8,000 µg/mL (preservative) and 488 - 500,000 µg/mL (whole formulation and chassis). After initial troubleshooting, CaMH was substituted with a commercially available brand (confidential) of TSB to minimise medium interactions with biocides.

Individual actives and 50:50 combinations of actives from FM104: MIC values of the individual actives ranged from 0.8 - 6.4 mg/L. Combinations of actives (50:50) showed similar results to individual actives, with some exceptions, possibly indicating a lack of synergy between the actives.

No differences in MIC values between BZK suppliers were observed. Differences between DDAC and ADAC (higher MIC values of ADAC) were observed. Therefore, lower MIC values DDAC are preferable, indicating DDAC is a better and more effective active for the formulation.

Novel biocidal formulation (FM104): after determining the MICs of the individual actives (and in combination), the MIC of FM104 (bulk liquid and liquid extracted directly from the wipes) were compared. Analytical quantification by high-performance liquid chromatography (HPLC) was performed to quantify the percentage of active ingredients in the wipes prior the experiment.

MIC values of FM104 similar to the MIC if the individual actives. There were minor changes in MIC/MBC when comparing the bulk liquid form and the liquid extracted from the wipes.

Preservative (POE) and chassis from FM104: higher MIC values were observed for POE than for the active ingredients. In fact, the preservative MIC was higher than in-use concentrations of this ingredient in the formulation. These results indicate only a small percentage of this ingredient is needed to be effective in the formulation, in order to avoid high doses which will negatively contribute to POE safety issues.

The MIC of FM104 (-actives) or FM104 (-BZK/DDAC), and FM104 (-actives, -preservatives) or FM104 (-BZK/DDAC/POE), were really high compared to the previous stress agents tested. In fact, the MIC of FM104 (-actives) is even higher than the MIC of the preservative by itself (MIC = 0.8 %).

A summary of all the MIC/MBC values, which correspond to the average of 3 biological replicates (with 3 technical replicates included in each), can be found in table below (**Table 7.2.**).

Table 7.2. MIC and MBC values of the tested agents against *S. aureus* ST 188, *E. faecalis* ST40 and *E. hirae* NCTC 13383.

	Minimum inhibitory concentration (µg/mL)	Minimum bactericidal concentration (µg/mL)
***Staphylococcus aureus* ST188**		
Actives and 50:50 combinations		
DDAC	0.8	0.8
ADAC	3.2 - 6.4	3.2 - 6.4
BZK – Supplier A	1.6	1.6
BZK – Supplier B	1.6	1.6
DDAC:BZK – Supplier A (50:50)	0.8	3.2
DDAC:BZK – Supplier B (50:50)	0.8 - 1.6	1.6
ADAC:BZK – Supplier A (50:50)	1.6	1.6
ADAC:BZK – Supplier B (50:50)	1.6	1.6
FM104		
FM104 (Bulk liquid)	0.8	0.8 - 1.6
FM104 (Liquid extracted from the wipe)	1.6	1.6
FM104 (Liquid extracted from the wipe adjusted for adsorption)	0.8	0.8 - 1.6
Preservative and Chassis		
Preservative (POE)	8,000	> 8,000
FM104 (-DDAC, -BZK) = Chassis	125,000	≥ 125,000
FM104 (-DDAC, -BZK, -POE)	125,000	125,000

	Minimum inhibitory concentration (µg/mL)	Minimum bactericidal concentration (µg/mL)
***Enterococcus faecalis* ST40**		
Actives and 50:50 combinations		
DDAC	1.6	1.6 - 3.2
ADAC	6.4	> 6.4
BZK – Supplier A	3.2	> 6.4
BZK – Supplier B	3.2	> 6.4
DDAC:BZK – Supplier A (50:50)	1.6	3.2
DDAC:BZK – Supplier B (50:50)	3.2	3.2
ADAC:BZK – Supplier A (50:50)	3.2	3.2
ADAC:BZK – Supplier B (50:50)	3.2	3.2
FM104		
FM104 (Bulk liquid)	1.6	3.2 - 6.4
FM104 (Liquid extracted from the wipe)	3.2	6.4
FM104 (Liquid extracted from the wipe adjusted for adsorption)	1.6	1.6 - 3.2
Preservative and Chassis		
Preservative (POE)	> 8,000	> 8,000
FM104 (-DDAC, -BZK) = Chassis	250,000	≥ 250,000
FM104 (-DDAC, -BZK, -POE)	250,000	250,000

	Minimum inhibitory concentration (µg/mL)	Minimum bactericidal concentration (µg/mL)
***Enterococcus hirae* NCTC 13383**		
Actives and 50:50 combinations		
DDAC	0.8 - 1.6	1.6
ADAC	6.4	> 6.4
BZK – Supplier A	3.2	3.2 - 6.4
BZK – Supplier B	3.2	3.2
DDAC:BZK – Supplier A (50:50)	1.6	3.2
DDAC:BZK – Supplier B (50:50)	1.6	3.2
ADAC:BZK – Supplier A (50:50)	3.2	3.2
ADAC:BZK – Supplier B (50:50)	3.2	6.4
FM104		
FM104 (Bulk liquid)	1.6	3.2
FM104 (Liquid extracted from the wipe)	3.2	3.2
FM104 (Liquid extracted from the wipe adjusted for adsorption)	1.6	1.6 - 3.2
Preservative and Chassis		
Preservative (POE)	> 8,000	> 8,000
FM104 (-DDAC, -BZK) = Chassis	250,000	≥ 250,000
FM104 (-DDAC, -BZK, -POE)	250,000	250,000

* MIC/MBC values correspond to the average of 3 biological replicates (with 3 technical replicates included/biological replicate).

* For confidential purposes, the ratios of the tested agents, and the names of the suppliers are not disclosed.

7.3.4. Evolution experiment

After performing susceptibility testing, an evolution experiment was performed to assess the changes over time of the selected populations when evolved under increased concentrations of the selected stresses, including a biocidal formulation, over a 1-month period of time.

Modifications of the *in vitro* bead-based evolution model (as explained in **Chapter 2**, **Section 2.5.2.**) included removal of the biofilm condition due to time constraints and the primary goal being to study potential resistance emergence which earlier data showed happened faster in planktonic conditions (**Chapter 4**) and reduction of the passage window (from 72 hours to 48 hours since no biofilm condition was added). In summary, the tested conditions included planktonic and control (no stress) for 3 different isolates, and 3 stresses (BZK+DDAC, FM104 and chassis). The concentrations of the stresses doubled in each passage for stress 1 and 2 (from 0.0125 to 12.8 µg/mL), and for stress 3 (from 0.0125, 93.75, 187.5 to 1000 µg/mL, and then increased by double to 256,000 µg/mL in each passage).

For the two tested enterococci, the experiment ran for a total of 10 passages (equivalent to 66 generations) for all the stress except for FM104 11 passages (73 generations). For *S. aureus* ST188, the experiment ran for a total of 9 passages (59 generations) for all the stresses except for FM104, with 11 passages (73 generations). The control condition for each isolate ran for 11 passages (73 generations).

Independent drug-free controls productivity (**APPENDIX XVI**) stayed relatively the same over time for the two enterococci isolates and *S. aureus* ST188. In the planktonic condition (**Figure 7.2.**), results differed between the different stresses:

Stress 1 (BZK+DDAC): Increasing concentrations of a 50:50 combination of both actives (with the current BZK supplier) were tested (**Figure 7.2. - A**). When analysing the planktonic condition, productivity started to decrease at exactly the MIC value (beyond 1.6 µg/mL for enterococci and 0.8 µg/mL for *S. aureus* ST1188) although isolates from the last exposures were very poor growers. Generally, isolates were able to grow slightly beyond the WT MIC of the 50:50 combination of BZK:DDAC, but never surpassed the MIC values of these actives individually.

Stress 2 (FM104): When stressed with increased concentrations of FM104 (bulk liquid) planktonic lineages were able to survive beyond the WT MIC for enterococci (1.6

µg/mL) and *S. aureus* ST188 (0.8 µg/mL), but productivity started to decrease exactly at the MIC level (**Figure 7.2. - B**). Isolates from the last exposure had a decrease in productivity.

Stress 3 (Chassis = FM104 minus actives): when stressed under increased concentrations of the chassis (**Figure 7.2. - C**), isolates did not survive beyond the WT MIC for enterococci (250,000 µg/mL) when productivity stopped at MIC levels. For *S. aureus* ST188, productivity already started to decrease a few passages before the WT MIC (125,000 µg/mL).

Overall, there is a decrease in productivity at the MIC level for all the stresses, and although some isolates were able to continue growing beyond the MIC (2X), growth was compromised at prior passages, and no conditions selected mutants with high MICs to the selective agents.

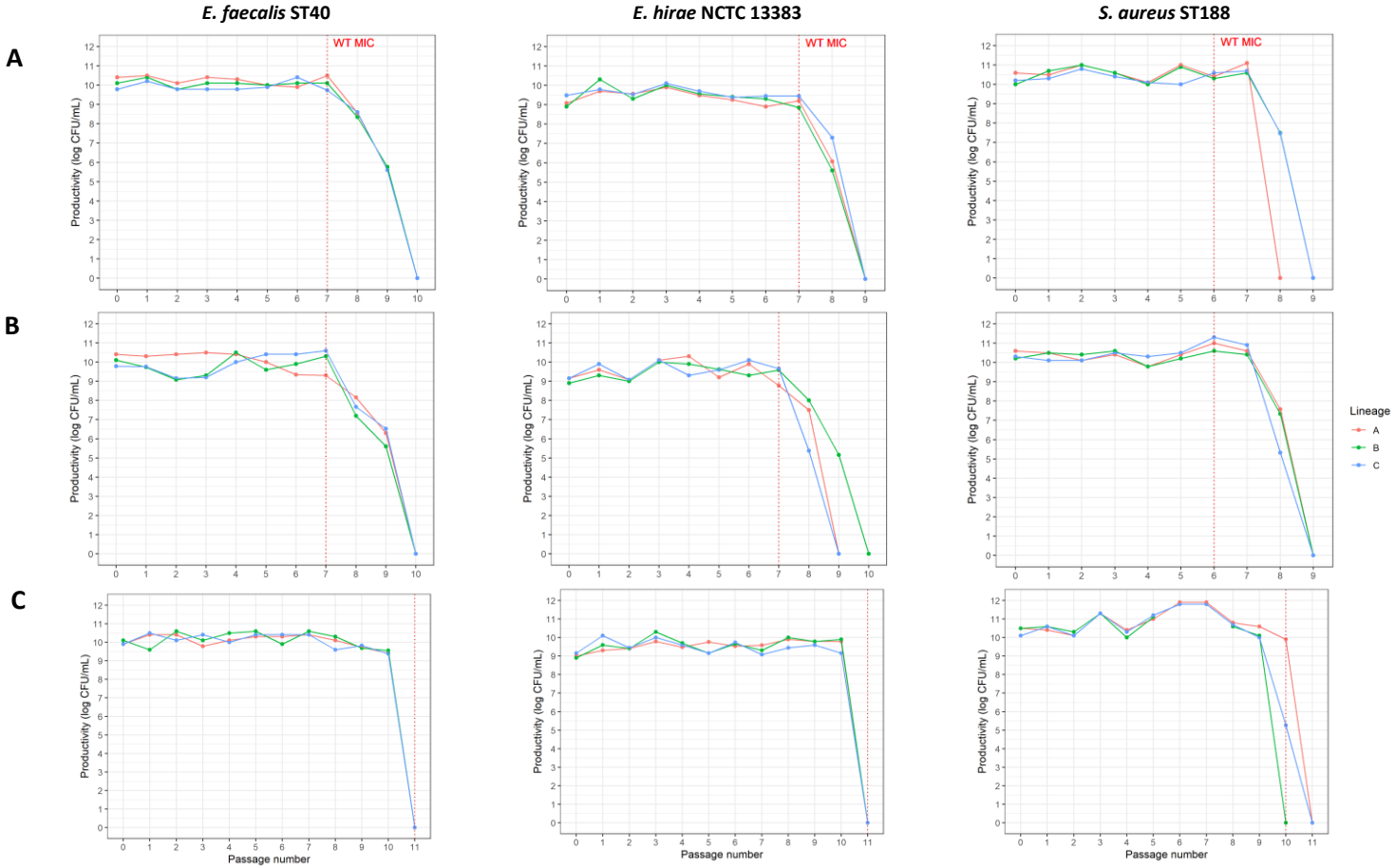

Figure 7.2. Productivity of planktonically evolved isolates for each stress. Productivity (expressed as CFU/mL) is plotted over each passage number for **(A)** Stress 1 (BZK+DDAC); **(B)** Stress 2 (FM104); **(C)** Stress 3 (Chassis); three independent lineages (A, B, C) included. The MIC of the WTs shown by dotted red lines for Stress 1 and Stress 2: 0.8 µg/mL (passage 6), 1.6 µg/mL (passage 7); for Stress 3: 125,000 µg/mL (passage 10), 250,000 µg/mL (passage 11).

7.3.5. Genotyping

Population samples from the late timepoints (for all stresses) were selected for WGS and compared to the reference genomes (as explained in **Chapter 5**). Sequencing analysis revealed a few SNPs were present in the evolved isolates when compared to the reference genomes. Overall, the tested stresses did not have an impact on any genes known to confer antibiotic or biocide tolerance, suggesting the potential for selection of cross-resistance of these agents is low.

A summary of the SNPs shared by 2 (or more) independent isolates is shown (**APPENDIX XVII**). For *E. faecalis* ST40, most SNPs were chromosomal but one was also identified in the plasmid (second contig), whereas for *S. aureus* ST188 and *E. hirae* NCTC 13383 evolved isolates, fewer SNPs were detected and all of them were present in the chromosome. For these isolates, there were cases with SNP changes present in all the evolved isolates when compared to the reference genome. Nonetheless, these have not been considered as real changes but as a change in the reference genome. To identify genomic changes potentially associated with the phenotypes observed, we subtracted changes present in our parent stains and ended up with 3 variant locations (for *S. aureus* ST188) and 1 variant location (for enterococci).

Many of the changes found were in hypothetical genes of uncharacterised function and in intergenic regions. In the case of intergenic SNPs, the genetic environment (upstream/downstream regions) was studied. There was one example in *S. aureus* ST188 evolved isolates, where the intergenic region is downstream of *ktrA,* a potassium uptake protein related to increased susceptibility to aminoglycoside antibiotics and cationic antimicrobials in *S. aureus* (Gries et al., 2013). This could potentially be linked to FM104 since the stress includes cationic antimicrobials, although no clear benefit to the isolate can be associated to this change.

When visualising phylogenies between the evolved isolates and the reference genomes, clear distributions can be observed in the trees for *E. faecalis* ST40 (**Figure 7.3. - A**) and *S. aureus* ST188 (**Figure 7.3. - B**) when grouped by stress. This indicates high relatedness between planktonic populations sampled from the same stress. Nonetheless, results for *E. hirae* NCTC 13383 (**Figure 7.3. - C**) showed differences between samples from the same stress.

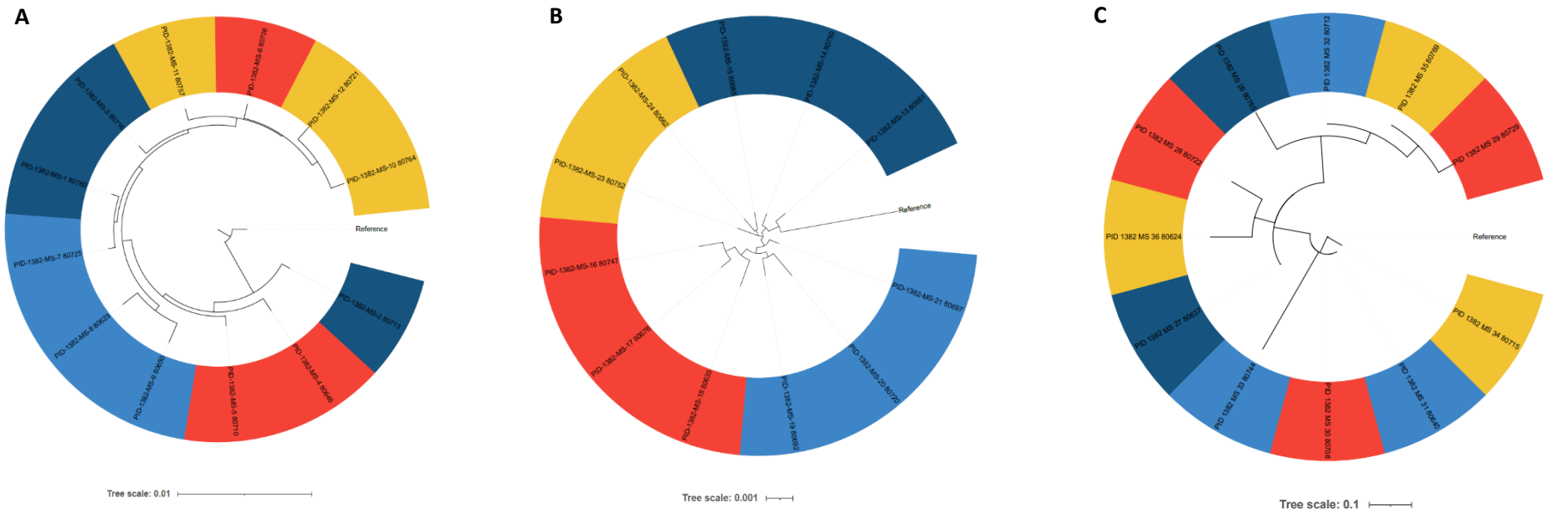

Figure 7.3. Phylogenetic trees from alignments of the evolved isolates with the reference wild-type genomes. Approximately-maximum-likelihood phylogenetic trees from Snippy-core (v4.4.3) alignments generated with FASTTREE (v2.1.10) and visualised with iTOL (v6.8.2) for **(A)** *E. faecalis* ST40; **(B)** *S. aureus* ST188; **(C)** *E. hirae* NCTC 11383. The phylogenetic circular trees were rooted using the reference strain. Results shows different groups selected by different stress conditions (BZK+DDAC highlighted in red, FM104 in yellow, and Chassis in blue); control condition (no stress) highlighted in navy. A total of 12 samples/isolate are represented, except for *S. aureus* ST188 where after quality checks, 11 samples are shown.

7.3.6. Phenotyping

Phenotyping assays to characterise the selected evolved isolates included testing for changes in the susceptibility pattern against the different biocidal stresses and assessing any potential cross-resistance to a panel of clinically relevant antibiotics. Stress 3 (chassis) was not tested as an antimicrobial since it is not representative of a real-world product, as formulations always include biocides as active ingredients.

Additionally, biofilm formation and growth differences compared to the WTs were determined.

7.3.6.1. Biocide-antibiotic cross-resistance

In general, low-level changes to the tested antibiotics were observed in the evolved isolates (**Figure 7.4.**), with some exceptions. Similarly to what was observed (**Chapter 5**), changes to cefotaxime susceptibility were observed in the two clinical isolates but this also occurred in control conditions and are likely to represent media adaptation and not a specific response to either tested agent.

In *E. faecalis* ST40 (**Figure 7.4. - A**), a 2-$\log_2$ fold decrease to gentamicin was observed for all the stresses, and in the control condition. A 2-$\log_2$ and 4-$\log_2$ fold increase were seen for penicillin and erythromycin respectively in *S. aureus* ST188 evolved isolates (under all stresses) but not in the control condition (**Figure 7.4. - B**). A decrease in the MIC of gentamicin compared to the WT was observed for *E. hirae* NCTC 13383 under all tested stresses (**Figure 7.4. - C**).

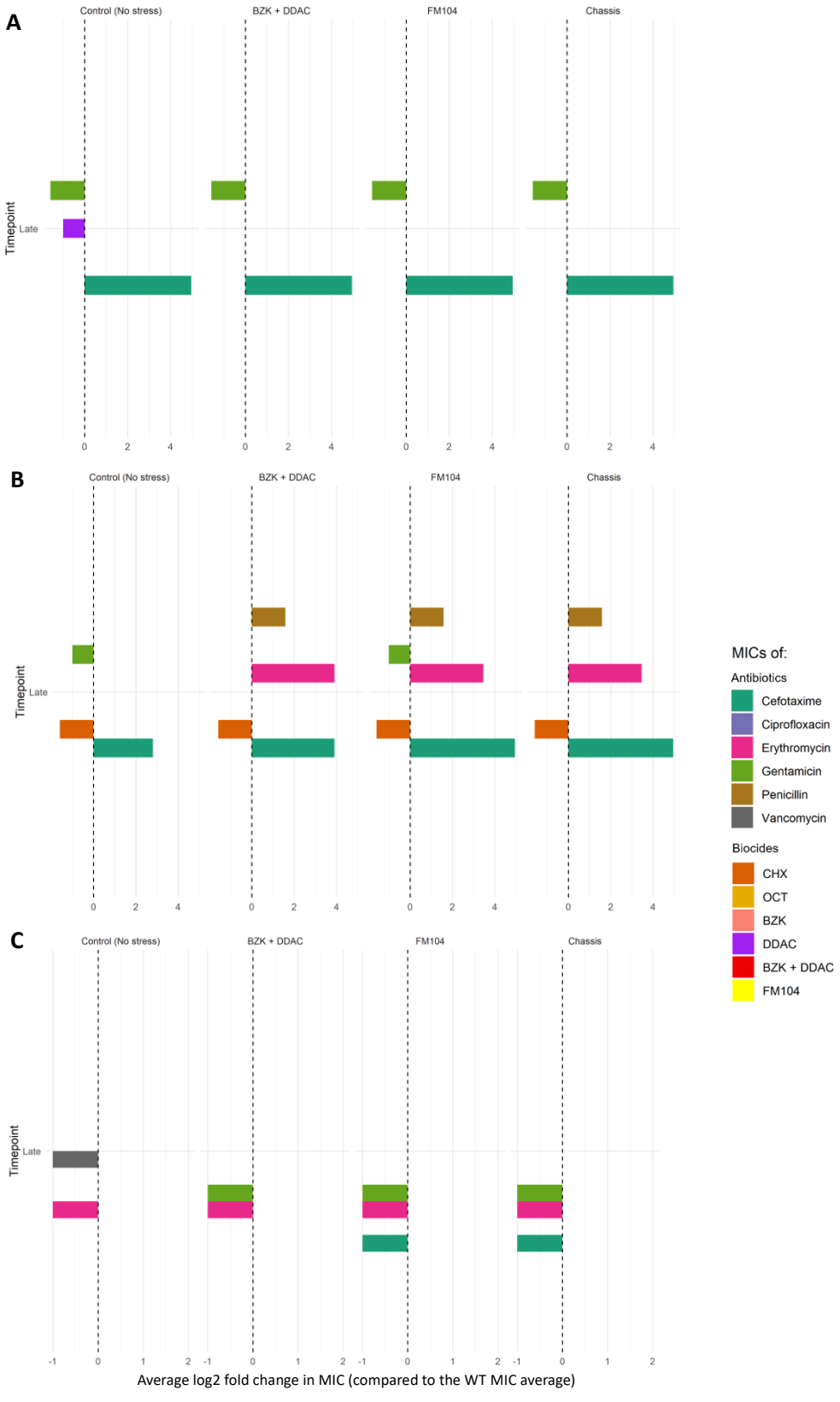

Figure 7.4. Susceptibility profiles of the evolved isolates. Control (no stress) and planktonic evolved **(A)** *E. faecalis* ST40; **(B)** *S. aureus* ST188; **(C)** *E. hirae* NCTC 13383 isolates shown. The average $\log_2$ fold change in MICs (compared to the WT MIC average) was calculated for different antimicrobials (antibiotics and biocides).

7.3.6.2. Colony morphology of the evolved isolates

Biofilm production was assessed for the evolved isolates from all the stresses and compared to the WT (**Figure 7.5.**), using the same Congo red scale scoring system as explained in **Chapter 5**. Overall, enterococci colonies were paler (1+), which was associated with less biofilm being produced compared to staphylococci, that had darker red colonies (3+). No changes in the evolved isolates were observed when compared to the WT, with two exceptions.

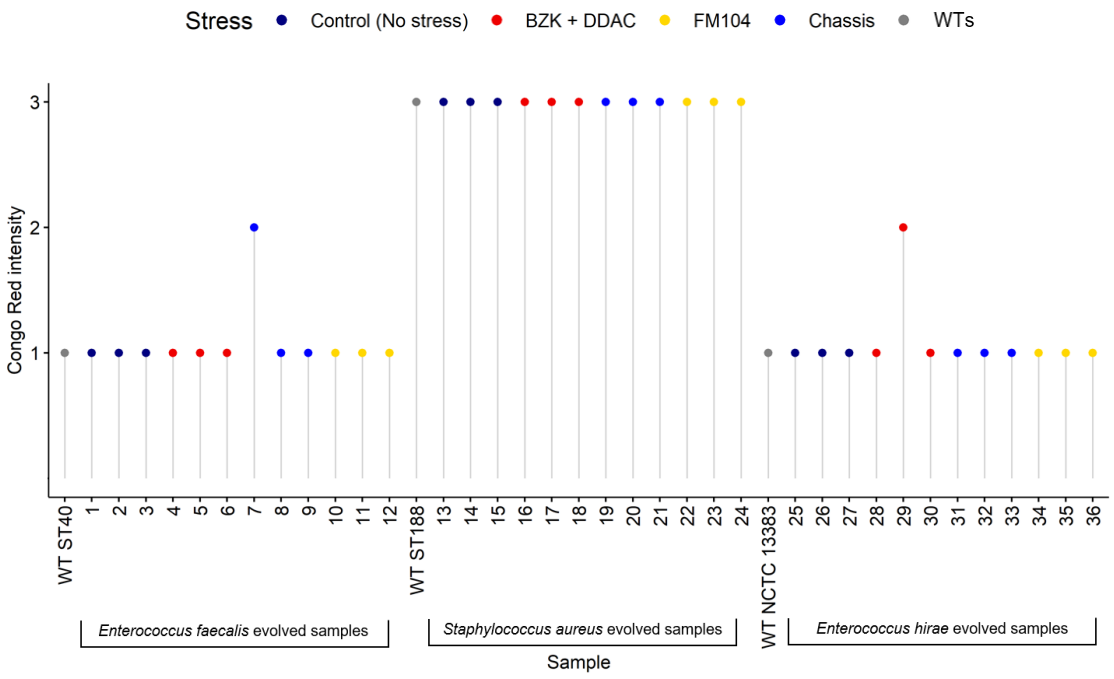

Figure 7.5. Congo red intensity of the WTs and the evolved samples. WTs (*E. faeca*lis ST188, *S. aureus* ST188 and *E. hirae* NCTC 13383) and the respective planktonic evolved samples under stress 1 (BZK+DDAC), stress 2 (FM104) and stress 3 (Chassis), and control (no stress) are shown. Lollipop plots show no changes in biofilm formation between WT and evolved sample under different stresses.

7.3.6.3. Growth curves

To determine any changes in fitness, growth was assessed over 18 hours for the selected evolved samples (from the late timepoints) and the control samples (no stress) and compared to the WTs (**Figure 7.6.**). Wilcoxon-Mann-Whitney tests showed non-statistically significant changes (*p-value* > 0.05) between the evolved isolates under biocidal stress (BZK+DDAC, FM104, chassis) and the WT.

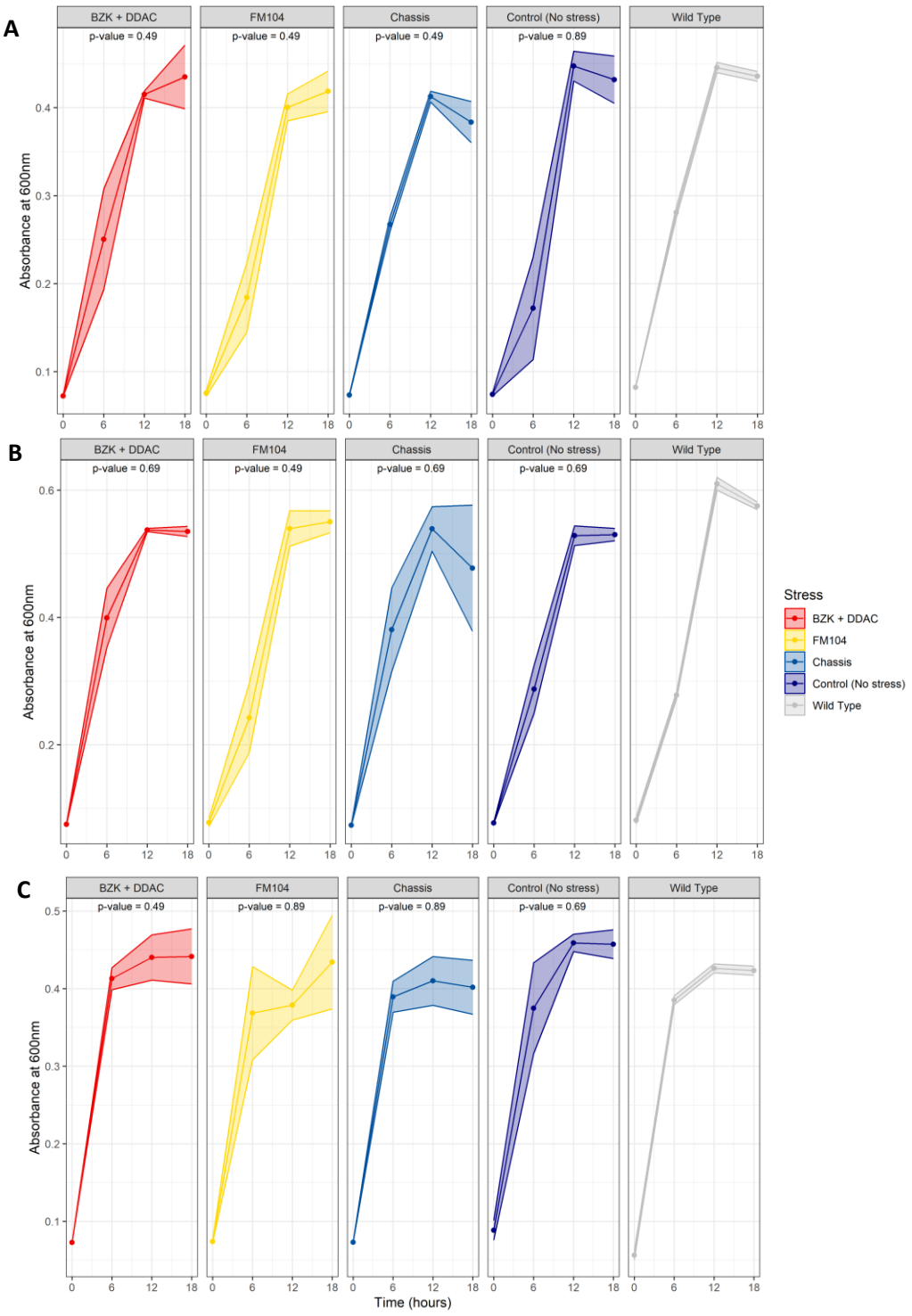

Figure 7.6. Growth curves for the evolved isolates. Absorbance (OD_{600nm}) was measured over 18 hours in TSB for **(A)** *E. faecalis* ST40; **(B)** *S. aureus* ST188; **(C)** *E. hirae* NCTC 13383 evolved isolates from the late timepoint for each stress; control (no stress) and WT included. The mean and standard deviation (represented as shaded areas in the plots) show the variability across the samples (3 samples/stress, with 3 technical replicates each) within each stress at each timepoint. Wilcoxon-Mann-Whitney showed non-statistically significant changes (*p-value* > 0.05) within conditions.

7.4. Discussion

During the iCASE placement at GAMA Healthcare Ltd., more realistic assays were used to assess the susceptibility to not only biocidal actives but also fully formulated biocidal products, and efficacy testing.

BS EN standard testing have shown that the novel FM104 formulation is effective at eliminating not only the reference *E. hirae* NCTC 13383 strain (commonly used for this standard testing) but also the two clinical isolates, since at least a 5-log reduction was obtained in both the BS EN 13727 and BS EN 16615 tests. These results are coherent with results from the current commercialised Clinell® formulation, which claims to be effective against *E. faecalis* (EN 13727), *E. hirae* (EN 13727, EN 16615) and *S. aureus* (EN 13727, EN 16615) in 10 seconds.

MIC and MBC assays provided useful information on each active, combination of actives, the novel FM104 formulation and the chassis, although it is important to highlight that biocides are often used at concentrations that exceed the MIC/MBC values. From our data, combinations of actives and the full formulation showed similar results to individual actives, and minor differences between bulk liquid and liquid extracted from biocidal wipes were observed. The concentration of the liquid extracted from the wipes usually differs on a surface from the concentration of the bulk liquid form. This could be due to the delivery vehicle, since it is delivered in the form of a wipe the concentration of the biocide added is not the same as the concentration in the actual surface, or even the material of the wipe could affect the performance. Therefore, small changes in the MIC/MBC are to be expected. Results also showed that the chassis (co-formulants) can eradicate bacterial growth, and no increased tolerance was observed. Nonetheless, the efficacy of the formulation is due to the active substance and not the co-formulants itself. Therefore, this combination will not be produced in a real-life scenario since efficacy data is generated with the active substances that exhibit the main biocidal activity of the product.

Data from the evolution experiment, which ran for around 70 generations, showed that planktonically evolved lineages under three different stresses (BZK+DDAC, FM104 and Chassis) were able to survive at increased concentrations but with a sharp decrease in productivity at or above the MIC levels. Even if biofilms were not incorporated in this evolution experiments (there is no biofilm claim in the BPR), the previous *in vitro* bead-based evolution experiment (**Chapter 4**) included the biofilm condition since these play an important role in infections and confer an increased tolerance to antimicrobials.

Sequencing of mutants identified no changes in any genes known to confer antibiotic or biocide tolerance suggesting the potential for selection of cross-resistance with these agents is low. Phenotypic characterisation elucidated low-level changes to the tested antibiotics, except in the case of erythromycin, where a 4-$\log_2$ fold increase in the MIC was seen in the *S. aureus* ST188 evolved isolates compared to the WT, although below the EUCAST clinical breakpoint. No observable differences in biofilm formation nor microbial growth between the WT and the evolved isolates were seen.

Commercial relevance

Whilst previously tested biocides (CHX/OCT) showed limited selection for tolerance and a limited impact on antibiotic susceptibility, unformulated products perform very differently to biocidal formulations, which include not only active ingredients but also co-formulants and other excipients that can impact product efficacy. Therefore, outcomes after exposure to different products containing CHX or OCT may vary. Additionally, depending on the application of these biocides (skin, surfaces, mucosal sites), performance might differ. Some studies have observed resistance to in-use concentrations of biocidal formulation. For example, adapted *E. faecalis* to increasing concentrations of DDAC for 70 days (Schwaiger et al., 2014), and clinical *K. pneumoniae*, where CHX-based formulations were tested (Bock et al., 2016), showed resistance to in-use concentrations of these formulations. For this reason, a novel formulation was tested in this chapter, although the concentrations disclosed here are significantly lower than the ones in the final FM104 product.

Considering the experimental set-ups (Vejzovic et al., 2022) in this context is also essential. For example, the *in vitro* assays performed in this chapter depend on the media used, since biocides could react with the growth media components leading to biocide neutralisation. For this reason, prior troubleshooting with different media was essential to minimise medium interactions with biocides. Additionally, *in vitro* evolution experiments included media control to better understand if bacterial adaptation is a consequence of adaptation to the experimental conditions of a real adaptation to the biocides. This experimental design is significant commercially since it highlights the need for appropriate controls should the regulators push for standardise methods for determining biocide and antibiotic cross-resistance.

To conclude, this data could support the new product regulatory submission, as it could be included in the technical file of the novel formulation enclosed within the application for BPR

approval of the biocidal product. Additionally, it could also guide product design to effectively create more intelligent formulations with the optimal active ingredients and ratios.

7.5. Conclusions

Understanding bacterial responses to different biocidal agents is key to intelligently formulating biocidal products that deliver efficacy and support IPC practices. The proposed protocol to predict development of biocide tolerance/resistance using different high throughput *in vitro* methods, had been a robust method to understand biocide susceptibility, molecular modes of action, and the risk of biocide tolerance and cross-resistance. Additionally, it provided us with a deeper insight into how different variables might influence the experimental results.

No consistent patterns of mutations were recovered or data suggesting any significant cross-resistance after exposure to GAMA Healthcare's novel Clinell® proprietary formulation, indicating FM104 is effective against the tested clinical isolates, has a distinct mode of action and shows no cross-resistance to the antimicrobials tested. This data supports continued development of FM104 which is not likely to select for resistance/cross-resistance.

CHAPTER 8: GENERAL DISCUSSION

“One sometimes finds what one is not looking for" – Alexander Fleming

8.1. General discussion

Healthcare-associated infections represent a critical threat to patient safety, leading to high morbidity and mortality rates. Biocides are widely used to control and prevent these infections and understanding how nosocomial pathogens respond to biocidal agents is key to improving infection prevention and control products and practices.

Biocides at in-use concentrations remain highly effective. Nonetheless, the risk of biocidal tolerance and/or resistance development after exposure to sub-inhibitory concentrations, and cross-resistance to antibiotics should be assessed and evidenced. Some studies have argued that even if this bacterial adaptation to biocides can be observed *in vitro*, the tested concentrations are still below in-use concentrations, and these scenarios are not comparable to real-world commercially available products. Nonetheless, investigating the impact of these exposures is essential to better understand the implications for clinical relevance.

The overall aim of this research was to understand how nosocomial pathogens adapt to different biocides in a biofilm context and to use this information to help develop improved biocidal formulations with the iCASE partner GAMA Healthcare Ltd.

A protocol to predict development of biocide tolerance/resistance, and cross-resistance to antibiotics has been proposed (**Figure 8.1.**). A previous approach by Knapp et al. (2015) developed a low-cost protocol that included phenotypic assessment in the core part. Our proposed protocol not only includes *in vitro* methods (MIC/MBC) to phenotypically characterise the isolates against biocidal actives, but also biocidal formulation (in liquid and wipe format), as well as the co-formulants. Additionally, other techniques such as experimental evolution and further characterisation of the evolved isolates on a genomic (WGS) and transcriptomic (RNA-Seq) level has also been included.

This pipeline offers to provide important information assessing both the potential for tolerance/resistance to any biocide to emerge, but also the impacts of this in terms of cross-resistance, biofilm formation and virulence. The information generated using this approach can support product development and regulatory submissions, whilst also providing biological insight into microbial adaptation.

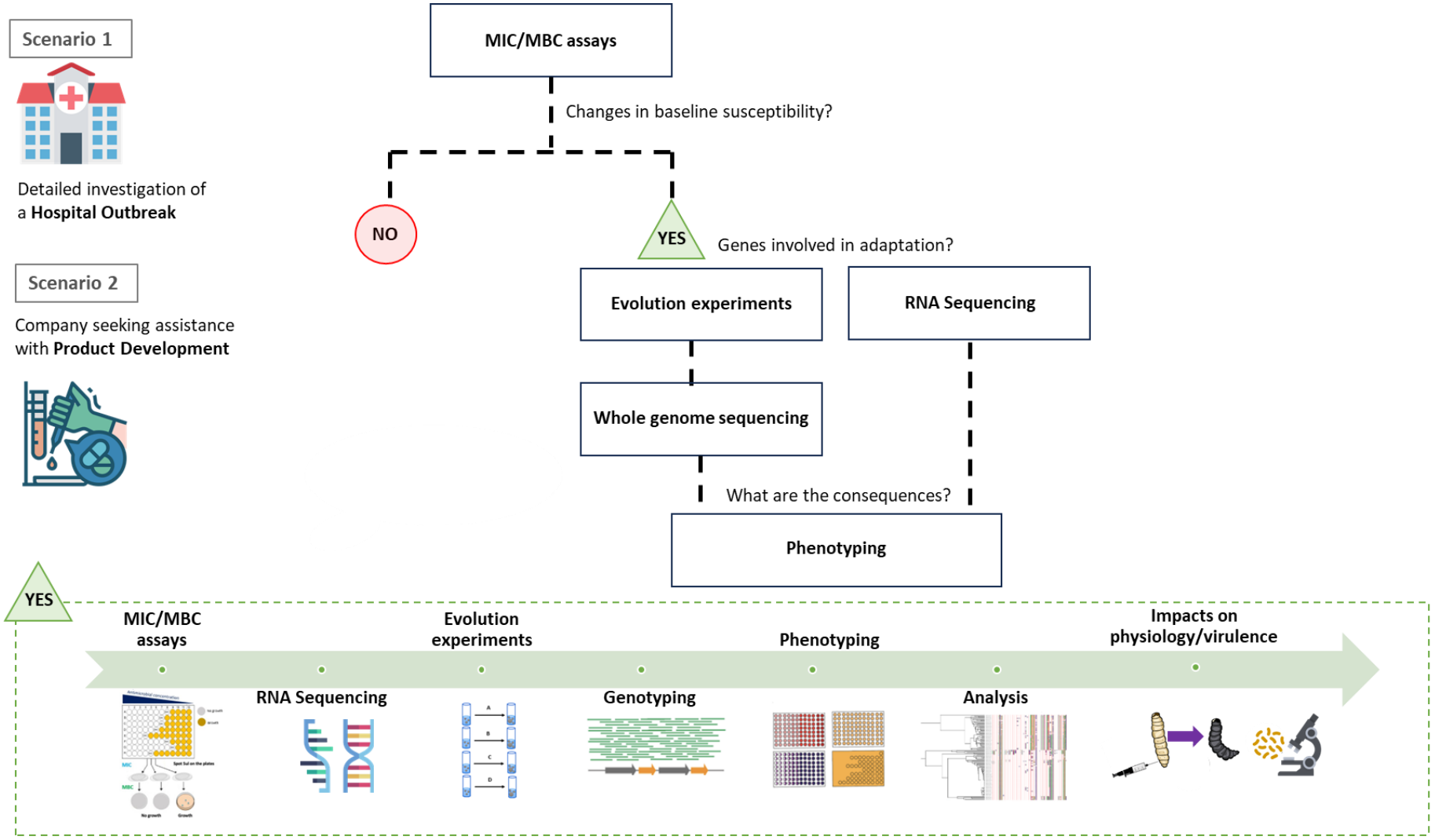

Figure 8.1. Proposed protocol to predict development of biocide tolerance/resistance and cross-resistance to antibiotics. Two-scenarios where this protocol could be applied are illustrated at the top-left of the diagram. Figure contains some icons from www.flaticon.com.

In this work, the proposed protocol provided important information at different levels:

Baseline susceptibility testing: MIC/MBC testing were used to measure biocide susceptibility against a panel of different agents providing robust data and showing some baseline susceptibility changes. Nonetheless, the absence of clinical breakpoints for biocides and standard definitions for tolerance/resistance makes interpretation of changes difficult. Developing databases with compiled information of MIC/MBC, and even ECOFF determination for biocides (Morrissey et al., 2014) could be key in monitoring biocide tolerance, resistance, and cross-resistance to antibiotics (Buxser, 2021).

RNA-Sequencing: responses to different agents (CHX, OCT) and a novel biocidal product (FM104) differed, with many more genes being upregulated and related to general stress response, heat shock proteins, and amino acid biosynthesis. RNA-Seq provided us with a better understanding of the genes involved in adaptation to biocidal stress under short-term exposures.

***In vitro* bead-based evolution model:** under prolonged exposures to biocidal stress, both species were able to adapt to grow beyond relatively low concentrations of both agents, although not to FM104, and this occurred in both planktonic and biofilm conditions. Although biofilms are often intrinsically more tolerant of many antimicrobials, the planktonic lineages exhibited an ability to adapt to higher concentrations of both biocides than the biofilm lineages. This may reflect the larger effective population size present in the planktonic lineages but shows there is no inherently greater ability to adapt to these biocides when grown as a biofilm for both species tested.

Whole genome-sequencing: sequencing of mutants repeatedly identified SNPs in *S. aureus* fatty acid kinase (*fakA*) from independent lineages, for both biofilm and planktonic conditions and both biocides. A mutation in the orthologue gene (*dak2*) was also identified in *E. faecalis*. The changes in FakA were mainly predicted to result in loss of function as a result of either introduction of stop codons or alteration of completely conserved residues within FakA.

Phenotyping assays: antimicrobial susceptibility testing results showed very limited changes in antimicrobial susceptibility followed exposure to either biocide and there were no

significant changes between isolates recovered from planktonic or biofilm conditions. As hypothesised, bacterial biofilms can evolve resistance or tolerance to biocides leading to low-level changes to susceptibility to various other antimicrobials. However, there were collateral impacts on fitness seen in populations able to grow in escalating concentrations of the biocides. Differences in the selective outcomes between the biocides and species were observed in biofilm formation which was also generally compromised more in *E. faecalis* after biocide exposure than in *S. aureus*.

FakA and its novel role in biocide tolerance: The repeated isolation of *fakA* mutants after biocide exposure strongly suggests a role for this gene in disinfectant tolerance. We hypothesised that loss of FakA function would result in altered membrane composition, with more lipids containing longer acyl chains (DeMars et al., 2020) which leads to less membrane fluidity. Ethidium bromide accumulation assays showed significantly lower accumulation in the evolved isolates than in the WT. Additionally, the MIC of daptomycin, a membrane targeting antibiotic (Alder, 2005), was increased in some *fakA* mutants. These results are consistent with our prediction that *fakA* impacts membrane composition and as a result susceptibility to agents targeting the membrane. In addition, TEM and 3D-SIM revealed differences in the cell wall between the WT and the evolved isolates showing increased frequency of invaginations in the plasmid membrane (mesosomes) in evolved isolates with a *fakA* mutation.

Testing real-world formulations: Whilst both biocides tested here showed limited selection for tolerance, in reality these are applied in formulation containing many other components (co-formulants and excipients) that can impact product efficacy. As hypothesized, biocidal products have differing potentials for selection of resistance or tolerance depending on formulation. No changes in genes known to confer antibiotic or biocide susceptibility were observed under FM104 stress.

8.2. Concluding remarks

Whilst combining the approaches above is perhaps a more detailed study than typical for many biocides, the required time and cost still represent a fraction of the cost of a new product development. Given the use of the data generated, this can be considered a good return.

Mutants with increased tolerance to cationic biocides such as CHX and OCT in *S. aureus* and *E. faecalis* could be selected in biofilm and planktonic conditions, and biofilms are not predisposed to developing tolerance. Adaptation was relatively limited with small changes in susceptibility and little evidence of antibiotic cross-resistance to clinically relevant antibiotics.

FakA appears to be a novel mediator of biocide sensitivity potentially acting by causing changes in membrane permeability. These findings could have a broader impact, since FakA homologs are present in different Gram-positive and Gram-negative bacteria, and we found these changes in some totally conserved residues in all homologues. Nonetheless, biocides have multiple targets, and it is likely that more genes that have yet to be described also play a role in reduced susceptibility to these cationic agents.

8.3. Future work

To gain further insights into the role of FakA in biocide tolerance, the next step in this project would be to further optimise the creation of a *fakA* deletion mutant in the tested clinical strains. Analysis of *fakA* in clinical isolates and comparison with biocide susceptibility will also help understand its importance. Additionally, understanding the biocide-membrane interactions would be essential to comprehend the mechanism of action and the risks of resistance, hence biomolecular analysis to better understand biocide binding to FakA could also be performed.

RNA-Sequencing to evaluate gene expression changes in the *fakA* evolved isolates could be performed. From our results, expression of genes involved in the synthesis of several branched-chain amino acids (BCAAs) were upregulated under biocide stress in the WTs. These BCAAs are elongated into branched-chain fatty acids by the FASII pathway, which are then incorporated into the membrane for phospholipid biosynthesis (Parsons and Rock, 2013). Comparison with the *fakA* evolved isolates, that have a decreased membrane fluidity, could provide further insight into these pathways.

Polymicrobial infections are common, and understanding the role of inter-species interactions in a biofilm is key. As a future experiment, mixed species biofilms could be incorporated into the evolution model. Additionally, CHX and OCT could be assessed in combination with other regularly used biocides since in some hospitals rotational practices are already applied. Furthermore, a reverse evolution experiment to test if these mutations are stable could also be conducted. Investigating the role of biocides in virulence, and the link to biofilm formation could also be assessed using the *in vivo* model of *G. mellonella*.

Biocides play a key role in infection prevention control, and in the fight against AMR. However, there are significant knowledge gaps when comparing these antimicrobials to antibiotics. Further exploration in this area is needed, with future research focusing on elucidating the modes of action, mechanisms of tolerance/resistance, and working towards a more harmonised methodology system.

REFERENCES

“A country without research is a country without development" – Margarita Salas

Abraham, N.M., Jefferson, K.K. 2010. A low molecular weight component of serum inhibits biofilm formation in staphylococcus aureus. *Microbial Pathogenesis*, 49, 388–391.

Afgan, E., Baker, D., Batut, B., Van Den Beek, M., Bouvier, D., Ech, M., Chilton, J., Clements, D., Coraor, N., Grüning, B.A., Guerler, A., Hillman-Jackson, J., Hiltemann, S., Jalili, V., Rasche, H., Soranzo, N., Goecks, J., Taylor, J., Nekrutenko, A., Blankenberg, D. 2018. The Galaxy platform for accessible, reproducible and collaborative biomedical analyses: 2018 update. *Nucleic Acids Research*, 46, W537–W544.

Alam, A., Bröms, J.E., Kumar, R., Sjöstedt, A. 2021. The Role of ClpB in Bacterial Stress Responses and Virulence. *Frontiers in Molecular Biosciences*, 8.

Alav, I., Kobylka, J., Kuth, M.S., Pos, K.M., Picard, M., Blair, J.M.A., Bavro, V.N. 2021. Structure, Assembly, and Function of Tripartite Efflux and Type 1 Secretion Systems in Gram-Negative Bacteria. *Chemical Reviews*, 121(9), 5479–5596.

Alder, J.D. 2005. Daptomycin, a new drug class for the treatment of Gram-positive infections. *Drugs of Today*, 41(2), 81–90.

Alfa, M.J. 2019. Biofilms on instruments and environmental surfaces: Do they interfere with instrument reprocessing and surface disinfection? Review of the literature. *American Journal of Infection Control*, 47, A39–A45.

Alhede, M., Kragh, K.N., Qvortrup, K., Allesen-Holm, M., van Gennip, M., Christensen, L.D., Jensen, P.Ø., Nielsen, A.K., Parsek, M., Wozniak, D., Molin, S., Tolker-Nielsen, T., Høiby, N., Givskov, M., Bjarnsholt, T. 2011. Phenotypes of non-attached Pseudomonas aeruginosa aggregates resemble surface attached biofilm. *PLoS One*, 6(11).

Allegranzi, B., Bagheri Nejad, S., Combescure, C., Graafmans, W., Attar, H., Donaldson, L., Pittet, D. 2011. Burden of endemic health-care-associated infection in developing countries: systematic review and meta-analysis. *The Lancet*, 377(9761), 228–241.

Almatroudi, A., Hu, H., Deva, A., Gosbell, I.B., Jacombs, A., Jensen, S.O., Whiteley, G., Glasbey, T., Vickery, K. 2015. A new dry-surface biofilm model: An essential tool for efficacy testing of hospital surface decontamination procedures. *Journal of Microbiological Methods*, 117, 171–176.

Alreshidi, M.M., Dunstan, R.H., Macdonald, M.M., Gottfries, J., Roberts, T.K. 2020. The Uptake and Release of Amino Acids by Staphylococcus aureus at Mid-Exponential and Stationary Phases and Their Corresponding Responses to Changes in Temperature, pH and Osmolality. *Frontiers in Microbiology*, 10.

Altschul, S.F., Gish, W., Miller, W., Myers, E.W., Lipman, D.J. 1990. Basic local alignment search tool. *Journal of Molecular Biology*, 215, 403–410.

Anderson, S.E., Shane, H., Long, C., Lukomska, E., Meade, B.J., Marshall, N.B. 2016. Evaluation of the irritancy and hypersensitivity potential following topical application of didecyldimethylammonium chloride. *Journal of Immunotoxicology*, 13, 557–566.

Andrews S. 2010. FastQC: a quality control tool for high throughput sequence data. http://www.bioinformatics.babraham.ac.uk/projects/fastqc

Andrews, A., Budd, E.L., Hendrick, A., Ashiru-Oredope, D., Beech, E., Hopkins, S., Gerver, S., Muller-Pebody, B. 2021. Surveillance of antibacterial usage during the COVID-19 pandemic in England, 2020. *Antibiotics*, 10(7), 841.

Ansari, S., Hays, J.P., Kemp, A., Okechukwu, R., Murugaiyan, J., Ekwanzala, M.D., Ruiz Alvarez, M.J., Paul-Satyaseela, M., Iwu, C.D., Balleste-Delpierre, C., Septimus, E., Mugisha, L., Fadare, J., Chaudhuri, S., Chibabhai, V., Wadanamby, J.M.R.W.W., Daoud, Z., Xiao, Y., Parkunan, T., Khalaf, Y., M'Ikanatha, N.M., van Dongen, M.B.M., Barkema, H.W., Strathdee, S., Benyeogor, E., Ighodalo, U.L., Prasad, K.P., M, C., Gu, Y., Essack, S., de Silva, D., Vellinga, A., Mommtaz Ghannam, W., Tsoho, N.A., Sakeena, M.H.F., Ilenwabor, R., Shetty, D. (Raj), Ayebare, A., Traore, Z.I., Henry, O., Kiran, A., Ilenwabor, R., Toro, L.F., Smail, A., Amulele, A., Founou, L.L., Sawant, P.S., Buregyeya, E., Castro-Sanchez, E., Moreno-Morales, J., Izadjoo, M., Gori, A., Goff, D., Blocker, A., Forte, G., Tahir, M.F., Diggle, M., Chakraborty, D., Asamoah, A.E., Aberi, H. 2021. The potential impact of the COVID-19 pandemic on global antimicrobial and biocide resistance: an AMR Insights global perspective. *JAC Antimicrobial Resistance*, 3(2).

ANSES. 2019. Opinion of the French Agency for Food, Environmental and Occupational Health & Safety on "Resistance to antimicrobial biocides." ANSES Opinion. Request No 2016-SA-0238.

Aranega-Bou, P., George, R. P., Verlander, N.Q., Paton, S., Bennett, A., Moore, G., Aiken, Z., Akinremi, O., Ali, A., Cawthorne, J., Cleary, P., Crook, D.W., Decraene, V., Dodgson, A., Doumith, M., Ellington, M., Eyre, D.W., George, Ryan P., Grimshaw, J., Guiver, M., Hill, R., Hopkins, K., Jones, R., Lenney, C., Mathers, A.J., McEwan, A., Moore, Ginny, Neilson, M., Neilson, S., Peto, T.E.A., Phan, H.T.T., Regan, M., Seale, A.C., Stoesser, N., Turner-Gardner, J., Watts, V., Walker, J., Sarah Walker, A., Wyllie, D., Welfare, W., Woodford, N. 2019. Carbapenem-resistant Enterobacteriaceae dispersal from sinks is linked to drain position and drainage rates in a laboratory model system. *Journal of Hospital Infection*, 102, 63–69.

Arnold, W.A., Blum, A., Branyan, J., Bruton, T.A., Carignan, C.C., Cortopassi, G., Datta, S., Dewitt, J., Doherty, A.C., Halden, R.U., Harari, H., Hartmann, E.M., Hrubec, T.C., Iyer, S., Kwiatkowski, C.F., Lapier, J., Li, D., Li, L., Muñiz Ortiz, J.G., Salamova, A., Schettler, T., Seguin, R.P., Soehl, A., Sutton, R., Xu, L., Zheng, G. 2023. Quaternary Ammonium Compounds: A Chemical Class of Emerging Concern. *Environmental Science & Technology.* 57(20), 7645–7665

Bae, T., Schneewind, O. 2006. Allelic replacement in Staphylococcus aureus with inducible counter-selection. *Plasmid*, 55, 58–63.

Bailey, A.M., Constantinidou, C., Ivens, A., Garvey, M.I., Webber, M.A., Coldham, N., Hobman, J.L., Wain, J., Woodward, M.J., Piddock, L.J.V. 2009. Exposure of Escherichia coli and Salmonella enterica serovar Typhimurium to triclosan induces a species-specific response, including drug detoxification. *Journal of Antimicrobial Chemotherapy*, 64(5), 973–985.

Bankevich, A., Nurk, S., Antipov, D., Gurevich, A.A., Dvorkin, M., Kulikov, A.S., Lesin, V.M., Nikolenko, S.I., Pham, S., Prjibelski, A.D., Pyshkin, A. V., Sirotkin, A. V., Vyahhi, N., Tesler, G., Alekseyev, M.A., Pevzner, P.A. 2012. SPAdes: A new genome assembly algorithm and its applications to single-cell sequencing. *Journal of Computational Biology*, 19, 455–477.

Barra, A.L.C., Dantas, L. de O.C., Morão, L.G., Gutierrez, R.F., Polikarpov, I., Wrenger, C., Nascimento, A.S. 2020. Essential Metabolic Routes as a Way to ESKAPE From Antibiotic Resistance. *Frontiers in Public Health*, 8(26).

Batra, R., Cooper, B.S., Whiteley, C., Patel, A.K., Wyncoll, D., Edgeworth, J.D. 2010. Efficacy and limitation of a Chlorhexidine-Based decolonization strategy in preventing

transmission of Methicillin-Resistant Staphylococcus aureus in an intensive care unit. *Clinical Infectious Diseases*, 50, 210–217.

Becker, K., Heilmann, C., Peters, G. 2014. Coagulase-negative staphylococci. *Clinical Microbiology Reviews*, 27, 870–926.

Bhardwaj, P., Hans, A., Ruikar, K., Guan, Z., Palmer, K.L. 2017. Reduced Chlorhexidine and Daptomycin Susceptibility in Vancomycin-Resistant Enterococcus faecium after Serial Chlorhexidine Exposure. *Antimicrobial Agents and Chemotherapy*, 62(1), e01235–17.

BICSc, British Institute of Cleaning Science. 2020. Cleaning and Disinfection Quality: Guidance standards for establishing and assessing cleaning and disinfection in UK Hospitals and other healthcare facilities. Available: https://www.bics.org.uk/wp-content/uploads/2020/04/V-3-Healthcare-Environmental-Cleaning-guide-and-standards-final.pdf (accessed 05.01.24).

Blair, J.M.A., Webber, M.A., Baylay, A.J., Ogbolu, D.O., Piddock, L.J.V. 2015. Molecular mechanisms of antibiotic resistance. *Nature Reviews Microbiology*, 13, 42–51.

Block, F.E., Ortega, R.A., Brown, C.W. 2018. Failure Mechanisms of Polymeric Medical Devices. *Journal of Clinical Engineering*, 43, 187–193.

Boaro, A., Ageitos, L., Torres, M.D.T., Blasco, E.B., Oztekin, S., de la Fuente-Nunez, C. 2023. Structure-function-guided design of synthetic peptides with anti-infective activity derived from wasp venom. *Cell Reports Physical Science*, 4(7).

Bock, L.J., Ferguson, P.M., Clarke, M., Pumpitakkul, V., Wand, M.E., Fady, P.E., Allison, L., Fleck, R.A., Shepherd, M.J., Mason, A.J., Sutton, J.M. 2021. Pseudomonas aeruginosa adapts to octenidine via a combination of efflux and membrane remodelling. *Communications Biology*, 4(1):1058.

Bock, L.J., Wand, M.E., Sutton, J.M. 2016. Varying activity of chlorhexidine-based disinfectants against Klebsiella pneumoniae clinical isolates and adapted strains. *Journal of Hospital Infection*, 93, 42–48.

Bonten, M.J., Willems, R., Weinstein, R.A. 2001. Vancomycin-resistant enterococci: why are they here, and where do they come from?. *The Lancet Infectious Diseases*, 1, 314–325.

Bose, J.L., Daly, S.M., Hall, P.R., Bayles, K.W. 2014. Identification of the Staphylococcus aureus vfrAB operon, a novel virulence factor regulatory locus. *Infection and Immunity*, 82, 1813–1822.

Bose, J.L., Fey, P.D., Bayles, K.W. 2013. Genetic tools to enhance the study of gene function and regulation in Staphylococcus aureus. *Applied Environmental Microbiology*, 79, 2218–2224.

Bowman, L., Palmer, T. 2021. The Type VII Secretion System of Staphylococcus. *Annual Review of Microbiology*, 75, 471–494.

Boyce, J.M. 2023. Quaternary ammonium disinfectants and antiseptics: tolerance, resistance and potential impact on antibiotic resistance. *Antimicrobial Resistance and Infection Control*, 12(1), 32.

Boyce, J.M. 2007. Environmental contamination makes an important contribution to hospital infection. *Journal of Hospital Infection*, 65, 50–54.

Bridier, A., de Sanchez-Vizuete, M.P., Le Coq, D., Aymerich, S., Meylheuc, T., Maillard, J.Y., Thomas, V., Dubois-Brissonnet, F., Briandet, R. 2012. Biofilms of a Bacillus subtilis

Hospital Isolate Protect Staphylococcus aureus from Biocide Action. *PLoS One*, 7(9), e44506.

BSI, British Standards Institution. 2012a. BS EN 13727:2012+A2:2015. Clinical disinfectants and antiseptics – Quantitative suspension test for the evaluation of bactericidal activity in the medical area – Test method and requirements (phase 2, step 1).

BSI, British Standards Institution. 2012b. BS EN 16615:2015. Chemical disinfectants and antiseptics. Quantitative test method for the evaluation of bactericidal and yeasticidal activity of non-porous surfaces with mechanical action employing wipes in the medical area (4-field test) – Test method and requirements (phase 2, step 2).

Butler, M.S., Henderson, I.R., Capon, R.J., Blaskovich, M.A.T. 2023. Antibiotics in the clinical pipeline as of December 2022. *Journal of Antibiotics*, 76(8), 431–473.

Buxser, S. 2021. Has resistance to chlorhexidine increased among clinically-relevant bacteria? A systematic review of time course and subpopulation data. *PLoS One*, 16(8), e0256336.

Cândido, E. de S., de Barros, E., Cardoso, M.H., Franco, O.L. 2019. Bacterial cross-resistance to anti-infective compounds. Is it a real problem? *Current Opinion in Pharmacology*, 48, 76–81.

Carling, P.C., Bartley, J.M. 2010. Evaluating hygienic cleaning in health care settings: What you do not know can harm your patients. *American Journal of Infection Control*, 38(5 Suppl 1), S41–S50.

Carson, R.T., Larson, E., Levy, S.B., Marshall, B.M., Aiello, A.E. 2008. Use of antibacterial consumer products containing quaternary ammonium compounds and drug resistance in the community. *Journal of Antimicrobial Chemotherapy*, 62(5), 1160–1162.

Carver, T., Harris, S.R., Berriman, M., Parkhill, J., McQuillan, J.A. 2012. Artemis: An integrated platform for visualization and analysis of high-throughput sequence-based experimental data. *Bioinformatics*, 28, 464–469.

Casey, A., Fox, E.M., Schmitz-Esser, S., Coffey, A., McAuliffe, O., Jordan, K. 2014. Transcriptome analysis of Listeria monocytogenes exposed to biocide stress reveals a multi-system response involving cell wall synthesis, sugar uptake, and motility. *Frontiers in Microbiology*, 5(68).

Cendra, M. del M., Blanco-Cabra, N., Pedraz, L., Torrents, E. 2019. Optimal environmental and culture conditions allow the in vitro coexistence of Pseudomonas aeruginosa and Staphylococcus aureus in stable biofilms. *Scientific Reports*, 9, 1–17.

Centeleghe, I., Norville, P., Hughes, L., Maillard, J.Y. 2022. Dual species dry surface biofilms; Bacillus species impact on Staphylococcus aureus survival and surface disinfection. *Journal of Applied Microbiology*, 133, 1130–1140.

Cerf, O., Carpentier, B., Sanders, P. 2010. Tests for determining in-use concentrations of antibiotics and disinfectants are based on entirely different concepts: “resistance” has different meanings. *International Journal of Food Microbiology*, 166, 247–254.

Chen, S., Zhou, Y., Chen, Y., & Gu, J. 2018. Fastp: An ultra-fast all-in-one FASTQ preprocessor. *Bioinformatics*, 34(17), i884–i890.

Charron, R., Boulanger, M., Briandet, R., Bridier, A. 2023. Biofilms as protective cocoons against biocides: from bacterial adaptation to One Health issues. *Microbiology*, 169(6).

Chiewchalermsri, C., Sompornrattanaphan, M., Wongsa, C., Thongngarm, T. 2020. Chlorhexidine allergy: Current challenges and future prospects. *Journal of Asthma and Allergy*, 13, 127–133.

Condell O, Power K.A., Händler K, Finn S, Sheridan A, Sergeant K, Renaut J, Burgess C.M., Hinton J.C., Nally J.E., Fanning S. 2014. Comparative analysis of Salmonella susceptibility and tolerance to the biocide chlorhexidine identifies a complex cellular defense network. *Frontiers in Microbiology*, 5(373).

Conlon, B.P., Rowe, S.E., Lewis, K. 2015. Persister Cells in Biofilm Associated Infections. *Advances in Experimental Medicine and Biology*, 831, 1–9.

Coombs, K., Rodriguez-Quijada, C., Clevenger, J.O., Sauer-Budge, A.F. 2023. Current Understanding of Potential Linkages between Biocide Tolerance and Antibiotic Cross-Resistance. *Microorganisms*. 11(8), 2000.

Cooper, V.S. 2018. Experimental Evolution as a High-Throughput Screen for Genetic Adaptations. *mSphere*, 3, 1–7.

Costerton, J.W., Cheng, K.J., Geesey, G.G., Ladd, T.I., Nickel, J.C., Dasgupta, M., Marrie, T.J. 1987. Bacterial Biofilms in Nature and Disease. *Annual Review of Microbiology*, 41, 435–464.

Costerton, J.W., Lewandowski, Z., Caldwell, D.E., Korber, D.R., Lappin-Scott, H.M. 1995. Microbial Biofilms. *Annual Review of Microbiology*, 49, 711–745.

Cowley, N.L., Forbes, S., Amézquita, A., McClure, P., Humphreys, G.J., McBain, A.J. 2015. Effects of formulation on microbicide potency and mitigation of the development of bacterial insusceptibility. *Applied and Environmental Microbiology*, 81(20), 7330–7338.

Croes, S., Deurenberg, R.H., Boumans, M.L.L., Beisser, P.S., Neef, C., Stobberingh, E.E. 2009. Staphylococcus aureus biofilm formation at the physiologic glucose concentration depends on the S. aureus lineage. *BMC Microbiology*, 9, 229.

Crooks, G.E., Hon, G., Chandonia, J.M., Brenner, S.E. 2004. WebLogo: A sequence logo generator. *Genome Research*, 14, 1188–1190.

Darby, E.M., Trampari, E., Siasat, P., Gaya, M.S., Alav, I., Webber, M.A., Blair, J.M.A. 2023. Molecular mechanisms of antibiotic resistance revisited. *Nature Reviews Microbiology*, 21(5), 280–295.

Debarati, P., Chakraborty, R., Mandal, S.M. 2019. Biocides and health-care agents are more than just antibiotics: Inducing cross to co-resistance in microbes. *Ecotoxicology and Environmental Safety*, 174, 601–610.

DeMars, Z., Singh, V.K., Bose, J.L. 2020. Exogenous fatty acids remodel Staphylococcus aureus lipid composition through fatty acid kinase. Journal of Bacteriology, 202(14).

Desbois, A.P., Coote, P.J. 2011. Wax moth larva (Galleria mellonella): An in vivo model for assessing the efficacy of antistaphylococcal agents. *Journal of Antimicrobial Chemotherapy*, 66, 1785–1790.

Dewachter, L., Fauvart, M., Michiels, J. 2019. Bacterial Heterogeneity and Antibiotic Survival: Understanding and Combatting Persistence and Heteroresistance. *Molecular Cell*, 76(2), 255–267.

DHSC, Department of Health and Social Care. 2024. Confronting antimicrobial resistance 2024 to 2029. London: HM Government. Available:

https://www.gov.uk/government/publications/uk-5-year-action-plan-for-antimicrobial-resistance-2024-to-2029/confronting-antimicrobial-resistance-2024-to-2029 (accessed 12.05.24)

DHSC, Department of Health and Social Care. 2019a. Contained and controlled: the UK's 20-year vision for antimicrobial resistance. London: HM Government. Available: https://assets.publishing.service.gov.uk/media/5c48896a40f0b616fe901e91/uk-20-year-vision-for-antimicrobial-resistance.pdf (accessed 12.03.24)

DHSC, Department of Health and Social Care. 2019b. Tackling antimicrobial resistance 2019-2024: The UK's five-year national action plan. London: HM Government. Available: https://assets.publishing.service.gov.uk/media/6261392d8fa8f523bf22ab9e/UK_AMR_5_year_national_action_plan.pdf (accessed 12.03.24)

Donlan, R.M., Costerton, J.W. 2002. Biofilms: Survival mechanisms of clinically relevant microorganisms. *Clinical Microbiology Reviews*, 15, 167–193.

Du, D., Wang-Kan, X., Neuberger, A., van Veen, H.W., Pos, K.M., Piddock, L.J.V., Luisi, B.F. 2018. Multidrug efflux pumps: structure, function and regulation. *Nature Reviews Microbiology*, 16(9), 523–539.

ECDC, European Centre for Disease Prevention and Control. 2024. Point prevalence survey of healthcare-associated infections and antimicrobial use in European acute care hospitals 2022-2023. Stockholm: ECDC. Available: https://www.ecdc.europa.eu/sites/default/files/documents/healthcare-associated-point-prevalence-survey-acute-care-hospitals-2022-2023.pdf (accessed 28.05.24)

ECDC, European Centre for Disease Prevention and Control. 2023a. Point prevalence survey of healthcare-associated infections and antimicrobial use in European acute care hospitals, 2016-2017. Stockholm: ECDC. Available: https://www.ecdc.europa.eu/sites/default/files/documents/healthcare-associated--infections-antimicrobial-use-point-prevalence-survey-2016-2017.pdf (accessed 14.02.24)

ECDC, European Centre for Disease Prevention and Control. 2023b. Antimicrobial consumption in the EU/EEA (ESAC-Net) - Annual Epidemiological Report for 2022. Stockholm: ECDC. Available: https://www.ecdc.europa.eu/sites/default/files/documents/AER-antimicrobial-consumption.pdf (accessed 14.02.24)

Edgeworth, J.D., Yadegarfar, G., Pathak, S., Batra, R., Cockfield, J.D., Wyncoll, D., Beale, R., Lindsay, J.A. 2007. An outbreak in an intensive care unit of a strain of methicillin-resistant Staphylococcus aureus sequence type 239 associated with an increased rate of vascular access device-related bacteremia. *Clinical Infectious Diseases*, 44(4). 493–501.

Edwards, N.W.M., Best, E.L., Goswami, P., Wilcox, M.H., Russell, S.J. 2020. Recontamination of healthcare surfaces by repeated wiping with biocide-loaded wipes: "One wipe, one surface, one direction, dispose" as best practice in the clinical environment. *International Journal of Molecular Sciences*, 21, 1–11.

Elena, S.F., Lenski, R.E. 2003. Evolution experiments with microorganisms: The dynamics and genetic bases of adaptation. *Nature Reviews Genetics*, 4(6), 457–469.

EUCAST, European Committee on Antimicrobial Susceptibility Testing. 2024a. Broth microdilution. EUCAST reading guide v.5.0. Available: https://www.eucast.org/ast_of_bacteria/mic_determination (accessed 28.02.24)

EUCAST, European Committee on Antimicrobial Susceptibility Testing. 2024b. Display of MIC and inhibition zone diameter distributions and ECOFFs. Available: https://mic.eucast.org/ (accessed 28.02.24)

Felgate, H., Sethi, D., Faust, K., Kiy, C., Härtel, C., Rupp, J., Clifford, R., Dean, R., Tremlett, C., Wain, J., Langridge, G., Clarke, P., Page, A.J., Webber, M.A. 2023. Characterisation of neonatal Staphylococcus capitis NRCS-A isolates compared with non NRCS-A Staphylococcus capitis from neonates and adults. *Microbial Genomics*, 9(10).

Ferdinand, A.S., Coppo, M.J.C., Howden, B.P., Browning, G.F. 2023. Tackling antimicrobial resistance by integrating One Health and the Sustainable Development Goals. *BMC Global and Public Health*, 1.

Feßler, A.T., Wang, Y., Wu, C., Schwarz, S. 2018. Mobile lincosamide resistance genes in staphylococci. *Plasmid*, 99, 22–31.

Flemming, H.C., Wingender, J., Szewzyk, U., Steinberg, P., Rice, S.A., Kjelleberg, S. 2016. Biofilms: An emergent form of bacterial life. *Nature Reviews Microbiology*, 14, 563–575.

Fox, L.J., Kelly, P.P., Humphreys, G.J., Waigh, T.A., Lu, J.R., McBain, A.J. 2022. Assessing the risk of resistance to cationic biocides incorporating realism-based and biophysical approaches. *Journal of Industrial Microbiology & Biotechnology*, 49(1).

Fraise, A. 1999. Choosing disinfectants. *Journal of Hospital Infection*. 43(4), 255–264.

Frank, M.W., Yao, J., Batte, J.L., Gullett, J.M., Subramanian, C., Rosch, J.W., Rock, C.O. 2020. Host fatty acid utilization by Staphylococcus aureus at the infection site. *mBio*, 11.

Frees, D., Gerth, U., Ingmer, H. 2014. Clp chaperones and proteases are central in stress survival, virulence and antibiotic resistance of Staphylococcus aureus. *International Journal of Medical Microbiology*. 304(2), 142–149.

Frieri, M., Kumar, K., Boutin, A. 2017. Antibiotic resistance. *Journal of Infection and Public Health*. 10(4), 369–378.

Fucini, G.B., Geffers, C., Schwab, F., Behnke, M., Sunder, W., Moellmann, J., Gastmeier, P. 2023. Sinks in patient rooms in ICUs are associated with higher rates of hospital-acquired infection: a retrospective analysis of 552 ICUs. *Journal of Hospital Infection*, 139, 99–105.

Furi, L., Ciusa, M.L., Knight, D., Di Lorenzo, V., Tocci, N., Cirasol, D., Aragones, L., Coelho, J.R., Freitas, A.T., Marchi, E., Moce, L., Visa, P., Northwood, J.B., Viti, C., Borghi, E., Orefici, G., Morrissey, I., Oggioni, M.R. 2013. Evaluation of reduced susceptibility to quaternary ammonium compounds and bisbiguanides in clinical isolates and laboratory-generated mutants of Staphylococcus aureus. *Antimicrobial Agents and Chemotherapy*, 57, 3488–3497.

Galié, S., García-Gutiérrez, C., Miguélez, E.M., Villar, C.J., Lombó, F. 2018. Biofilms in the food industry: Health aspects and control methods. *Frontiers in Microbiology*, 9.

García-Solache, M., Rice, L.B. 2019. The enterococcus: A model of adaptability to its environment. *Clinical Microbiology Reviews*, 32(2).

Garratt, I., Aranega-Bou, P., Sutton, J.M., Moore, G., Wanda, M.E. 2021. Long-Term Exposure to Octenidine in a Simulated Sink Trap Environment Results in Selection of Pseudomonas aeruginosa, Citrobacter, and Enterobacter Isolates with Mutations in Efflux Pump Regulators. *Applied and Environmental Microbiology*, 87, 1–14.

Ge, S.X., Son, E.W., Yao, R. 2018. iDEP: An integrated web application for differential expression and pathway analysis of RNA-Seq data. *BMC Bioinformatics*, 19.

Gibbens, J.C., Pascoe, S.J.S., Evans, S.J., Davies, R.H., Sayers, A.R. 2001. A trial of biosecurity as a means to control Campylobacter infection of broiler chickens. *Preventive Veterinary Medicine*, 48(2), 85–99.

Gómez-Casanova, N., Gutiérrez-Zufiaurre, M.N., Blázquez de Castro, A.M., Muñoz-Bellido, J.L. 2024. Genomic Insights into Staphylococcus aureus Isolates Exhibiting Diminished Daptomycin Susceptibility. *Pathogens*, 13.

Gries, C.M., Bose, J.L., Nuxoll, A.S., Fey, P.D., Bayles, K.W. 2013. The Ktr potassium transport system in Staphylococcus aureus and its role in cell physiology, antimicrobial resistance and pathogenesis. *Molecular Microbiology*, 89, 760–773.

Griffiths, P.A., Babb, J.R., Bradley, C.R., Fraise, A.P. 1997. Glutaraldehyde-resistant Mycobacterium chelonae from endoscope washer disinfectors, *Journal of Applied Microbiology,* 82(4), 519–526.

Grosser, M.R, Richardson, A.R. 2016. Method for Preparation and Electroporation of S. aureus and S. epidermidis. *Methods in Molecular Biology*, 1373, 51–57.

Guérin, A., Bridier, A., Le Grandois, P., Sévellec, Y., Palma, F., Félix, B., Roussel, S., Soumet, C., Karpíšková, R., Pomelio, F., Skjerdal, T., Ricao, M., Bojan, P., Oevermann, A., Wullings, B., Bulawová, H., Castro, H., Lindström, M., Korkeala, H., Šteingolde, Ž., Szymczak, B., Gareis, M., Amar, C. 2021. Exposure to quaternary ammonium compounds selects resistance to ciprofloxacin in listeria monocytogenes. *Pathogens,* 10, 1–11.

Guest, J.F., Keating, T., Gould, D., Wigglesworth, N. 2020. Modelling the annual NHS costs and outcomes attributable to healthcare-associated infections in England. *BMJ Open*, 10.

Gurevich, A., Saveliev, V., Vyahhi, N., Tesler, G. 2013. QUAST: Quality assessment tool for genome assemblies. *Bioinformatics*, 29, 1072–1075.

Hardy, K., Sunnucks, K., Gil, H., Shabir, S., Trampari, E., Hawkey, P., Webber, M. 2018. Increased usage of antiseptics is associated with reduced susceptibility in clinical isolates of Staphylococcus aureus. *mBio*, 9.

Harrison, F., Blower, A., de Wolf, C., Connelly, E. 2023. Sweet and sour synergy: exploring the antibacterial and antibiofilm activity of acetic acid and vinegar combined witmedical-grade honeys. *Microbiology*, 169.

Harrison, F., Roberts, A.E.L., Gabrilska, R., Rumbaugh, K.P., Lee, C., Diggle, S.P. 2015. A 1,000-year-old antimicrobial remedy with antistaphylococcal activity. *mBio*, 6.

Hassan, K.A., Elbourne, L.D.H., Li, L., Gamage, H.K.A.H., Liu, Q., Jackson, S.M., Sharples, D., Kolstø, A.B., Henderson, P.J.F., Paulsen, I.T. 2015. An ace up their sleeve: A transcriptomic approach exposes the AceI efflux protein of Acinetobacter baumannii and reveals the drug efflux potential hidden in many microbial pathogens. *Frontiers in Microbiology*, 6.

Hassan, K.A., Jackson, S.M., Penesyan, A., Patching, S.G., Tetu, S.G., Eijkelkamp, B.A., Brown, M.H., Henderson, P.J.F., Paulsen, I.T. 2013. Transcriptomic and biochemical analyses identify a family of chlorhexidine efflux proteins. *PNAS*, 110, 20254–20259.

Hassan, K.A., Liu, Q., Elbourne, L.D.H., Ahmad, I., Sharples, D., Naidu, V., Chan, C.L., Li, L., Harborne, S.P.D., Pokhrel, A., Postis, V.L.G., Goldman, A., Henderson, P.J.F., Paulsen, I.T. 2018. Pacing across the membrane: the novel PACE family of efflux pumps is widespread in Gram-negative pathogens. *Research in Microbiology*, 169, 450–454.

Heath, R.J., Rubin, J.R., Holland, D.R., Zhang, E., Snow, M.E., Rock, C.O. 1999. Mechanism of Triclosan Inhibition of Bacterial Fatty Acid Synthesis. *The Journal of Biological Chemistry*, 274(16), 11110–11114.

Heberle, H., Meirelles, V. G., da Silva, F. R., Telles, G. P., & Minghim, R. 2015. InteractiVenn: A web-based tool for the analysis of sets through Venn diagrams. *BMC Bioinformatics*, 16(1).

Hegstad, K., Langsrud, S., Lunestad, B.T., Scheie, A.A., Sunde, M., Yazdankhah, S.P. 2010. Does the wide use of quaternary ammonium compounds enhance the selection and spread of antimicrobial resistance and thus threaten our health?. *Microbial Drug Resistance*, 16, 91–104.

Hill, K.E., Malic, S., McKee, R., Rennison, T., Harding, K.G., Williams, D.W., Thomas, D.W. 2010. An in vitro model of chronic wound biofilms to test wound dressings and assess antimicrobial susceptibilities. *Journal of Antimicrobial Chemotherapy*, 65, 1195–1206.

Horner, C., Mawer, D., Wilcox, M. 2012. Reduced susceptibility to chlorhexidine in staphylococci: Is it increasing and does it matter?. *Journal of Antimicrobial Chemotherapy*. 77(11), 2547–2559.

Hover, B.M., Kim, S.H., Katz, M., Charlop-Powers, Z., Owen, J.G., Ternei, M.A., Maniko, J., Estrela, A.B., Molina, H., Park, S., Perlin, D.S., Brady, S.F. 2018. Culture-independent discovery of the malacidins as calcium-dependent antibiotics with activity against multidrug-resistant Gram-positive pathogens. *Nature Microbiology*, 3, 415–422.

Htun, H.L., Hon, P.Y., Holden, M.T.G., Ang, B., Chow, A. 2019. Chlorhexidine and octenidine use, carriage of qac genes, and reduced antiseptic susceptibility in methicillin-resistant Staphylococcus aureus isolates from a healthcare network. *Clinical Microbiology and Infection*, 25, 1154.e1–1154.e7.

Hu, H., Johani, K., Gosbell, I.B., Jacombs, A.S.W., Almatroudi, A., Whiteley, G.S., Deva, A.K., Jensen, S., Vickery, K. 2015. Intensive care unit environmental surfaces are contaminated by multidrug-resistant bacteria in biofilms: Combined results of conventional culture, pyrosequencing, scanning electron microscopy, and confocal laser microscopy. *Journal of Hospital Infection*, 91, 35–44.

Hübner, N.O., Siebert, J., Kramer, A. 2010. Octenidine dihydrochloride, a modern antiseptic for skin, mucous membranes and wounds. *Skin Pharmacology and Physiology*, 23(5), 244–258.

Hunt, M., Mather, A.E., Sánchez-Busó, L., Page, A.J., Parkhill, J., Keane, J.A., Harris, S.R. 2017. ARIBA: Rapid antimicrobial resistance genotyping directly from sequencing reads. *Microbial Genomics*, 3.

Hutchings, M., Truman, A., Wilkinson, B. 2019. Antibiotics: past, present and future. *Current Opinion in Microbiology,* 51, 72–80.

Ioannou, C.J., Hanlon, G.W., Denyer, S.P. 2007. Action of disinfectant quaternary ammonium compounds against Staphylococcus aureus. *Antimicrobial Agents and Chemotherapy,* 51, 296–306.

Jackson, N., Czaplewski, L., Piddock, L.J.V. 2018. Discovery and development of new antibacterial drugs: Learning from experience?. J*ournal of Antimicrobial Chemotherapy.* 73(6), 1452–1459.

Jennings, J., James, D.E., Wares, K.D., Campbell-Train, A., Siani, H. 2024. Chemical resistance testing of plastics – Material compatibility of detergent and disinfectant products. *Journal of Hospital Infection*, https://doi.org/10.1016/j.jhin.2024.04.023.

Jones, I.A., Joshi, L.T. 2021. Biocide use in the antimicrobial era: A review. *Molecules*, 26(8), 2276.

Jumper, J., Evans, R., Pritzel, A., Green, T., Figurnov, M., Ronneberger, O., Tunyasuvunakool, K., Bates, R., Žídek, A., Potapenko, A., Bridgland, A., Meyer, C., Kohl, S.A.A., Ballard, A.J., Cowie, A., Romera-Paredes, B., Nikolov, S., Jain, R., Adler, J., Back, T., Petersen, S., Reiman, D., Clancy, E., Zielinski, M., Steinegger, M., Pacholska, M., Berghammer, T., Bodenstein, S., Silver, D., Vinyals, O., Senior, A.W., Kavukcuoglu, K., Kohli, P., Hassabis, D. 2021. Highly accurate protein structure prediction with AlphaFold. *Nature*, 596, 583–589.

Kaiser, N., Klein, D., Karanja, P., Greten, Z., Newman, J. 2009. Inactivation of chlorhexidine gluconate on skin by incompatible alcohol hand sanitizing gels. *American Journal of Infection Control,* 37, 569–573.

Kampf, G. 2023. Proposal for a definition to describe resistance to biocidal active substances and disinfectants. *Journal of Hospital Infection*. 139, 251–252.

Kampf, G. 2019a. Antibiotic resistance can be enhanced in Gram-positive species by some biocidal agents used for disinfection. *Antibiotics*, 8(1), 13.

Kampf, G. 2019b. Adaptive bacterial response to low level chlorhexidine exposure and its implications for hand hygiene. *Microbial Cell*, 6(7), 307–320.

Kampf, G. 2018. Biocidal agents used for disinfection can enhance antibiotic resistance in gram-negative species. *Antibiotics*, 7(4), 110.

Kawamura-Sato, K., Wachino, J., Kondo, T., Ito, H., Arakawa, Y. 2008. Reduction of disinfectant bactericidal activities in clinically isolated Acinetobacter species in the presence of organic material. *Journal of Antimicrobial Chemotherapy*, 61, 568–576.

Khan, R., Kong, H.G., Jung, Y.H., Choi, J., Baek, K.Y., Hwang, E.C., Lee, S.W. 2016. Triclosan Resistome from Metagenome Reveals Diverse Enoyl Acyl Carrier Protein Reductases and Selective Enrichment of Triclosan Resistance Genes. *Scientific Reports*, 6.

Kholina, E.G., Kovalenko, I.B., Bozdaganyan, M.E., Strakhovskaya, M.G., Orekhov, P.S. 2020. Cationic Antiseptics Facilitate Pore Formation in Model Bacterial Membranes. *Journal of Physical Chemistry*, 124, 8593–8600.

Kim, D., Langmead, B., & Salzberg, S. L. 2015. HISAT: A fast spliced aligner with low memory requirements. *Nature Methods*, 12(4), 357–360.

Kim, D., Song, L., Breitwieser, F.P., Salzberg, S.L. 2016. Centrifuge: Rapid and sensitive classification of metagenomic sequences. *Genome Research*, 26, 1721–1729.

Kleerebezem, M., Quadri, L.E.N., Kuipers, O.P., De Vos, W.M. 1997. Quorum sensing by peptide pheromones and two-component signal- transduction systems in Gram-positive bacteria. *Molecular Microbiology*, 24, 895–904.

Knapp, L., Amézquita, A., McClure, P., Stewart, S., Maillard, J.Y. 2015. Development of a protocol for predicting bacterial resistance to microbicides. *Applied and Environmental Microbiol*ogy, 81, 2652–2659.

Knight, G.M., Glover, R.E., McQuaid, C.F., Olaru, I.D., Gallandat, K., Leclerc, Q.J., Fuller, N.M., Willcocks, S.J., Hasan, R., van Kleef, E., Chandler, C.I.R. 2021. Antimicrobial resistance and COVID-19: Intersections and implications. *eLife*, 10.

Koburger, T., Hübner, N.O., Braun, M., Siebert, J., Kramer, A. 2010. Standardized comparison of antiseptic efficacy of triclosan, PVP-iodine, octenidine dihydrochloride, polyhexanide and chlorhexidine digluconate. *Journal of Antimicrobial Chemotherapy*, 65, 1712–1719.

Köck, R., Denkel, L., Feßler, A.T., Eicker, R., Mellmann, A., Schwarz, S., Geffers, C., Hübner, N.O., Leistner, R. 2023. Clinical Evidence for the Use of Octenidine Dihydrochloride to Prevent Healthcare-Associated Infections and Decrease Staphylococcus aureus Carriage or Transmission-A Review. *Pathogens*, 12(4), 612.

Kõljalg, S., Naaber, P., Mikelsaar, M. 2002. Antibiotic resistance as an indicator of bacterial chlorhexidine susceptibility. *Journal of Hospital Infection*, 51, 106–113.

Kolmogorov, M., Yuan, J., Lin, Y., Pevzner, P.A. 2019. Assembly of long, error-prone reads using repeat graphs. *Nature Biotechnology*, 37, 540–546.

Konrat, K., Schwebke, I., Laue, M., Dittmann, C., Levin, K., Andrich, R., Arvand, M., Schaudinn, C. 2016. The bead assay for biofilms: A quick, easy and robust method for testing disinfectants. *PLoS One*, 11, 1–13.

Kramer, A., Schwebke, I., Kampf, G. 2006. How long do nosocomial pathogens persist on inanimate surfaces? A systematic review. *BMC Infectious Diseases*, 6.

Kreiswirth, B.N., Löfdahl, S., Betley, M.J., O'Reilly, M., Schlievert, P.M., Bergdoll, M.S., Novick, R.P. 1983. The toxic shock syndrome exotoxin structural gene is not detectably transmitted by a prophage. *Nature*, 305, 709–712.

Kuiack, R.C., Tuffs, S.W., Dufresne, K., Flick, R., McCormick, J.K., McGavin, M.J., 2023. The fadXDEBA locus of Staphylococcus aureus is required for metabolism of exogenous palmitic acid and in vivo growth. *Molecular Microbiology*, 120, 425–438.

La Rosa, S.L., Diep, D.B., Nes, I.F., Brede, D.A. 2012. Construction and application of a luxABCDE reporter system for real-time monitoring of Enterococcus faecalis gene expression and growth. *Applied and Environmental Microbiology,* 78, 7003–7011.

Lade, H., Park, J.H., Chung, S.H., Kim, I.H., Kim, J.M., Joo, H.S., Kim, J.S. 2019. Biofilm formation by Staphylococcus aureus clinical isolates is differentially affected by glucose and sodium chloride supplemented culture media. *Journal of Clinical Medicine*, 8(11):1853.

Lam, M.M.C., Seemann, T., Tobias, N.J., Chen, H., Haring, V., Moore, R.J., Ballard, S., Grayson, L.M., Johnson, P.D.R., Howden, B.P., Stinear, T.P. 2013. Comparative analysis of the complete genome of an epidemic hospital sequence type 203 clone of vancomycin-resistant Enterococcus faecium. *BMC Genomics*, 14.

Langsrud, S., Sundheim, G., Holck, A.L. 2004. Cross-resistance to antibiotics of Escherichia coli adapted to benzalkonium chloride or exposed to stress-inducers. *Journal of Applied Microbiology*. 96(1), 201–208.

Laroque, S., Garcia Maset, R., Hapeshi, A., Burgevin, F., Locock, K.E.S., Perrier, S. 2023. Synthetic Star Nanoengineered Antimicrobial Polymers as Antibiofilm Agents: Bacterial Membrane Disruption and Cell Aggregation. *Biomacromolecules*, 24, 3073–3085.

Larsson, D.G.J., Gaze, W.H., Laxminarayan, R., Topp, E. 2023. AMR, One Health and the environment. *Nature Microbiology*, 8(5), 754–755.

Laxminarayan, R. 2022. The overlooked pandemic of antimicrobial resistance. *The Lancet.* 399(10325), 606–607.

Laxminarayan, R., Van Boeckel, T., Frost, I., Kariuki, S., Khan, E.A., Limmathurotsakul, D., Larsson, D.G.J., Levy-Hara, G., Mendelson, M., Outterson, K., Peacock, S.J., Zhu, Y.G. 2020. The Lancet Infectious Diseases Commission on antimicrobial resistance: 6 years later. *The Lancet Infectious Diseases*, 20(4), e51–e60.

Ledwoch, K., Dancer, S.J., Otter, J.A., Kerr, K., Roposte, D., Rushton, L., Weiser, R., Mahenthiralingam, E., Muir, D.D., Maillard, J.Y. 2018. Beware biofilm! Dry biofilms containing bacterial pathogens on multiple healthcare surfaces; a multi-centre study. *Journal of Hospital Infection*, 100, e47–e56.

Lee, J.Y.H., Carter, G.P., Pidot, S.J., Guérillot, R., Seemann, T., Gonçalves da Silva, A., Foster, T.J., Howden, B.P., Stinear, T.P., Monk, I.R. 2019. Functional genomics reveals extensive diversity in Staphylococcus epidermidis restriction modification systems compared to Staphylococcus aureus. *bioRxiv.* https://doi.org/10.1101/644856.

Lenski, R.E., Rose, M.R., Simpson, S.C., Tadler, S.C. 1991. Long-Term Experimental Evolution in Escherichia coli. I. Adaptation and Divergence During 2,000 Generations. *The American Naturalist,* 138, 1315–1314.

Leonard, C., Crabb, N., Glover, D., Cooper, S., Bouvy, J., Wobbe, M., Perkins, M. 2023. Can the UK 'Netflix' Payment Model Boost the Antibacterial Pipeline?. *Applied Health Economy and Health Policy*, 21, 365–372.

Letunic, I., Bork, P. 2006. Interactive Tree Of Life (iTOL): an online tool for phylogenetic tree display and annotation. *Bioinformatics*, 23(1), 127–128.

Lewis, K. 2020. The Science of Antibiotic Discovery. *Cell*, 181, 29–45.

Lewis, K. 2013. Platforms for antibiotic discovery. *Nature Reviews Drug Discovery,* 12, 371–387.

Li, H. 2018. Minimap2: Pairwise alignment for nucleotide sequences. *Bioinformatics*, 34, 3094–3100.

Li, H., Handsaker, B., Wysoker, A., Fennell, T., Ruan, J., Homer, N., Marth, G., Abecasis, G., & Durbin, R. 2009. The Sequence Alignment/Map format and SAMtools. *Bioinformatics*, 25(16), 2078–2079.

Li, L., Short, F.L., Hassan, K.A., Naidu, V., Pokhrel, A., Nagy, S.S., Prity, F.T., Shah, B.S., Afrin, N., Baker, S., Parkhill, J., Cain, A.K., Paulsen, I.T. 2023. Systematic analyses identify modes of action of ten clinically relevant biocides and antibiotic antagonism in Acinetobacter baumannii. *Nature Microbiology* 8, 1995–2005.

Lim, K.-S., Kam, P.C.A. 2008. Chlorhexidine - Pharmacology and Clinical Applications. *Anaesthesia and Intensive Care*, 36, 502–512.

Liao, Y., Smyth, G. K., & Shi, W. 2014. FeatureCounts: An efficient general purpose program for assigning sequence reads to genomic features. *Bioinformatics*, 30(7), 923–930.

Ling, L.L., Schneider, T., Peoples, A.J., Spoering, A.L., Engels, I., Conlon, B.P., Mueller, A., Schäberle, T.F., Hughes, D.E., Epstein, S., Jones, M., Lazarides, L., Steadman, V.A., Cohen, D.R., Felix, C.R., Fetterman, K.A., Millett, W.P., Nitti, A.G., Zullo, A.M., Chen, C., Lewis, K. 2015. A new antibiotic kills pathogens without detectable resistance. *Nature*, 517, 455–459.

Love, M. I., Huber, W., & Anders, S. 2014. Moderated estimation of fold change and dispersion for RNA-seq data with DESeq2. *Genome Biology*, 15(12).

Lister, J.L., Horswill, A.R. 2014. Staphylococcus aureus biofilms: Recent developments in biofilm dispersal. *Frontiers in Cellular and Infection Microbiology*, 4.

Lopez, M.S., Tan, I.S., Yan, D., Kang, J., McCreary, M., Modrusan, Z., Austin, C.D., Xu, M., Brown, E.J. 2017. Host-derived fatty acids activate type VII secretion in Staphylococcus aureus. *PNAS*, 114, 11223–11228.

Loveday, H.P., Wilson, J.A., Pratt, R.J., Golsorkhi, M., Tingle, A., Bak, A., Browne, J., Prieto, J., Wilcox, M. 2014. epic3: National Evidence-Based Guidelines for Preventing Healthcare-Associated Infections in NHS Hospitals in England, *Journal of Hospital Infection*. 86 (Suppl 1), S1–S70.

Lu, J., Breitwieser, F.P., Thielen, P., Salzberg, S.L. 2017. Bracken: Estimating species abundance in metagenomics data. *PeerJ Computer Science*, 3:e104.

Ma, Y., Guo, Z., Xia, B., Zhang, Y., Liu, X., Yu, Y., Tang, N., Tong, X., Wang, M., Ye, X., Feng, J., Chen, Y., Wang, J. 2022. Identification of antimicrobial peptides from the human gut microbiome using deep learning. *Nature Biotechnology*, 40, 921–931.

Maasch, J.R.M.A., Torres, M.D.T., Melo, M.C.R., de la Fuente-Nunez, C. 2023. Molecular de-extinction of ancient antimicrobial peptides enabled by machine learning. *Cell Host Microbe*, 31, 1260–1274.e6.

Macià, M.D., Rojo-Molinero, E., Oliver, A. 2014. Antimicrobial susceptibility testing in biofilm-growing bacteria. *Clinical Microbiology and Infection*, 20(100), 981–990.

Mack, W.N., Mack, J.P., Ackerson, A.O. 1975. Microbial film development in a trickling filter. *Microbial Ecology*, 2, 215–226.

Maillard, J.-Y. 2018. Resistance of Bacteria to Biocides. *Microbiology Spectrum*, 6(2).

Maillard, J.-Y. 2005. Antimicrobial biocides in the healthcare environment: efficacy, usage, policies, and perceived problems. *Therapeutics and Clinical Risk Management, 1*, 307–320.

Maillard, J.-Y., Bloomfield, S., Coelho, J.R., Collier, P., Cookson, B., Fanning, S., Hill, A., Hartemann, P., Mcbain, A.J., Oggioni, M., Sattar, S., Schweizer, H.P., Threlfall, J. 2013. Does Microbicide Use in Consumer Products Promote Antimicrobial Resistance? A Critical Review and Recommendations for a Cohesive Approach to Risk Assessment. *Microbial Drug Resistance*, 19, 344–354.

Maillard, J.Y., Centeleghe, I. 2023. How biofilm changes our understanding of cleaning and disinfection. *Antimicrobial Resistance and Infection Control*, 12, 95.

Maillard, J.Y., Pascoe, M. 2024. Disinfectants and antiseptics: mechanisms of action and resistance. *Nature Reviews Microbiology*, 22(1), 4–17

Malanovic, N., Buttress, J.A., Vejzovic, D., Ön, A., Piller, P., Kolb, D., Lohner, K., Strahl, H. 2022. Disruption of the Cytoplasmic Membrane Structure and Barrier Function Underlies the Potent Antiseptic Activity of Octenidine in Gram-Positive Bacteria. *Applied and Environmental Microbiology*, 88.

Matthews, T.C., Bristow, F.R., Griffiths, E.J., Petkau, A., Adam, J., Dooley, D., Kruczkiewicz, P., Curatcha, J., Cabral, J., Fornika, D., Winsor, G.L., Courtot, M., Bertelli, C., Roudgar, A., Feijao, P., Mabon, P., Enns, E., Thiessen, J., Keddy, A., Isaac-Renton, J., Gardy, J.L., Tang, P., IRIDA Consortium, T., Carriço, J.A., Chindelevitch, L., Chauve, C., Graham, M.R., McArthur, A.G., Taboada, E.N., Beiko, R.G., Brinkman, F.S., Hsiao, W.W., Van Domselaar, G., The IRIDA Consortium. 2018. The Integrated Rapid Infectious Disease Analysis (IRIDA) Platform. *BioRxiv*. https://doi.org/10.1101/381830.

Mazzola, P.G., Christina, T., Penna, V., Da, A.M., Martins, S. 2003. Determination of decimal reduction time (D value) of chemical agents used in hospitals for disinfection purposes. *BMC Infectious Diseases*, 3.

Mc Carlie, S., Boucher, C.E., Bragg, R.R. 2020. Molecular basis of bacterial disinfectant resistance. *Drug Resistance Updates*, 48.

McArthur, A.G., Waglechner, N., Nizam, F., Yan, A., Azad, M.A., Baylay, A.J., Bhullar, K., Canova, M.J., De Pascale, G., Ejim, L., Kalan, L., King, A.M., Koteva, K., Morar, M., Mulvey, M.R., O'Brien, J.S., Pawlowski, A.C., Piddock, L.J.V., Spanogiannopoulos, P., Sutherland, A.D., Tang, I., Taylor, P.L., Thaker, M., Wang, W., Yan, M., Yu, T., Wright, G.D. 2013. The comprehensive antibiotic resistance database. *Antimicrobial Agents Chemotherapy,* 57, 3348–3357.

McBain, A.J., Rickard, A.H., Gilbert, P. 2002. Possible implications of biocide accumulation in the environment on the prevalence of bacterial antibiotic resistance. *Journal of Industrial Microbiology and Biotechnology*. 29(6), 326–330.

McDonnell, G., Russell, A.D. 1999. Antiseptics and disinfectants: Activity, action, and resistance. *Clinical Microbiology Reviews*, 12, 147–179.

McMurry, L.M., Oethinger, M., Levy, S. 1998. Triclosan targets lipid synthesis. *Nature*, 394(6693), 531–532.

Medaney, F., Dimitriu, T., Ellis, R.J., Raymond, B. 2016. Live to cheat another day: Bacterial dormancy facilitates the social exploitation of β-lactamases. *ISME Journal*, 10, 778–787.

Medaka: Sequence correction provided by ONT Research. https://github.com/nanoporetech/medaka

Mehla, J., Malloci, G., Mansbach, R., López, C.A., Tsivkovski, R., Haynes, K., Leus, I. V., Grindstaff, S.B., Cascella, R.H., D'Cunha, N., Herndon, L., Hengartner, N.W., Margiotta, E., Atzori, A., Vargiu, A. V., Manrique, P.D., Walker, J.K., Lomovskaya, O., Ruggerone, P., Gnanakaran, S., Rybenkov, V. V., Zgurskaya, H.I. 2021. Predictive Rules of Efflux Inhibition and Avoidance in Pseudomonas aeruginosa. *mBio,* 12, 1–19.

Messler, S., Klare, I., Wappler, F., Werner, G., Ligges, U., Sakka, S.G., Mattner, F. 2019. Reduction of nosocomial bloodstream infections and nosocomial vancomycin-resistant Enterococcus faecium on an intensive care unit after introduction of antiseptic octenidine-based bathing. *Journal of Hospital Infection*, 101, 264–271.

Moellering, R.C. 1992. Emergence of Enterococcus as a Significant Pathogen. *Clinical Infectious Diseases*, 14(6), 1173–1176.

Monahan, L.G., Turnbull, L., Osvath, S.R., Birch, D., Charles, I.G., Whitchurch, C.B. 2014. Rapid conversion of Pseudomonas aeruginosa to a spherical cell morphotype facilitates tolerance to carbapenems and penicillins but increases susceptibility to antimicrobial peptides. *Antimicrobial Agents Chemotherapy*, 58, 1956–1962.

Monk, I.R., Shah, I.M., Xu, M., Tan, M.W., Foster, T.J. 2012. Transforming the untransformable: Application of direct transformation to manipulate genetically Staphylococcus aureus and Staphylococcus epidermidis. *mBio*, 3.

Morais, D.S., Guedes, R.M., Lopes, M.A. 2016. Antimicrobial approaches for textiles: From research to market. *Materials*, 9(6), 498.

Morrissey, I., Oggioni, M.R., Knight, D., Curiao, T., Coque, T., Kalkanci, A., Martinez, J.L., Baldassarri, L., Orefici, G., Yetiş, Ü., Rödger, H.J., Visa, P., Mora, D., Leib, S., Viti, C. 2014. Evaluation of epidemiological cut-off values indicates that biocide resistant subpopulations are uncommon in natural isolates of clinically-relevant microorganisms. *PLoS One*, 9(1).

Morvan, C., Halpern, D., Kénanian, G., Pathania, A., Anba-Mondoloni, J., Lamberet, G., Gruss, A., Gloux, K., 2017. The Staphylococcus aureus FASII bypass escape route from FASII inhibitors. *Biochimie*. 141, 40–46.

Murray, B.E. 1990. The Life and Times of the Enterococcus. *Clinical Microbiology Reviews*, 3(1), 46–65.

Murray, C.J., Ikuta, K.S., Sharara, F., Swetschinski, L., Robles Aguilar, G., Gray, A., Han, C., Bisignano, C., Rao, P., Wool, E., Johnson, S.C., Browne, A.J., Chipeta, M.G., Fell, F., Hackett, S., Haines-Woodhouse, G., Kashef Hamadani, B.H., Kumaran, E.A.P., McManigal, B., Agarwal, R., Akech, S., Albertson, S., Amuasi, J., Andrews, J., Aravkin, A., Ashley, E., Bailey, F., Baker, S., Basnyat, B., Bekker, A., Bender, R., Bethou, A., Bielicki, J., Boonkasidecha, S., Bukosia, J., Carvalheiro, C., Castañeda-Orjuela, C., Chansamouth, V., Chaurasia, S., Chiurchiù, S., Chowdhury, F., Cook, A.J., Cooper, B., Cressey, T.R., Criollo-Mora, E., Cunningham, M., Darboe, S., Day, N.P.J., De Luca, M., Dokova, K., Dramowski, A., Dunachie, S.J., Eckmanns, T., Eibach, D., Emami, A., Feasey, N., Fisher-Pearson, N., Forrest, K., Garrett, D., Gastmeier, P., Giref, A.Z., Greer, R.C., Gupta, V., Haller, S., Haselbeck, A., Hay, S.I., Holm, M., Hopkins, S., Iregbu, K.C., Jacobs, J., Jarovsky, D., Javanmardi, F., Khorana, M., Kissoon, N., Kobeissi, E., Kostyanev, T., Krapp, F., Krumkamp, R., Kumar, A., Kyu, H.H., Lim, C., Limmathurotsakul, D., Loftus, M.J., Lunn, M., Ma, J., Mturi, N., Munera-Huertas, T., Musicha, P., Mussi-Pinhata, M.M., Nakamura, T., Nanavati, R., Nangia, S., Newton, P., Ngoun, C., Novotney, A., Nwakanma, D., Obiero, C.W., Olivas-Martinez, A., Olliaro, P., Ooko, E., Ortiz-Brizuela, E., Peleg, A.Y., Perrone, C., Plakkal, N., Ponce-de-Leon, A., Raad, M., Ramdin, T., Riddell, A., Roberts, T., Robotham, J.V., Roca, A., Rudd, K.E., Russell, N., Schnall, J., Scott, J.A.G., Shivamallappa, M., Sifuentes-Osornio, J., Steenkeste, N., Stewardson, A.J., Stoeva, T., Tasak, N., Thaiprakong, A., Thwaites, G., Turner, C., Turner, P., van Doorn, H.R., Velaphi, S., Vongpradith, A., Vu, H., Walsh, T., Waner, S., Wangrangsimakul, T., Wozniak, T., Zheng, P., Sartorius, B., Lopez, A.D., Stergachis, A., Moore, C., Dolecek, C., Naghavi, M. 2022. Global burden of bacterial antimicrobial resistance in 2019: a systematic analysis. *The Lancet,* 399, 629–655.

Myall, A., Price, J.R., Peach, R.L., Abbas, M., Mookerjee, S., Zhu, N., Ahmad, I., Ming, D., Ramzan, F., Teixeira, D., Graf, C., Weiße, A.Y., Harbarth, S., Holmes, A., Barahona, M.

2022. Prediction of hospital-onset COVID-19 infections using dynamic networks of patient contact: an international retrospective cohort study. *The Lancet Digit Health*, 4, e573–e583.

Nadimpalli, M.L., Chan, C.W., Doron, S. 2021. Antibiotic resistance: a call to action to prevent the next epidemic of inequality. *Nature Medicine*, 27(2), 187–188.

NAO, National Audit Office. 2000. The Management and Control of Hospital Acquired Infection in Acute NHS Trusts in England. HC 230, 1990-00. London: The Stationary Office. Available: https://www.nao.org.uk/wp-content/uploads/2000/02/9900230.pdf (accessed 28.01.24)

NBIC, National Biofilms Innovation Centre. 2023. The Need for Funding in Biofilm Standardisation Background: NBIC Position Paper. University of Southampton. 7 pp. Available: https://doi.org/10.5258/biofilms/013 (accessed 04.06.24)

Neuhaus, S., Feßler, A.T., Dieckmann, R., Thieme, L., Pletz, M.W., Schwarz, S., Al Dahouk, S. 2022. Towards a Harmonized Terminology: A Glossary for Biocide Susceptibility Testing. *Pathogens*, 11(12), 1455.

Neyfakh, A.A., Borsch, C.M., Kaatz2, G.W. 1993. Fluoroquinolone Resistance Protein NorA of Staphylococcus aureus Is a Multidrug Efflux Transporter. *Antimicrobial Agents Chemotherapy*. 37(1), 128–129.

NICE, National Institute for Health and Care Excellence. 2021. Models for the evaluation and purchase of antimicrobials.

NICE, National Institute for Health and Care Excellence. 2017. Healthcare-associated infections: prevention and control in primary and community care. NICE Clinical Guideline No. CG139. Available: https://www.nice.org.uk/guidance/cg139 (accessed 06.02.24)

NICE, National Institute for Health and Care Excellence. 2014. Infection prevention and control. NICE Quality Standard No. 61. Available: https://www.nice.org.uk/guidance/qs61 (accessed 06.02.24)

Nicolae Dopcea, G., Dopcea, I., Nanu, A.E., Diguţă, C.F., Matei, F. 2020. Resistance and cross-resistance in Staphylococcus spp. strains following prolonged exposure to different antiseptics. *Journal of Global Antimicrobial Resistance*, 21, 399–404.

NIH, National Institutes of Health. 2002. Research on Microbial Biofilms. Report No. PA-03-047. Available: https://grants.nih.gov/grants/guide/pa-files/PA-03-047.html (accessed 04.05.24)

Nordholt, N., Kanaris, O., Schmidt, S.B.I., Schreiber, F. 2021. Persistence against benzalkonium chloride promotes rapid evolution of tolerance during periodic disinfection. *Nature Communications,* 12(1), 6792.

OECD, Organisation for Economic Co-operation and Development. 2022. Antimicrobial Resistance in the EU/EEA A One Health Response. Available: https://www.oecd.org/health/Antimicrobial-Resistance-in-the-EU-EEA-A-One-Health-Response-March-2022.pdf (accessed 04.05.24)

O'Neill, J. 2016. Tackling Drug-Resistant Infections Globally: final report and recommendations. The Review on Antimicrobial Resistance. London: HM Government and Wellcome Trust. Available: https://amr-

review.org/sites/default/files/160518_Final%20paper_with%20cover.pdf (accessed 04.05.24)

Page, A.J., Langridge, G.C. 2019. Socru: Typing of genome level order and orientation in bacteria. *bioRxiv*. https://doi.org/10.1101/543702.

Pahil, K.S., Gilman, M.S.A., Baidin, V., Clairfeuille, T., Mattei, P., Bieniossek, C., Dey, F., Muri, D., Baettig, R., Lobritz, M., Bradley, K., Kruse, A.C., Kahne, D. 2024. A new antibiotic traps lipopolysaccharide in its intermembrane transporter. *Nature*, 625, 572–577.

Pal, C., Bengtsson-Palme, J., Rensing, C., Kristiansson, E., Larsson, D.G.J. 2014. BacMet: Antibacterial biocide and metal resistance genes database. *Nucleic Acids Research*, 42(Database issue), D737–D743.

Parks, D.H., Imelfort, M., Skennerton, C.T., Hugenholtz, P., Tyson, G.W. 2015. CheckM: Assessing the quality of microbial genomes recovered from isolates, single cells, and metagenomes. *Genome Research*, 25(7), 1043–1055.

Parsons, J.B., Broussard, T.C., Bose, J.L., Rosch, J.W., Jackson, P., Subramanian, C., Rock, C.O. 2014a. Identification of a two-component fatty acid kinase responsible for host fatty acid incorporation by Staphylococcus aureus. *PNAS*, 111, 10532–10537.

Parsons, J.B., Frank, M.W., Jackson, P., Subramanian, C., Rock, C.O. 2014b. Incorporation of extracellular fatty acids by a fatty acid kinase-dependent pathway in Staphylococcus aureus. *Molecular Microbiology*, 92, 234–245.

Parsons, J.B., Rock, C.O. 2013. Bacterial lipids: Metabolism and membrane homeostasis. *Progress in Lipid Res*earch, 52(3), 249–276.

Payne, D.J., Gwynn, M.N., Holmes, D.J., Pompliano, D.L. 2007. Drugs for bad bugs: Confronting the challenges of antibacterial discovery. *Nature Reviews Drug Discovery,* 6, 29–40.

Peleg, A.Y., Monga, D., Pillai, S., Mylonakis, E., Moellering, R.C., Eliopoulos, G.M. 2009. Reduced susceptibility to vancomycin influences pathogenicity in Staphylococcus aureus infection. *Journal of Infectious Diseases*, 199, 532–536.

Percival, S.L., Suleman, L., Vuotto, C., Donelli, G. 2015. Healthcare-Associated infections, medical devices and biofilms: Risk, tolerance and control. *Journal of Medical Microbiology,* 64(Pt 4), 323–334.

Percival, S.L., Williams, D., Randle, J., Cooper, T. 2014. Biofilms in Infection Prevention and Control: A Healthcare Handbook. *Elsevier*. ISBN: 9780123977519.

Pereira, B.M.P., Tagkopoulos, I. 2019. Benzalkonium chlorides: Uses, regulatory status, and microbial resistance. *Applied and Environmental Microbiol*ogy, 85(13), e00377–19.

Pereira, B.M.P., Wang, X., Tagkopoulos, I. 2021. Biocide-Induced Emergence of Antibiotic Resistance in Escherichia coli. *Frontiers in Microbiology*, 12.

Pereira, B.M.P., Wang, X., Tagkopoulos, I. 2020. Short-and Long-Term Transcriptomic Responses of Escherichia coli to Biocides: a Systems Analysis. *Applied and Environmental Microbiology*, 86(14), e00708–20.

Pereira, T.C., Barros, P.P. de, de Oliveira Fugisaki, L.R., Rossoni, R.D., Ribeiro, F. de C., Menezes, R.T. de, Junqueira, J.C., Scorzoni, L. 2018. Recent advances in the use of Galleria mellonella model to study immune responses against human pathogens. *Journal of Fungi*, 4(4), 128.

PHE, Public Health England. 2020. English Surveillance Programme for Antimicrobial Utilisation and Resistance (ESPAUR). Report 2019 to 2020. London. Available: https://webarchive.nationalarchives.gov.uk/ukgwa/20211022024510/https://www.gov.uk/government/publications/english-surveillance-programme-antimicrobial-utilisation-and-resistance-espaur-report (accessed 04.04.24)

PHE, Public Health England. 2012. Healthcare-Associated Infection Operational Guidance and Standards for Health Protection Units. London. Available: https://www.gov.uk/government/publications/healthcare-associated-infection-hcai-operational-guidance-and-standards (accessed 04.04.24)

Plantinga, N.L., Wittekamp, B.H.J., Leleu, K., Depuydt, P., Van den Abeele, A.M., Brun-Buisson, C., Bonten, M.J.M. 2016. Oral mucosal adverse events with chlorhexidine 2 % mouthwash in ICU. *Intensive Care Medicine*, 42(4), 620–621.

Poltak, S.R., Cooper, V.S. 2011. Ecological succession in long-term experimentally evolved biofilms produces synergistic communities. *ISME Journal*, 5, 369–378.

Poole, K. 2002. Mechanisms of bacterial biocide and antibiotic resistance. *Journal of Applied Microbiology Symposium,* 92 Suppl, 55S–64S.

Porter, L., Sultan, O., Mitchell, B.G., Jenney, A., Kiernan, M., Brewster, D.J., Russo, P.L. 2024. How Long do Nosocomial Pathogens Persist on Inanimate Surfaces? A Scoping Review. *Journal of Hospital Infection.* 147, 25–31.

Powell, D. 2013. Degust: RNA-seq exploration, analysis and visualisation. https://doi.org/10.5281/zenodo.3258932

Prax, M., Lee, C.Y., Bertram, R. 2013. An update on the molecular genetics toolbox for staphylococci. *Microbiology,* 159(3), 421–435.

Price, M.N., Dehal, P.S., Arkin, A.P. 2009. Fasttree: Computing large minimum evolution trees with profiles instead of a distance matrix. *Molecular Biology and Evol*ution, 26, 1641–1650.

Quigley, J., Peoples, A., Sarybaeva, A., Hughes, D., Ghiglieri, M., Achorn, C., Desrosiers, A., Felix, C., Liang, L., Malveira, S., Millett, W., Nitti, A., Tran, B., Zullo, A., Anklin, C., Spoering, A., Ling, L.L., Lewis, K. 2020. Novel antimicrobials from uncultured bacteria acting against mycobacterium tuberculosis. *mBio,* 11, 1–13.

R Core Team, 2021. R: A language and environment for statistical computing. R Foundation for Statistical Computing. Viena, Austria. https://www.R-project.org

Raj, S., Omar, B., Hamidah, T., Suhana, A., Asiha, N. 2007. Mesosomes are a definite event in antibiotic-treated Staphylococcus aureus ATCC 25923. *Tropical Biomedicine*, 24(1), 105–109.

Raoofi, S., Kan, F.P., Rafiei, S., Hosseinipalangi, Z., Mejareh, Z.N., Khani, S., Abdollahi, B., Talab, F.S., Sanaei, M., Zarabi, F., Dolati, Y., Ahmadi, N., Raoofi, N., Sarhadi, Y., Masoumi, M., Hosseini, B. sadat, Vali, N., Gholamali, N., Asadi, S., Ahmadi, S., Ahmadi, B., Chomalu, Z.B., Asadollahi, E., Rajabi, M., Gharagozloo, D., Nejatifar, Z., Soheylirad, R., Jalali, S., Aghajani, F., Navidriahy, M., Deylami, S., Nasiri, M., Zareei, M., Golmohammadi, Z., Shabani, H., Torabi, F., Shabaninejad, H., Nemati, A., Amerzadeh, M., Aryankhesal, A., Ghashghaee, A. 2023. Global prevalence of nosocomial infection: A systematic review and meta-analysis. *PLoS One*, 18.

Ridder, M.J., Daly, S.M., Triplett, K.D., Seawell, N.A., Hall, P.R., Bose, J.L. 2020. Staphylococcus aureus fatty acid kinase FakA modulates pathogenesis during skin infection via proteases. *Infection and Immunity,* 88.

Robinson, T.P., Bu, D.P., Carrique-Mas, J., Fèvre, E.M., Gilbert, M., Grace, D., Hay, S.I., Jiwakanon, J., Kakkar, M., Kariuki, S., Laxminarayan, R., Lubroth, J., Magnusson, U., Ngoc, P.T., Van Boeckel, T.P., Woolhouse, M.E.J. 2016. Antibiotic resistance is the quintessential One Health issue. *Transactions of the Royal Society of Tropical Medicine and Hygiene,* 110(7), 377–380.

Rodríguez-Baño, J., Rossolini, G.M., Schultsz, C., Tacconelli, E., Murthy, S., Ohmagari, N., Holmes, A., Bachmann, T., Goossens, H., Canton, R., Roberts, A.P., Henriques-Normark, B., Clancy, C.J., Huttner, B., Fagerstedt, P., Lahiri, S., Kaushic, C., Hoffman, S.J., Warren, M., Zoubiane, G., Essack, S., Laxminarayan, R., Plant, L. 2021. Key considerations on the potential impacts of the COVID-19 pandemic on antimicrobial resistance research and surveillance. *Transactions of the Royal Society of Tropical Medicine and Hygiene,* 115(10), 1122–1129.

Rosenman, K.D., Reilly, M.J., Wang, L. 2021. Calls to a State Poison Center Concerning Cleaners and Disinfectants From the Onset of the COVID-19 Pandemic Through April 2020. *Public Health Reports*, 136(1), 27–31.

Roy, R., Tiwari, M., Donelli, G., Tiwari, V. 2018. Strategies for combating bacterial biofilms: A focus on anti-biofilm agents and their mechanisms of action. *Virulence*, 9(1), 522–554.

RStudio Team. 2021. RStudio: Integrated Development Environment for R. Boston, US. RStudio PBC. http://www.rstudio.com/

Russell A.D. 2001. Mechanisms of bacterial insusceptibility to biocides. *American Journal of Infection Control,* 29(4), 259–261.

Russell, A.D. 1999. Bacterial resistance to disinfectants: Present knowledge and future problems. *Journal of Hospital Infection*, 43, 57–68.

Rutala, W.A., Weber, D.J. 2016. Disinfection, sterilization, and antisepsis: An overview. *American Journal of Infection Control*, 44, e1–e6.

Rutala, W.A., Weber, D.J. 2004. The benefits of surface disinfection. *American Journal of Infection Control*, 32, 226–231.

Rutter, J.D., Angiulo, K., Macinga, D.R. 2014. Measuring residual activity of topical antimicrobials: Is the residual activity of chlorhexidine an artefact of laboratory methods?. *Journal of Hospital Infection*, 88, 113–115.

Rzycki, M., Drabik, D., Szostak-Paluch, K., Hanus-Lorenz, B., Kraszewski, S. 2021. Unraveling the mechanism of octenidine and chlorhexidine on membranes: Does electrostatics matter?. *Biophysical Journal*, 120, 3392–3408.

Sabirova, J.S., Hernalsteens, J.P., De Backer, S., Xavier, B.B., Moons, P., Turlej-Rogacka, A., De Greve, H., Goossens, H., Malhotra-Kumar, S. 2015. Fatty acid kinase A is an important determinant of biofilm formation in Staphylococcus aureus USA300. *BMC Genomics*, 16.

SCENIHR, Scientific Committee on Emerging and Newly Identified Health Risks. 2010. Research strategy to address the knowledge gaps on the antimicrobial resistance effects of biocides. Available at: chrome-extension://efaidnbmnnnibpcajpcglclefindmkaj/https://ec.europa.eu/health/scientific_committees/emerging/docs/scenihr_o_028.pdf (accessed 28.01.24).

Schenk, S., Laddaga, R.A. 1992. Improved method for electroporation of Staphylococcus aureus. *FEMS Microbiology Lett*ers, 94, 133–138.

Schneider, T.D., Stephens, R.M. 1990. Sequence logos: a new way to display consensus sequences. Nucleic Acids Research, 18(20), 6097–6100.

Schug, A.R., Scholtzek, A.D., Turnidge, J., Meurer, M., Schwarz, S., Feßler, A.T. 2022. Development of Quality Control Ranges for Biocide Susceptibility Testing. *Pathogens*, 11.

Schwaiger, K., Harms, K.S., Bischoff, M., Preikschat, P., Mölle, G., Bauer-Unkauf, I., Lindorfer, S., Thalhammer, S., Bauer, J., Hölzel, C.S. 2014. Insusceptibility to disinfectants in bacteria from animals, food and humans-is there a link to antimicrobial resistance?. *Frontiers in Microbiol*ogy, 5.

Schweizer, H.P. 2001. Triclosan: a widely used biocide and its link to antibiotics. *FEMS Microbiology Lett*ers, 202, 1–7.

Schwengers, O., Jelonek, L., Dieckmann, M. A., Beyvers, S., Blom, J., & Goesmann, A. 2021. Bakta: Rapid and standardized annotation of bacterial genomes via alignment-free sequence identification. *Microbial Genomics*, 7(11).

Seemann, T. 2016. MLST: Scan contig files against PubMLST typing schemes. https://github.com/tseemann/mlst

Seemann, T. 2015. Snippy: fast bacterial variant calling from NGS reads. https://github.com/tseemann/snippy

Seemann, T. 2014. Prokka: rapid prokaryotic genome annotation. *Bioinformatics*, 30, 2068–2069.

Seiser, S., Janker, L., Zila, N., Mildner, M., Rakita, A., Matiasek, J., Bileck, A., Gerner, C., Paulitschke, V., Elbe-Bürger, A. 2021. Octenidine-based hydrogel shows anti-inflammatory and protease-inhibitory capacities in wounded human skin. *Scientific Reports,* 11.

Sethi, D.K., Felgate, H., Diaz, M., Faust, K., Kiy, C., Clarke, P., Härtel, C., Rupp, J., Webber, M.A. 2021. Chlorhexidine gluconate usage is associated with antiseptic tolerance in staphylococci from the neonatal intensive care unit. *JAC Antimicrobial Resistance,* 3.

Sheehan, G., Dixon, A., Kavanagh, K. 2019. Utilization of Galleria mellonella larvae to characterize the development of Staphylococcus aureus infection. *Microbiology*, 165, 863–875.

Shepherd, M.J., Moore, G., Wand, M.E., Sutton, J.M., Bock, L.J. 2018. Pseudomonas aeruginosa adapts to octenidine in the laboratory and a simulated clinical setting, leading to increased tolerance to chlorhexidine and other biocides. *Journal of Hospital Infection*, 100, e23–e29.

Shukla, R., Peoples, A.J., Ludwig, K.C., Maity, S., Derks, M.G.N., De Benedetti, S., Krueger, A.M., Vermeulen, B.J.A., Harbig, T., Lavore, F., Kumar, R., Honorato, R. V., Grein, F., Nieselt, K., Liu, Y., Bonvin, A.M.J.J., Baldus, M., Kubitscheck, U., Breukink, E., Achorn, C., Nitti, A., Schwalen, C.J., Spoering, A.L., Ling, L.L., Hughes, D., Lelli, M., Roos, W.H., Lewis, K., Schneider, T., Weingarth, M. 2023. An antibiotic from an uncultured bacterium binds to an immutable target. *Cell*, 186, 4059–4073.e27.

Siani, H., Maillard, J.Y. 2015. Best practice in healthcare environment decontamination. *European Journal of Clinical Microbiology and Infectious Diseases*. 34(1), 1–11.

Sievers, F., Wilm, A., Dineen, D., Gibson, T.J., Karplus, K., Li, W., Lopez, R., McWilliam, H., Remmert, M., Söding, J., Thompson, J.D., Higgins, D.G. 2011. Fast, scalable generation of high-quality protein multiple sequence alignments using Clustal Omega. *Molecular Systems Biology,* 7.

Silva, M.T., Sousa, J.C.F., Polónia, J.J., Macedo, M.A.E., Parente, A.M. 1976. Bacterial mesosomes: Real structures of artifacts? *Biochimica et Biophysica Acta (BBA) – Biomembranes*, 443, 92–105.

Singh, V.K., Syring, M., Singh, A., Singhal, K., Dalecki, A., Johansson, T. 2012. An insight into the significance of the DnaK heat shock system in Staphylococcus aureus. *International Journal of Medical Microbiology*, 302, 242–252.

Smith, D.R.M., Shirreff, G., Temime, L., Opatowski, L. 2023. Collateral impacts of pandemic COVID-19 drive the nosocomial spread of antibiotic resistance: A modelling study. *PLoS Medicine*, 20.

Smith, K., Hunter, I.S. 2008. Efficacy of common hospital biocides with biofilms of multi-drug resistant clinical isolates. *Journal of Medical Microbiology,* 57, 966–973.

Sobhanipoor, M.H., Ahmadrajabi, R., Nave, H.H., Saffari, F. 2021. Reduced Susceptibility to Biocides among Enterococci from Clinical and Non-Clinical Sources. *Infection & Chemotherapy,* 53, 696–704.

Sommers, K.J., Michaud, M.E., Hogue, C.E., Scharnow, A.M., Amoo, L.E., Petersen, A.A., Carden, R.G., Minbiole, K.P.C., Wuest, W.M. 2022. Quaternary Phosphonium Compounds: An Examination of Non-Nitrogenous Cationic Amphiphiles That Evade Disinfectant Resistance. *ACS Infectious Diseases,* 8, 387–397.

Sønderholm, M., Kragh, K.N., Koren, K., Jakobsen, T.H., Darch, S.E., Alhede, M., Jensen, P.Ø., Whiteley, M., Kühl, M., Bjarnsholt, T. 2017. Pseudomonas aeruginosa Aggregate Formation in an Alginate Bead Model System Exhibits In Vivo-Like Characteristics. *Applied and Environmental Microbiol*ogy, 83, e00113-17.

Song, Y., Rubio, A., Jayaswal, R.K., Silverman, J.A., Wilkinson, B.J. 2013. Additional Routes to Staphylococcus aureus Daptomycin Resistance as Revealed by Comparative Genome Sequencing, Transcriptional Profiling, and Phenotypic Studies. *PLoS One*, 8.

Spagnolo, F., Trujillo, M., Dennehy, J.J. 2021. Why Do Antibiotics Exist?. *mBio*, 12(6).

Spaulding, E. 1968. Chemical disinfection of medical and surgical materials. C. Lawrence (Ed.), Block *Disinfection, Sterilization and Preservation*. Philadelphia: Lea & Febiger, 517–531.

Stapels, D.A.C., Ramyar, K.X., Bischoff, M., Von Köckritz-Blickwede, M., Milder, F.J., Ruyken, M., Eisenbeis, J., McWhorter, W.J., Herrmann, M., Van Kessel, K.P.M., Geisbrecht, B. V., Rooijakkers, S.H.M. 2014. Staphylococcus aureus secretes a unique class of neutrophil serine protease inhibitors. *PNAS*, 111, 13187–13192.

Stapleton, M.R., Horsburgh, M.J., Hayhurst, E.J., Wright, L., Jonsson, I.M., Tarkowski, A., Kokai-Kun, J.F., Mond, J.J., Foster, S.J. 2007. Characterization of IsaA and SceD, two putative lytic transglycosylases of Staphylococcus aureus. *Journal of Bacteriology*, 189, 7316–7325.

Stapleton, P.D., Taylor, P.W. 2002. Methicillin resistance in Staphylococcus aureus: mechanisms and modulation. *Science Progress,* 85(Pt 1), 57–72.

Stark, R., Grzelak, M., Hadfield, J. 2019. RNA sequencing: the teenage years. *Nature Review Genet*ics, 20(11), 631–656.

Stathis, C., Victoria, N., Loomis, K., Nguyen, S.A., Eggers, M., Septimus, E., Safdar, N. 2021. Review of the use of nasal and oral antiseptics during a global pandemic. *Future Microbiol*ogy, 16(2), 119–130.

Subramanian, C., Cuypers, M.G., Radka, C.D., White, S.W., Rock, C.O. 2022. Domain architecture and catalysis of the Staphylococcus aureus fatty acid kinase. *Journal of Biological Chemistry,* 298.

Sugimoto, S., Sato, F., Miyakawa, R., Chiba, A., Onodera, S., Hori, S., Mizunoe, Y. 2018. Broad impact of extracellular DNA on biofilm formation by clinically isolated Methicillin-resistant and -sensitive strains of Staphylococcus aureus. *Scientific Reports*, 8(1), 2254.

Szklarczyk, D., Kirsch, R., Koutrouli, M., Nastou, K., Mehryary, F., Hachilif, R., Gable, A.L., Fang, T., Doncheva, N.T., Pyysalo, S., Bork, P., Jensen, L.J., Von Mering, C. 2023. The STRING database in 2023: protein-protein association networks and functional enrichment analyses for any sequenced genome of interest. *Nucleic Acids Research,* 51, D638–D646.

Tacconelli, E., Carrara, E., Savoldi, A., Harbarth, S., Mendelson, M., Monnet, D.L., Pulcini, C., Kahlmeter, G., Kluytmans, J., Carmeli, Y., Ouellette, M., Outterson, K., Patel, J., Cavaleri, M., Cox, E.M., Houchens, C.R., Grayson, M.L., Hansen, P., Singh, N., Theuretzbacher, U., Magrini, N., Aboderin, A.O., Al-Abri, S.S., Awang Jalil, N., Benzonana, N., Bhattacharya, S., Brink, A.J., Burkert, F.R., Cars, O., Cornaglia, G., Dyar, O.J., Friedrich, A.W., Gales, A.C., Gandra, S., Giske, C.G., Goff, D.A., Goossens, H., Gottlieb, T., Guzman Blanco, M., Hryniewicz, W., Kattula, D., Jinks, T., Kanj, S.S., Kerr, L., Kieny, M.P., Kim, Y.S., Kozlov, R.S., Labarca, J., Laxminarayan, R., Leder, K., Leibovici, L., Levy-Hara, G., Littman, J., Malhotra-Kumar, S., Manchanda, V., Moja, L., Ndoye, B., Pan, A., Paterson, D.L., Paul, M., Qiu, H., Ramon-Pardo, P., Rodríguez-Baño, J., Sanguinetti, M., Sengupta, S., Sharland, M., Si-Mehand, M., Silver, L.L., Song, W., Steinbakk, M., Thomsen, J., Thwaites, G.E., van der Meer, J.W., Van Kinh, N., Vega, S., Villegas, M.V., Wechsler-Fördös, A., Wertheim, H.F.L., Wesangula, E., Woodford, N., Yilmaz, F.O., Zorzet, A. 2018. Discovery, research, and development of new antibiotics: the WHO priority list of antibiotic-resistant bacteria and tuberculosis. *The Lancet Infectious Diseases*, 18, 318–327.

Theuretzbacher, U., Outterson, K., Engel, A., Karlén, A. 2020. The global preclinical antibacterial pipeline. *Nature Reviews Microbiology,* 18(5), 275–285.

Thieme, L., Hartung, A., Makarewicz, O., Pletz, M.W. 2020. In vivo synergism of ampicillin, gentamicin, ceftaroline and ceftriaxone against Enterococcus faecalis assessed in the Galleria mellonella infection model. *Journal of Antimicrobial Chemother*apy, 75, 2173–2181.

Trampari, E., Holden, E.R., Wickham, G.J., Ravi, A., Martins, L. de O., Savva, G.M., Webber, M.A. 2021. Exposure of Salmonella biofilms to antibiotic concentrations rapidly selects resistance with collateral trade-offs. *npj Biofilms and Microbiomes*, 7, 1–13.

UKHSA, UK Health Security Agency. 2023. English surveillance programme for antimicrobial utilisation and resistance (ESPAUR). Report 2022 to 2023. London. Available: https://www.gov.uk/government/publications/english-surveillance-programme-antimicrobialutilisation-and-resistance-espaur-report (accessed 06.05.24)

UKHSA, UK Health Security Agency. 2022. English surveillance programme for antimicrobial utilisation and resistance (ESPAUR). Report 2021 to 2022. London. Available: https://webarchive.nationalarchives.gov.uk/ukgwa/20231002172235/https://www.gov.uk/government/publications/english-surveillance-programme-antimicrobial-utilisation-and-resistance-espaur-report (accessed 06.05.24)

UKHSA, UK Health Security Agency. 2021. English surveillance programme for antimicrobial utilisation and resistance (ESPAUR). Report 2020 to 2021. London. Available: https://webarchive.nationalarchives.gov.uk/ukgwa/20221020175458/https://www.gov.uk/government/publications/english-surveillance-programme-antimicrobial-utilisation-and-resistance-espaur-report (accessed 06.05.24)

Van Belkum, A., Bachmann, T.T., Lüdke, G., Lisby, J.G., Kahlmeter, G., Mohess, A., Becker, K., Hays, J.P., Woodford, N., Mitsakakis, K., Moran-Gilad, J., Vila, J., Peter, H., Rex, J.H., Dunne, W.M., Jr, & JPIAMR AMR-RDT Working Group on Antimicrobial Resistance and Rapid Diagnostic Testing. 2019. Developmental roadmap for antimicrobial susceptibility testing systems. *Nature Reviews Microbiology,* 17(1), 51–62.

Varadi, M., Anyango, S., Deshpande, M., Nair, S., Natassia, C., Yordanova, G., Yuan, D., Stroe, O., Wood, G., Laydon, A., Zídek, A., Green, T., Tunyasuvunakool, K., Petersen, S., Jumper, J., Clancy, E., Green, R., Vora, A., Lutfi, M., Figurnov, M., Cowie, A., Hobbs, N., Kohli, P., Kleywegt, G., Birney, E., Hassabis, D., Velankar, S. 2022. AlphaFold Protein Structure Database: Massively expanding the structural coverage of protein-sequence space with high-accuracy models. *Nucleic Acids Research*, 50, D439–D444.

Vaser, R., Sović, I., Nagarajan, N., Šikić, M. 2017. Fast and accurate de novo genome assembly from long uncorrected reads. *Genome Res*earch, 27, 737–746.

Vejzovic, D., Iftic, A., Ön, A., Semeraro, E.F., Malanovic, N. 2022. Octenidine's Efficacy: A Matter of Interpretation or the Influence of Experimental Setups?. *Antibiotics*, 11.

Velez, R., Sloand, E. 2016. Combating antibiotic resistance, mitigating future threats and ongoing initiatives. *Journal of Clinical Nursing,* 25, 1886–1889.

Vickery, K., Deva, A., Jacombs, A., Allan, J., Valente, P., Gosbell, I.B. 2012. Presence of biofilm containing viable multiresistant organisms despite terminal cleaning on clinical surfaces in an intensive care unit. *Journal of Hospital Infection*, 80, 52–55.

Vijayakumar, R., Sandle, T. 2019. A review on biocide reduced susceptibility due to plasmid-borne antiseptic-resistant genes—special notes on pharmaceutical environmental isolates. *Journal of Applied Microbiology,* 126(4), 1011–1022.

Wade, J.J., Casewell, M.W. 1991. The evaluation of residual antimicrobial activity on hands and its clinical relevance. *Journal of Hospital Infection*, 18, 23–28.

Walker, B.J., Abeel, T., Shea, T., Priest, M., Abouelliel, A., Sakthikumar, S., Cuomo, C.A., Zeng, Q., Wortman, J., Young, S.K., Earl, A.M. 2014. Pilon: An integrated tool for comprehensive microbial variant detection and genome assembly improvement. *PLoS One*, 9.

Waller, C., Marzinek, J.K., McBurnie, E., Bond, P.J., Williamson, P.T.F., Khalid, S. 2023. Impact on S. aureus and E. coli Membranes of Treatment with Chlorhexidine and Alcohol Solutions: Insights from Molecular Simulations and Nuclear Magnetic Resonance. *Journal of Molecular Biology,* 435(11).

Walsh, C.T., Wright, G. 2005. Introduction: Antibiotic resistance. *Chemical Reviews,* 105(2), 391–394.

Wand, M.E., Bock, L.J., Bonney, L.C., Sutton, J.M. 2017. Mechanisms of increased resistance to chlorhexidine and cross-resistance to colistin following exposure of Klebsiella pneumoniae clinical isolates to chlorhexidine. *Antimicrobial Agents and Chemother*apy, 61.

Wand, M.E., Mark Sutton, J. 2022. Efflux-mediated tolerance to cationic biocides, a cause for concern? *Microbiology*, 168(11).

Wang, M., Buist, G., van Dijl, J.M. 2022. Staphylococcus aureus cell wall maintenance – the multifaceted roles of peptidoglycan hydrolases in bacterial growth, fitness, and virulence. *FEMS Microbiology Reviews*, 46(5).

Wang, Y., Liu, Qingyun, Liu, Qian, Gao, Q., Lu, H., Meng, H., Xie, Y., Huang, Q., Ma, X., Wang, H., Qin, J., Li, Q., Li, T., Xia, Q., Li, M. 2018. Phylogenetic analysis and virulence determinant of the host-Adapted Staphylococcus aureus lineage ST188 in China. *Emerging Microbes & Infections*, 7(1), 45.

Webber, M.A., Coldham, N.G., Woodward, M.J., Piddock, L.J.V. 2008a. Proteomic analysis of triclosan resistance in Salmonella enterica serovar Typhimurium. *Journal of Antimicrobial Chemotherapy*, 62, 92–97.

Webber, M.A., Piddock, L.J.V., 2003. The importance of efflux pumps in bacterial antibiotic resistance. *Journal of Antimicrobial Chemotherapy*, 51, 9–11.

Webber, M.A., Randall, L.P., Cooles, S., Woodward, M.J., Piddock, L.J.V. 2008b. Triclosan resistance in Salmonella enterica serovar Typhimurium. *Journal of Antimicrobial Chemotherapy*, 62, 83–91.

Webber, M.A., Whitehead, R.N., Mount, M., Loman, N.J., Pallen, M.J., Piddock, L.J.V. 2015. Parallel evolutionary pathways to antibiotic resistance selected by biocide exposure. *Journal of Antimicrobial Chemotherapy*, 70, 2241–2248.

Weber, D.J., Rutala, W.A., Sickbert-Bennett, E.E. 2019. Use of germicides in health care settings—is there a relationship between germicide use and antimicrobial resistance: A concise review. *American Journal of Infection Control*. 47S, A106–A109.

Weber, D.J., Rutala, W.A., Sickbert-Bennett, E.E. 2007. Outbreaks associated with contaminated antiseptics and disinfectants. *Antimicrobial Agents Chemotherapy*, 51(12), 4217–4224.

Wellington, E.M.H., Boxall, A.B.A., Cross, P., Feil, E.J., Gaze, W.H., Hawkey, P.M., Johnson-Rollings, A.S., Jones, D.L., Lee, N.M., Otten, W., Thomas, C.M., Williams, A.P. 2013. The role of the natural environment in the emergence of antibiotic resistance in Gram-negative bacteria. *The Lancet*, 13(2), 155–165.

Wessler, S., Schneider, G., Backert, S. 2017. Bacterial serine protease HtrA as a promising new target for antimicrobial therapy? Cell Communication and Signaling. *Cell*, 15(1), 4.

Whitchurch, C.B., Tolker-Nielsen, T., Ragas, P.C., Mattick, J.S. 2002. Extracellular DNA Required for Bacterial Biofilm Formation. *Science*. 295(5559), 1487.

Whitehead, R.N., Overton, T.W., Kemp, C.L., Webber, M.A. 2011. Exposure of Salmonella enterica serovar Typhimurium to high level biocide challenge can select multidrug resistant mutants in a single step. *PLoS One*, 6.

WHO, World Health Organisation. 2024. WHO Bacterial Priority Pathogens List, 2024: bacterial pathogens of public health importance to guide research, development and strategies to prevent and control antimicrobial resistance. WHO, Geneva. Available: https://www.who.int/publications/i/item/9789240093461 (accessed 18.05.24)

WHO, World Health Organisation. 2022a. Global Antimicrobial Resistance and Use Surveillance System (GLASS) Report 2022. WHO, Geneva. Available: https://www.who.int/publications/i/item/9789240062702 (accessed 02.04.24)

WHO, World Health Organisation. 2022b. Global report on infection prevention and control. WHO, Geneva. Available: https://www.who.int/publications/i/item/9789240051164 (accessed 04.04.24)

WHO, World Health Organisation. 2019a. WHO releases the 2019 AWaRe Classification Antibiotics. WHO, Geneva. Available: https://www.who.int/news/item/01-10-2019-who-releases-the-2019-aware-classification-antibiotics (accessed 02.05.24)

WHO, World Health Organisation. 2019b. Minimum requirements for infection prevention and control programmes. WHO, Geneva. Available: https://www.who.int/publications/i/item/9789241516945 (accessed 02.05.24)

WHO, World Health Organisation. 2017. WHO publishes list of bacteria for which new antibiotics are urgently needed. Media Centre. News Release. WHO, Geneva. Available: https://www.who.int/news/item/27-02-2017-who-publishes-list-of-bacteria-for-which-new-antibiotics-are-urgently-needed (accessed 08.02.24).

WHO, World Health Organisation. 2016. Guidelines on core components of infection prevention and control programmes at the national and acute health care facility level. WHO, Geneva. Available: https://www.who.int/publications/i/item/9789241549929 (accessed 05.05.24)

WHO, World Health Organisation. 2015. Global action plan on antimicrobial resistance. WHO, Geneva. Available: https://www.who.int/publications/i/item/9789241509763 (accessed 05.05.24)

WHO, World Health Organisation. 2011. Report on the burden of endemic health care-associated infection worldwide. WHO, Geneva. Available: https://www.who.int/publications/i/item/report-on-the-burden-of-endemic-health-care-associated-infection-worldwide (accessed 04.05.24)

Wick, R., 2017. Filtlong. https://github.com/rrwick/Filtlong.

Wickham, H., 2016. ggplot2: Elegant Graphics for Data Analysis. *Springer-Verlag*. New York. ISBN: 978-3-319- 24277-4. https://ggplot2.tidyverse.org.

Wilson, L.A., Rogers Van Katwyk, S., Fafard, P., Viens, A.M., Hoffman, S.J. 2020. Lessons learned from COVID-19 for the post-antibiotic future. *Global Health*. 16.

World Bank. 2017. Drug-resistant infections: A Threat to Our Economic Future. Washington, DC: World Bank. License: Creative Commons Attribution CC BY 3.0 IGO. Available: https://documents1.worldbank.org/curated/en/323311493396993758/pdf/final-report.pdf (accessed 04.06.24)

Wong, F., Zheng, E.J., Valeri, J.A., Donghia, N.M., Anahtar, M.N., Omori, S., Li, A., Cubillos-Ruiz, A., Krishnan, A., Jin, W., Manson, A.L., Friedrichs, J., Helbig, R., Hajian, B., Fiejtek, D.K., Wagner, F.F., Soutter, H.H., Earl, A.M., Stokes, J.M., Renner, L.D., Collins, J.J. 2023.

Discovery of a structural class of antibiotics with explainable deep learning. *Nature*, 626, 177–185.

Wong, H.S., Townsend, K.M., Fenwick, S.G., Trengove, R.D., O'Handley, R.M. 2010. Comparative susceptibility of planktonic and 3-day-old Salmonella Typhimurium biofilms to disinfectants. *Journal of Applied Microbiology*, 108, 2222–2228.

Wood, D.E., Salzberg, S.L. 2014. Kraken: ultrafast metagenomic sequence classification using exact alignments. *Genome Biology*, 15(3), R46.

Wu, D., Lu, R., Chen, Y., Qiu, J., Deng, C., Tan, Q. 2016. Study of cross-resistance mediated by antibiotics, chlorhexidine and Rhizoma coptidis in Staphylococcus aureus. *Journal of Global Antimicrobial Resistance,* 7, 61–66.

Wu, G., Yang, Q., Long, M., Guo, L., Li, B., Meng, Y., Zhang, A., Wang, H., Liu, S., Zou, L. 2015. Evaluation of agar dilution and broth microdilution methods to determine the disinfectant susceptibility. *Journal of Antibiotics*, 68, 661–665.

Xie, X., Liu, X., Li, Y., Luo, L., Yuan, W., Chen, B., Liang, G., Shen, R., Li, H., Huang, S., Duan, C. 2020. Advanced Glycation End Products Enhance Biofilm Formation by Promoting Extracellular DNA Release Through sigB Upregulation in Staphylococcus aureus. *Frontiers in Microbiology,* 11.

Xijin Ge, S., Jung, D., Yao, R. 2020. ShinyGO: a graphical gene-set enrichment tool for animals and plants. *Bioinformatics*, 36(8), 2628–2629.

Yanisch-Perron, C., Vieira, J., Messing, J. 1984. Improved Ml3 phage cloning vectors and host strains: nucleotide sequences of the M13mp18 and pUC19 vectors. *Gene*, 33(1), 103–119.

Yasir, M., Keith Turner, A., Bastkowski, S., Baker, D., Page, A.J., Telatin, A., Phan, M.D., Monahan, L., Savva, G.M., Darling, A., Webber, M.A., Charles, I.G. 2020. TraDIS-Xpress: A high-resolution whole-genome assay identifies novel mechanisms of triclosan action and resistance. *Genome Research*, 30, 239–249.

Zaborowska, M., Tillander, J., Brånemark, R., Hagberg, L., Thomsen, P., Trobos, M. 2017. Biofilm formation and antimicrobial susceptibility of staphylococci and enterococci from osteomyelitis associated with percutaneous orthopaedic implants. *Journal of Biomedical Materials Research Part B Applied Biomaterials*, 105, 2630–2640.

Zampaloni, C., Mattei, P., Bleicher, K., Winther, L., Thäte, C., Bucher, C., Adam, J.-M., Alanine, A., Amrein, K.E., Baidin, V., Bieniossek, C., Bissantz, C., Boess, F., Cantrill, C., Clairfeuille, T., Dey, F., Di Giorgio, P., du Castel, P., Dylus, D., Dzygiel, P., Felici, A., García-Alcalde, F., Haldimann, A., Leipner, M., Leyn, S., Louvel, S., Misson, P., Osterman, A., Pahil, K., Rigo, S., Schäublin, A., Scharf, S., Schmitz, P., Stoll, T., Trauner, A., Zoffmann, S., Kahne, D., Young, J.A.T., Lobritz, M.A., Bradley, K.A. 2024. A novel antibiotic class targeting the lipopolysaccharide transporter. *Nature*, 625, 566–571.

Zeng, W., Xu, W., Xu, Y., Liao, W., Zhao, Y., Zheng, X., Xu, C., Zhou, T., Cao, J., 2020. The prevalence and mechanism of triclosan resistance in Escherichia coli isolated from urine samples in Wenzhou, China. *Antimicrobial Resistance and Infection Control*, 9(1), 161.

Zhang, X., de Maat, V., Guzmán Prieto, A.M., Prajsnar, T.K., Bayjanov, J.R., de Been, M., Rogers, M.R.C., Bonten, M.J.M., Mesnage, S., Willems, R.J.L., van Schaik, W. 2017. RNA-seq and Tn-seq reveal fitness determinants of vancomycin-resistant Enterococcus faecium during growth in human serum. *BMC Genomics*, 18.

Zheng, G., Filippelli, G.M., Salamova, A. 2020. Increased Indoor Exposure to Commonly Used Disinfectants during the COVID-19 Pandemic. *Environmental Science and Technology Letters,* 7, 760–765.

Zhou, G., Wang, Y.S., Peng, H., Li, S.J., Sun, T. L, Shi, Q.S., Garcia-Ojalvo, J., Xie, X.B. 2023. Proteomic signatures of synergistic interactions in antimicrobials. *Journal of Proteomics*, 270.

Zhu, L., Lin, J., Ma, J., Cronan, J.E., Wang, H. 2010. Triclosan resistance of Pseudomonas aeruginosa PAO1 is due to FabV, a triclosan-resistant enoyl-acyl carrier protein reductase. *Antimicrobial Agents and Chemotherapy*, 54, 689–698.

Zhu, X.Q., Wang, X.M., Li, H., Shang, Y.H., Pan, Y.S., Wu, C.M., Wang, Y., Du, X.D., Shen, J.Z. 2017. Novel lnu(G) gene conferring resistance to lincomycin by nucleotidylation, located on Tn6260 from Enterococcus faecalis E531. *Journal of Antimicrobial Chemotherapy*. 72, 993–997.

Zischka, M., Künne, C.T., Blom, J., Wobser, D., Sakinç, T., Schmidt-Hohagen, K., Dabrowski, P.W., Nitsche, A., Hübner, J., Hain, T., Chakraborty, T., Linke, B., Goesmann, A., Voget, S., Daniel, R., Schomburg, D., Hauck, R., Hafez, H.M., Tielen, P., Jahn, D., Solheim, M., Sadowy, E., Larsen, J., Jensen, L.B., Ruiz-Garbajosa, P., Quiñones Pérez, D., Mikalsen, T., Bender, J., Steglich, M., Nübel, U., Witte, W., Werner, G. 2015. Comprehensive molecular, genomic and phenotypic analysis of a major clone of Enterococcus faecalis MLST ST40. *BMC Genomics*, 16.

APPENDICES

“You can begin anytime, even though it takes a lifetime to be good " – Esther Lederberg

APPENDIX I: List of bacterial isolates used in the optimisation experiments

Table A.I. List of bacterial isolates used in the optimisation experiments.

Isolate number	Species	Sample type	Country
60	*Staphylococcus aureus*	Gut swab	UK
353	*Staphylococcus aureus*	Nose swab	UK
33	*Staphylococcus capitis*	Gut swab	UK
379	*Staphylococcus capitis*	Nose swab	UK
677	*Staphylococcus capitis*	Ear swab	UK
118	*Staphylococcus epidermidis*	Skin swab	UK
447	*Staphylococcus epidermidis*	Skin swab	UK
16TB0527	*Staphylococcus epidermidis*	Hip tissue	UK
16TB0528	*Staphylococcus epidermidis*	Hip tissue	UK
16TB0529	*Staphylococcus epidermidis*	Hip tissue	UK
16TB0532	*Staphylococcus epidermidis*	Skin swab	UK
16TB0533	*Staphylococcus epidermidis*	Skin swab	UK
567	*Staphylococcus epidermidis*	Nose swab	UK
W01 - 42 - a	*Staphylococcus epidermidis*	Gut swab	Germany
349	*Staphylococcus haemolyticus*	Ear swab	UK
W02 - 16 - t	*Staphylococcus hominis*	Throat swab	Germany

APPENDIX II: Standard Operating Procedure: *In vitro* bead-based biofilm evolution experiment for *Staphylococcus aureus* and *Enterococcus faecalis*

QUADRAM INSTITUTE BIOSCIENCE

STANDARD OPERATING PROCEDURE

Quadram Institute
Science Health Food Innovation

Title: In vitro biofilm evolution experiment for Staphylococcus aureus and Enterococcus faecalis

Applies to staff in: Containment level 2, floor 2 laboratory	***Reference number: MFC-MW-029***
Author: Maria Solsona Gaya	***Approver: Dr Mark Webber***
Issue date: 15 June 2023	***Review date: 14 June 2025***
QA and H&S Review: R Walding	***Version Number: 002***

AUTHORISATION: I confirm that this SOP is an accurate description of the procedure or method in use.

DECLARATION. The safety information contained in this document is to the best of my knowledge an accurate statement of the known and foreseeable hazards to health and of the safety precautions, which are to be followed to minimise the risks to health in the process. All users of this SOP are adequately trained to be competent in the process.

Approved by ISP/NC Leader, or Research Leader, or Senior Scientist, or Senior Administrator

Signed:	Print: Mark Webber	Date: 15 June 2023

TITLE: IN VITRO BIOFILM EVOLUTION EXPERIMENT FOR STAPHYLOCOCCUS AUREUS AND ENTEROCOCCUS FAECALIS

1. PURPOSE OF PROCEDURE/METHOD AND ITS SCOPE

To determine how staphylococcal and enterococcal biofilms and planktonic cells evolve in response to stress factors such as biocides.

2. EQUIPMENT AND REAGENTS NEEDED

2.1. Equipment

- Class II Microbiological safety cabinet
- Lab coat
- Sheildskin orange nitrile gloves
- Fume cupboard (for antimicrobial stock preparation)
- Microbiology Safety cabinet
- 5 mL Universal tubes
- Tweezers (for bead transfer between tubes)
- Reservoirs
- Single and multi-channel pipettes
- Sterile tips
- Sterile 24-well microtiter plates and 96-well microtiter plates
- Absorbent paper roll
- Stainless steel beads from different sizes (Diameter: 6 mm and 3 mm)

    https://simplybearings.co.uk/shop/p221124/6mm-Diameter-%20Grade-100-%20AISI-316-Stainless-Steel-Ball-%20Bearings/product_info.html

    https://simplybearings.co.uk/shop/p221112/3mm-Diameter- Grade-100-AISI-316-Stainless-Steel-Ball- Bearings/product_info.html

2.2. Reagents

- O/N bacterial liquid cultures
- Appropriate medium (TSB)
- Biocide solutions (CHX and OCT) of appropriate concentrations
- Dimethyl sulfoxide (DMSO)
- 70 % Ethanol
- 20 % Glycerol in PBS

3. STEPS IN PROCEDURE (INCLUDING SAFETY INFORMATION)

For all the steps below, it is essential to:

- Work in a containment level 2 laboratory.
- Wear appropriate personal protective equipment (PPE): lab coat, gloves and safety glasses.
- Observe local safety rules.

Biocide preparation:

All the biocide powders should be weighed in the ventilated weighing station to avoid inhalation.

Biocide	Solubility	Stock Concentration	Working concentration	Volume
Chlorhexidine digluconate	Water	106 mg/mL	1024 µg/mL	10 mL
Octenidine dihydrochloride	DMSO	5 mg/mL	1024 µg/mL	10 mL

* The purchased stock of CHX (stored in the cold room) is too concentrated (20 % v/v) so a 1:10 dilution is needed to obtain a 2 % (v/v) CHX stock to work with. Alternatively, a 0.2 % (v/v) CHX stock can also be prepared to prevent errors (e.g., avoid pipetting small volumes).

Carry out all the following procedures using aseptic technique, you should not wear gloves when using a Bunsen burner as this can cause serious burns. If using a respiratory pathogen use a Microbiological Safety cabinet for all manipulations with live organisms.

This experiment aims to repeatedly expose bacteria in a biofilm and planktonic conditions to stress. The following procedure has been optimised for *Staphylococcus aureus* and *Enterococcus faecalis* to allow 72 h exposure steps. The timeframe may need adjustment according to the specifics of an experiment. The standard timeframe of activities are as follows:

Day 1:

- Streak the strains of interest on TSA plates.
    - For further information on agar plates and glycerol stocks see SOP General Bacteria Growth MFC_MW_014

Day 2:

- Start 5 mL TSB O/N cultures by picking a single colony with a loop from the plate prepared on Day 1 and re-suspending it into the medium.

Bead preparation

- Prepare the beads in a Duran bottle to store them for a longer period of time. Firstly, wash the beads with sterile water and make sure the water is not filled up more than half of the volume of the bottle. Then, autoclave the bottle with water, as it will conduct the heat better than air. After autoclaving, decant the water and replace it with 70 % ethanol.

Day 3:

Inoculation

- Inoculate 1 to 5 mL of the appropriate medium with 1:100 inoculum from the O/N culture (e.g., in 5 mL of TSB add 50 µL from the O/N bacterial culture). Use 5 mL glass bottles.
- Incubate the O/N at 37 °C in the orbital shaker, shaking at 200 rpm.
    - Samples: It is important to include more than one lineage (e.g., 4 lineages are a good number) and a planktonic culture with no beads in as a control.

Bead decontamination

- Soak the beads in 70 % ethanol for 20 minutes and air dry them for 1-2 minutes on absorbent paper.
- Alternatively, take the beads directly from the Duran bottle and air dry them for 1-2 minutes on absorbent paper. Use a balance spoon to easily pick the 3 mm beads from the Duran bottle (Pasteur pipettes are too narrow for the 3 mm beads).
- Add the appropriate number of beads in each culture. In this case, 3 beads of the same size will be used:
    - One will be used for the biofilm transfer.
    - One will be stored.
    - The third one will be used for the analysis or be stored as a back-up.

Incubation

- Place the samples in an orbital shaker (40 rpm) inside a refrigerated incubator (22 °C).

[**Note 1:** The chosen temperature (22 °C) has been tested for *Staphylococcus haemolyticus* with no optimal results. The preferred temperature for this specie is 30 °C].

Day 5:

[**Note 2:** For the bead transfer you will need multiple pairs of tweezers, e.g., 3 pairs, which will need to be soaked in ethanol and air dried in rotation before used for the transfer of the next bead. Tweezers need to be autoclaved after each passage].

[**Note 3:** It is also advisable to work on an absorbent material to avoid the beads rolling around if they fall on the bench].

Bead washing

- For each bead you want to transfer, prepare a 24-well microtiter plate, and fill it with 1 mL of PBS per bead. All the beads taken from the culture will need to be washed before being stored, analysed, or used as an inoculum for the biofilm transfer.
- Transfer the bead and let it wash for 5 minutes under slow rotation or slowly shaking by hand inside the hood (Important to shake gently + slowly).

Inoculation - Transfer

- For each sample prepare 5 mL of TSB in universal tubes and add the stress factors (biocides) at the appropriate concentrations (depending on the chosen MIC). To calculate the quantity of biocide that needs to be added, start from the working concentration.

(Always make sure that you keep transferring the planktonic culture, 100 µL inoculum is appropriate and that you include samples with "No biocides + bead" as a control).

- Transfer the washed bead in the universal tube with the fresh medium and the stress factor where appropriate. Add three decontaminated beads of a different size to the same tube.
- Incubate at 22 °C in the orbital shaker, shaking at 40 rpm.

Sampling

- For each bead you want to store prepare a 1.5 mL Eppendorf tube filled with 1 mL 20 % glycerol in PBS. Alternatively, use a 2 mL 96-well deepwell (better than Eppendorf for a long-term storage) plate filled with 20 % glycerol in PBS; seal the plate with adhesive PCR plate foil.

    - Biofilm stock: After washing the bead of interest, transfer it to the deepwell and store it at -20 °C. Add 2 mL 20 % glycerol in PBS.

    - Planktonic stock: Include also stocks from the planktonic tubes by adding 1 mL planktonic culture to 1 mL 20 % glycerol in PBS to the 96-well deepwell.

    - Planktonic stock from the Biofilm condition: 1 mL 20 % glycerol in PBS + 1 mL planktonic from the biofilm tube to the 96-well deepwell.

Analysis

- Where appropriate, use the third bead and after washing it, transfer it to an Eppendorf tube filled with 1 mL of PBS. Run planktonic alongside (do not add PBS and do not vortex).
- Vortex at 1200 rpm, 21 °C for 2 minutes for the biofilm to detach from the surface and use it for a serial dilution series and CFU counting experiment.

CFU counting:

- Use a 96-well microtiter plate to carry out the serial dilutions up to the 10^{-8} in 200 µL final volume. To do this, add 20 µL of the sample and 180 µL of PBS. Shake the tube before pipetting.

- Using a multichannel pipette, take 5 µL of the whole row and spot it in a TSA square plate (No need to spot 10^{0} dilution). Include 3 replicates.

- On the next day the CFU counting (check CFU/calculations section) can be carried out. It is also possible to make bead glycerol stocks from the 10^{-1} dilution to have multiple copies of your isolate.

CFU calculations:

- To calculate the CFU/bead for biofilm and planktonic:

Biofilm → X * (200/5) * $10^{\text{dilution-1}}$ * (1000/20)

Initially, the CFU is multiplied by "200/5", because 5 µL of the culture were spotted from the 200ul well into the agar. Then, that is multiplied by "$10^{\text{dilution-1}}$" to get the CFU of the top spot on the plate. Finally, the result is multiplied by "1000/20" because the beads were resuspended in 1000 µL (1 mL) and 20 µL of these were added on the top well of the 96-well plate to do the dilutions.

Planktonic → X * (200/5) * $10^{\text{dilution-1}}$ * (5000/20) * (1/5)

Initially, the CFU is multiplied by "200/5", because 5 µL of the culture were spotted from the 200ul well into the agar. Then, that is multiplied by "$10^{\text{dilution-1}}$" to get the CFU of the top spot on the plate. Afterwards, the result is multiplied by "5000/20" because 20 µL were directly taken from the 5 ml planktonic culture in the glass tube (CFU/5 mL). Finally, to get CFU/ml the result is divided by 5.

- To calculate CFU/mm^2, the CFU/bead is divided by the area of the sphere. So, as the beads have different radius, divide by 113.1 mm^2 (6 mm beads) and by 28.27 mm^2 (when using the 3 mm beads).

Experimental timeline:

Passage window → After previous optimizations, the selected passage window is 72 hours. So, the sampling, analysis and transfer steps will be repeated every Monday and Thursday for the duration of the experiment.

[**Note 4:** After the first serial passage, start the second passage from the "Bead washing" step and do the next passages every 72 hours (e.g., on Monday and Thursday). Alternatively, the schedule frequency can vary as passage window could also be 48 hours (e.g., Tuesday and Thursday)].

[**Note 5:** The bead biofilm evolution model can be performed with a continuous stable exposure to antimicrobials (Static model – same MIC) or an increasing exposure to antimicrobials (Ladder model – increasing MIC)].

Disposal of waste:

All waste contaminated with biological substances are to be disposed of in autoclave bin. Any spillages should be cleared with paper towel, and the area treated with BioGuard. All waste created should also be disposed of in autoclave bins.

SAFETY INFORMATION

Principal Hazards:

- Chemical hazards: Biocides (see hazard statements below)
- Biological hazards: Make sure you are familiar with all the risks involving the use of microorganisms. Check the Risk assessment for the microorganism you are planning to use.

Method Steps involving Higher Risk (and precautions to minimise risk): *Salmonella, E. coli* and *Klebsiella* are hazard group 2 organisms and as such should be handled in a containment lab 2 and all steps carried out at this risk level. Culture volumes should remain below 5 ml so that spills can be easily contained.

Read Risk Assessment – COSHH Assessments for *Staphylococcus spp. and Enterococcus spp.* and Hazard Group 2 Organisms.

Essential Precautions:

- Work in a ventilated weigh station for the biocide powder handling.
- Work in ACDP level 2 lab when handling ACDP level 2 organisms. Use a safety cabinet if handling respiratory pathogens (e.g., *Haemophilus*, *Streptococcus*)

Personal Protective Clothing: Lab coat, Shieldskin gloves and safety specs.

Any restrictions on use: Trained personnel only.

Exceptions or Warnings: Should be included at relevant step in the procedure.

4. RISK ASSESSMENT

The overall risk is LOW if the guidelines in this SOP are followed carefully.

All individuals using this procedure will be shown the risk assessment and given appropriate information, instruction and training in the risks and precautions necessary, including the use of any personal protective equipment required.

SOP HEALTH RISK ASSESSMENT			
[1] Activity:	*In vitro* biofilm evolution experiment		
[2] Location of activity:	Containment level 2 laboratory, floor 2		
[3] Who is involved:	Webber group, and researchers in the MFC QIB		
[4] Frequency of activity:	Variable		
[5] Duration of Activity:	Variable		
[6] Chemical Hazard Name:	**Hazard Statements**	**Route of Exposure** *	**Quantity Used**
Chlorhexidine digluconate	○ **H318** - Causes serious eye damage. ○ **H410** - Very toxic to aquatic life long lasting effects.	S, I	Max 5 mL
Octenidine dihydrochloride	○ The product is **not classified as hazardous** within the meaning of Regulation (EU) No 1272/2008. 2008. ○ In normal use conditions and in its original form, the product itself does not involve any other risk for health and the environment.	S, I, B	Max 1 g

DMSO	○ **Not a hazardous substance** or mixture according to Regulation (EC) No 1272/2008. ○ This substance/mixture contains no components considered to be either persistent, bioaccumulative and toxic (PBT), or very persistent and very bioaccumulative (vPvB) at levels of 0.1 % or higher. Rapidly absorbed through skin.	S	Max 25 mL
Ethanol	○ **H225 -** Highly flammable liquid and vapour. ○ **H319** - Causes serious eye irritation.	S	250 mL stock

[7] Details of biological agents of risk to human health:	**GMRA Number**
Salmonella spp. COSHH Hazard Group 2 microorganisms	N/A
Klebsiella spp. COSHH Hazard Group 2 microorganisms	N/A
Staphylococcus spp. COSHH Hazard Group 2 microorganisms	N/A
Other enteric pathogens at COSHH Hazard Group 2	N/A

[8] Other Hazards:		Please ■ as necessary			
Hot or Cold Burns	☐	Ionising Radiation**	☐	Ultraviolet or Infra-Red	☐
Dust	☐	Noise	☐	Pollen Sensitizer	☐
Repetitive Action	☐	Extreme Cold Environment (< 0 °C)	☐	Lifting / Manual Handling	☐
Asphyxiation	☐	Cuts	☐	Electrical	☐
Slips / trips / falls	☐	Display Screen Equipment	☐	Nanomaterials (man-made particles, tubes, rods, or fibres ≤100nm in size)	☐
Other (give details)	☐				

[9] Control Measures:		Please ■ as necessary			
Fume Cupboard	☐	Microbiological Safety Cabinet	■	Total Containment Cabinet	☐

Ventilated Bench	■	Spill Tray	☐	Trained personnel only	■
Signs	☐	Reduce frequency/alternate activity	☐	Reduce duration of activity	☐
Sub divide a load	☐	2 persons lift of equipment	☐	Not for more than 1 hour	☐
Regular, short breaks	☐	Alternate activities	☐	Other (give details)	☐
[10] Personal Protection:		Please ■ as necessary			
Lab coat	■	Safety Glasses	■	Face Shield	☐
Goggles	☐	Gloves *(Shieldskin orange nitrile)*	■	Protective Gloves *(specify)*	☐
Ear defenders	☐	Other (give details)	☐		
[11] Is personal monitoring and/or health surveillance required?			Yes	☐	No ■
Details:					
[12] Restrictions:		Please ■ as necessary			
No lone working	☐	Not to be left unattended	☐	Named persons only	☐
In restricted area	☐	Risk Assessment Required for New or Expectant Workers	☐	Under constant supervision	☐
Not by under 18's	■	Other (give details)	☐		
[13] Level of Residual Risk:		Please ■ as necessary			
Low	■	Medium	☐	High	☐
Name of Assessor:		Maria Solsona Gaya		Date:	2 Nov 2020

* Route of exposure; S = skin, I = ingestion, B = inhalation

5. DOCUMENTS

Chemical Tables: http://intranet/cms/2256

Good Laboratory Practice in the Use of Chemicals: http://intranet/cms/2199

Link to Laboratory Waste Disposal: http://intranet/cms/968

Biosafety Handbook: http://intranet/cms/970

6. RELATED PROCEDURES

SOP MFC-MW-003: *In vitro* Biofilm Evolution Experiment (Author: Gregory Wickham/Version Number: 001).

SOP MFC-MW-014: General Bacteria Growth.

7. DOCUMENT HISTORY

Issue Number	Reason for update
001	First issue
002	SOP reviewed, changes to method made

8. APPENDIX

Staff Training record for SOP (Link to: *In vitro* biofilm evolution experiment for *Staphylococcus aureus* and *Enterococcus faecalis.* Training.doc).

APPENDIX III: Calibration curves for *S. aureus* ST188 and *E. faecalis* ST40

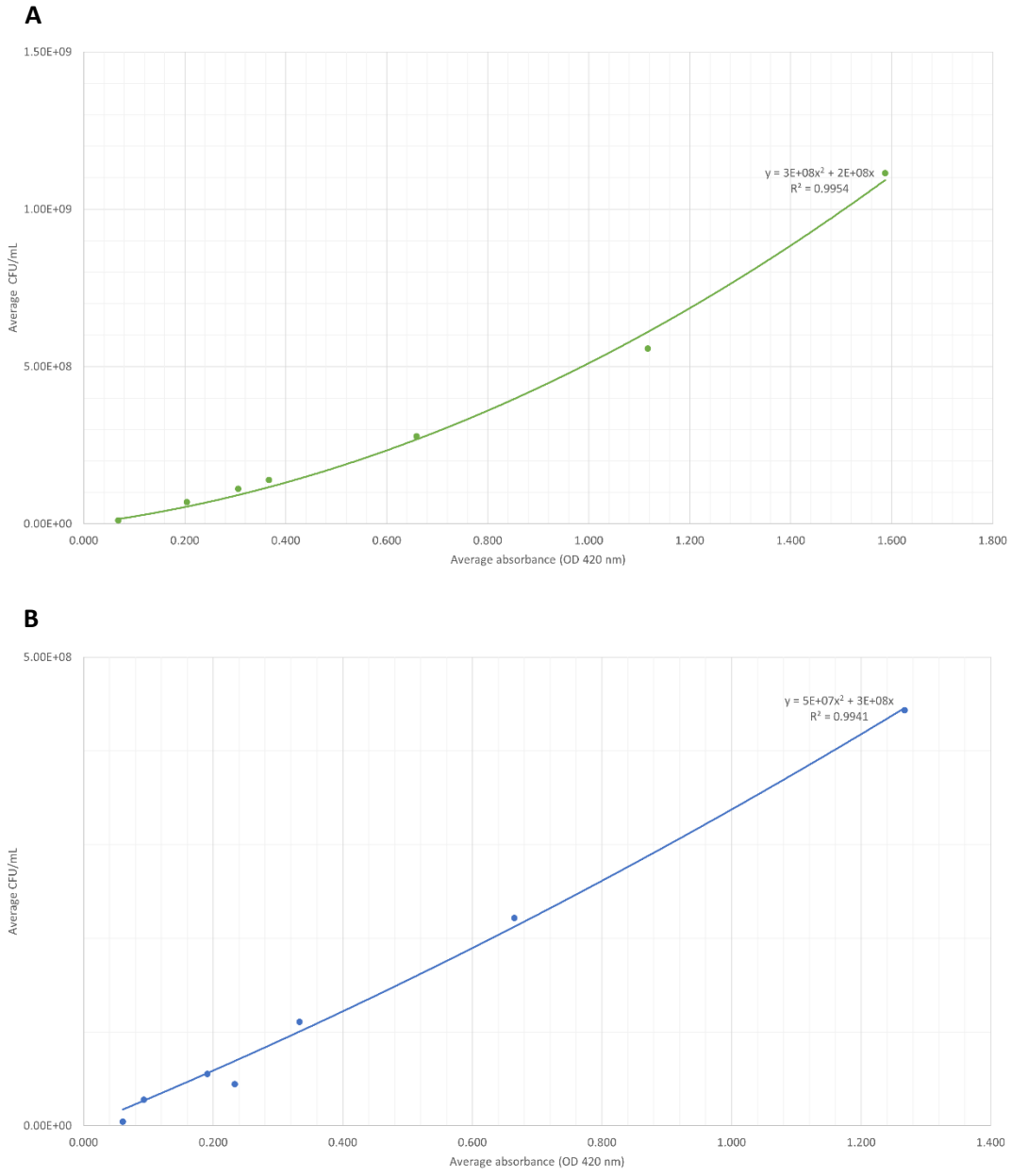

Figure A.III. Calibration curves for (A) *S. aureus* ST188 and (B) *E. faecalis* ST40. Average of the total viable counts (average CFU/mL) from three biological replicates (2 technical replicates in each) is plotted against the optical density ($OD_{420\,nm}$) following the optical density standardisation protocol from GAMA Healthcare Ltd.

APPENDIX IV: Primer list

Table A.IV. Primers used to create Δ*fakA* mutants.

ID	Name	Sequence (5'→ 3')	Tm (°C)	Role
1	pKOR1_UP_*fakA*_F	GGGGG**GGGCCC**CCAAATTATATTGATAGTTCGAATTTCACTATGAAC	57	To amplify flanking region 1 and for PCR Up
2	Flank1_KpnI_*fakA*_R	GGGGG**GGTACC**AAGTTGTCCTCCTAAGCTTTCTTGCCTGTATTATTCA CACGTACACC	68	To amplify flanking region 1
3	Flank2_SacI_*fakA*_F	GGGGG**GAGCTC**CTATTTTAGTGATATTGCGGGTTAAAAGTATCGTTC TCGAGTTG	64	To amplify flanking region 2
4	pKOR1_Down_*fakA*_R	GGGGGG**GGTACC**CCTACATCACCTTGAAGTAATCGATGCATACGTATTG	62	Used for PCR Down
5	Flank2_XmaI_*fakA*_R	GGGGGGG**GTCGAC**CCCTACATCACCTTGAAGTAATCGATGCATACGTAG	62	To amplify flanking region 2
6	pKOR1_Down_*fakA*_F	GAAAGCTTAGGAGGACAACTTGAAATG**CAGCTG**GCTATTTTAGTGATAT TGCGGGTTAAAAGTATCGTTCTCGAGTTG	65	Used for PCR Down
7	pKOR1_UP_*fakA*_R	CTTTTAACCCGCAATATCACTAAAATAGC**GTCGAC**CATTTCAAGTTGTCCT C CTAAGCTTTCTTGCCTGTATTATTCACACGTACAC	68	Used for PCR Up

* Restriction sites are indicated in bold.

* Tm: Melting temperature; F: Forward; R: Reverse; Flank1: Flanking region 1 kb upstream *fakA* gene (Approach 1); Flank2: Flanking region 1 kb downstream *fakA* gene (Approach 1); UP: Flanking region 1 kb upstream *fakA* gene (Approach 2); DOWN: Flanking region 1 kb downstream *fakA* gene (Approach 2).

APPENDIX V: Detailed PCR programmes used to construct Δ*fakA* mutants

Table A.V. PCR programmes used in the cloning strategy (Step 1) to create Δ*fakA* mutants.

Step	Temperature (°C)	Duration
Stage 1: 1 cycle		
Initial denaturation	95	20 seconds
Stage 2: 28 cycles* or 22 cycles**		
Denaturation	95	15* or 30** seconds
Annealing	60	30 seconds
Elongation	72	1* or 2** minutes
Stage 3: 1 cycle		
Final elongation	72	7* minutes
Hold	4	∞

* Denaturation and elongation times differed for Approach 1 (*) and Approach 2 (**), depending on the insert size. Settings were also used for colony PCR, depending on the approach.

APPENDIX VI: Calculation of the theoretical bead surface occupied by bacterial cells

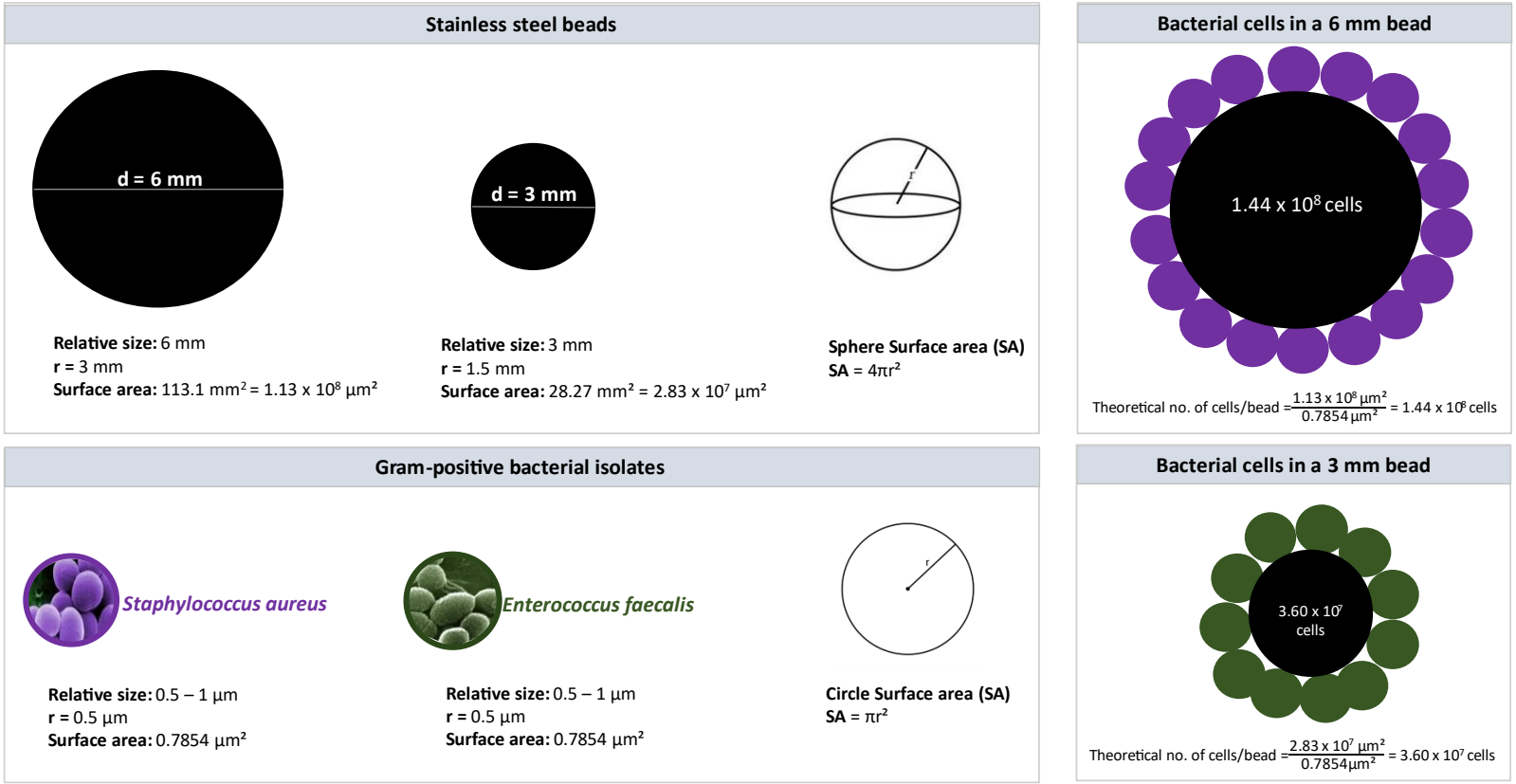

Figure A.VI. Calculation of the theoretical bead surface occupied by bacterial cells. The surface area of the sphere was calculated for the beads from different diameters (6 mm and 3 mm) and the surface area of the circle was calculated for the Gram-positive cocci (*S. aureus* and *E. faecalis*). The theoretical number of bacterial cells for each bead is shown on the right**.**

APPENDIX VII: Survival of *E. faecalis* ST40 and *S. aureus* ST188 in the control condition

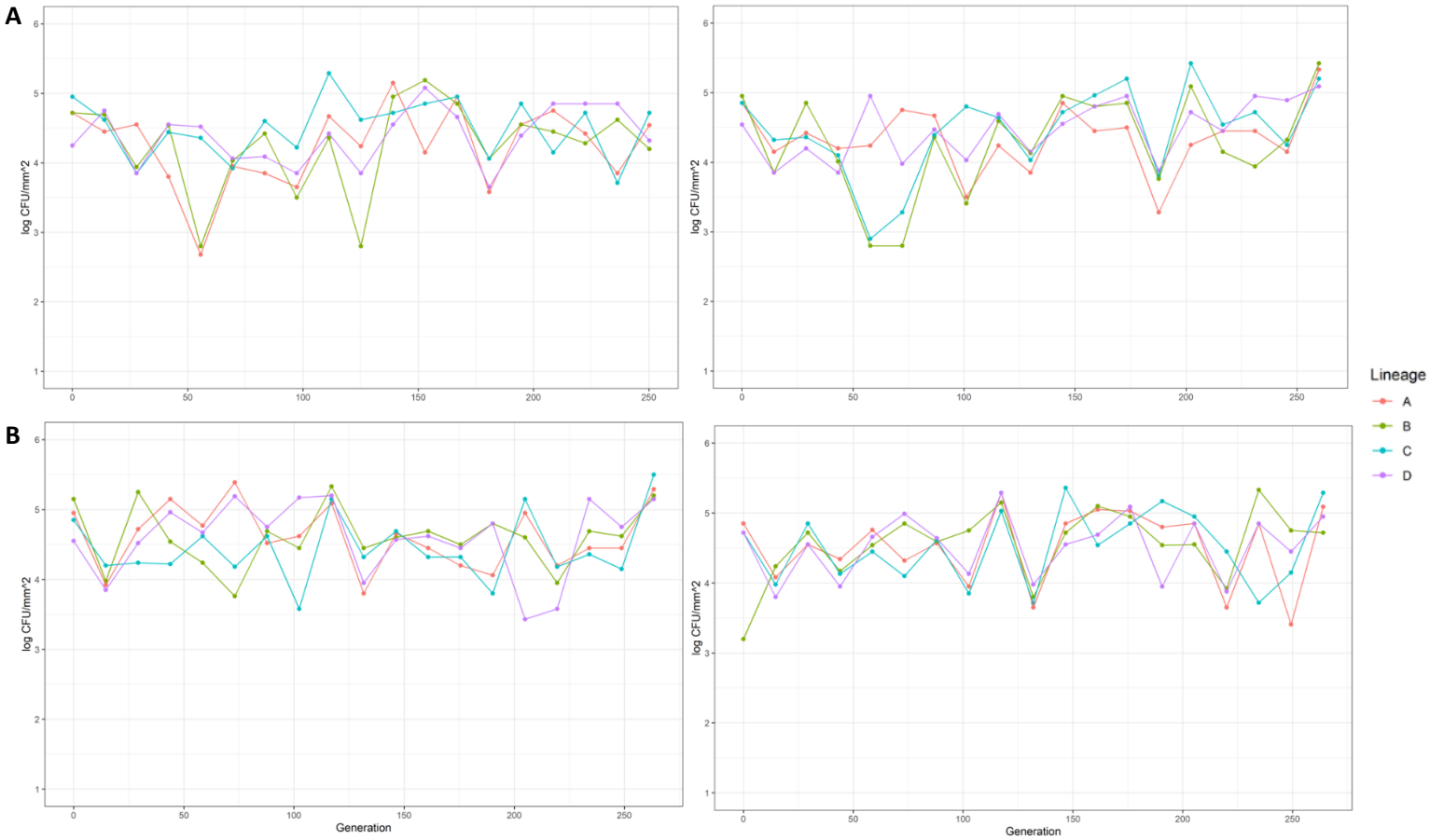

Figure A.VII. Survival of (A) *E. faecalis* and (B) *S. aureus* in the control condition (no stress with beads). Controls for the CHX experiment (left panels) and OCT experiment (right panels) shown. Productivity (expressed as CFU/mm^2) is plotted against the generation time (passage window: 72 hours).

APPENDIX VIII: Wilcoxon-Mann-Whitney test to assess differences within conditions for each sample in *E. faecalis* isolates exposed to CHX

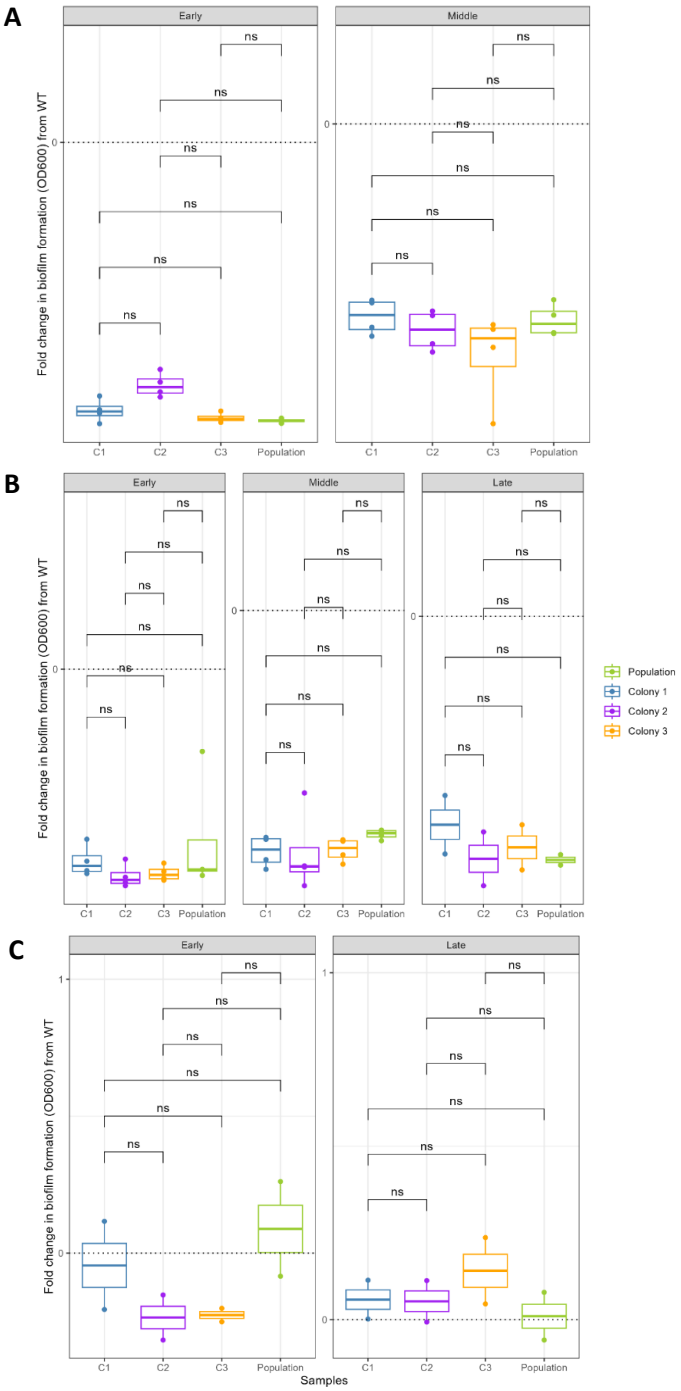

Figure A.VIII. Biofilm biomass production in *E. faecalis* isolates exposed to CHX for (A) biofilm; (B) planktonic; (C) control (no stress). Boxplots representing crystal violet staining with medians are shown; populations and individual isolates are represented in different colours. Fold changes in biofilm formation (OD_{600nm}) from the WT (black dotted line) are shown. Wilcoxon-Mann-Whitney test applied to study differences within conditions for each sample (population and random colonies); *ns* indicates non-statistically significant changes (*p-value* > 0.05).

APPENDIX IX: Wilcoxon-Mann-Whitney test to assess differences within conditions for each sample in *E. faecalis* isolates exposed to OCT

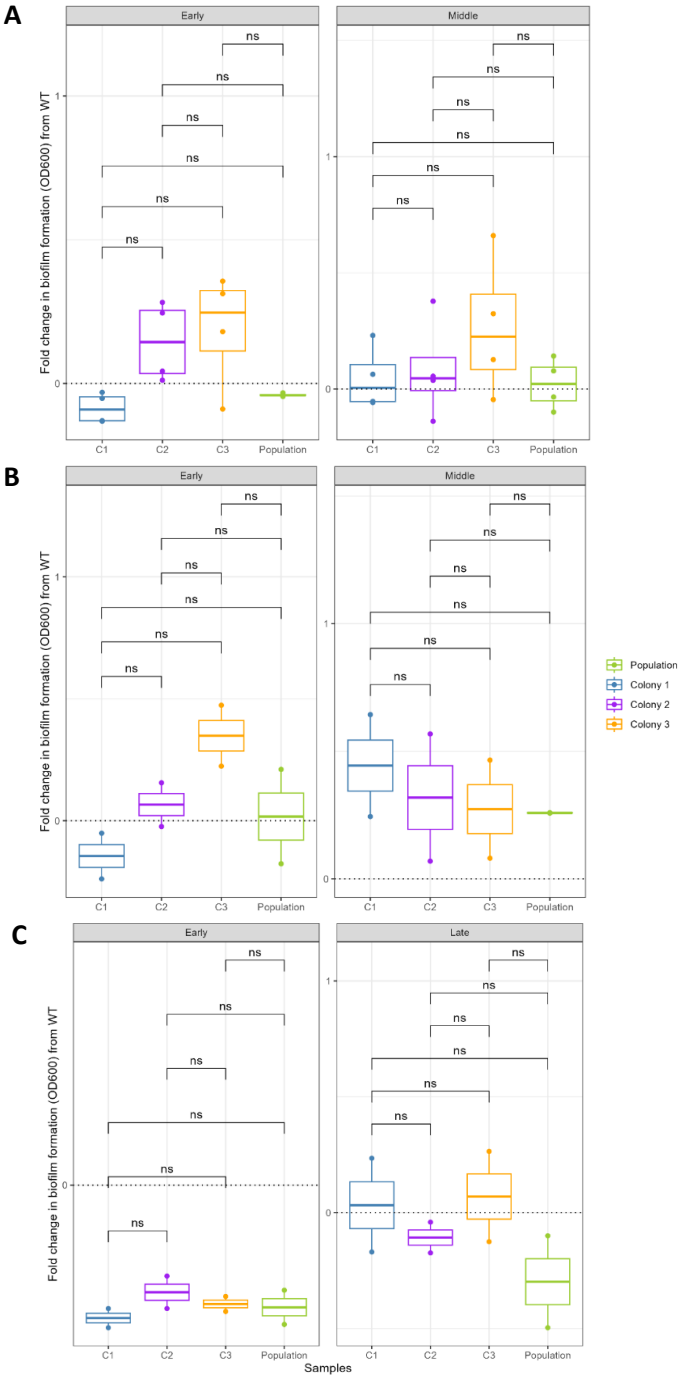

Figure A.IX. Biofilm biomass production in *E. faecalis* isolates exposed to OCT for (A) biofilm; (B) planktonic; (C) control (no stress). Boxplots representing crystal violet staining with medians are shown; populations and individual isolates are represented in different colours. Fold changes in biofilm formation (OD_{600nm}) from the WT (black dotted line) are shown. Wilcoxon-Mann-Whitney test applied to study differences within conditions for each sample (population and random colonies); *ns* indicates non-statistically significant changes (*p-value* > 0.05).

APPENDIX X: Wilcoxon-Mann-Whitney test to assess differences within conditions for each sample in *S. aureus* isolates exposed to CHX

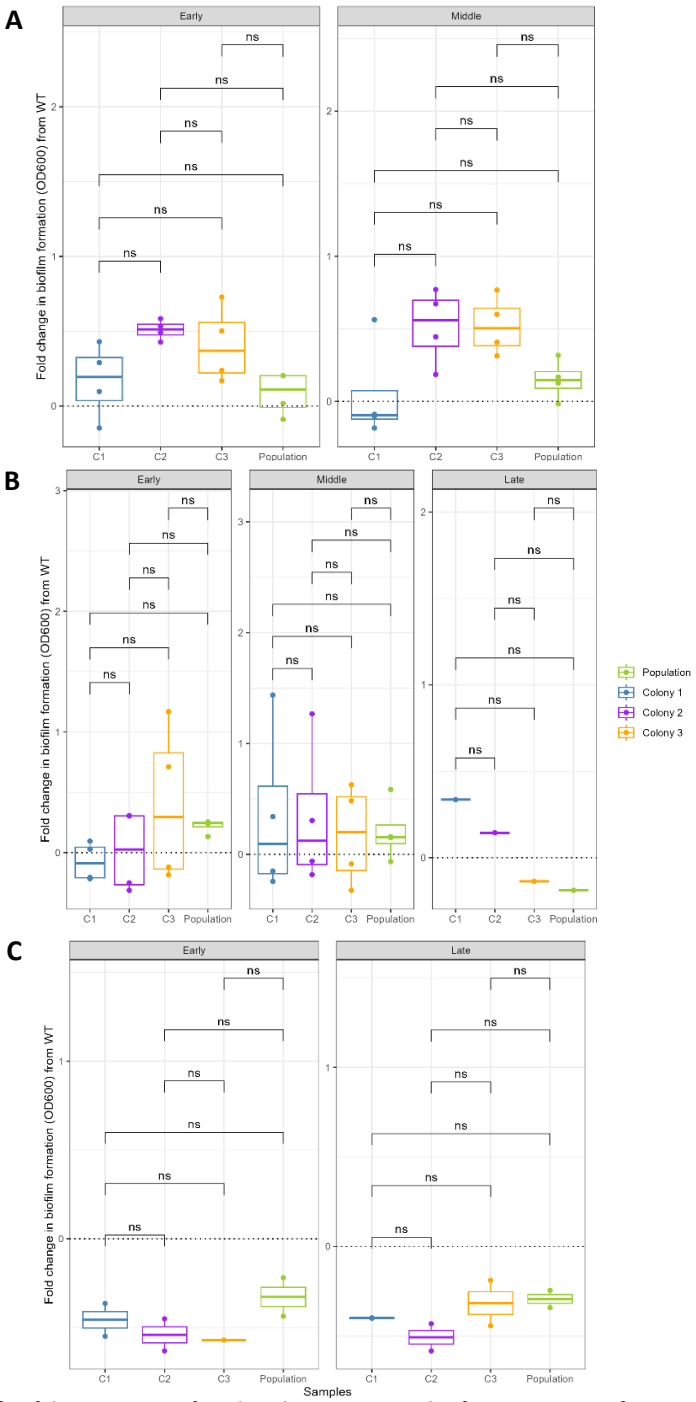

Figure A.X. Biofilm biomass production in *S. aureus* isolates exposed to CHX for (A) biofilm; (B) planktonic; (C) control (no stress). Boxplots representing crystal violet staining with medians are shown; populations and individual isolates are represented in different colours. Fold changes in biofilm formation (OD_{600nm}) from the WT (black dotted line) are shown. Wilcoxon-Mann-Whitney test applied to study differences within conditions for each sample (population and random colonies); *ns* indicates non-statistically significant changes (*p-value* > 0.05).

APPENDIX XI: Wilcoxon-Mann-Whitney test to assess differences within conditions for each sample in *S. aureus* isolates exposed to OCT

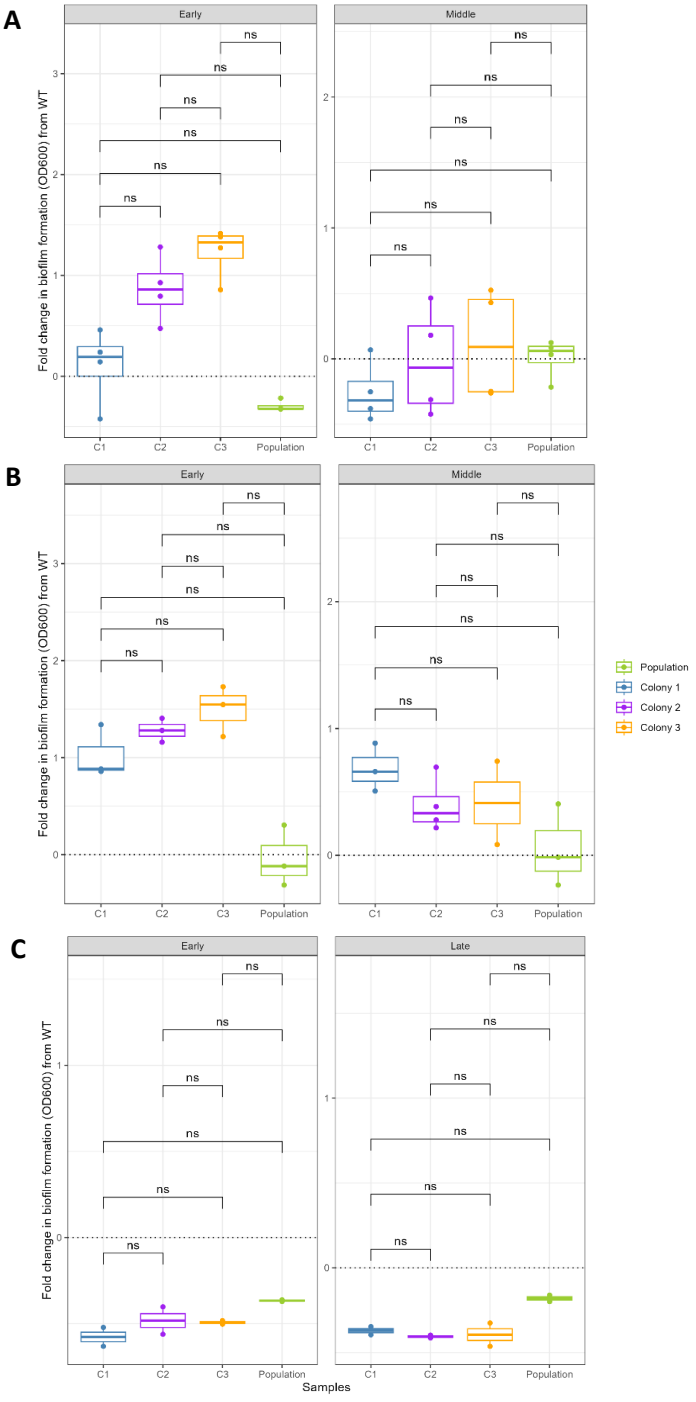

Figure A.XI. Biofilm biomass production in *S. aureus* isolates exposed to OCT for (A) biofilm; (B) planktonic; (C) control (no stress). Boxplots representing crystal violet staining with medians are shown; populations and individual isolates are represented in different colours. Fold changes in biofilm formation (OD_{600nm}) from the WT (black dotted line) are shown. Wilcoxon-Mann-Whitney test applied to study differences within conditions for each sample (population and random colonies); *ns* indicates non-statistically significant changes (*p-value* > 0.05).

APPENDIX XII: Distribution of the MICs in *E. faecalis* ST40 evolved isolates

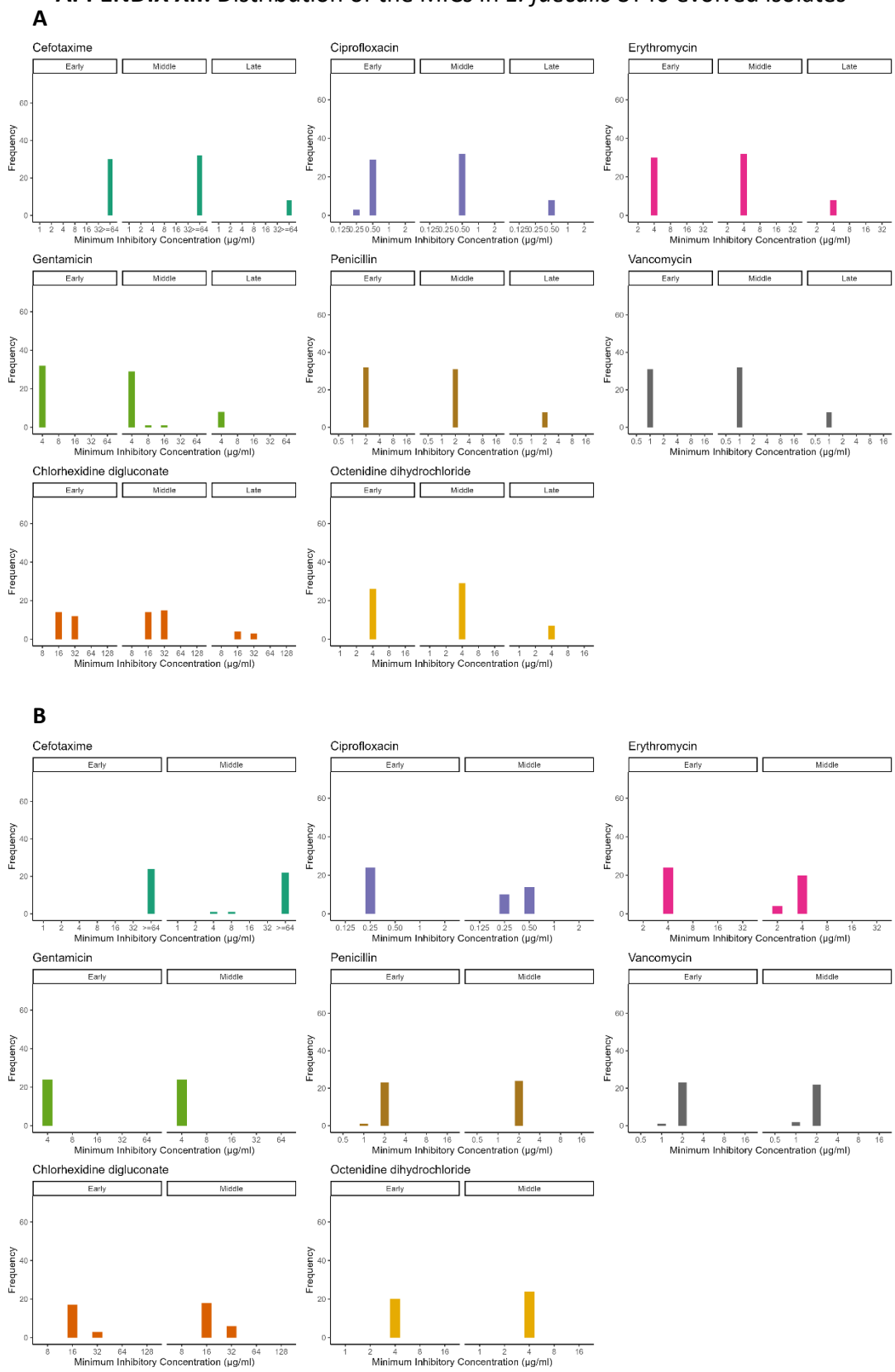

Figure A.XII. Distribution of the MICs of 6 different antibiotics and 2 biocides against *E. faecalis* evolved isolates. (A) CHX-evolved isolates and **(B)** OCT-evolved isolates shown. The heigh of the barplots indicates the MIC value with higher frequency across the samples.

APPENDIX XIII: Distribution of the MICs in *S. aureus* ST188 evolved isolates

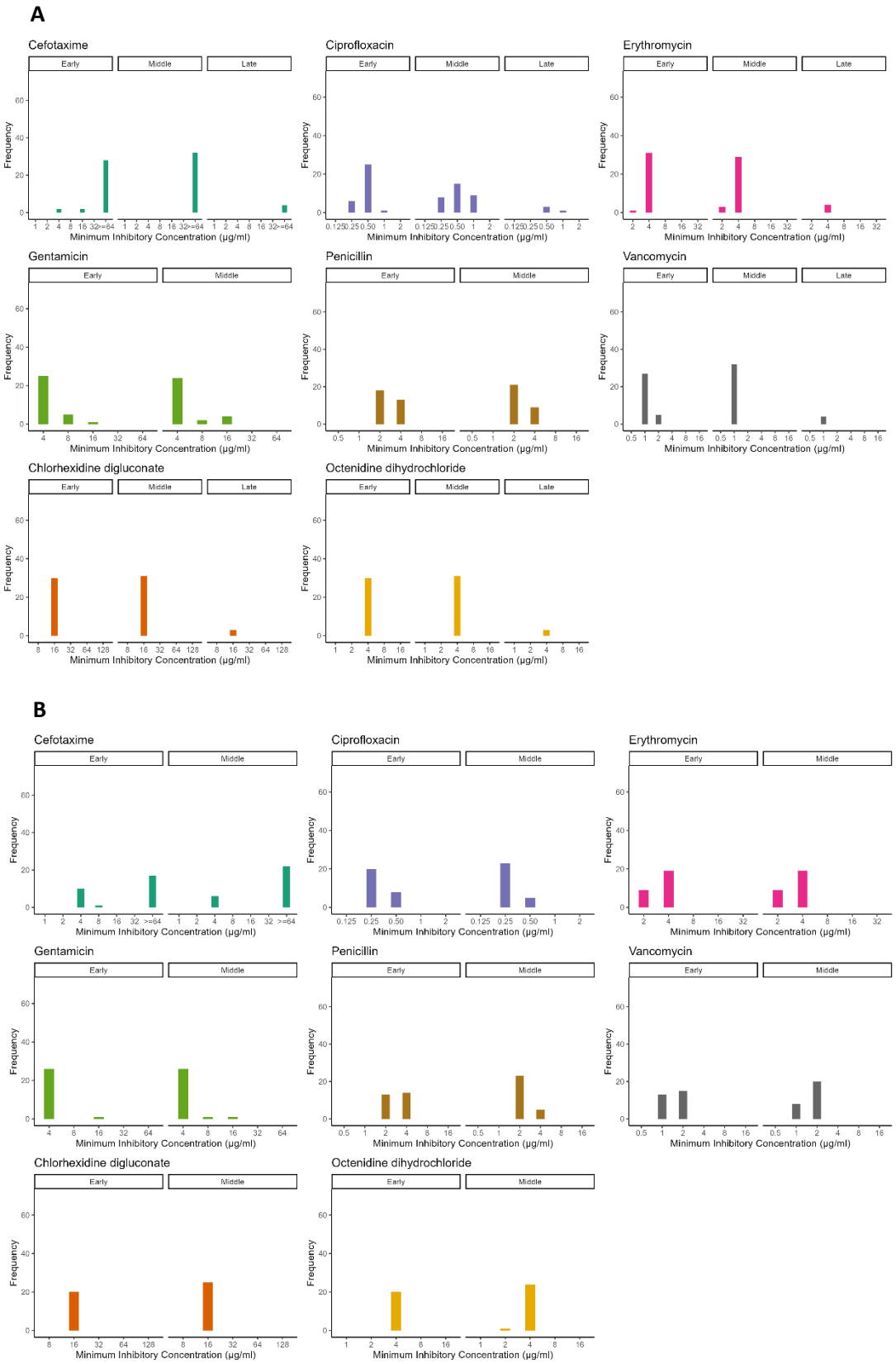

Figure A.XIII. Distribution of the MICs of 6 different antibiotics and 2 biocides against *S. aureus* evolved isolates. (A) CHX-evolved isolates and **(B)** OCT-evolved isolates shown. The heigh of the barplots indicates the MIC value with higher frequency across the samples.

APPENDIX XIV: Summarised sequencing details for *S. aureus* ST188, *E. faecalis* ST40 and *S. aureus* NCTC 12973

Table A.XIV. Summarised sequencing details for *S. aureus* ST188, *E. faecalis* ST40 and *S. aureus* NCTC 12973.

Isolate number	Genome size (Mbp)	Depth of coverage	Centrifuge (v0.15)	MLST	N50 (Kbp)	GC content (%)	AMR genes		
							AMR detection pipeline (v0.1.0)	ARIBA (v2.12.2)	BacMet (v2.0)
NCTC 12973	2.8	40X	*S. aureus*	ST 5 arcC(1) aroE(4) glpF(1) gmk(4) pta(12) tpi(1) yqiL(10)	138	32.67	*blaZ*	*arlR, arlS, blaZ, mepA, mepR, mgrA, tet38*	*arsB, arsC, copZ, farB, mepA, norB, perR, sdpR, tetA*
312	2.9	30X	*E. faecalis*	ST 40 gdh(3) gyd(6) pstS(23) gki(12) aroE(9) xpt(10) yqiL(7)	114	37.33	*lsa*(A), *tet*(M)	*dfrE, emeA, lsaA*	*bltD, copB, copY, graR graS, merR, tetA*
678	2.8	40X	*S. aureus*	ST 188 arcC(3) aroE(1) glpF(1) gmk(8) pta(1) tpi(1) yqiL(1)	138	32.65	*blaZ*	*arlR, arlS, blaZ, mepA, mepR, mgrA, tet38*	*arsB, arsC, copZ, farB, fabI, mepA, norB, perR, sdpR, tetA*

APPENDIX XV: Ethidium bromide accumulation in isolates with *fakA* mutations previously exposed to biocides

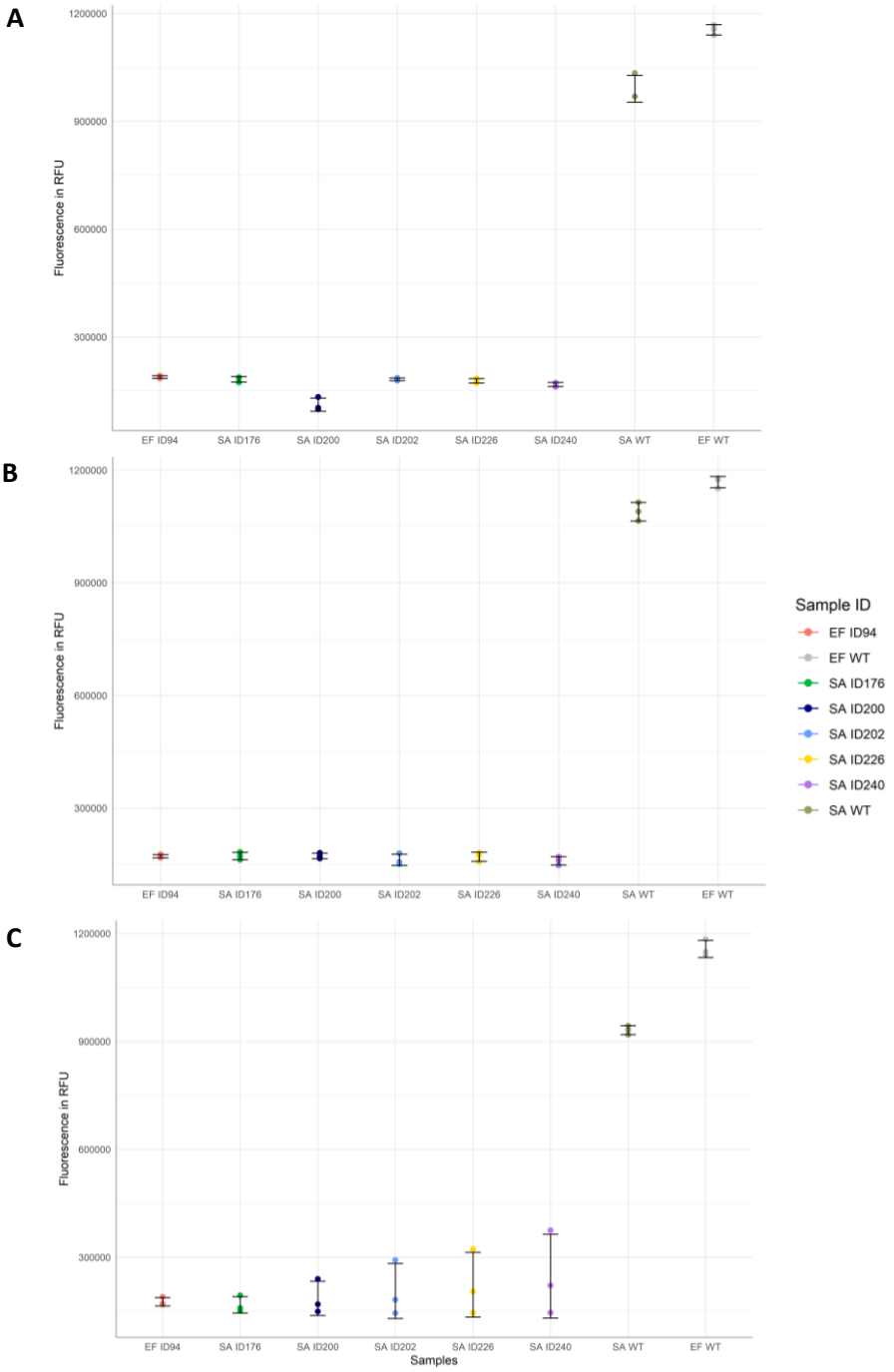

Figure A.XV. Ethidium bromide accumulation in isolates with *fakA* mutations previously exposed to biocides. 30-minute exposures to **(A)** ½ MIC of CHX; **(B)** ½ MIC of OCT; **(C)** ½ MIC of FM104 are shown. EtBr accumulation was measured based on fluorescence (excitation: 301 nm, emission: 603 nm) of cultures over 6 hours for *S. aureus* (SA) and *E. faecalis* (EF) evolved isolates and the WTs. Accumulation shown here was measured after 2 h 30 minutes of incubation representing a steady state; points show 3 independent replicates per sample with error bars indicating the mean and standard deviation values of the samples.

APPENDIX XVI: Productivity of the control lineages

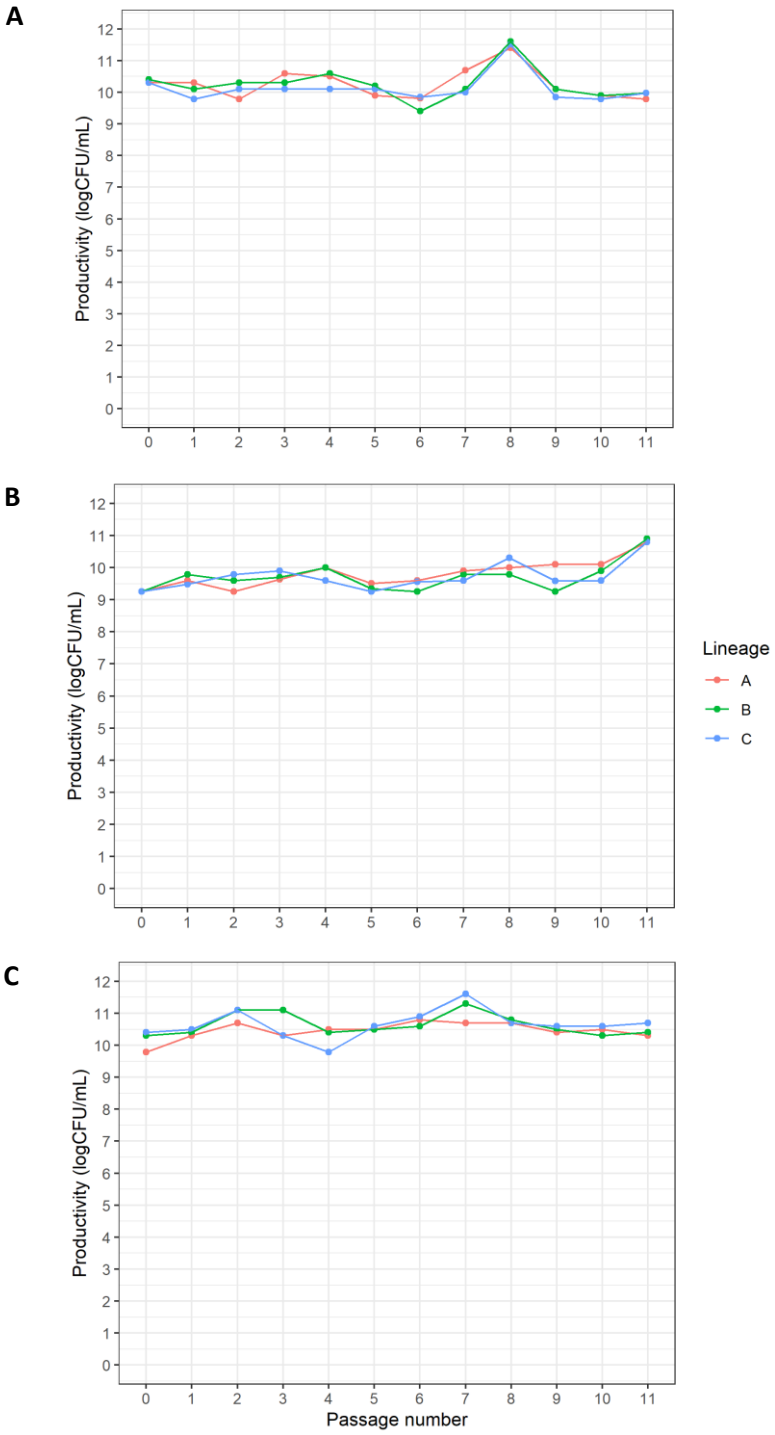

Figure A.XVI. Productivity of the control lineages. (A) *E. faecalis* ST40; **(B)** *E. hirae* NCTC 13383; **(C)** *S. aureus* ST188 control lineages are shown. Productivity (expressed as CFU/mL) is plotted over each passage number for the control condition (with no stress) for the experiment; three independent lineages (A, B, C) included. Independent drug-free controls ran for 11 passages (73 generations), and productivity stayed relatively the same over time.

APPENDIX XVII: Summary of the SNPs in annotated and hypothetical genes from the evolution experiment at GAMA Healthcare Ltd.

Table A.XVII. Summary of the SNPs in annotated and hypothetical genes in isolates evolved under different stresses (BZK+DDAC, FM104, Chassis).

Location	Gene	Function	Genome position	Mutation	Group	Number of isolates with the change	Effect
			***Enterococcus faecalis* ST40**				
Chromosome	Hypothetical (CIJKNMKJ_00329)	Unknown	325671	T -> C	Control, Stress 3	3	Synonymous variant (Ser -> Ser)
Plasmid (Contig 2)	-	Unknown	1006	C -> A	Control, Stress 1, Stress 2, Stress 3	5	Unknown
			***Staphylococcus aureus* ST188**				
Chromosome	Hypothetical (OOEOKIHE_02011)	Unknown	2128406	C -> T	Control, Stress 1, Stress 3	7	Synonymous variant (Leu -> Leu)
Chromosome	Hypothetical (OOEOKIHE_00881)	Unknown	902925	G -> A	Stress 1, Stress 3	2	Missense variant (Val -> Ile)
Chromosome	*cna*	Collagen-binding adhesin, virulence factor	2213804	GT -> AC (*)	Control, Stress 1, Stress 2, Stress 3	7	Missense variant (Ser -> Asn)
			***Enterococcus hirae* NCTC 13383**				
Chromosome	*capD*	UDP-glucose 4-epimerase	196580	C -> A	Control, Stress 1, Stress 2, Stress 3	4	Missense variant (Arg -> Ser)

* Multiple nucleotide polymorphism (MNP) indicated by (*).